Toxoplasma gondii : Knock-out approaches to study the function of dense granule proteins in the host-parasite interaction

Valeria Bellini

Communauté
UNIVERSITÉ Grenoble Alpes

THÈSE

Pour obtenir le grade de

DOCTEUR DE LA COMMUNAUTE UNIVERSITE GRENOBLE ALPES

Spécialité : **Virologie - Microbiologie - Immunologie**

Arrêté ministériel : 25 mai 2016

Présentée par

Valeria BELLINI

Thèse dirigée par **Corinne MERCIER, Maître de Conférences, Université Grenoble Alpes**, et
Co-dirigée par **Marie-France DELAUW, Directeur de Recherche, CNRS**

préparée au sein du **Laboratoire Techniques de L'Ingénierie Médicale et de la Complexité - Informatique, Mathématiques et Applications.**
dans **l'École Doctorale Chimie et Sciences du Vivant**

Toxoplasma gondii : approches moléculaires (analyse de mutants « knocked-out ») pour l'étude de la fonction de protéines de granules denses dans l'interaction hôte-parasite

Thèse soutenue publiquement le **13 Avril 2017**,
devant le jury composé de :

Monsieur Marc BLOCK
Professeur Université Grenoble Alpes, INSERM U1209, UMR 5309 CNRS, Université Grenoble Alpes, Président
Monsieur Sébastien BESTEIRO
Chargé de Recherche INSERM, UMR 5235 CNRS, Université de Montpellier, Rapporteur
Monsieur Mathieu GISSOT
Chargé de Recherche CNRS, INSERM U1019, CNRS UMR 8204, Université Lille Nord de France, Institut Pasteur de Lille, Rapporteur
Madame Patricia RENESTO
Directeur de Recherche CNRS, UMR 5525 CNRS, Université Grenoble Alpes, Examinateur

Invité :
Monsieur Jean-François DUBREMETZ
Directeur de Recherche émérite CNRS

Communauté
UNIVERSITÉ Grenoble Alpes

THESIS MANUSCRIPT

To obtain the diploma of

Philosophiæ doctor (PhD) in Life Sciences

Specialty: **Virology - Microbiology - Immunology**

Presented by:

Valeria BELLINI

Thesis directed by:
Corinne MERCIER and **Marie-France DELAUW**

Research Laboratory:
TIMC-IMAG, CNRS UMR 5525 – Université Grenoble Alpes
Research group: **"Natural Barrier and Infectivity"**
Doctoral School: **"Chemistry and Life Sciences of Grenoble"**

Toxoplasma gondii:
Knock-out approaches to study the function of dense granule proteins in the host/parasite interaction

Thesis defended on Thursday**, April 13th, 2017**

Reviewing committee:

Pr. Marc BLOCK, chair person
PR Ex. Université Grenoble Alpes, INSERM U1209, UMR 5309 CNRS, Université Grenoble Alpes
Dr. Sebastien BESTEIRO, rapporteur
CR-HDR INSERM, UMR CNRS 5235, Université de Montpellier II
Dr. Mathieu GISSOT, rapporteur
CR-HDR CNRS, INSERM U1019, CNRS UMR 8204, Université Lille Nord de France, Institut Pasteur de Lille
Dr Patricia Renesto, examiner
DR CNRS, CNRS UMR 5525, Université Grenoble Alpes, Grenoble

Invited:
Dr. Jean-François DUBREMETZ
DR CNRS (retired)

Acknowledgements

This study is the result of a short but very intensive work. Short, because these three years have gone so fast … and, intensive because obtaining meaningful results and compiling them into a story … has not been easy. If now all the results I have collected stand as a readable story, this is because of the help and support from many persons to whom I am most grateful and that I would like to thank here:

- my advisors Corinne and Marie-France for their continuous support during my PhD preparation and my experiments. Your experiences have helped me all along these three years of research and during the preparation of this thesis manuscript. Special thanks to Corinne for having selected me during the first call of the ParaFrap program, providing me with the opportunity to work in the Grenoble's team. Thank you for your precious advices during these years, your patience and having taken the time to proofread and amend all my writings through these three years despite your long list of university appointments. Thank you Marie-France for having accepted me in your team and for your strong support, when important decisions had to be taken. Thank you for your scientific advices that allowed me to improve my experience, they will be important for my future career.

- I am particularly thankful to my thesis committee for having accepted to read my thesis manuscript and assess my work: thanks to my rapporteurs Drs Sébastien Besteiro and Mathieu Gissot for their time; Dr. Patricia Renesto, who has accepted to examine it; Pr. Marc Block, who has accepted to be the chair person of this committee and Dr. Jean-François Dubremetz, I had the pleasure to meet at the last ParaFrap congress. I really feel honored to count you all as the members of my thesis committee;

- My sincere thanks go to our collaborators without whom this work would not have been possible: Dr D. Bzik and his team for sharing his collections of knocked-out parasites and our exchanges; Dr. Yves Usson, for his patience and the time he has spent in helping me with the analysis of confocal images; Dr Jean-Michel Saliou, for his efficiency in the proteomic analyses and his help in the interpretation of the results; Bastien Touquet and Dr Delphine Aldebert for having helped me with the high throughput immunofluorescence analyses and their advices; Dr. Pietro Lupetti and Dr. Eugenio Paccagnini, for having provided me with the opportunity to join their team and learn more about transmission electron microscopy.

- I will not forget my present and past colleagues of the BNI team: Pierre Cavailles, for his optimism, even when nothing seemed to make sense in the results, and his precious scientific advises; Corinne Loeuilletn for her help, her time spent doing the last precious experiments, and of course, her rigor in managing the lab; Cordelia Bisanz, for having made the complementation possible and for her help; Catherine Lemaire, for her smiles and her important advices in molecular biology. I have learnt a lot from you all! Delphine Jublot and Sara Cristinelli, you have supported me through all these days, becoming my friends more than my colleagues! Thanks also to Céline Colombani-Massera, Graciane Pètre, Salima Kamche, and the internship students.

And finally, many thanks to my friends and my family for their never-stopping support!

Valeria BELLINI, February 2017

Education

2009-2011: Master degree in Health Biology. University of Siena. Faculty of Mathematical, Physical and Natural Sciences**,** Siena, Italy.
2011: 4-month internship in Immunology for the preparation of my Master's degree**,** Pasteur Institute, Unit of Antiviral Immunity, Biotherapy and Vaccines, Paris, France. Director: Marie-Lyse Gougeon. Fellowship: Erasmus placement project.
2012-2013: 10-month internship in Immunology and Parasitology, Centre de Physiopathologie Toulouse Purpan (CPTP), INSERM UMR1043 / CNRS UMR5282, Toulouse III University, CHU Purpan, Toulouse, France. ATIP-AVENIR team: Parasites Eucaryotes Intracellulaires : Immunité et Physiopathologie. Director: Nicolas Blanchard.
Fellowship*:* European Unipharma Graduate Program, 2012-2013. National competition of "La Sapienza" University, Rome, Italy.

Lab Training during the preparation of my PhD

Animal experimentation for biologists (level 1), Université Grenoble Alpes (UGA), Grenoble.

Trainings during the preparation of my PhD

October 2013: Introductory training workshop in Parasitology of the ParaFrap LabEx, Laboratoire de Parasitologie-Mycologie, Faculté de Médicine, Montpellier
January 2015: Bioinformatics training course of the ParaFrap LabEx on the use of the "EuPathDB" database (Eukaryotics Pathogen Database Resources), Laboratoire de Parasitologie-Mycologie, Faculté de Médicine, Montpellier
2015-2016: Label Recherche Entreprise et Innovation (REI), 3rd edition, Ecole Doctorale Chimie et Sciences du Vivant (EDCSV), Grenoble
June 2016: Training in scientific writing and oral presentation. Training of the ParaFrap Labex, Pasteur Institute, Paris.

Trained students during the preparation of my PhD

2013: Anouar BITTAME (2 weeks), 3ème, Cité Scolaire Internationale de Grenoble.
2014: Julie VEDEL (3 months), BTS Bio-Analyses et Contrôles, Lycée Louise Michel. Now continuing with a "Licence Pro" degree.
2014: Aude GERBAUD (33 days), IUT de Lyon 1, training on a side project not reported in this manuscript. Now continuing with an Engineer School in Nice.
2015: Amélie DONCHET (39 days), Licence 3 de Biologie. Université Grenoble Alpes. Now continuing with a Master 2 degree in Grenoble.
2015: Mashal AHMED (39 days), Master 1 Biologie Moléculaire et Cellulaire. Université Grenoble Alpes. Now continuing with the preparation of a PhD in Immunology in Grenoble.

Participation to meetings during the preparation of my PhD

September 2014: First biannual PARAFRAP conference: "From basic research to intervention strategies against parasites". Les Embiez Island, Marseille, France.

Valeria Bellini, Corinne Loeuillet, Pierre Cavaillès, Barbara Fox, David Bzik, Nicolas Blanchard, Marie-France Cesbron-Delauw and Corinne Mercier. *"Contribution of the dense granule proteins to the formation of brain cysts and the establishment of latent infection"* (poster presentation).

October 2016: Second biannual PARAFRAP conference: "From basic research to intervention strategies against parasites". Les Embiez Island, Marseille, France.

Valeria Bellini, Corinne Loeuillet, Barbara A. Fox, David J. Bzik, Bastien Touquet, Delphine Aldebert, Pietro Lupetti, Yves Usson, Pierre Cavailles, Corinne Mercier and Marie-France Cesbron-Delauw. *"Toxoplasma gondii: contribution of the dense granule protein GRA5 to the formation of brain cysts and the establishment of latent infection"* (poster presentation).

List of publications

1.Valeria Bellini, Corinne Loeuillet, Céline Massera, Marie-France Cesbron-Delauw, Pierre Cavaillès. Cyst detection in Toxoplasma gondii infected mice and rats brains. Bio-protocol Vol 5, Iss 7, 4/5/2015.

2.Leah M Rommereim*, Valeria Bellini*, Barbara A. Fox, Graciane Pètre, Camille Rak, Bastien Touquet, Delphine Aldebert; Jean-François Dubremetz, Marie-France Cesbron-Delauw, Corinne Mercier, David J Bzik. (2016). Phenotypes associated with knockouts of eight dense granule gene loci (GRA2-9) in virulent Toxoplasma gondii" **(* co-first authors**) PloS One. 11:e0159306

3.Valeria Bellini, Corinne Loeuillet, Jean-Michel Saliou, Delphine Jublot, Cordelia Bisanz, Barbara A. Fox, David J. Bzik, Eugenio Paccagnini, Bastien Touquet, Delphine Aldebert, Pietro Lupetti, Yves Usson, Pierre Cavailles, Corinne Mercier* and Marie-France Delauw*. GRA5 regulates the recruitment of host organelles around the vacuole formed by cystogenic Toxoplasma parasites. *in preparation* (* equal contributions).

List of Joined Documents

This thesis manuscript includes, in the "Results" section, the three papers to which I have contributed, and which will constitute the three chapters of this section:

1 . Leah M Rommereim*, Valeria Bellini*, Barbara A. Fox, Graciane Pètre, Camille Rak, Bastien Touquet, Delphine Aldebert; Jean-François Dubremetz, Marie-France Cesbron-Delauw, Corinne Mercier, David J Bzik. (2016). Phenotypes associated with knockouts of eight dense granule gene loci (GRA2-9) in virulent Toxoplasma gondii" **(* co-first authors**) PloS One. 11:e0159306

Pages 84-107 of this manuscript

2. Valeria Bellini, Corinne Loeuillet, Jean-Michel Saliou, Delphine Jublot, Cordelia Bisanz, Barbara A. Fox, David J. Bzik, Eugenio Paccagnini, Bastien Touquet, Delphine Aldebert,' Pietro Lupetti, Yves Usson, Pierre Cavailles, Corinne Mercier* and Marie-France Delauw*. GRA5 regulates the recruitment of host organelles around the vacuole formed by cystogenic Toxoplasma parasites. *in preparation* (* equal contributions).

Pages 108-109 of this manuscript

3. Valeria Bellini, Corinne Loeuillet, Céline Massera, Marie-France Cesbron-Delauw, Pierre Cavaillès. Cyst detection in Toxoplasma gondii infected mice and rats brains. Bio-protocol Vol 5, Iss 7, 4/5/2015.

Paqes 163-169 of this manuscript

Index

Abbreviations

Ahr: Aryl Hydrocarbon Receptor
AMA1: Apical Membrane Antigen 1
AP: Apetala
APC: Antigen Presenting Cell
ASP: Aspartyl Protease
ATG5: Autophagy-related Protein 5
BAG: Bradyzoite Antingen
CAMLG: Calcium signal-Modulating cyclophilin Ligand
CARM: Coactivator Associated Arginine Methyltransferase
CCR: C-C Chemokine Receptor
CPC: Cathepsin C
CNS: Central Nervous System
Cy: Cyclophilin
DAG: DiAcylGlycerol
DC: Dendritic Cell
DG: Dense Granule
DHFR: DiHydroFolate Reductase
eiIF2: Eukaryotic Initiation Factor 2
ENO: Enolase
ER: Endoplasmic Reticulum
ESA: Excreted-Secreted Antigen
GAG: GlycoAmino Glycan
GAP: Glideosome-Associated-Protein
GAS: Gamma Activated Sequence
GBP: Guanylate Binding Protein
GCN: General Control Nonderepressible
GLC: Gas Liquid Chromatography
GPI: GlycosylPhosphate Inositol
GRA: Dense Granule Protein
GTPase: Guanosine Triphosphatehydrolase
HAUSP: Herpes virus-Associated Ubiquitin Specific Protease deubiquitinase
HDAC: Histone DeAcetylase
HIV: Human Immunodeficiency Virus
HPLC: High Pressure Liquid Chromatography
HSCT: Hematopioetic Stem Cell Transplant
HOST: HOst Sequestering Tubulostructure
HSP: Heat Shock Protein
IF2K: Initiation Factor 2 Kinase
Ig: Immunoglobulin
IFN-γ: Interferon-gamma
IFN-γR: Interferon-gamma Receptor
IL: InterLeukin
IMC: Inner Membrane Complex
iNOS: inducible Nitric Oxide Synthase
IRF8: Interferon Regulatory Factor 8
IRG: Immunity Related Guanosine Triphosphatase
IST: Inhibitor of STAT1-dependent Transcription
KO: KnockOut
LDH: Lactate DesHydrogenase
LCAT: Lipolytic Lecithin:Cholesterol Acyltransferase
LD: Lethal Dose
5 LO: 5 Lipoxygenase
LPC: LysoPhosphatidylCholine
LXA4: Lipoxin A4
MAF1: Mitochondrial Association Factor1
MHC ClI: Major Histocompatibility Complex Class I
MIC: Microneme protein
MJ: Moving Junction
MNN: Membranous Nanotubular Network
MTOC: MicroTubule Organization Center
MyD88: Myeloid Differentiation primary response gene 88
MYR1: Myc-Regulation-1
NFAT: Nuclear Factor of Activated T-cells
NF-κB: Nuclear Factor Kappa B
NK: Natural Killer cell
NLS: Nuclear Localization Signal
NO: Nitric Oxide
NTPase: Nucleotide Triphosphate isomerases
OPN: Osteopontin
PA: Phosphatidic Acid
PAMP: Pathogen-Associated Molecular Pattern
PCR-RFLP: Polymerase Chain Reaction-Restriction Fragment Length Polymorphism
PEXEL: Plasmodium Export ELement

PH (domain): Pleckstrin Homology (domain)
PI: Post-Infection
PPM: Parasite Plasma Membrane
PV: Parasitophorous Vacuole
PVM: Parasitophorous Vacuole Membrane
ROM: Rhomboid protease
ROP: Rhoptry protein
ROS: Reactive Oxygen Species
SAG1: Surface Antigen 1
SET: Histone lysine methyltransferase containing a SET domain
SRS: SAG1-Related Sequences
STAT1: Signal Transducer and Activator of Transcription 1
SUV: Small Unilamellar Vesicle
TE: ToxoEncephalitis
TEM: Transmission Electron Microscopy
Th1: T Helper 1 cell
TLC: Thin Layer Chromatography
TLR: Toll-Like Receptor
TNF-α: Tumor Necrosis Factor α
VLP: Virus-Like Particle

INTRODUCTION

CHAPTER I
TOXOPLASMA GONDII AND TOXOPLASMOSIS

Toxoplasma gondii is a ubiquitous protozoan parasite that belongs to the Apicomplexa phylum. All the Apicomplexa (such as *Plasmodium, Eimeria, Cprytosporidium, Neospora* and *Theileria*) are intracellular parasites and agents of a wide variety of diseases in animals and humans.
T. gondii, in particular, is able to infect all warm-blooded animals, causing one of the most common parasite infections, toxoplasmosis. As an obligate intracellular parasite, *T. gondii* replicates within a parasitophorous vacuole (PV), which is a structure formed by the parasite within the host cell at the time of invasion. During the acute phase of infection, the intracellular parasite escapes the host immune response and colonizes the whole infected organism. In organs where the pressure of the host immune system is weaker such as in the brain, the PV differentiates into a cyst, while the fast dividing tachyzoite stage (characteristic of the acute stage of infection) differentiates into the slowly dividing or quiescent bradyzoite stage. This differentiation is typical of the chronic phase of infection. Within these quiescent cysts bradyzoites can persist for the entire life of the infected individual.

I-1 *TOXOPLASMA GONDII*: HISTORY AND PHYLOGENY

T. gondii was identified for the first time in 1908 independently by Nicolle and Manceaux, who isolated a protozoan from the tissues of a North African rodent, *Ctenodactylus gundi*, and by Splendore, who discovered the same parasite in a rabbit in Brazil (Nicolle and Manceaux, 1909; Splendore, 1909). The name "*Toxoplasma gondii*" was attributed to the isolated protozoan by Nicolle and Manceaux according to the parasite shape (*toxon*= arc or bow, *plasma*= life) and the infected host.
Following this primary identification, several *Toxoplasma*-like infections were described in various animal species, including humans in the 1920s. Step by step, knowledge on human toxoplasmosis increased, particularly during the 1970/80s. When the immunodeficiency syndrome (AIDS) became epidemic, *T. gondii* became the major cause of morbidity and mortality in patients infected by the human immunodeficiency virus (HIV). The complete parasite life cycle and the different ways by which the parasite can be transmitted were discovered between the 1960s and the 1970s by Hutchison (Hutchison, 1965) and later by Frenkel and Dubey (Frenkel *et al*., 1969).
Within the Alveolata super-phylum *T. gondii* is a protozoon that belongs to the Apicomplexa phylum, the Conoidasida class, the Eucoccidiorida order, the Sarcocystidae family, the Toxoplasmatinae sub-family, in which one single genus (Toxoplasma) and one single species (*T. gondii)* has been described (**Figure 1**). The parasites of the Apicomplexa phylum are characterized by a highly developed structure called the apical complex at their anterior region, and which is used for host cell invasion.

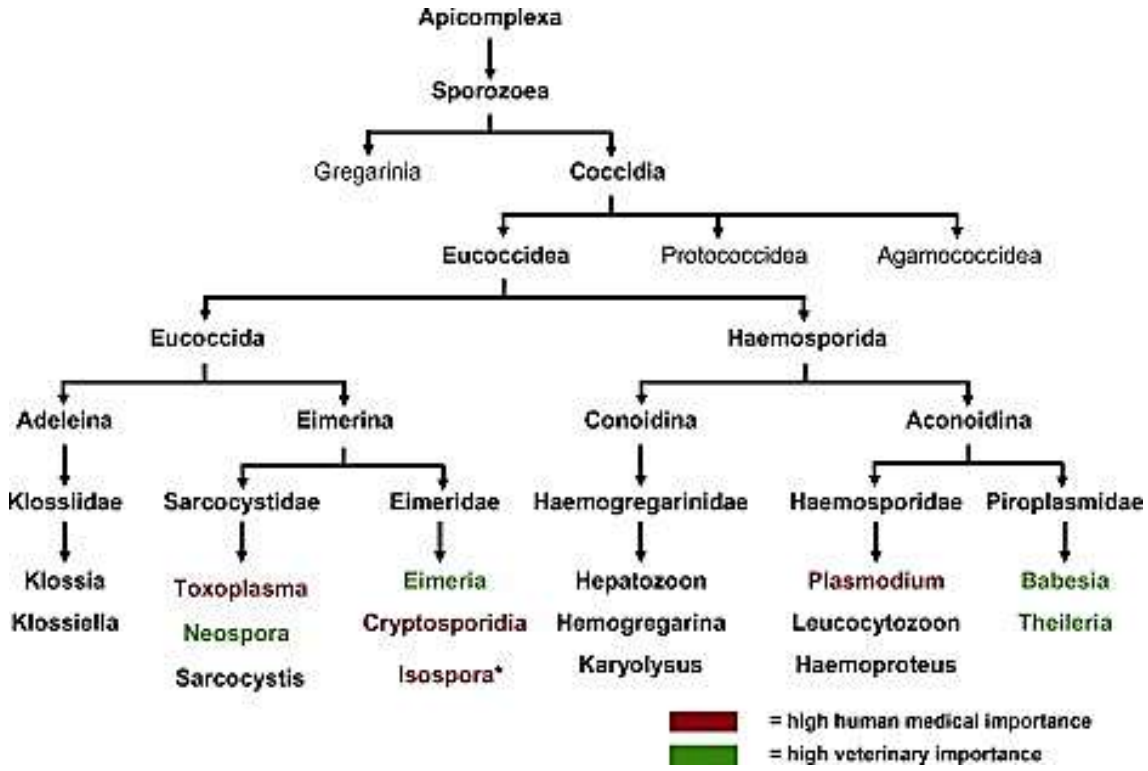

Figure 1. Phylogenetic tree of Apicomplexa parasites.
The distinction between parasites of human medical and/or veterinary importance is based on the molecular analyses by Beck *et al.,* 2009.

Among the Apicomplexa, *T. gondii* is the most experimentally tractable: easy to amplify *in vitro* and readily amenable to genetic manipulations, it became the parasite model *i*) to study the molecular and cellular mechanisms of cell invasion and *ii*) to explore the genetic bases of virulence in intracellular protozoan parasites.

I-2 THE PARASITE LIFE CYCLE

Toxoplasma gondii differs from the other Apicomplexa parasites by its ability to infect a wide range of hosts. All the warm-blooded animals (carnivores, herbivores and birds), including humans, constitute its intermediate hosts. In their tissues the parasite exhibits an incomplete life cycle and multiplies only as asexual stages**.** In cats and other Felids, that are the parasite's definitive hosts, *T. gondii* develops a complete life cycle with both sexual- and asexual stages (**Figure 2**).

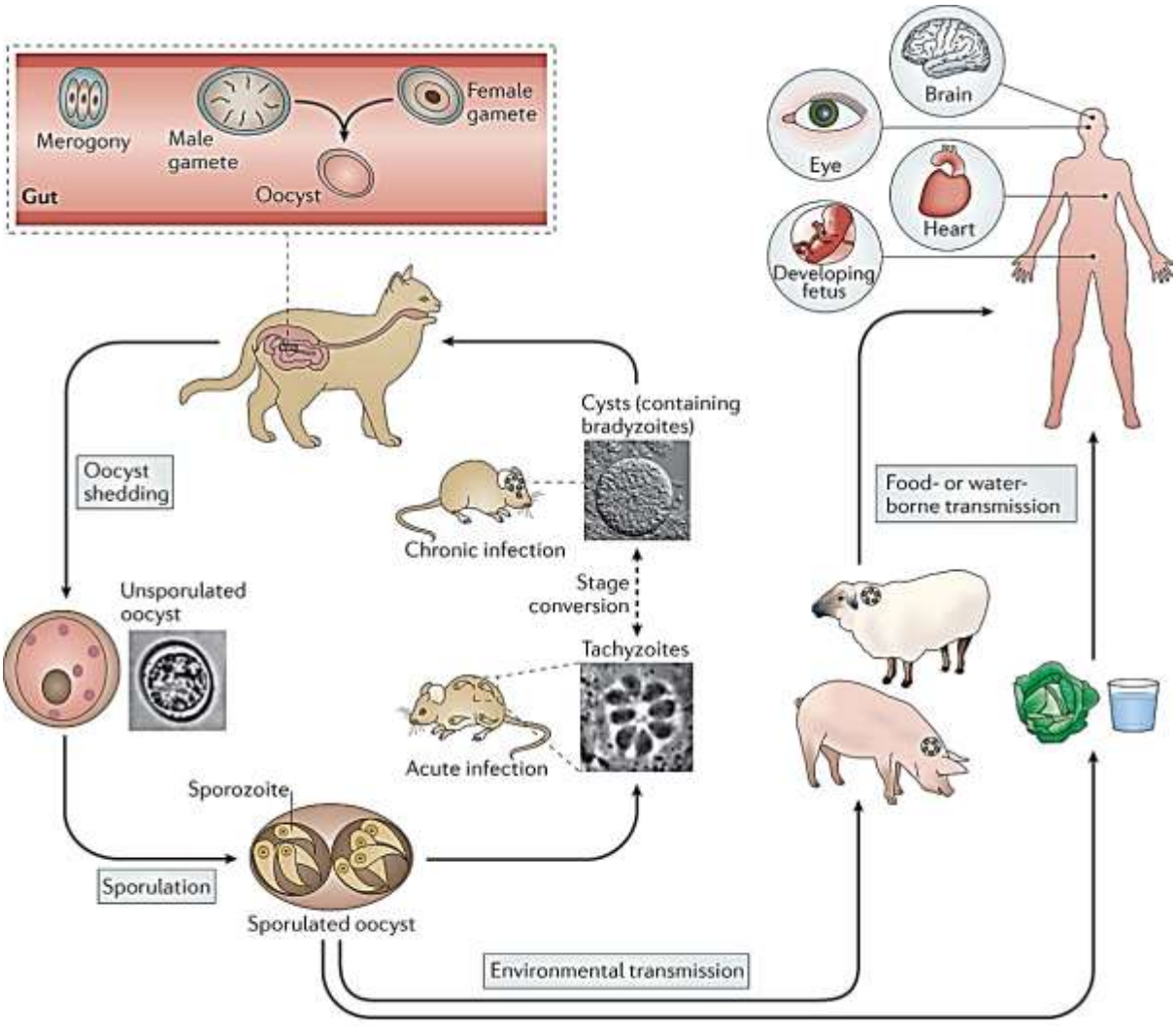

Figure 2. Transmission and life cycle of *Toxoplasma gondii*.
Except for congenital infections, the parasite is acquired by the oral route. In intermediate hosts the parasite can be encountered as 2 different stages, the tachyzoite and the bradyzoite, respectively. In definitive Felid hosts, the same stages as those encountered in intermediate hosts are described. However, sexual stages also develop in the digestive tract, leading to excretion of parasite eggs called oocysts, which must sporulate in the environment (last step of maturation) to become infectious for both intermediate and definitive hosts. Oocysts contain infectious sporozoites. From Hunter and Sibley, 2012.

I-2.1) The asexual cycle occurs in intermediate hosts

The intermediate hosts (all warm-blooded animals) can be infected by ingestion of mature oocysts present on contaminated vegetables or in contaminated water, or by ingestion of tissue cysts present in infected raw or undercooked meat (**Figure 2**). The oocysts and the cysts represent indeed the

dissemination and infectious structures of the parasite (**Figure 2**). They contain, respectively, infectious sporozoites and bradyzoites. Consecutively to the digestion of the oocyst/cyst wall in the intestinal tract, the zoites they contain rapidly differentiate into tachyzoites, which constitute the fast dividing and disseminating stage of the parasite. Once these tachyzoites have infected the intestinal epithelium, they divide actively (by an asexual type of division process called endodyogeny), disseminate throughout the body *via* the vascular system and reach muscle tissues and the brain. This acute infection is usually rapidly controlled by the host immune response, which is initiated as soon as the first contact with the parasite and fully develops 7 to 10 days post-infection (PI). This host innate immune response is crucial for both the host and the parasite since *i),* if uncontrolled, the infection would kill the host and *ii)* it participates to the differentiation of tachyzoites to bradyzoites and the formation of cysts in tissues, where the immune pressure is lower, *i.e.* the muscles, the brain, the eyes and the testicles. Tissue cysts cannot be eliminated by the immune system and they may remain viable for the entire life-time of the infected host, meaning that the chronic phase of infection lasts as long as the infected host survives (Dubey *at al*., 1970; Ferguson *et al*., 1975).

I-2.2) The sexual cycle in definitive hosts

Definitive hosts (Felids) can be infected by the parasite after eating oocysts present on the ground, on vegetables and in contaminated water, or by carnivorism of infected mice and birds, which contain tissue cysts in their brain and muscles.
In addition to the differentiation processes which have been described for intermediate hosts (see the paragraph 1.2-1), some tachyzoites differentiate into merozoites in the gut. These merozoites initiate the parasite sexual cycle: they differentiate into micro- and macrogemetes. Fertilization leads to the formation of immature oocysts, which are released into the intestinal lumen and are eventually ejected into the external environment with the cat feces. Sporulation (*i.e.* maturation) of these oocysts takes place outdoor and leads to mature oocysts, which are resistant to chemical- or physical agents, can remain viable for extended periods of time and contain highly infectious sporozoites (Dubey *at al*., 1970; Ferguson *et al*., 1975).

I-3 *TOXOPLASMA GONDII*: CLONAL LINEAGES

Due to its complex life cycle that alternates between sexual replication in Felids and asexual replication in a wide-range of warm-blooded animals including humans, *T. gondii* has a worldwide distribution. In the recent years, molecular analyses of strains sampled mainly in North America,

Europe and South America have revealed significant differences among the parasite populations described in the two hemispheres.

Despite the presence of a sexual cycle, the population structure of *T. gondii* isolated in North America and Europe is remarkably clonal. The majority of isolates belongs to one of the three major clonal lineages, *i.e.* types I, II, or III (Howe and Sibley, 1995; Sibley and Boothroyd, 1992). A fourth clonal lineage, type 12, has been described in North America from isolates of wild animals (Khan *et al.,* 2011). In contrast, an entirely distinct pattern is observed in Central and South America. Various lineages that show greater genetic diversity within- and divergence between the groups have indeed been observed, reflecting more frequent recombination events (Khan *et al*., 2007; Lehmann *et al*., 2006; Pena *et al*., 2008).

To date, one can regret that there is no standard nomenclature for Toxoplasma genotypes. The historical nomenclature indeed refers to the clonal lineages called types I, II, III as well as to other atypical strains (Howe and Sibley, 1995; Grigg *et al.,* 2001; Su *et al.,* 2003). Several molecular techniques, such as polymerase chain reaction-restriction fragment length polymorphisms analysis (PCR-RFLP) (Howe and Sibley, 1995; Su *et al.,* 2010; 2012), microsatellite DNA analysis (Ajzenberg *et al.,* 2002; 2010) and multi-locus DNA sequence typing of introns (Khan *et al.,* 2007; 2011) allowed to refine the population structure of *T. gondii*. PCR-RFLP analysis of 10 markers on 1,457 strains isolated from domestic and wild animals with chronic infection identified 189 genotypes. Among them, 10 genotypes (#1 to #10) were shown to compose the conventional Types I, II and III (**Table 1**). The genotypes #1, #2, and #3, which correspond respectively to Type II clonal, Type III and Type II variant, were identified worldwide and are particularly highly prevalent in Europe. In North America the prevalent genotypes are #1, #2, #3, #4 and #5. Genotypes #2 and #3 (Type III and II variant) are prevalent in Africa, while genotypes #9 and #10 (Chinese1 and Type I) are more often encountered in East Asia. The Type 12, described as a dominant lineage in wild life in North America, is associated with high mortality in sea otters along the coast of California. In Central and South America *T. gondii* strains display a highly diverse population structure, in which no genotype appears to be clearly dominant. The 10 genotypes the most represented are #2, #6, #7, #8, #11, #3, #65, #13, #19 and #146. Of these genotypes, #2 (Type III) is predominant and is found in many countries of the region (Shwab *et al.,* 2014; Su *et al.,* 2010; 2012; Miller *et al.,* 2008).

The various genotypes have been linked to different levels of virulence, which is defined in mice for Toxoplasma infections. Virulent type I strains kill laboratory- and outbred strains of mice within 10-12 days with a lethal dose (LD) of 1 parasite, while type II and III strains are less virulent (median LD $\geq 10^3$ parasites) (Sibley and Boothroyd, 1992; Taylor *et al*., 2006). Strain type-dependent virulence was shown to be linked to the polymorphism of secreted proteins such as PV membrane (PVM)-associated ROP5/ROP18 complexes that allow resistance to interferon-γ (IFN-γ) activated immunity-related GTPases (IRG) dependent innate killing mechanisms (see paragraph 1.4-1b).

Conventional genotypes	ToxoDB PCR-RFLP genotypes	Representative isolates	References
Type I, type 1	#10	GT1	Su *et al*., 2012
Type II, type 2 (type 2 clonal)	#1	PTG	Su *et al*., 2012
Type II, type 2 (type 2 variant)	#3	PRU	Su *et al*., 2012
Type III, type 3	#2	VEG	Su *et al*., 2012
Type 12, atypical, exotic	#4	B41	Khan *et al*., 2011; Su *et al*. 2012
Type 12, atypical, exotic, includes Type X and Type A	#5	ARI	Khan *et al*., 2011; Su *et al*., 2012
Type BrI, atypical, exotic, Africa 1	#6	FOU, TgCatBr2	Pena *et al*., 2008; Mercier *et al*., 2010; Su *et al*., 2012
Type BrII, atypical, exotic	#11	TgCatBr1	Pena *et al*., 2008; Su *et al*., 2012
Type BrIII, atypical, exotic	#8	P89 (TgPgUs15), TgCatBr3	Pena *et al*., 2008; Su *et al*., 2012
Type BrIV, atypical, exotic	#17	MAS, TgCkBr147	Pena *et al*., 2008; Su *et al*., 2012
Chinese 1, atypical, exotic	#9	TgCtPRC4	Dubey *et al*., 2007; Chen *et al*., 2011; Su *et al*., 2012

Table 1. Genotype designation of major *Toxoplasma gondii* lineages
From Shwab *et al*., 2014.

Together, these studies suggested a clonal population structure in the Northern hemisphere and an epidemic population structure in the Southern hemisphere. The reasons of this geographical difference could be related to various causes:

i) the transformation of European, North American and East Asian landscapes during history, which led to the reduced presence of wild animals correlated to an increased number of genetically uniform domestic animals (Shwab *et al.,* 2014);

ii) a "founder effect" in the Northern hemisphere. Strains of South or Central America could have been introduced from these regions into other continents by maritime trading of goods and transport of infected animals, such as rodents or pet animals (Lehmann *et al.,* 2006). Competition or recombination between these strains during their successive

replications could thus be the reason for the current clonal population structure in the Northern hemisphere;

iii) the diversity and the high number of animal hosts in tropical and sub-tropical regions may have allowed the selection of different *T. gondii* genotypes, enabling a wider variety of strains to proliferate (Shwab *et al.,* 2014).

I-4 TOXOPLASMOSIS IN HUMANS

I-4.1) The immune response during toxoplasmosis

In immunocompetent individuals the infection by *Toxoplasma gondii* is controlled by the activity of the immune system. Consecutively to a non-specific innate immune response, the infection is controlled mainly by a T helper-1 (Th1) cell-mediated specific immune response that is predominantly mediated by IFN-γ mainly produced by natural killer cells (NK), T cells and neutrophils (Yarovinsky, 2014).

The immune response during the acute phase of infection limits the parasite replication, allows the differentiation of tachyzoites into bradyzoites and the development of intracellular cysts, which are characteristic of the chronic phase. Moreover, the immunity acquired following the first infection controls the reactivation of encysted parasites and allows long specific protection against new parasite infections (Capron and Dessaint, 1988).

a) The innate immune response

Following parasite infection patrolling neutrophils, monocytes, and dendritic cells (DC) are recruited at the site of infection (Liu *et al.,* 2006; Dunay *et al.,* 2008). A critical function of these innate immune cells is their ability to "sense" the presence of pathogens by their recognition of pathogen motifs called pathogen-associated molecular patterns (PAMP) by their receptors called toll-like receptors (TLR). Mice lacking the adapter myeloid differentiation factor 88 (MyD88), which is required for signaling downstream most TLR, were shown to be acutely susceptible to toxoplasmosis (Scanga *et al.,* 2002). This is indeed MyD88, which relays the production of interleukin-12 (IL-12) by these innate immune cells, IL-12 being the cytokine that allows the activation of Th1 cells.

Many TLR, such as TLR2, 4, 7, 9, 11 and 12 are involved in sensing the presence of *T. gondii*. For examples:

i) TLR11 was shown to recognize profilin, which is an essential actin-binding protein that regulates parasite motility and host cell invasion (Plattner *et al.,* 2008), and which is also released from parasites. Various studies showed that TLR11 (present in endolysosomes), in

association with the TLR12 receptor, mediates the recruitment of MyD88 to initiate the downstream signaling cascade that triggers the production of IL-12 (Andrade *et al.,* 2013; Raetz *et al.,* 2013). However, the precise mechanism behind this TLR11-TLR12 cooperation remains to be clarified;

ii) TLR7 and TLR9 have been implicated in the detection of *Toxoplasma* RNA and genomic DNA, respectively (Andrade *et al.,* 2013);

iii) TLR2 and TLR4 were shown to recognize the glycosylphosphatidylinositol (GPI) moiety of the major parasite surface proteins (Debierre-Grockiego *et al.,* 2007).

Many studies were performed to define the immune cells (neutrophils, DC, NK cells, macrophages) that produce the pro-inflammatory cytokines, such as IL-12 and/or tumor necrosis factor α (TNF α), which amplify the Th1 specific response and the production of IFN-γ (**Figure 3**). Interestingly, neutrophils were described as being rapidly recruited at the site of infection to be an early source of IL-12 released from their internal stores independently of the presence of IFN-γ (Bliss *et al.,* 2000; Sturge *et al.,* 2013). They are also important cells to protect TLR11-depleted mice from *T. gondii* infection (Sturge *et al.,* 2013) and to activate and recruit indirectly more DCs in order to amplify the IL-12 production. Infected mice depleted in neutrophils exhibit a low level of IL-12 correlated with an increased parasite proliferation (Bliss *et al.,* 2001).

Interestingly, parasitized DC (as well as microglia) were shown to exhibit a hyper-migratory phenotype *in vitro*, associated with enhanced parasite dissemination in mice (Lambert *et al*., 2006). Recent studies showed that the PVM-associated protein Tg14-3-3 is the mediator of this DC hyper-motility (Weidner *et al*., 2016). *In vivo* models confirmed the major role of DC and more particularly, that of the $CD8\alpha^+$ subset, as the primary source of IL-12 (Mashayekhi *et al.,* 2011; Raetz *et al.,* 2013). Recent findings indeed showed that naive $CD8\alpha^+$ DC selectively express the transcription factor "IFN regulatory factor 8" (IRF8), which leads to their specific production of IL-12 (Sturge and Yarovinsky, 2014). Activation of this DC subset was shown to be crucial to initiate the adaptive immune response. Within the first few days that follow an oral infection, infected DCs migrate from the intestine (first site of parasite infection) to the mesenteric- and draining lymph nodes (Courret *et al.,* 2006; Luu and Coombes, 2015). In the para-cortical region of these lymph nodes activated DCs initiate a vigorous immune response that primes naive T cells (Chtanova *et al.,* 2009).

By contrast, TNFα was shown to be mostly produced by macrophages and monocytes via other signaling pathways (not activated by TLR11), such as that involving nuclear factor κ B (NF-κB).

The NK cells play an important role in the innate response to Toxoplasma infection due to their production of large amounts of IFN-γ and their cytotoxicity against the parasite. They can also promote adaptive immune responses. Two different studies indeed showed that, in absence of $CD4^+$ T cells, NK cells help the $CD8^+$T cell response (Combe *et al.,* 2005), while their IFNγ production optimizes the $CD4^+$ T cell response (Goldszmid *et al.,* 2007).

b) The adaptive immune response

The adaptive immune response is represented by the activity of both $CD4^+$ and $CD8^+$ T cells. Early studies showed that mice lacking T cells do not survive latent infection (Hunter *et al*., 1994), while depletion in T cells during the chronic phase re-activates the disease (Gazzinelli *et al.,* 1992). $CD4^+$T cells play important roles both during the early stage of infection by their contribution to optimal B- and $CD8^+$ T cell responses, and during the chronic phase by their production of IFN-γ (Dupont *et al*., 2012).

Once released, IFN-γ binds to the IFNγ receptor (IFN-γR), which eventually leads to the activation of the transcription factor "signal transducer and activator of transcription 1" (STAT1) (Kim *et al.,* 2007). In macrophages and monocytes STAT1 induces the transcription of many genes implicated in antimicrobial responses, such as the gene encoding inducible nitric oxide synthase (iNOS), which leads to the production of nitric oxide (NO). Activation of macrophages by IFN-γ also leads to their production of toxic reactive-oxygen species (ROS) (Arsenijevic *et al.,* 2001). The production of both NO and ROS constitutes two main mechanisms by which macrophages efficiently kill the parasites that are protected by their PV (**Figure 3**). In addition, in the hours that follow invasion, mouse macrophages as well as non-hematopoietic cells up-regulate two families of defense proteins, namely IRGs and guanylate-binding proteins (GBPs) (Butcher*, et al.*, 2005; Howard *et al.,* 2011; Yamamoto *et al.,* 2012), that are recruited to the PV, attack it, leading to rapid parasite death (**Figure 3**).

Activated $CD8^+$ T cells not only produce IFN-γ but also kill infected cells. The $CD8^+$ T cell response is initiated when naive $CD8^+$ T cells encounter their cognate antigen presented by a class I major histocompatibility complex (MHCI) at the surface of an antigen-presenting cell (APC), accompanied by co-stimulatory and cytokine signals (Dupont *et al*., 2012). The first studies on the $CD8^+$ T cell response characterized the Surface Antigen 1 (SAG1) as a major target of $CD8^+$ T cells (Khan *et al.,*1988). Other T epitopes have since been characterized in GRA3, GRA4, GRA6, GRA7 and ROP7 (Frickel *et al.,* 2008; Blanchard *et al.,* 2008; Tan *et al*., 2010). These T epitopes have been shown to be presented in the context of the H2-Ld allele of MHCI, while the T epitope from the Tgd_057 antigen is presented in the context of the H2-Kb allele of MHCI (Wilson *et al.,* 2010). Among these T epitopes, that described in the C-terminal region of GRA6 was shown to be restricted to $GRA6_{II}$ (which is the GRA6 protein expressed by type II parasites) (Blanchard *et al.,* 2008; Dupont *et al*., 2012).

Another important arm for the resistance to toxoplasmosis is the humoral response. B cells produce specific antibodies that help kill the parasites (Dupont *et al*., 2012). As mentioned before, the optimal B cell response requires $CD4^+$ T cell activity, as confirmed by mice deficient- or depleted in $CD4^+$T cells, which display lower specific antibody titers (Johnson *et al.,* 2002). Although the humoral immune response plays a second role in parasite elimination, various classes of antibodies (immunoglobulins A (IgA), IgE, IgM and IgG) are produced and are crucial for the protection against new *Toxoplasma*

infections (Yap and Sher, 1999). In humans, detection of specific IgG and IgM are at the basis of most of the toxoplasmosis diagnosis tests (see paragraph 1.5-1).

c) Control of the inflammatory response

As for any other infection, the intensity of the immune response mounted against *T. gondii* must be tightly regulated to avoid immune-pathologic effects due to excessive inflammation.

Soon after infection and upon stimulation by still unidentified parasite antigens, DC up-regulate 5-lipoxygenase (5LO), which leads to the production of Lipoxin A4 (LXA4). This eicosanoid links the aryl hydrocarbon receptor (Ahr) that translocates to the nucleus, blocking the production of IL-12 (Aliberti *et al*., 2002; Sanchez *et al*., 2016). This transitory paralysis of DCs that occurs ~ 24 hours PI and lasts for about one week is supposed to give time to the parasite for efficient dissemination, while diminishing the negative effects of a too strong inflammatory response.

Although systemic infection with *T. gondii* triggers a transient increase in activated T $CD4^+$ Th1 cells (see the above paragraph), it was recently shown that it was also correlated with a decrease in the size of the naive $CD4^+$ T lymphocytes pool, destruction of the thymus epithelium and disruption of the thymus architecture, leading to an immunocompromised state that promotes chronic infection (Kugler *et al*., 2016).

Among the mechanisms that dampen the inflammatory response, IL-10 and IL-27 secreted by macrophages, DC, NK cells, B and T cells during both the acute and the chronic phases of infection limit the accessory and adaptive cells responses (Hunter et al., 1994; Moore *et al.,* 2001; Hall *et al*., 2012) (**Figure 3**).

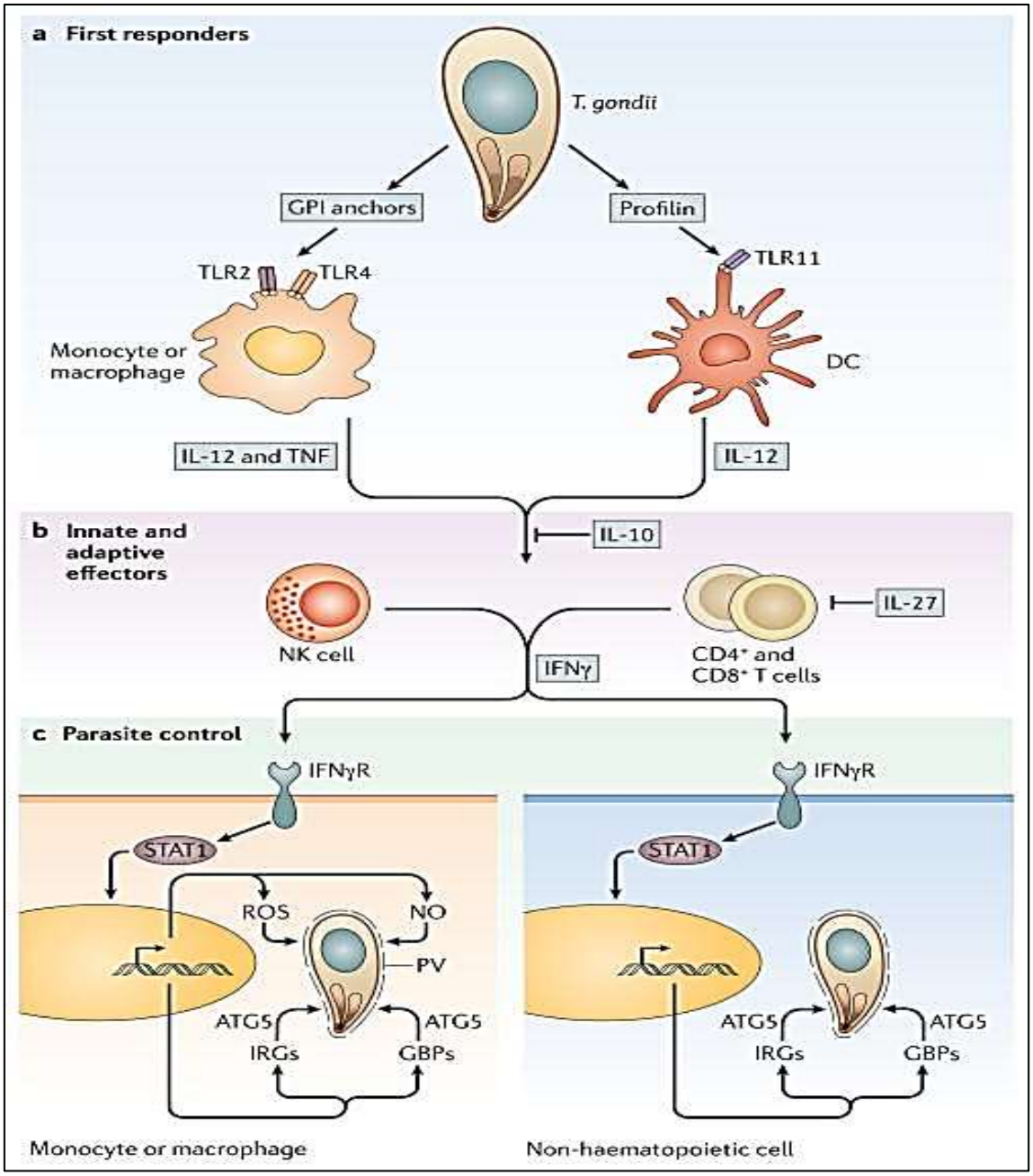

<u>Figure 3.</u> Schematic representation of important steps of the immune response against *T. gondii*
a)Neutrophils (not represented on this scheme), monocytes, macrophages and DC are the first cells to respond to the infection. Recognition of secreted profilin by TLR11 at the surface of DC triggers their production of IL-12. In addition to IL12 monocytes and macrophages also produce TNFα in response to their TLR2 and TLR4 detection of parasite GPI-anchored proteins. **b)** IL-12 and TNFα pro-inflammatory cytokines induce NK cells, $CD4^+$ and $CD8^+$ T cells to produce IFNγ. IL-10 and IL-27 are key cytokines that modulate these major defense pathways and prevent the overproduction of Th1-type cytokines. **c)** The production of IFNγ during the innate and adaptive phases is responsible for activating the cells that control parasite proliferation. Binding of IFNγ to its macrophage surface receptor (IFNγR) activates the STAT1 transcription factor. In response to STAT1, monocytes and macrophages up-regulate their production of NO and ROS, while both mouse hematopoietic

and non-hematopoietic cells up-regulate the two families of intracellular defense proteins (IRG and GBP). The function of IRG and GBP depends on autophagy protein 5 (ATG5). From Hunter and Sibley, 2012

I-4.2) Pathogenicity

Toxoplasmosis is one of the most common parasitic zoonoses worldwide. Epidemiological studies have shown that the prevalence of toxoplasmosis differs between countries, between the regions of a given country and between different communities in a given region. Climate, socio-economic factors, food habits and the age at which infection occurs play important roles in the parasite distribution. Low seroprevalences (10 to 30%) have been observed in North America, South-East Asia, and Northern Europe. Moderate seroprevalences (30 to 50%) have been found in countries of Central and Southern Europe, while high prevalences are common in Latin America and tropical African countries (Robert-Gagneaux and Dardé, 2012).

Toxoplasmosis is usually an asymptomatic- or a paucisymptomatic disease in over 80% of the cases or it leads to mild flu-like symptoms in immune-competent patients. However, it is more serious in immune-compromised patients (Luft and Remington, 1992) or during pregnancy because transmission of tachyzoites to the developing fetus can be devastating, making *T. gondii* a leading cause of congenital neurological birth defects in humans (Swisher *et al*., 1994).

a) Toxoplasmosis in immune-competent patients

The recently acquired infection, which corresponds to the acute phase of infection, is asymptomatic in more than 80% of immune-competent individuals. In some cases, patients may experience fever or cervical lymphadenopathy, sometimes associated with myalgia, asthenia, and various aspecific clinical signs. These symptoms usually resolve spontaneously within a few weeks or within a month at the most (Montoya and Liesenfeld, 2004).

Tissue cysts, typical of the latent infection, are normally well controlled by the immune system. However, recent studies showed that the chronic phase of toxoplasmosis could be linked to the development of mental disorders and, in particular, schizophrenia and bipolar disorders. Schizophrenic patients indeed display an increased prevalence of specific antibodies against *T. gondii* (Torrey *et al*., 2007; Mortensen *et al.,* 2007; de Barros *et al*., 2017).

The severity of infection is also related to the genotype of the infecting parasite strain. As stated above, the low prevalence and the low severity of infection in North America and Europe is correlated with type II strains. The strains present in South America usually lead to more severe infections. Acquisition of toxoplasmosis during childhood or adulthood in Brazil was for example shown to account for high levels of visual impairment and toxoplasmosis is a leading cause of blindness in South America (De Boer *et al*., 2003). Recently, new “atypical” strains, which caused lethal infections in immune-competent individuals, were isolated in French Guiana. During these infections, the subjects

developed fatal pneumonitis, myocarditis, meningo-encephalitis, or polymyositis (inflammatory myopathies) (Carme *et al*., 2002; Robert-Gagneaux and Dardé, 2012).

b) Toxoplasmosis in immune-compromised patients

The host immune background is of prime importance to restrict and control the infection by *T*. *gondii*. Various factors impair the protective cellular immune response such as HIV infection, immunosuppressive therapies administered in the context of haematopoietic stem cells- (HSCT) or solid organ transplant, or a therapy against cancer.

In immune-compromised patients who had been infected before their immune-depression, toxoplasmosis is life-threatening, resulting in the rupture of brain cysts and reactivation of the latent disease: bradyzoites present in the central nervous system (CNS) indeed reverse to tachyzoites, which cause severe encephalitis that can be fatal if not treated in time. In HIV-infected patients toxoplasmic encephalitis (TE) is the predominant manifestation of the disease, while pulmonary or disseminated toxoplasmosis are more characteristic of transplant patients (Robert-Gagneaux and Dardé, 2012).

In the case of solid organ transplanted patients, toxoplasmosis occurs when the transplanted organ is from a *Toxoplasma*-seropositive donor and the immunosuppressive therapy is at its maximum. The *Toxoplasma*-seronegative recipient is then exposed for the first time to the parasite, and develops a severe primary infection. By contrast, for HSCT patients, the highest risk is that of reactivation of the infection that occurred prior to the transplantation. To prevent the infection, serological screening of both donors and recipients is necessary to identify the potential risks of toxoplasmosis (Derouin and Pelloux, 2008).

c) Congenital toxoplasmosis

Congenital infection results from the transmission of tachyzoites to a fetus consecutively to the primary infection of the mother-to-be. The frequency of vertical transmission and the severity of fetal damages depend on the stage of pregnancy, when maternal infection occurs. The placenta is indeed an efficient barrier at the beginning of the gestation, *i.e*. during the first trimester, efficiently limiting the passage of parasites, while its permeability increases over the course of pregnancy. The rate of transmission rises to 30-50% in pregnant women infected during their second trimester and reaches 60-70% in women infected during their third trimester of pregnancy. Conversely, the severity of fetal infection is inversely proportional: the clinical manifestations of congenital toxoplasmosis are more severe when the infection is acquired at the beginning of the gestation. In these cases, the CNS is commonly affected causing encephalomyelitis, which can lead to fetal death (Hampton, 2015). Congenital infections also constitute important veterinary problems, as they are responsible for a high percentage of spontaneous abortions in sheep breeding (Buxton, 1998).

I-5 DIAGNOSIS, TREATMENTS AND VACCINES

I-5.1) The diagnosis of toxoplasmosis

To date, a serious issue of *T. gondii* infection still remains congenital toxoplasmosis. This is why systematic screening of toxoplasmosis is commonly performed in pregnant women in various countries of Western and central Europe, *i.e.* France, Austria, Slovenia, Belgium, Italy, Germany and Spain. The diagnosis can be performed using various biological methods (tissue histology, PCR, serology), but the diagnosis techniques performed in routine are serological tests (automated or semi-automated immunoassays most of the time; Villard *et al*., 2016). Serology allows the detection of *Toxoplasma*-specific IgM and IgG antibodies. High levels of IgM antibodies characterize the acute phase of infection, while IgG are the signature of a more ancient infection. Because IgM can persist for years in some cases, dating the infection relies now on the determination of IgG avidity, which is low at the beginning of infection and increases as the infection becomes more ancient (Hill and Dubey, 2002).

I-5.2) Treatments available against toxoplasmosis

The common treatment against toxoplasmosis is a combination of pyrimethamine (inhibitor of the dihydrofolate reductase enzyme, DHFR) and sulfonamide (inhibitor of dihydropteroate synthase), administered with folinic acid (leucovorin). Since the parasite synthesizes folates *de novo* (unlike its mammalian host, it is unable to use preformed dietary folates), the combination of pyrimethamine-sulfonamide aims at blocking the biosynthesis of parasite folate, thus its nucleic acids and consequently, parasite replication, while leucovorin is used to decrease the toxic effects of pyrimethamine (Katlama *et al.,* 1996). However, there are limitations to the use of this drug combination:

i) the drugs, in particular sulfonamides, are not always well tolerated and they generate important secondary effects. Other molecules such as clindamycin (lincosamide antibiotic that binds to the 50s ribosomal subunit of bacteria and thus targets the protozoan mitochondrion) can be used as alternative treatments to the combination of sulfonamide-pyrimethamine. Atovaquone (hydroxy-1,4-naphthoquinone; structural toxic analog of Protozoa ubiquinone - coenzyme Q - and thus inhibitor of the mitochondrial electron transport system, thus resulting in a default of the biosynthesis of pyrimidines) is another possible drug in patients unable to tolerate sulfonamides and clindamycin (Oz, 2014);

ii) the teratogenic effect of pyrimethamine prevents its use in pregnant women, for whom a single molecule, spiramycin, has received the agreement and can be administered to

reduce the parasite transmission. However, spiramycin has no effect on the severity of the disease in an already infected fetus;

iii) importantly, even if the combination pyrimethamine-sulfonamides/leucovorin targets efficiently proliferating tachyzoites during the acute phase of infection, it remains useless against the tissue cysts that are characteristic of the latent infection. Only atovaquone was shown to reduce the number of brain cysts in infected hamsters (Gormley *et al*., 1998).

Studies performed on the metabolic activity of the apicoplast showed that some herbicides or their enzymatic analogs could become efficient anti-parasitic drugs (Bisanz *et al*., 2006; Nagamune *et al*., 2008; Endeshaw *et al*., 2010).

I-5.3) Vaccines against toxoplasmosis

a) Available vaccine against sheep congenital toxoplasmosis

Only a few vaccines against veterinary protozoan diseases, among which the commercial "Ovilis Toxovax" (Intervet), have been developed with success. Used against congenital toxoplasmosis in sheep, "Ovilis Toxovax" consists in an injectable suspension of attenuated parasites of the strain S48, which was was originally isolated from a case of ovine abortion in New Zealand. Following approximately 3,000 passages in mice, this strain lost its ability to differentiate into tissue cysts in mice and into oocysts in cats (Buxton and Innes, 1995; Innes *et al*., 2009) and it is thus used to prevent abortions due to toxoplasmosis in sheep. This kind of live vaccine cannot be used in humans because of its high risk of parasite reactivation.

b) Development of a vaccine against human toxoplasmosis

To be protective, a vaccine has to stimulate both the humoral- and the cellular immune responses, which is difficult to achieve with sub-unit- or inactivated vaccines. Conversely, even if live vaccines are more efficacious, they present high risks of reactivation and are not easy to use because of their short shelf-life and the precautions that must be taken to preserve their efficacy.

No vaccine is currently available against human toxoplasmosis and the development of an efficacious vaccine remains a priority.

Two main classes of antigens are considered as potential vaccine candidates:

i) surface antigens and in particular, the tachyzoite major surface antigen, SAG1 (Wu *et al.,* 2012; Dziadek *et al.,* 2012);

ii) Excretory-Secretory Antigens (ESAs), which represent 90% of the circulating antigens and are highly immunogenic. The production of monoclonal antibodies against ESAs showed that dense granule proteins (GRA) constitute major components of these ESAs. Many of these GRA were described as constituting potential vaccine candidates (Golkar

et al., 2007; Jongert *et al.,* 2008; Hiszczynska-Sawicka *et al.,* 2011; Min *et al.,* 2012; Ching *et al*., 2016).

The recent studies related to vaccine development proposed multi-epitope DNA vaccines composed of $CD8^+$ T cell-elliciting- and $CD4^+$ helper T lymphocyte epitope(s) administered with lipid adjuvant (El Bissati *et al*., 2016), coated with calcium phosphate nanoparticles (Rahimi *et al*., 2017) or recombinant proteins formulated in Poly (DL-lactide-co-glycolide microspheres (Allahyari *et al*., 2016), or virus-like particles (VLPs) (Lee *et al*., 2016) to increase both the cellular and humoral responses and consequently induce a higher protection in animal models.

Interestingly, vaccination of mice bearing highly aggressive ovarian cancer with a safe, non-replicating, non-cyst forming vaccine strain of *T*. *gondii* (type I uracil auxotrophic mutant) was shown to effectively reverse tumor-associated immune suppression and activate potent anti-tumor immunity (Baird *et al*., 2013). This attenuated parasite strain was also shown to stimulate immunity to pancreatic cancer (Sanders *et al*., 2015). Thus, the use of knocked-out Toxoplasma parasites could represent an interesting strategy to develop vaccines against some cancers. Recently, the anti-tumor response against established ovarian cancer was shown to be dependent on proteins secreted by the parasite before- or at the time of invasion (respectively, ROP and GRA proteins, see chapters III and IV) (Fox *et al*., 2016).

CHAPTER II
TOXOPLASMA GONDII:
INVASION AND EARLY STEPS OF THE PARASITOPHOROUS VACUOLE FORMATION

Toxoplasma gondii is an obligate intracellular pathogen that infects any kind of nucleated cell. The host cell invasion is an active mechanism, which leads to the formation of a PV, an intracellular compartment in which the parasite resides safely and replicates.
After a brief introduction on the organelles that can be found in a tachyzoite cell, I will focus on the invasion process and the early steps of this PV formation.

II-1 SUB-CELLULAR ORGANIZATION OF THE TOXOPLASMA TACHYZOITE

The tachyzoite is the parasite invasive stage that disseminates during the acute stage of infection in both intermediate and definitive hosts. The tachyzoite is a crescent-shaped cell (approximately 7 x 2 μm), with a slightly pointed anterior end important for cell motility, and a rounded posterior end. The tachyzoite is a eukaryotic cell, with typical organelles of a eukaryotic cell (a nucleus, a Golgi apparatus, an endoplasmic reticulum (ER), a plant-like vacuole and ribosomes), but it is also organized in a unique manner, comprising: *i)* an unusual cytoskeleton composed of sub-pellicular microtubules and intermediate filaments as well as a conoid; *ii)* endosymbiosis-derived organelles (one mitochondrion and one non-photosynthetic apicoplast); *iii)* three types of Apicomplexa-specific secretory organelles (micronemes, rhoptries, and dense granules (DG)). The conoid as well as the micronemes and the rhoptries define the apical complex of the parasite, which is crucial to invasion; *iv)* acidocalcisomes, which constitute calcium storage compartments, all these organelles being enclosed in a membranous complex named the pellicle (60 nm wide) (**Figure 4**). It is composed of an outer membrane, the plasmalemna (plasma membrane), and the inner membrane complex (IMC) (Vivier and Petitprez, 1969). The parasite plasma membrane (PPM) displays a micropore located in the apical part of the cell, anterior to the nucleus. This microprore consists in a circular invagination of the PPM and might be involved in endocytosis (Nichols *et al.*, 1994). The IMC consists in fused plates formed by flattened vesicles derived from the ER-Golgi system (Vivier and Petitprez, 1969). The IMC covers the whole periphery of the parasite and is interrupted only at *i)* the apical part to give space to the conoid, *ii)* the rounded posterior part of the cell, and *iii)* the micropore. The IMC is strictly associated with *i)* 22 sub-pellicular microtubules which run from the post-conoidal ring to two thirds of the parasite length, and *ii)* a network of intermediate filaments (8-10 nm) that extend from the anterior- to the posterior part of the parasite. The sub-pellicular microtubules and this network of intermediate filaments play a role

in determining the cell polarity and the parasite shape. They are also involved in cell motility or "gliding" (see paragraph II) (Morissette and Sibley, 2002).

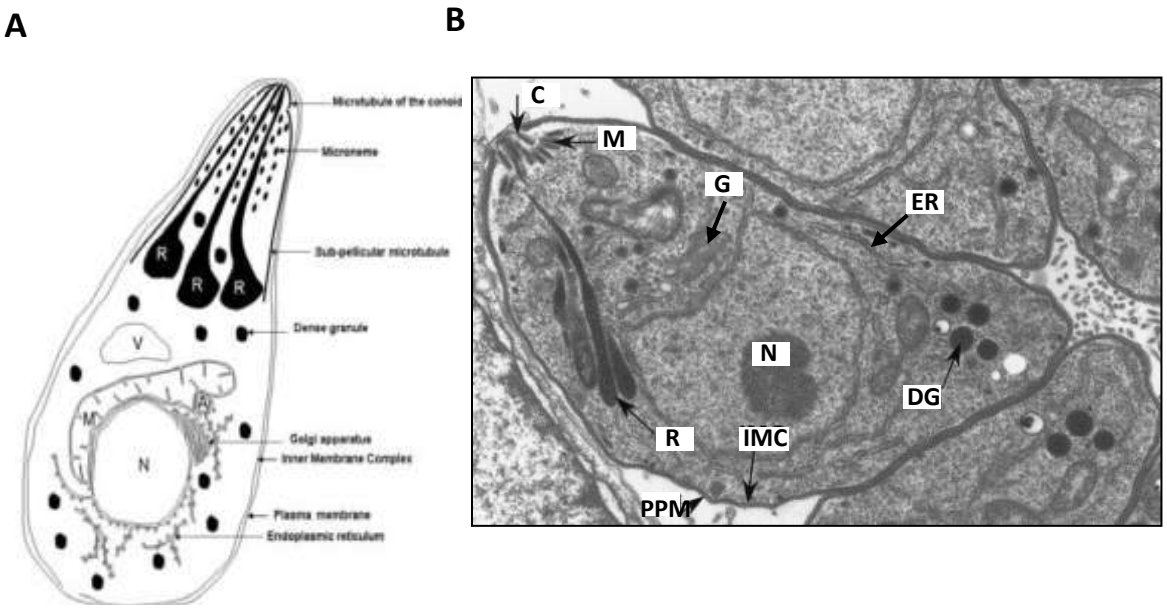

Figure 4. Ultrastructure of a Toxoplasma tachyzoite cell.
A- Schematic representation of a *Toxoplama gondii* tachyzoite. A, apicoplast; M, mitochondrion; N, nucleus; R, rhoptry; V, vacuole. From Mercier *et al*., 2012. **B-** *Toxoplasma gondii* ultrastructure as observed by Transmission Electron Microscopy (TEM). The pellicle is formed by the inner membrane complex (IMC) and the parasite plasma membrane (PPM). C, conoid, M, micronemes; G, Golgi apparatus; R, rhoptries; ER, endoplasmic reticulum; DG, dense granules; N, nucleus. Adapted from Dubremetz, 1998.

Host cell invasion by *T. gondii* differs from the phagocytosis- and endocytosis processes, which are typical of other intracellular pathogens*, e.g.* viruses, bacteria or parasites such as *Trypanosoma cruzi* (Weissenhorn *et al.,* 2007; Fernandes and Andrews, 2012; Cossart and Helenius, 2014; Ribet and Cossart, 2015; Pizarro-Cerdá *et al*., 2016). Toxopalsma invasion is indeed a rapid and active process: in less than 20 seconds the parasite mobilizes its apical cytoskeleton and its secretory organelles to invade the cell and form its PV. This particular mechanism of "active invasion" thus contrasts with the zipper- or trigger-mechanisms of invasion used by bacteria, endocytosis of enveloped viruses or the subversion of plasma membrane injury repair mechanism used by *T. cruzi*.
Entry into the host cell by Toxoplasma consists in several sequential steps initiated by weak attachment of the parasite to the cell surface *via* its surface proteins, followed by the release of proteins from the micronemes (**Figure 4**) and the rhoptries (**Figure 4**). Some of the microneme protein complexes contribute to host cell attachment and provide a physical link between host cell receptors and the parasite actin-myosin motor, thus providing the force necessary for host cell invasion. The proteins from the upper part of the rhoptries (called the "neck" of the rhoptries), together with particular microneme proteins, are more particularly involved in the formation of a moving junction

(MJ) involved in *i)* the selection of the host cell proteins that are integrated into what will constitute the PVM and *ii)* the firm anchorage of the PV to the host cell cytoskeleton (**Figure 5**). I will briefly review below these early steps that lead to the formation of the PV, which will also give me the opportunity to describe the parasite organelles involved in this process.

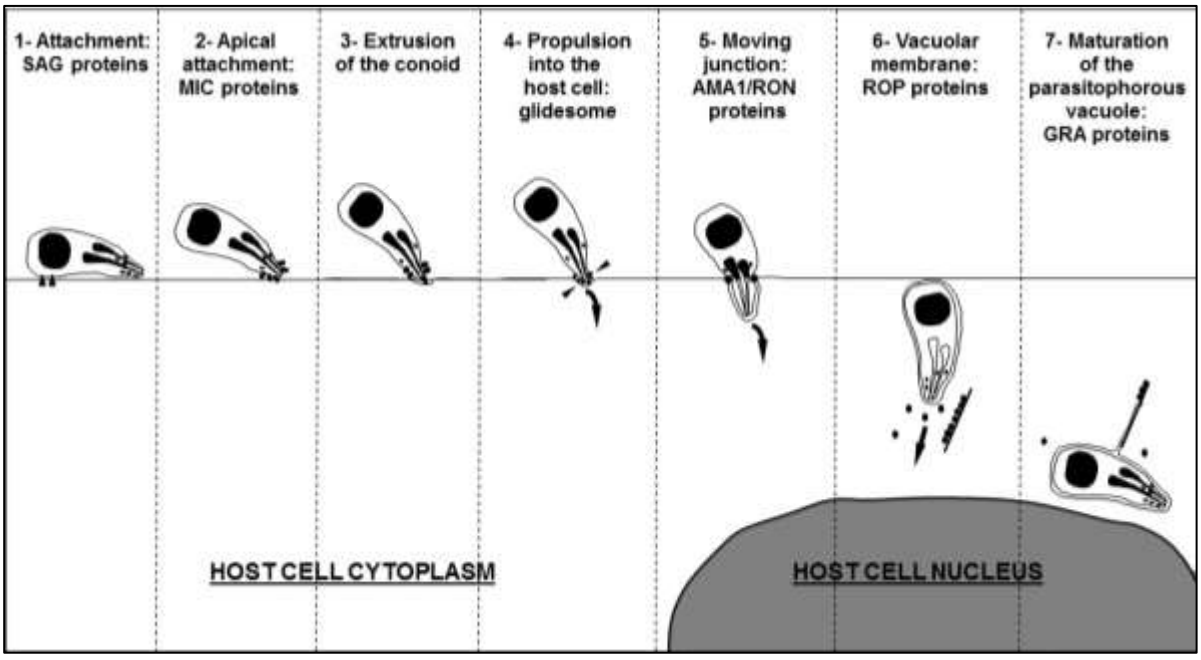

Figure 5. Step-wise invasion process of *T. gondii* into the host cell
Consecutively to weak, non-orientated attachment to the host cell *via* its surface proteins (SAG), Toxoplasma re-orientates and presents its apical tip to the host cell surface. The microneme proteins (MIC adhesins) secreted from the apical part allow weak attachment to host cell glycoaminoglycans (GAGs). Following ***i)*** extrusion of its conoid to probe the surface of the host cell and define the most favorable region for invasion and ***ii)*** mobilization of its glideosome, the parasite secretes the proteins contained in the neck of its rhoptries. In conjunction with microneme proteins such as AMA1, these RON proteins form a moving junction that progresses along the parasite in the same time as the parasite does push forward into the host cell and incurves the host cell plasma membrane. This moving junction is responsible for the selection of the host proteins that are integrated into the PVM and the firm anchorage of the PV to the host cell cytoskeleton. Once the PVM has enclosed the parasite, the proteins secreted from the basis of the rhoptries (ROP) contribute to the remodeling of the PVM, while proteins secreted from the dense granules (GRA) allow the PV to become functional. In the mean time reprogramming of the host cell expression program is ensured by both rhoptry and dense granule-like proteins. Adapted from Mercier and Cesbron-Delauw, 2012.

II-2 LOOSE, NON-ORIENTATED ATTACHMENT TO THE HOST CELL SURFACE: THE SAG PROTEINS

The plasma membrane is covered by ˜ 200 types of GPI-anchored proteins also called surface antigens (SAG) and SAG1-related Sequences (SRS) (He *et al*., 2002). Among these SAG and SRS, SAG1 is the most abundant protein (and the first one described). During the very early step of host cell invasion, the positive charges that are included in the top groove formed by SAG dimers establish weak interactions with the negative charges of the host cell surface glycosaminoglycans (GAGs) (Naguleswaran *et al.,* 2003), thus ensuring low affinity, non-orientated attachment of the parasite to the host cell (He *et al*., 2002; Boulanger *et al*., 2010). The diversity in SAG proteins could explain why Toxoplasma recognizes a large variety of GAGs and is thus capable of invading any kind of nucleated cell.

II-3 APICAL ATTACHMENT: ROLE OF THE MICRONEME PROTEINS

Fifty to 100 micronemes (250 nm x 50 nm) (**Figure 4**) are present at the apical tip of each invasive cell. Because they are closely associated with the cytoplasmic face of the IMC, they appear as an arc at the anterior part of the parasite.

II-3.1) Microneme proteins and their secretion

Various proteins have been identified within the micronemes, among which, MIC1-12, M2AP (MIC2-Associated Protein), AMA1 (Apical Membrane Antigen 1), and proteases such as SUB-1 (Subtilase 1) or ROM1 (Rhomboid-1) (Cowper *et al*., 2012; Dowse and Soldati, 2005). Among the MIC proteins one can distinguish transmembrane- from soluble proteins.
Three major complexes have been described as being involved in the attachment to host cells. The transmembrane proteins MIC2, MIC6 and MIC8 contain one single transmembrane α-helix in their C-terminal region that allows the anchorage of the protein in the PPM. Furthermore, both MIC2 and MIC6 play the role of escorters for their respective associated soluble MICs (M2AP in the case of MIC2 or MIC1 and MIC4 in the case of MIC6) to target them to the micronemes (Meissner *et al*., 2002).
Microneme proteins display numerous, frequently repeated, adhesive domains homologous to those found in higher eukaryotic cells, as exemplified for some of the MIC represented on **Figure 6**. Most of the MIC proteins, such as the essential protein MIC2, are indeed adhesins which are secreted from the apical part of the parasite during the early invasion process and which are involved in recognition of- and attachment to the host cell (Keeley and Soldati, 2004), as developed below.

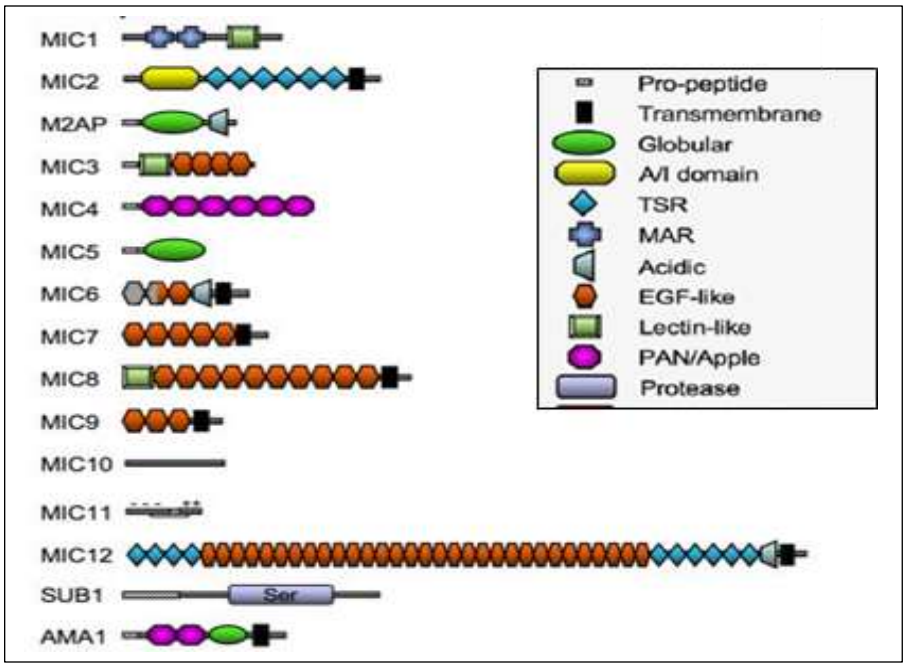

Figure 6. Schematic representation of some Toxoplasma MIC proteins and their different domains.
TSR: Thrombospondin-1 type 1 domain; MAR: Microneme Adhesive Repeat; EGF: Epidermal Growth Factor; PAN/Apple: Plasminogen apple. Adapted from Carruthers and Tomley, 2008.

Recent studies on the signaling pathways that regulate microneme secretion showed that it is *i)* induced by exposure to a single host agonist protein, *i.e.* serum albumin, *ii)* centrally controlled in a protein kinase G-dependent manner that correlates with increased cGMP levels, and *iii)* that this pathway is further augmented by elevation of intracellular Ca^{2+} (Brown *et al*., 2016). Recent observations are consistent with a mechanism of calmodulin (TgCaM)-based recruitment and activation of cytoplasmic Ca^{2+}-regulated phosphatase calcineurin for calcium-based signaling within the apical complex of the parasite (Paul *et al*., 2015). In addition, increased extracellular kalium level triggers a signaling cascade, which leads to the interconversion of diacylglycerol (DAG) to phosphatidic acid (PA). An acylated pleckstrin-homology (PH) domain-containing protein (APH) identified on the microneme surface was shown to sense PA during microneme secretion and to be necessary for microneme exocytosis (Bullen *et al*., 2016). The fusion event between micronemes and the PPM was shown to involve the SNARE-like protein DOC2.1 (Farrell *et al*., 2012).

II-3.2) Weak attachment to host cell receptors by microneme proteins

Recent studies have shown that the microneme proteins secreted at the surface of the parasite recognize carbohydrate motifs, which decorate the surface of host cells. For example, following its secretion onto the parasite surface, the microneme adhesive repeat region (MARR) located in the N-

terminal region of TgMIC1 was shown to recognize a wide range of sialylated glycans on host cell receptors (Garnett *et al*., 2009). Furthermore, carbohydrate microarrays revealed the basis of the interaction between TgMIC4 and a variety of galactose (Gal)-terminating oligosaccharides at the surface of host cells (Marchant *et al*., 2012).

Following exocytosis microneme adhesins undergo proteolytic processing by 3 types of proteases, termed respectively microneme protein protease 1 (MPP1), MPP2, and MPP3. MPP1 is responsible for the intramembrane cleavage of the transmembrane adhesins MIC2, MIC6, and AMA1, resulting in the shedding of their extracellular domains into the supernatant (Carruthers *et al*., 2000; Opitz *et al*., 2002). MPP1 activity depends on ROM proteases, which are membrane-spanning serine proteases that display the unique characteristic of cleaving their substrates within their transmembrane domains. ROM4, which plays a critical role in cleaving adhesins within their transmembrane segment, allows the parasite to disengage from its host cell receptors and completely enter the host cell (Shen *et al*., 2014).

II-4 EXTRUSION OF THE CONOID

At this point the parasite re-orientates itself to present its apical part to the host cell surface and it extrudes its conoid (400 nm in diameter at its base and 250 nm high) (**Figure 7**), which is made of 10 to 14 curved tubulin sheets that form a hollow cone at the apical part of the parasite (Hu *et al*., 2002). Two apical rings limit the upper part of the conoid, just beneath the plasma membrane at the apical tip of the parasite. Two polar rings limit the basis of the conoid. The outer polar ring, made of dense material, covers the interior part of the IMC, while the inner ring anchors the 22 sub-pellicular microtubules that provide the scaffold which shapes the parasite. Within the conoid a pair of adjacent microtubules extends for 1 µm into the cytoplasm from an apical vesicle that adheres to the plasma membrane (Hu *et al.,* 2002b) (**Figure 7**).

The conoid is a structure that plays a pivotal mechanical role during the invasion process because it can extend (the exact term being “extrude”) in a Ca^{2+} dependent-manner (Del Carmen *et al*., 2009) and retract repeatedly and, by pressing on the host plasma membrane, it creates the first mechanical push that leads to the PV formation.

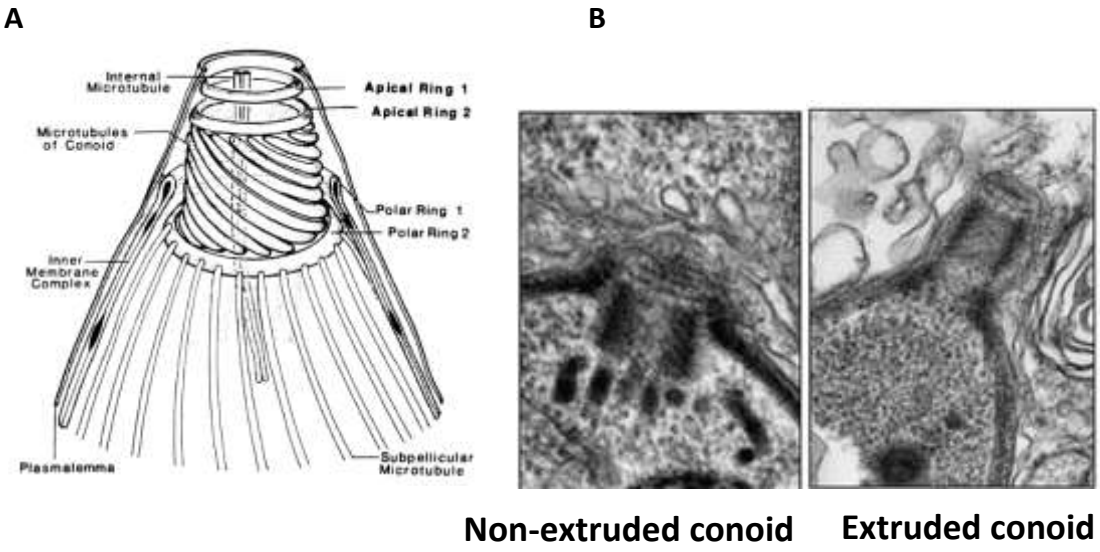

Figure 7. The conoid of *Toxoplasma gondii*
A- Schematic representation of the conoid. From Dubey *et al.,* 1998. **B-** Electron microscopy micrograph of a non-extruded (left panel) *versus* extruded conoid (right panel). Adapted from Graindorge *et al.,* 2016.

II-5 PROPULSION INTO THE HOST CELL: MOBILIZATION OF THE GLIDEOSOME

Toxoplasma parasites do not exhibit specialized motility structures such as cilia or a flagellum. Nonetheless, they are highly motile: they are able to move on an artificial substrate (such as a glass slide coated with proteins) or a cell surface by a specific type of movement dubbed "gliding", which relies on the anterior-posterior polarity of the parasite (**Figure 8A**). Gliding consists in a succession of several stereotyped movements: *i)* circular gliding (1.5 µm/s); *ii)* upright twirling, which consists in a 360° rotation, when the parasite posterior part is attached to a substrate (0.5 rotation/s); and *iii)* helical rotations (1-3 µm/s) (Hakansson *et al.*, 1999) (**Figure 8A**). The gliding movements, when occurring on a glass slide coated with proteins to ensure parasite attachment, lead to the shedding of components from the PPM, including surface proteins such as SAG1 (Hakansson *et al.*, 1999; Sibley, 2003).

Gliding as well as invasion and egress from infected cells are powered by rearward translocation of apically secreted transmembrane adhesins *via* their interaction with the parasite actin-myosin motor, which is coupled to glideosome-associated proteins (GAPs), the whole complex (actin-myosin associated with GAPs) forming the glideosome invasion machinery, which is located cortically between the PPM and the IMC (Keely and Soldati, 2004), and whose molecular composition varies according to the anterior-posterior axis of the parasite (Boucher and Bosch, 2015). Specifically, the forward movement, whatever the level in the anterior-posterior axis, is powered by a class XIV neck-less myosin molecular motor (Myo A or Myo C), which progresses on short (100 nm long) and-

unstable actin filaments located between the PPM and the external face of the IMC (**Figure 8B**). Mobilization of this driving force relies initially on the bridging of transmembrane adhesins such as TgMIC2 or TgMIC6 to their respective (unidentified) host cell receptors, followed by the transduction of this binding signal across the PPM to actin *via* the transmembrane adhesin. Myosin which progresses along actin filaments, then relays the binding signal to the sub-pellicular microtubules located in the parasite cytoplasm, *via* the glideosome complex constituted of Myosin-Light Chain (MLC-1), and several GAPs (**Figure 8B**).

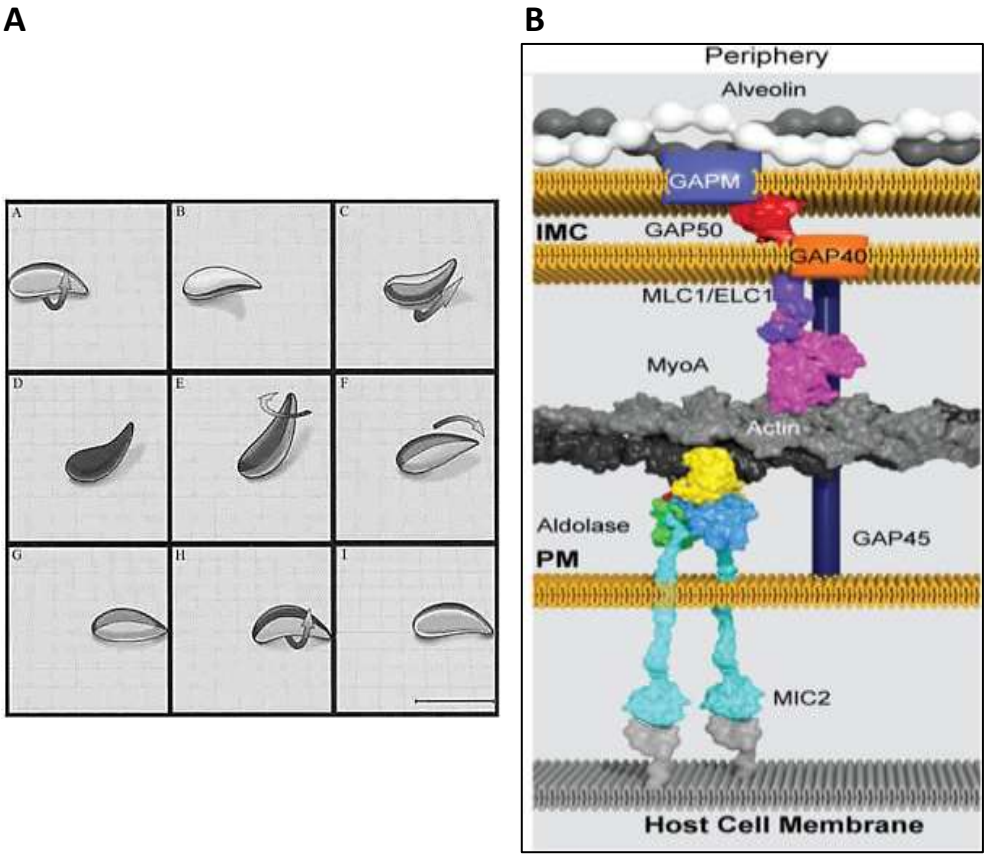

Figure 8. **Propulsion into the host cell by mobilization of the glideosome**
A-Scheme of Toxoplasma helical rotations. From Hakansson *et al*., 1999. **B-** Schematic representation of the Toxoplasma invasion machinery. The actin-myosin motor (grey/black and magenta) is bridged by tetrameric aldolase (multicolor) to the extracellular adhesins MIC2 or MIC6 (cyan), which connect to unknown cellular receptors on the host cell membrane (grey). The motor is anchored to the IMC *via* its interaction with MTIP MLC1/ELC1 (purple). The myosin-MLC1 motor interacts with a GAP protein that spans the space comprised between the PPM and IMC membranes. These motor complexes interact with GAP40 (orange) and GAP50 (red) located in the IMC. GAPMs (blue) are located on the cytosolic side of the IMC membrane and interact with alveolins (white/grey). From Boucher and Bosch, 2015

Although the above described model of active invasion powered by a parasite actin-dependent myosin motor defines the prevailing mechanism for Toxoplasma entry into its host cells (Drewry and Sibley, 2015), an alternative mechanism has been recently described. Since parasites deficient in MyoA remain invasive and are still capable of gliding (Egarter *et al.,*2014; Bichet *et al.,* 2016), other mechanisms that could allow parasite motility and invasion have been proposed: *i)* a model based on osmotic forces generated in the parasite cytosol that could be converted into motility or *ii)* the host cell membrane dynamics could contribute energetically to parasite invasion (Egarter *et al.,* 2014; Bichet *et al.,* 2016). Note also that the actin-myosin system of the parasite was recently reported to function in attachment of the parasite to the surface substrate, and not necessarily as force generator (Whitelaw *et al*., 2017).

II-6 FORMATION OF THE MOVING JUNCTION (MJ): COLLABORATION BETWEEN MIC AND RON PROTEINS

Each Toxoplasma cell contains 6-12 rhoptries in their apical part (**Figure 4**). These rather long, club-shaped organelles (2 x 0.2 µm) exhibit a bulbous base and an extended electron-dense duct, which opens to the apical membrane. Rhoptries were shown to contain both proteins (respectively ROP proteins in their bulbous part, and RON proteins in their neck) and lipids. Rhoptries constitute the most acidic organelles in the parasite and they contain for example specialized hydrolases, which are typical of lysosomes (Que *et al.,* 2002; Ngo *et al.,* 2004).

At the time of secretion from the micronemes the area located between the extended conoid and the cell surface forms a depression in the host cell membrane. This depression called the Moving Junction (MJ) (**Figure 9A**), moves as a circumferential ring at the penetration site. The MJ does not correspond to a region of fusion between the host cell membrane and the PPM. It is instead constituted by a tight apposition (< 6 nm) between both membranes and it was shown to be crucial for the self-propulsion of the parasite into the host cell (Aikawa *et al.,* 1978).

Contrary to the other microneme proteins, TgAMA1 is not implicated in the first step of invasion (*i.e.* recognition of host cell receptors) but, with the protein complex from the rhoptries' neck RON2/RON4/RON5/RON8, it contributes to the formation of the MJ (Carruthers and Boothroyd, 2007). TgAMA1, which starts being secreted onto the parasite surface during gliding, accumulates upon re-orientation of the parasite. TgAMA1 was described as a transmembrane protein of the PPM. Interestingly transmembrane RON2 in complex with the soluble complex RON4/RON5/RON8 was shown to be secreted into the host cell, RON2 spanning the host cell plasma membrane, while RON4/RON5/RON8 interact with the RON2 N-terminal region, which is exposed in the host cell cytoplasm (Alexander *et al.,* 2005; Besteiro *et al.,* 2009; Straub *et al.,* 2009, 2011). Reorganization of

host cell actin at the MJ site caused by the activation of the Arp2/3 complex (a conserved actin nucleator abundantly recruited at sites of dynamic actin remodeling, and essential for the formation of many F-actin-based structures) was shown to be linked to the presence of RON8 in the host cell cytoplasm (Gonzales *et al.,* 2009; Chabra and Higgs, 2007)

In conclusion, the molecular interaction between the N-terminal region of TgAMA1 with the C-terminal region of TgRON2 allows *i)* a close apposition between the PPM and the host cell membrane, *ii)* firm attachment of the parasite to the host cell and *iii)* the constitution of a molecular sieve that prevents both the multi-pass transmembrane proteins and the protein complexes from the host cell plasma membrane to be internalized into the forming PVM (**Figure 9B**). In particular, the resulting PVM lacks proteins involved in the regulation of endosomal fusion. This phenomenon explains why the PV remains an isolated organelle, which does not fuse with host endosomes or lysosomes. Once the parasite entry is complete the MJ closes at the posterior end of the parasite and the host cell plasma membrane reseals, finally liberating the PVM enclosing the parasite into the host cell cytoplasm (Aikawa *et al.,* 1978; Lebrun *et al.,* 2005).

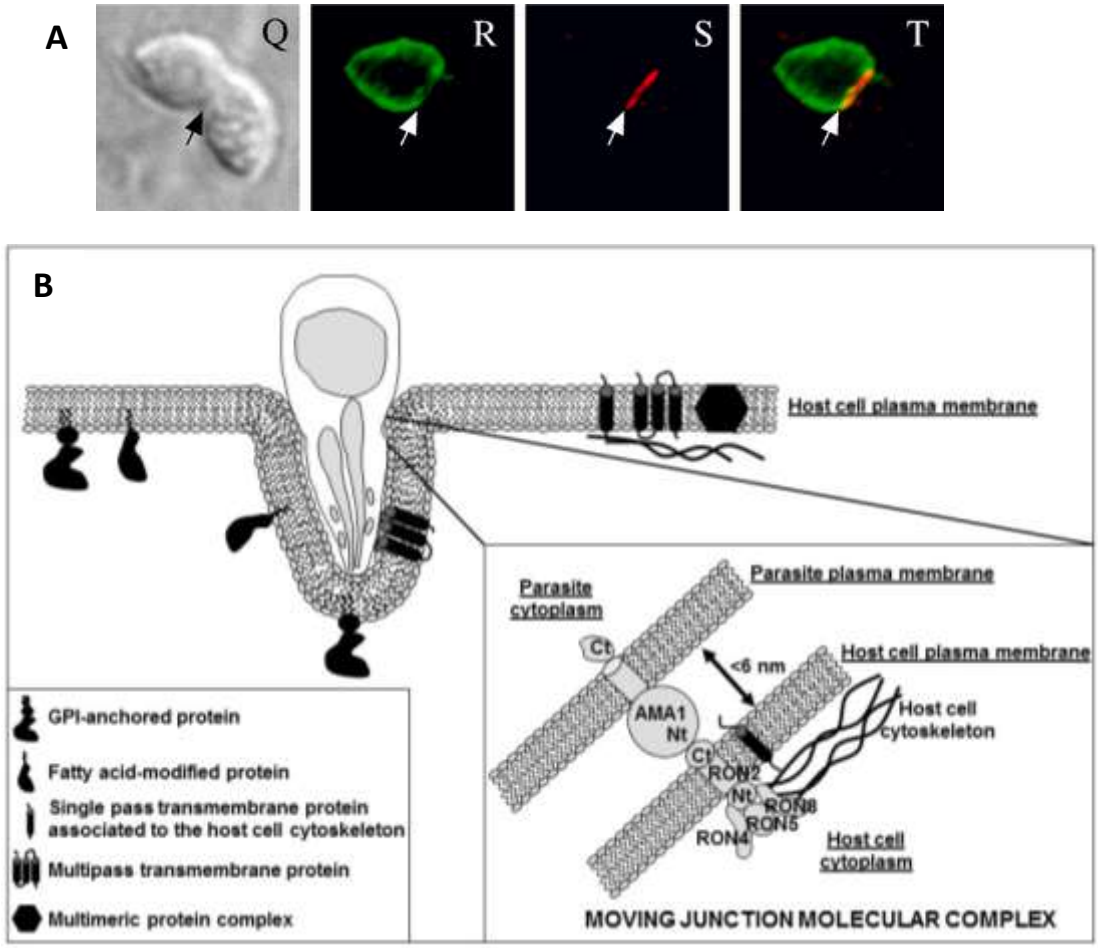

Figure 9. The moving junction of *Toxoplasma gondii*
A-Immunofluorescence labeling of RON4 (red) at the moving junction (indicated by the arrow) during parasite invasion. The labeling of SAG1 (green) indicates the part of the parasite that remains outside the host cell. Adapted from Alexander *et al.,* 2005. **B-**Schematic representation of the AMA1/RON2/RON4/RON5/RON8 protein complex that forms the Toxoplasma moving junction. The microneme protein AMA1, which remains anchored in the parasite plasma membrane interacts by its N-terminal region with the C-terminal region of RON2, which has been secreted from the rhoptry neck into the host cell plasma membrane. The soluble complex RON4/RON5/RON8 also secreted from the rhoptry neck into the host cell cytoplasm, interacts with the RON2 C-terminal region and with the host cell cytoskeleton *via* RON8, thus firmly anchoring the AMA1/RON2 complex to the host cell. Except from firmly anchoring the parasite to its host cell, the moving junction also plays a crucial role as a molecular sieve to prevent host cell multi-pass transmembrane proteins and protein complexes from the host cell plasma membrane to be integrated into what will constitute the parasitophorous vacuole membrane. Adapted from Mercier and Cesbron-Delauw, 2012

Other RON proteins have been described in the rhoptries' neck, among which the high molecular weight hetero-complex RON9/RON10 (Lamarque *et al.*, 2012). In contrast to RON10, in which no particular domain was identified, RON9 was found to contain a Sushi domain composed of *i)* a

repetition of ankyrin motifs involved in protein-protein interactions and *ii)* a set of repetitions enriched in proline (P), glutamic acid (D), aspartic acid (E), and serine (S) or threonine (T) (PEST sequences), which are targets for rapid degradation. Although depletion in RON9 or RON10 leads to loss of the entire complex, no defects in *in vitro* parasite intracellular development nor in parasite virulence were described (Lamarque *et al.*, 2012), indicating that the RON9/RON10 protein complex is not involved in the MJ formation.

II-7 PROTEINS FROM THE RHOPTRIES' BULB AND FORMATION OF THE PARASITOPHOROUS VACUOLE

Rhoptries contain both lipids (cholesterol as well as phospholipids) and proteins. However, thin-layer chromatographies (TLC) and enzymatic assays on rhoptry-enriched fractions showed that the major components of rhoptries are proteins and cholesterol: the lipid to protein ratio is 0.26 and the cholesterol to phospholipids ratio is >1 (Foussard *et al.,* 1991). It has been suggested that, at the time of invasion, secretion of lipids from the rhoptries may facilitate the PVM formation (Foussard *et al.,* 1991). However, further analyses showed that cholesterol is already present in this membrane at the time of invasion and that parasites depleted in 16 to 23% of their cholesterol are still capable of invasion (Coppens and Joiner, 2003). Re-evaluation of rhoptry lipids, by high pressure liquid chromatography (HPLC) and capillary gas-liquid chromatography (GLC) confirmed that rhoptries display a low content in cholesterol (Besteiro *et al.,* 2008). Together, these findings suggested that the cholesterol present in the PVM largely derives from the host cell rather than from the parasite.
The first identification of rhoptry proteins was based on sub-cellular fractionation and generation of monoclonal antibodies. More recently, proteomic analyses on purified rhoptries allowed the characterization of 38 other tachyzoite proteins localized either in the bulb- or in the neck of the rhoptries (Bradley *et al.*, 2005). All these proteins contain a signal peptide and many of them present a transmembrane domain or a GPI anchor, suggesting their association with membranes.
Among these rhoptry proteins, toxofilin (27 kDa) is involved in the control of parasite actin polymerization during invasion and motility (Poupel *et al.*, 2000) and once secreted into host cells, it controls the cortical actin cytoskeleton to facilitate Toxoplasma invasion (Delorme-Walker *et al.*, 2012).
The large family of ROP2/ROP4/ROP5/ROP7/ROP8/ROP14/ROP16/ROP17/ROP18 has received much attention. This family, which comprises at least 44 members, is constituted of rhoptry kinases (16 predicted proteins) or pseudo-kinases, which share several features such as a C-terminal putative transmembrane domain, a C-terminal kinase-like domain, and a N-terminal region rich in basic amino acids (El Hajj *et al.*, 2006; Saeij *et al.*, 2007; Peixoto *et al.*, 2010). At least two members of this family,

ROP16 and ROP18, exhibit the conserved glycine loop and the aspartic acid critical for phosphotransferase activity (El Hajj *et al*., 2006; 2007*).* Many components of the ROP2 family, such as ROP2, ROP4, ROP5, ROP7, ROP8, ROP14, and ROP18 have been described as being associated with the PVM (El Hajj *et al.*, 2006; Taylor *et al*., 2006; El Hajj *et al.*, 2007a; El Hajj et *al.*, 2007b).

Even if there is no formal proof of the involvement of rhoptries in the PV formation, their exocytosis correlates with the host cell membrane invagination at the beginning of the invasion process (Hakansoon *et al.,* 2001). The natural secretagogue that triggers rhoptry discharge remains unknown. In a similar way to what happens during invasion of Plasmodium merozoites into erythrocytes (Singh *et al*., 2010), rhoptry discharge could occur subsequently to the binding of microneme proteins to their host cell receptors and the consecutive restoration of intracellular Ca^{2+} concentration. Furthermore, the mechanisms by which ROP proteins could be delivered to the PVM or to other cellular locations is not entirely elucidated. Using a strategy of systematic protein tagging, all the rhoptry proteins secreted into the PV compartment at the time of invasion were shown to be trafficked to the PVM *via* the intravacuolar network (Reese *et al*., 2009). In addition, the secretion of the rhoptry bulbs was shown to occur during the spike of conductivity that occurs across the host cell membrane at the time of invasion (Suss-Toby *et al*., 1996). Knowing that the secretion of exosome-like vesicles dubbed “evacuoles” into the host cell cytoplasm had been demonstrated (Hakansson *et al*., 2001) and that these evacuoles could be labeled with antibodies specific to ROP proteins, Ravindran and Boothroyd (2008) proposed that these evacuoles (composed of both rhoptry lipids and proteins as well as some dense granule proteins) would align along host microtubules and assemble into filament-like ”beads on a string” to deliver ROP proteins to the PVM or to the host cell nucleus (**Figure 10**). Two microdomain components of the host plasma membrane, GPI and cholesterol, respectively, were recently shown to play important roles in the formation of evacuoles but not the PV, whereas GPI deficiency causes an increase of evacuoles’ size, cholesterol depletion results in a decrease of their number (Tahara *et al*., 2016).

Surprisingly, except for ROP9 (P36) and ROP14, most rhoptry proteins have no homologues within the Apicomplexa phylum, (Reichmann *et al.*, 2002), which suggests that these proteins have been under evolutionary pressure to make the parasite able to infect a wide range of host cells.

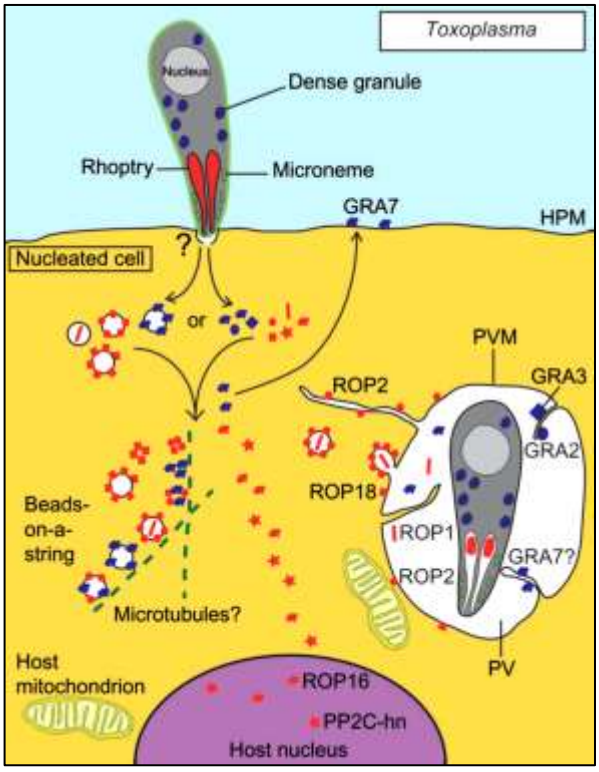

Figure 10. Possible traffic of ROP proteins in the host cell

At the time of invasion, the parasite secretes ROP proteins into the nascent PV as well as into the host cell cytoplasm *via* evacuoles. These exosome-like structures may organize themselves along host microtubules to traffic to the PVM of a PV already present in the host cell or to the host cell nucleus. Adapted from Ravindran and Boothroyd, 2008

CHAPTER III
MATURATION OF THE PARASITOPHOROUS VACUOLE: ROLE OF THE DENSE GRANULE PROTEINS

Once detached from the host cell plasma membrane, the PV undergoes a final step of maturation, which is characterized by the secretion of proteins from the DGs (**Figure 5**). These proteins contribute to the PV maturation, its functional development and later, its differentiation into an intracellular cyst. Although the precise function of most of these dense granule proteins remains to be determined, their specific location in the PV places them in the perfect location to interact with the host cell. In this chapter, I will first summarize what is currently known about the ultrastructure of the PV, the dense granule organelles, then the various dense granule proteins, their major characteristics, and I will finish by the possible functions that these proteins might play in the host/parasite interaction.

III-1 THE PARASITOPHOROUS VACUOLE OF *TOXOPLASMA GONDII*

All the Apicomplexa parasites did not evolve the same type of PV. For example, *Toxoplasma* and *Plasmodium* PVs result from two different strategies of intracellular parasitism. Although the initial invasion relies on a common active process, which involves sequential secretion from their apical secretory organelles and mobilization of their glideosome (chapter II), their resulting PVs differ in their architecture and metabolism, leading to two distinct modes of parasite replication, endodyogeny *versus* schizogony, respectively (see chapter IV). Consecutively to its formation, the PV of Toxoplasma (**Figure 11)**, which is initially located underneath the host plasma membrane, "plunges" into the host cell cytoplasm to re-locate close to the host cell nucleus envelope and this is in this particular cell location that parasites start to divide. The mechanism behind this PV migration remains to be investigated (Magno *et al.,* 2005a).

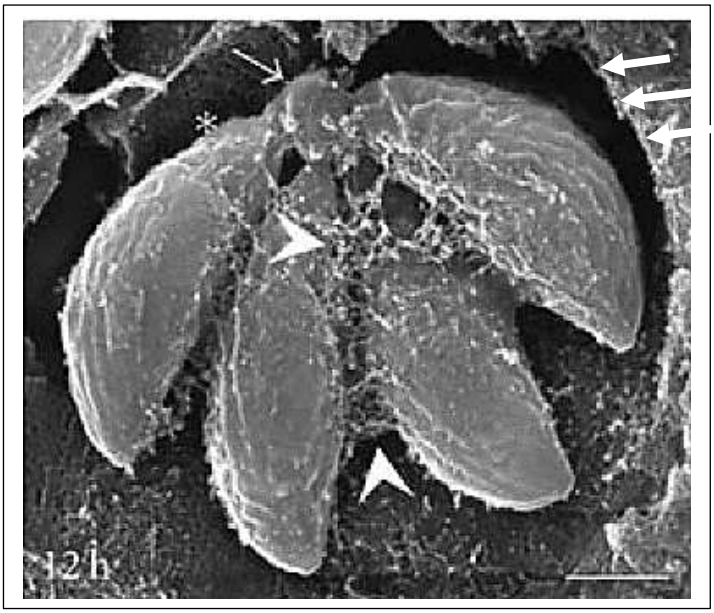

Figure 11. Scanning electron micrograph of a Toxoplasma parasitophorous vacuole containing 4 tachyzoites 12 hours post-invasion by Type I (RH) parasites.
The arrowheads indicate the membranous nanotubular network that links the parasites together and to the parasitophorous vacuole membrane (white thick arrows). The residual body of division is indicated by a thin arrow. The asterisk indicates the posterior part of one of the parasites. Adapted from Muniz-Hernandez *et al*., 2011.

Many features characterize the PV of *T. gondii* (**Figure 11)** and they will be developed below.

III-1.1) The PV is a compartment with a neutral pH

The PV of *T. gondii* is a compartment with a neutral pH, very likely due to the presence of proteases inhibitors (see below) and because the PV does not fuse with host lysosomal or endosomal compartments (see below). This neutral pH favors safe multiplication of the parasites.

III-1.2) The PV recruits host mitochondria and elements of the host endoplasmic reticulum

Shortly after invasion host mitochondria and elements of the host ER are recruited to the PV (de Melo *et al*., 1992; Schatten and Ris, 2004; de Melo and De Souza, 1997; Magno *et a*l., 2005b). This recruitment, in particular that of host mitochondria, was described as a dynamic process, in which host microtubules and host kinesins are involved (Sinai *et al*., 1997).

The interactions between the PV and host cell organelles may represent an efficient way to import nutrients and energy (ATP) into the PV. Both host mitochondria and ER elements were indeed shown to be a key source of phospholipids (Gupta *et al*., 2005). Specifically, the host mitochondria seem to be the main source of lipoic acid, an essential molecule for Toxoplasma since it is necessary for its Kreb's cycle and parasite replication (Crawford *et al*., 2006).

Various studies tried to identify the parasite factors involved in the association of the PV with host mitochondria. ROP2 was the first protein described as a candidate (Sinai *et al*, 2001). However, parasites lacking the *rop2* gene have the same ability as wild type parasites to recruit host mitochondria (Pernas and Boothroyd, 2010). A subsequent work demonstrated that this recruitment is strain-dependent: type I and type III parasites are able to attract host mitochondria contrary to type II strains (Pernas *et al*., 2014) (**Figure 12**). Furthermore, recruitment of host mitochondria and ER elements to the PV was recently shown to be increased in GPI-deficient mammalian cells (Tahara *et al*., 2016).

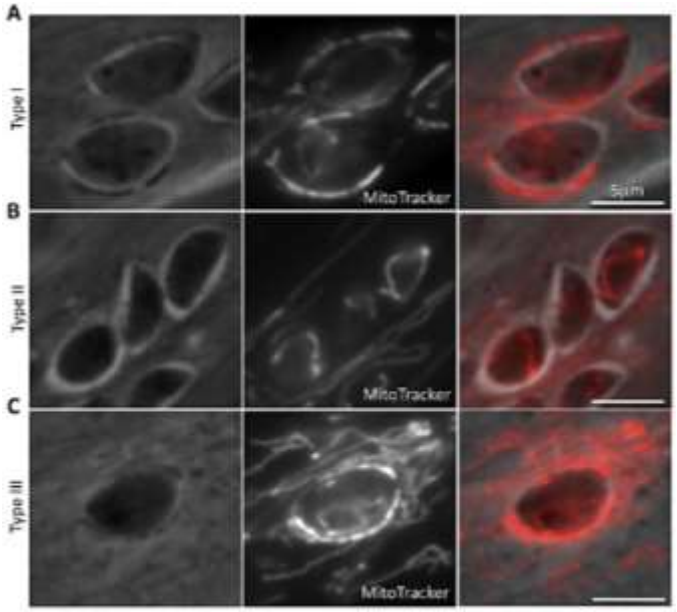

Figure12. Association of host mitochondria to the parasitophorous vacuole in host cells infected by types I, II, III parasites

IFA using mitotracker showed that the host mitochondria association is strain-dependent. Cells infected by **A,** type I (RH), **B,** type II (Me49) or **C**, type III (CEP) parasites. From Pernas *et al*., 2014

Recent data actually identified one of the dense granule proteins, MAF1, as a crucial factor for the association of host mitochondria to the PV of type I parasites (see below).

Contrary to the recruitment of host mitochondria, the factors that allow the recruitment of host ER elements to the PV are not well understood. Some dense granule proteins might be involved in their recruitment (see below).

III-1.3) Re-organization of the host cytoskeleton around the PV

One of the first modifications that appears during PV development, is the reorganization of the host intermediate filaments and microtubules around the PV (Cintra and de Souza, 1985; Andrade *et al*., 2001; Sehgal *et al*., 2005). The intermediate filaments seem to contribute to the positioning of the PV near the host nucleus (Halonen and Weidner, 1994).
The repositioning of host microtubules around the PV was shown to depend on the detachment of the host microtubule organization center (MTOC) from the host nuclear envelope and its subsequence recruitment to the external face of the PV (**Figure 13**) (Coppens *et al.,* 2006; Nolan *et al.,* 2015). Remodeling of the microtubules was shown to depend on tubulin polymerization and de-polymerization. The host microtubules would be involved in the acquisition of nutrients from the host. Host endolysosomal structures were indeed shown as being often associated with host microtubules, which have been described as conduits for the delivery of host nutrients such as cholesterol and shingolipids into the PV through specific vacuolar membranous structures called HOSTS (described below) (Coppens *et al*., 2006; Romano *et al*., 2013).

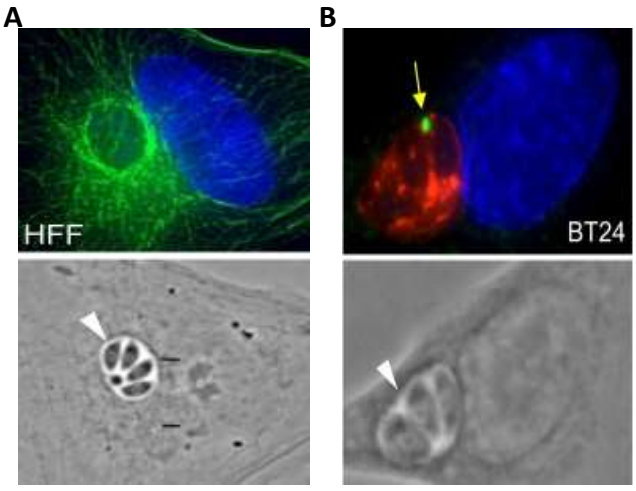

Figure 13. Reorganization of the host microtubules in cells infected by *T. gondii*
IFA of host microtubules **(A)** or host MTOC (**B**, yellow arrow) in *T. gondii* (RH)-infected cells. The arrowheads show the PV of *T. gondii.* Adapted from Nolan *et al*., 2015.

III-1.4) The PV is characterized by intriguing membranous systems

a) The PV is limited by a permeable membrane, the PVM

The PVM (**Figure 11)** derives originally from the host cell membrane but it is rapidly modified by the parasite (see chapter II). The PVM of *Toxoplasma*, *Plasmodium* and *Eimeria* is selectively permeable to small molecules up to 1,300-1,900 Da (such as glucose, amino acids, nucleotides and ions), which diffuse passively into the PV *via* pore like-molecules (Desai and Rosenberg, 1997; Schwab *et al.,* 1994; Werner-Meier and Entzeroth, 1997). Specific GRA proteins were recently shown to participate to the formation of these pores. Some bigger metabolites, like sterols, are actively scavenged from the host cell to the PV through sterol transporters located in the PVM (Ehrenman *et al.,* 2010).

b) An intricate network of membranous tubules

A network of membranous tubes (40-60 nm in diameter; 200-500 nm in length) extends between the parasites and connects them together and to the PVM. This intravacuolar network, also called the membranous nanotubular network (MNN), is formed at the posterior part of the parasite 15-30 minutes PI and persists until parasites' egress (Magno *et al.,* 2005a) (**Figure 11)**. I will show that the study of some of the dense granule proteins has led to a better understanding of the formation of this network.

c) Host Organelles Sequestering Tubulo-structures (HOSTs)

HOSTs are deep invaginations of the PVM into the PV lumen: these membranous tubules have a diameter of 95-115 nm. They are 1.2 µm long, contain a single, shortened host microtubule, and an electron dense coat that is regularly organized along their long axis (**Figure 14**). The HOSTs would be involved in the acquisition of host endolysosomal vesicles into the PV to ensure the internalization of lipids that the parasite cannot synthetize (Coppens *et al*., 2006).

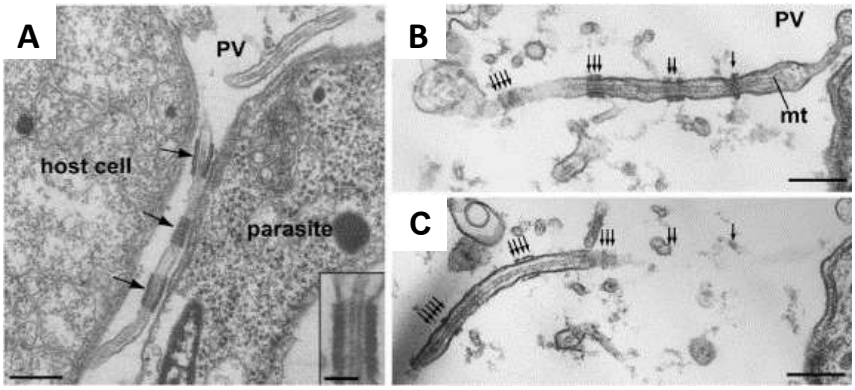

Figure 14. Transmission electron micrographs of H.O.S.T. structures.
A- An electron dense coat (arrows) is regularly organized along the H.O.S.T. Scale bar: 150 nm. **B-** Inset in (A) shows a detailed transverse section of the coat. Scale bar: 50 nm. **B-C** Serial sections of the same H.O.S.T. revealing their ramification in the PV and association with at least five coated structures constricting their diameter. From Coppens *et al*., 2006

d) the PVM forms thin membranous projections into the host cell cytoplasm

One or 2 (more rarely a higher number) thin membranous projections run from the PVM into the host cytosol, suggesting a dynamic nature of this latter membrane. However, nothing is currently known about the exact nature and function(s) of these projections. Whether the formation of these PVM extensions is a feature of mature- or developing vacuoles remains to be investigated.

The labeling of infected cells by antibodies specific to dense granule proteins revealed very early that these proteins are very abundant in the PV. In the next sections I will thus review the dense granules, the proteins which have been identified so far in these organelles and their potential functions.

III-2 THE DENSE GRANULES

DGs constitute the third type of secretory organelles described in *T. gondii.* These organelles are not present in all Apicomplexa. They have indeed been only described in parasites that form tissue cysts, *i.e*. the genera *Eimeria*, *Toxoplasma, Neospora* and *Sarcocystis* (Cesbron-Delauw *et al.,* 2008). In *T. gondii*, the number of DGs varies with the parasite stage: up to 15 DGs can be detected in a single tachyzoite, while only 8-10 and 5-6 have been described in the bradyzoite and merozoite stages, respectively. Since the 1960s DGs have been described by TEM as one single population of microspheres of 200 nm in diameter. Contrary to the rhoptries and the micronemes, DGs are dispersed in the parasite cytoplasm on each side of the nucleus. The density of these organelles, as observed by TEM, suggested that they could be important protein storage compartments (**Figure 15**). To this date, their natural secretagogue remains unknown and very few events of secretion have been

captured. The most recently reported one is presented on **Figure 15**: it shows the fusion between a dense granule and the PPM (in the anterior part of the parasite) and spreading of the dense material on each side of the fusion site, within the tightly fitting PV.

Recent studies have shown that newly synthesized dense granules are transported from the Golgi to the parasite's periphery by class 27 TgMyoF motors moving along filamentous actin (Heaslip *et al*., 2016). Once they reach the proximity of the IMC, the DGs would not fuse with the IMC itself for secretion but they would instead traverse the IMC through small gaps in the IMC plates (Dubremetz *et al.*, 1993). If the granule does not encounter a potential exit site, the TgMyoF motors linked to the granule would initiate a directed run parallel to the IMC (Heaslip *et al*., 2016).

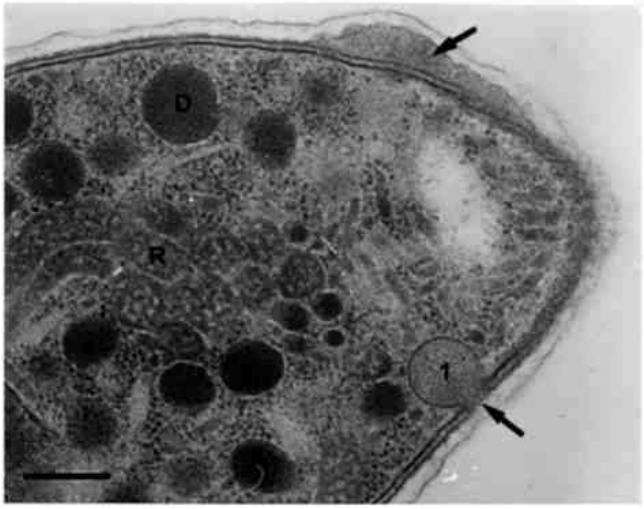

Figure 15. Transmission electron micrograph showing the apical part of a tachyzoite with several dense granules including a fusion event
The dense granules appear as electron dense globules (D). Secretion of the dense granule content (upper arrow) into the tightly fitting parasitophorous vacuole by fusion of the dense granule organelle with the lateral side of the parasite is indicated by the lower arrow. R, rhoptry. Bar: 350 nm. From de Souza *et al*., 2006.

III-3 THE DENSE GRANULE PROTEINS AND THEIR MOLECULAR FEATURES

The characterization of dense granule proteins started when the production of monoclonal antibodies against *in vitro* excreted-secreted antigens (ESAs) and sub-cellular fractionation of tachyzoites identified proteins in the dense granules (Cesbron-Delauw *et al.*, 1989; Charif *et al.*, 1990; Leriche and Dubremetz, 1991).

The first identified protein which was localized in the dense granules of both the tachyzoite and the bradyzoite stages, was called P23, by reference to its apparent molecular weight in sodium-dodecyl-sulfate polyacrylamide gel electrophoresis (SDS-PAGE) (Cesbron-Delauw *et al.,* 1989). Because of a growing number of proteins identified in the dense granules, Sibley and collaborators proposed in

1991 to use a common "GRAX" nomenclature for all the proteins which would be localized in the dense granules ("GRA" to refer to the dense GRAnules and "X" to the chronological order of identification): P23 was thus renamed GRA1 (Sibley *et al*., 1991). The dense granule proteins for which a function could be determined, were named after their function and not after their localization. One can regret that proteins have been recently named "GRAX" despite their lack of localization in the same dense granules as those that contain the historical GRA proteins (see the next paragraphs).
Up to now contamination of dense granule organelles with other types of organelles during their purification prevented the determination of the dense granules' full proteome. Nevertheless, during the last two decades at least 19 GRA proteins dubbed "canonical GRAs" have been co-localized in the same dense granules as those containing the firstly described DG proteins and a growing number of proteins (that we will call "GRA-like" proteins) are also localized in what could be a second set of dense granules (Mercier and Cesbron-Delauw, 2015; Nadipuram *et al*., 2016; Bougdour *et al*., 2014). I will review below these different categories of proteins secreted into the PV after invasion from dense granules and their related subset.

III-3.1) The canonical dense granule proteins

The members of this increasing family do not share homologies between them (except for GRA38, GRA39 and GRA40) or with any protein of known function. They were defined as GRA proteins because of their co-localization with GRA1 (or GRA2, GRA3) in the same dense granules, after having used an immune-EM technique (gold standard) or a specific immunofluorescence technique that allows the permeabilization of *i)* the host cell plasma membrane, *ii)* the PVM, *iii)* the PPM and *iv)* the dense granules' limiting membrane, without altering these compartments (*i.e.* fixation of infected cells in 4% methanol-free formaldehyde and permeabilization in 0.1 % triton-X100). Permabilization of both the host cell plasma membrane and the PVM without alteration of the PPM by the use of 0.002 % saponine as permeabilizing agent allows the detection of all these GRA proteins only in the PV.

Analysis of the amino acid sequences showed that the "canonical" dense granule proteins (**Figure 16**) share several features:

i) their gene is unique and they are abundantly expressed, with a peak of expression at both the tachyzoite and the bradyzoite stages;

ii) except for GRA20, they contain a canonical- or a non-canonical N-terminal hydrophobic sequence, which plays the role of a signal peptide. This correlates with their secretory profile, since the GRA proteins are secreted into the PV starting 3 minutes PI, with a peak of secretion 10-30 minutes PI (**Figure 15**);

iii) the monomeric proteins exhibit a low apparent molecular weight (20-75 kDa, with the exception of GRA38, GRA39 and GRA40 which are ˜ 100 kDa) (**Figure 16**). A difference between their calculated- and their apparent molecular weight suggested post-translational modifications (Mercier *et al.,* 2005). Although several N- and O-glycosylation sites were described in their amino acid sequences, only GRA2 (Zinecker *et al.*, 1998), GRA4 (Achbarou *et al.*, 1991) and GRA6 (Travier, 2007) were shown to be O-glycosylated. The phosphorylation of GRA2 (Mercier *et al.*, unpublished data) and GRA6 (Labruyère *et al.,* 1999), which occurs in the PV compartment, and the failure to label GRA1 and GRA5 with [^{32}P]-ATP (Mercier *et al*., unpublished data) could not account for the aberrant migration of these proteins, when extracted from extracellular parasites and analyzed by SDS-PAGE. In contrast, GRA4 and GRA8, which are proline-rich proteins (Carey *et al.*, 2000), may be modified by the peptidyl prolyl cis-isomerase activity of cyclophilin-18 (TgCy-18) that was found in both the DGs and the PV (see below) (High *et al.*, 1994). Although other post-translational modifications cannot be excluded, the apparent high molecular weight of the GRA proteins could thus be due to their particular resistance to denaturation by SDS;

iv) except for GRA1, GRA38, GRA39 and GRA40 which are soluble, the GRA proteins contain within their amino acid sequence, one hydrophobic α–helix or amphipathic α-helix(ces) (**Figure 16**) that allow the association of the respective proteins with the PV membranes consecutively to their secretion (see next paragraph). However, despite membrane association of most GRA proteins, a fraction of all these proteins remains soluble in the PV;

v) several of these canonical GRA proteins were shown to be part of high molecular weight protein complexes, both in the DGs and in the PV (Labruyère *et al.,* 1999; Braun *et al*., 2007);

vi) they are maintained in the PV up to the parasite's egress or the differentiation of the PV into a cyst;

vii) they would play major roles in the maturation of the newly formed PV into a metabolically active compartment, the biogenesis of the cyst wall, and they could also be major partners of host cell proteins (see below) (Mercier and Cesbron-Delauw, 2015).

Interestingly, the recent fusion of GRA17 to the biotin ligase BirA*, and its use as bait to purify its biotinylated partners by streptavidin chromatography (BioID technology) allowed the identification (by tandem mass spectrometry) of 13 novel GRA proteins (GRA28-40), all co-labelled with GRA14 in the dense granules and secreted into the PV. Among these proteins, GRA38, GRA39 and GRA40, which are ˜ 100 kDa, were more particularly studied because of their homology, their immunogenicity and the fact that they are soluble proteins (Nadipuram *et al.,* 2016).

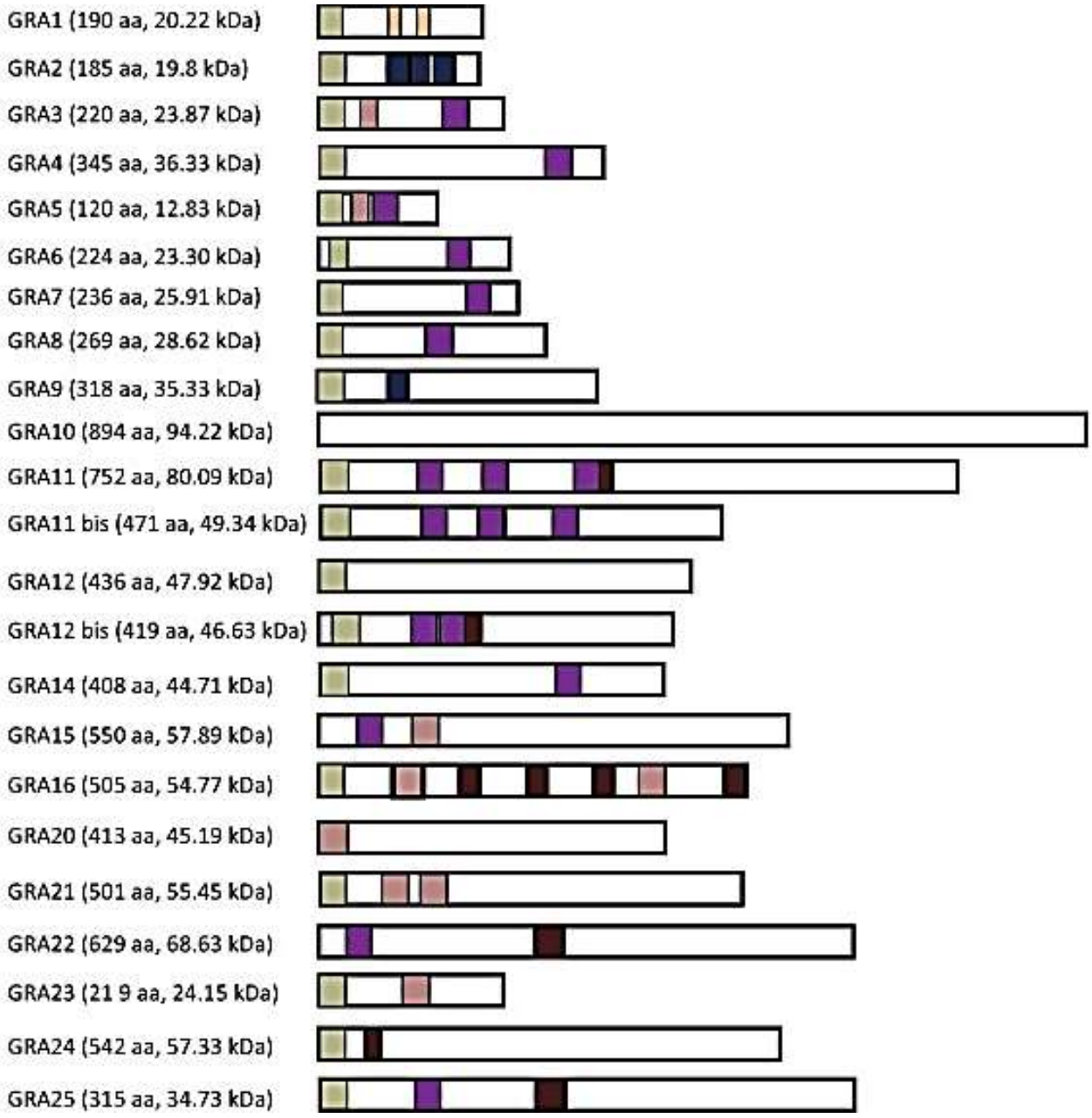

Figure 16. Schematic representation of the type II (ME49) proteins identified as dense granule (GRA) proteins in ToxoDB version 12.0.

signal peptide; PEXEL-like motif (RxLxE/Q/D:processing- and PVM targeting signal); hydrophobic alpha helix; Ca^{2+}-binding EF hand; nuclear localization signal. From Mercier and Cesbron-Delauw, 2015.

III-3.2) The dense granule proteins named after their function

Many proteins which were localized in the DGs and fit most of the "canonical GRA" features, have been named after their function (or their potential function) rather than their localization within the same dense granules as the "canonical GRA" proteins. Among these, one finds:

i) enzymes, such as 1/ the nucleotide triphosphate isomerases (NTPases I and NTPases II). These soluble proteins of the PV may help in the import of purines from the host cell and the regulation of vacuolar [ATP], avoiding premature egress of the parasites (Bermudes *et al*., 1994; Silverman *et al*., 1998); 2/ the cathepsins TgCPC1 and TgCPC2, named as such because they exhibit the typical catalytic site of cathepsins in their sequences (Que *et al*., 2007); 3/ the cyclophilins (TgCy-18 and TgCy-20), which exhibit *in vitro* peptidyl-prolyl cis/trans isomerase (PPIase or rotamase) activity, while *in vivo*, TgCyp18 recruits cells and enhances the growth of host cells at the site of infection for maintenance of the interaction (Ibrahim *et al*., 2010);

ii) serine protease inhibitors from the Kazal family (TgPI-1 and TgPI-2), whose exact function *in vivo* remains unknown, even if, *in vitro*, TgPI-1 is a broad-spectrum inhibitor capable of neutralizing trypsin, chymotrypsin and elastase, and TgPI-2 appears to be specific for trypsin (Morris and Carruthers, 2003, Morris *et al.*, 2002);

iii) an osteopontin-like protein (OPN) (Cortez *et al*., 2007);

iv) an Inhibitor of STAT1-dependent transcription (TgIST) (Olias *et al.,* 2016; Gay *et al.,* 2016);

v) a mitochondria association factor 1 (MAF1). MAF1 is a small protein of 446 amino acids, with an N-terminal signal peptide. It is expressed during both the tachyzoite and the bradyzoite stages (Pernas *et al*., 2014; Adomako-Ankomach *et al*., 2016).

III-3.3) The "GRA-like proteins"

These proteins were named "GRA" proteins, because they are secreted into the PV after invasion. However, their co-localization with historical dense granule proteins in the dense granules of Toxoplasma was sometimes not reported (example of GRA15) or is not perfect (example of GRA24; **Figure 17**). Contrary to the canonical dense granule proteins, these "GRA-like" proteins are moderately expressed and importantly, their expression is not maximal during cyst development. In a similar manner to the dense granules proteins, they would be stored in Toxoplasma secretory vesicles, which are similar to- but distinct from the dense granules that can be labelled with antibodies specific of the historical GRA proteins. Whether these vesicles constitute a subset of the dense granules or another type of secretory vesicles remains to be determined (Mercier and Cesbron-Delauw, 2015).

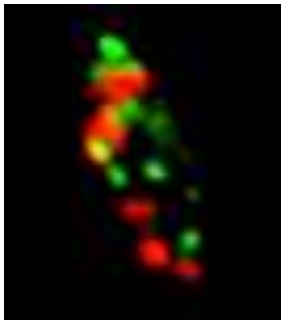

Figure 17. Extracellular tachyzoite immune-labelled for GRA24-HA (green) and GRA7 (red) and showing that both proteins are very likely stored in two types of secretory vesicles. From Braun *et al*., 2013

Among these proteins, one can include GRA15 (Rosowski *et al*., 2011), GRA16 (Bougdour *et al.*, 2013) and GRA24 (Braun *et al*., 2013). Interestingly, both GRA16 and GRA24 present in their amino acid sequences, nuclear localization signals (NLS) (**Figure 16**), which is in agreement with their final location in the host cell nucleus (see below), while both GRA15 and GRA16 display a PEXEL motif that would help them cross the PVM (**Figure 16**).
In a similar manner to these "GRA" proteins, Myc-regulation-1 (TgMYR1) contains a PEXEL motif, which is cleaved by aspartyl protease TgASP5 (Hammoudi *et al.*, 2015; Curt-Varesano *et al*., 2016) at the level of the Golgi, which allows the transport of this protein across the PVM after its secretion into the PV (see below), where it is phosphorylated.
Lipolytic lecithin: cholesterol acyltransferase (TgLCAT), which is stored in a subset of dense granules, is a 83 kDa protein, which displays a potential transmembrane domain in its N-terminal region and potential binding sites for lipids. TgLCAT is secreted by the parasite into the PV but, unlike other LCAT enzymes, it is cleaved into two proteolytic fragments that share the residues of the catalytic triad and need to be reassembled to reconstitute enzymatic activity (Pszenny *et al*., 2016).

III-4 DIFFERENTIAL TARGETING OF THE DENSE GRANULE PROTEINS

Secretion of the dense granule proteins into the PV takes place shortly after invasion and the peak of secretion occurs 10-30 minutes PI (Carruthers and Sibley, 1997). After secretion, the dense granule proteins reach various locations, either within the PV or in the infected cell.

III-4.1) Proteins that remain in the vacuolar lumen

So far, only a limited number of dense granule proteins have been shown to remain soluble in the vacuolar lumen. These are GRA1, GRA38, GRA39, GRA40, TgIPs and the NTPases (**Figure 18**).

III-4.2) Proteins targeted to the various membrane systems of the PV

Most of the canonical GRA proteins were described as being associated with either the PVM and/or the MNN and/or the HOSTs and/or the PVM extensions (**Figure 18**):

i) GRA2, GRA4, GRA6, GRA9 and GRA12 associate with the MNN (Charif *et al.,* 1990; Dubremetz *et al.,*1993; Sibley *et al.,* 1994; Lecordier *et al.,* 1995; Bonhomme *et al.,* 1998; Labruyère *et al.,* 1999; Adjogble *et al.,* 2004; Michelin *et al*., 2009);

ii) GRA3, GRA5, GRA7, GRA8, GRA10, GRA14, GRA19, GRA20, GRA21, GRA22 and GRA23 associate primarily with the PVM and its thin extensions (although some of these GRA could also be readily detected at the MNN) (Achbarou *et al.*, 1991; Bonhomme *et al.*, 1998; Carey *et al.*, 2000; Dubremetz *et al.*, 1993; Lecordier *et al.*, 1993; Sinai *et al.*, 1997; Rome *et al.*, 2008; Hsiao *et al*., 2013; Okada *et al*., 2013; Masatani *et al*., 2013). This is also the case of GRA15, GRA24, as well MAF1 and MYR1, even if this PVM-localization is not definitive for both GRA16 and GRA24 (see below) (Rosowski *et al*., 2011; Braun *et al*., 2013; Pernas *et al*., 2014; Franco *et al*., 2016);

iii) so far, GRA7 is the only GRA protein to be detected as being associated with the H.O.S.T.S (Coppens *et al.,* 2006).

As mentioned above, the ability of these GRA proteins to interact with PV membranes is in agreement with the presence, in their amino acid sequence, of potential membrane-association domains. Specifically, GRA3, GRA5, GRA6, GRA7, GRA8, GRA12, GRA14, GRA25 display one potentially transmembrane hydrophobic α-helix (**Figure 16**). One or several amphipathic α-helix(ces) has/have been described in GRA2 (several) and GRA9 (only one) (Adjogble *et al*., 2004; Travier *et al*., 2008) (**Figure 16**). These putative membrane-association domains have been experimentally validated in the cases of both GRA2 and GRA5 (Mercier *et al.,* 1998; Lecordier *et al.,* 1999). Topologically, the GRA5 N-terminal domain was shown to be exposed to the host cell cytoplasm, whereas its C-terminal region faces the PV lumen (Lecordier *et al.,* 1999). The opposite topology was observed for GRA14 (Rome *et al.,* 2008). Although the specific topology of most PVM-associated GRA proteins remains to be elucidated, it has been shown that the N-terminal hydrophilic sequence of both GRA5 and GRA6 is responsible for their specific targeting to the PVM and the MNN, respectively (Gendrin *et al.*, 2008; Gendrin *et al.*, 2010). The hydrophilic N-terminal domain of GRA2 was also shown to be important for proper association of the protein with the MNN (Travier *et al*., 2008). Intriguingly, despite the

presence in their amino acid sequence of a potential transmembrane α-helix (**Figure 16**), GRA4 (Labruyère *et al*., 1999) and GRA23 (Masatani *et al*., 2013) have been demonstrated as being associated with the PV membranes by protein-protein interactions relying mainly on hydrogen bonds. In a similar manner, GRA19, GRA20, and GRA21, which lack a potential transmembrane domain in their amino acid sequence, may be associated with the PVM *via* protein-protein interactions (Hsiao *et al*., 2013; Mercier and Cesbron-Delauw, 2015).
Together, these characteristics suggest a model by which the interaction of the hydrophilic N-terminal domain of the GRA proteins with specific lipids would be responsible for their specific targeting to their respective vacuolar membrane (Cesbron-Delauw *et al*., 2008). Although the lipid composition of the PV membranes remains unknown, preliminary results on the specific interaction of GRA7 with phosphoinositids (Coppens *et al.*, 2006) and the GRA6 N-terminal domain with negatively charged lipids (Gendrin *et al*., 2010) are in agreement with this model.

III-4.3) Proteins exposed to the cytosolic phase of the PV or targeted to the host cell nucleus

A growing number of GRA-like- or dense granule proteins is shown to be targeted to the cytosolic face of the PVM or the host cell nucleus. This is the case, so far, of MAF1 (cytosolic face of the PVM), GRA15, GRA16, GRA24 and TgIST (host cell nucleus). How these proteins are transported across the PVM and the mechanisms by which they are targeted to the host cell nucleus are key questions to understand the host cell/parasite interaction.

a) Transport across the PV membrane

In Plasmodium, a PEXEL motif (Hiller *et al*., 2004; Marti *et al.,* 2004) directs proteins to export across the PVM. This PEXEL motif is the cleavage site for plasmepsin V and allows the release of a mature protein with a N-terminal xE/Q/D that is competent for export through the Plasmodium translocon of exported proteins (PTEX) after unfolding of the protein to be exported (Spillman *et al*., 2015). In Toxoplasma, the PEXEL motif observed in GRA16 was found to be cleaved by the aspartyl protease TgASP5, a Golgi-resident homolog of PfPMV (Coffey *et al*., 2015; Hammoudi *et al*., 2015), and which mediates the transport of the protein into the host cell. This enzyme was also shown to be important for the correct transport of GRA24 into the host cell nucleus, even if this latter protein does not contain any PEXEL motif (Curt-Varesano *et al*., 2016; Coffey *et al*., 2015). It thus seems that, in Toxoplasma such as in Plasmodium, two different routes of protein export into the host cell operate, one which allows the transport of GRA16, GRA19, GRA20 or TgMyr1 across the PV and which is dependent on TgASP5 and a still uncharacterized translocon machinery embedded in the PVM, and a second one, that allows the transport of GRA24 or MAF1 across the PVM, and which is independent

on TgASP5. Interestingly, the PVM-resident protein TgMYR1 was shown to be crucial for the transport of GRA24 to the host cell nucleus (Franco *et al*., 2016), which suggests that it could be part of the PVM translocon. However, to this date, none of these two transport machineries across the PVM are identified.

b) Transport of the proteins across the host cell cytoplasm and to the host cell nucleus

To our knowledge, how Toxoplasma proteins, which have been translocated from the PV compartment into the host cell, are transported across the host cytoplasm and into the nucleus, remains unknown.

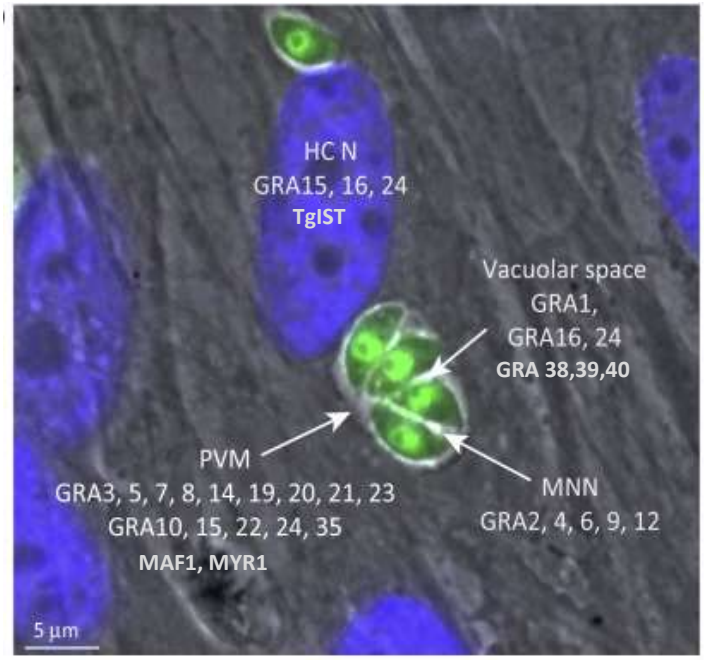

Figure18 Schematic representation of the final localization of the dense granule proteins.
After their secretion into the parasitophorous vacuole:

- GRA1, GRA38, GRA39, GRA40, TgIPs and NTPases remain soluble within the vacuolar space;
- GRA2, GRA4, GRA6, GRA9 and GRA12 are targeted to the membranous naotubular network;
- GRA3, GRA5, GRA7, GRA8, GRA10, GRA14, GRA15, GRA19, GRA20, GRA21, GRA22, GRA23, GRA24, GRA35 as well MAF1 and MYR1 associate with parasitophorous vacuole membrane;
- GRA15, GRA16, GRA24 transported by TgIST and GRA28 are targeted to the host cell nucleus.

HCN, host cell nucleus; MNN, membranous nanotubular network; PVM, parasitophorous vacuole membrane.
Adapted from Mercier and Cesbron-Delauw, 2015

III-5 FUNCTIONS OF THE DENSE GRANULE PROTEINS

Identification of specific domains in the amino acid sequence of some GRA proteins could evoke possible functions, as for examples two calcium-binding "EF-Hand" domains in GRA1 (Cesbron-Delauw *et al.,* 1989), a binding ER domain in the C-terminal end of GRA3 (Henriquez *et al*., 2005), a P-loop involved in an ATP/GTP-binding- and a RGD adhesion domain in GRA4 and GRA7, respectively (Mercier *et al*., 2005; Ahn *et al*., 2005). However, for most of the GRA proteins, this crude analysis was not sufficient to have a clue about their possible functions. The construction of parasite lines deficient for one or more *gra* gene(s) was thus the technical approach of choice to unravel the possible functions of the GRA proteins. Due to the amenability of type I parasites to genetic manipulations, the first Δ*gra* KO lines were constructed in the tachyzoite stage of the type I, virulent RH strain. It is important to notice that efficient construction of these KO lines (except for GRA1 and GRA10, Rommereim *et al*., 2016) showed that most of the GRA proteins are not essential for the parasite survival *in vitro*. Whether these proteins are involved in the parasite virulence remains unclear, due to contrasting results. A recent work, studying Δ*gra2-9* mutants has indeed shown that the loss of each single *gra* gene does not affect the parasite replication rate, contrary to what was observed for the double *gra* depletions *gra4-gra6, gra3-gra5, gra3-gra7* (Rommereim *et al.,* 2016). This study also concluded that GRA2-9 are not involved in parasite virulence, since no significant difference in the percentage of mice deaths was detected after an intra-peritoneal infection of 100 tachyzoites of wild-type *versus* Δ*gra2-9* parasites. By contrast, previous work had shown that GRA2, GRA6 and GRA7 may be important for parasite virulence. In these studies, mice had been inoculated with 10 tachyzoites into the peritoneum (Mercier *et al*., 1998), or at atypical sites, *i.e*. sub-cutaneously (Alagan *et al*., 2014) or in the footpad (Shastri *et al*., 2014), respectively. This studies thus highlighted the importance of the infection protocols to draw conclusions.

Since it is difficult to review all the possible functions of these dense granule proteins, I have chosen to consider their functions in comparison to their specific targeting: I will thus first consider the functions of the dense granule proteins that remain within the PV, then those of the proteins which are targeted to the PVM and can thus easily interact with the infected host cell and finally, I will review the proteins which are targeted to the host cell nucleus.

III-5.1) Functions within the PV

Analysis of the phenotypes of various Δ*gra* mutants led to interesting findings.

a) GRA2 and GRA6 contribute to the formation of the MNN

While the phenotypic analysis of many Δ*gra* KO parasites did not show particular phenotypes (Rommereim *et al.,* 2016), the deletion of *gra2* and/or *gra6* hampered the development of a normal MNN (Mercier *et al*., 1998b; 2002; Travier *et al*., 2008; Muniz-Hernandez *et al*., 2011; Lopez *et al*., 2015; Rommereim *et al.,* 2016). During the first 30 minutes PI GRA2 and GRA6 localize at the posterior end of the parasite, which is then invaginated. In this invagination, both the proteins were localized at the tubular membranes and vesicles that will further extend into the vacuolar space to generate the MNN (Labruyère *et al.,* 1999; Sibley *et al.,* 1995). In the absence of GRA2 the MNN was replaced by aggregated material, while in Δ*gra6* parasites the MNN was replaced by small vesicles (Mercier *et al.,* 2002; Travier *et al*., 2008; Lopez *et al*., 2015) (**Figure 19A-C**).

Moreover, the N-terminal hydrophilic domain of GRA6 was shown to display affinity for negatively charged phospholipids and to be crucial for association of the protein with the MNN (Gendrin *et al.,* 2010). The N-terminal domain and the amphipathic α–helices of GRA2 were also shown to be crucial to the MNN formation and to target GRA6 to the posterior pole of the parasite, where the MNN forms (Travier *et a*l., 2008). Finally, incubation of recombinant GRA2 and GRA6 with small unilamellar vesicles (SUVs) allowed their deformation into membranous tubules which resemble those observed within the PV (Lopez *et al*.,2015). Together, these data suggested a model where GRA6 stabilizes the MNN, whose formation is initiated by GRA2 (Mercier *et al.,* 2002; Travier *et al.,* 2008; Gendrin *et al.,* 2010; Lopez *et al.*, 2015).

b) GRA7 limits hyper-formation of the MNN

Recent data showed that parasites deleted of their *gra7* gene exhibit a hyper-formation of the MNN (**Figure 19D**) (Rommereim *et al.,* 2016). Knowing also that GRA7 deforms liposomes into tubular membranes (Coppens *et al.,* 2006) and that it interacts with GRA2 and GRA6 (Braun *et al.,* 2007), these observations could indicate that the association of GRA7, GRA2 and GRA6 may regulate the formation of the MNN.

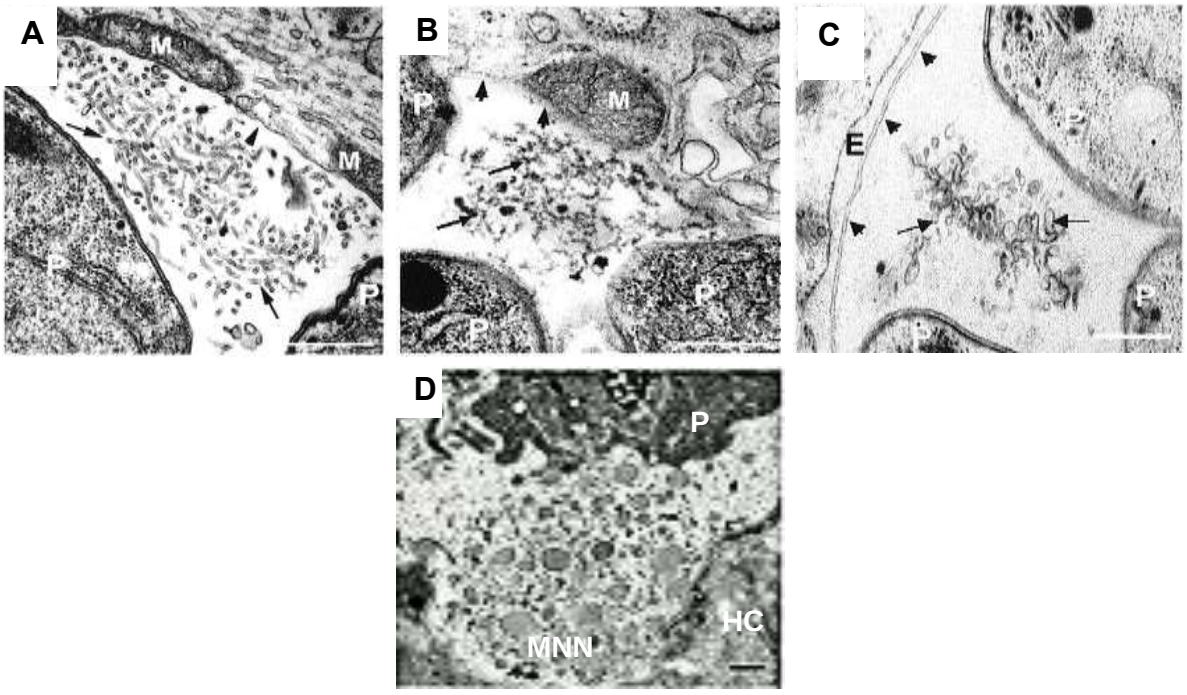

Figure 19. Transmission electron micrographs of the parasitophorous vacuole content from various Δ*gra* mutants constructed in type I parasites (RH strain).
A-Wild-type membranous nanotubular network (MNN). **B-** In Δ*gra2* the MNN is replaced by aggregated material. **C-** In Δ*gra6* the MNN is replaced by small vesicles. **D-** In Δ*gra7* the membranous tubules forming network are more abundant. The parasitophorous vacuole membrane is indicated by the arrowheads and the MNN by arrows. HC, host cytosol; E, host endoplasmic reticulum, M, host mitochondrion; MNN, intravacuolar membranous nanotubular network; P, parasite. Bar: 500 nm in **A-C** and 2 μm in **D**. **A-C,** adapted from Mercier *et al*., 2002 and **D,** from Rommereim *et al*., 2016.

Although GRA proteins such as GRA2, GRA6 and GRA7 are directly linked to the formation and/or regulation of the MNN, many other secreted proteins likely contribute to its formation, shaping, maintenance, etc. Interestingly, the deletion of *Tgasp5*, which is required for the cleavage of PEXEL motifs present in many proteins that are translocated through the PVM (see above paragraph), leads to the formation of aggregated material within the PV space in a similar manner to what was observed in the Δ*gra2* mutant (Coffey *et a*l., 2015), suggesting that one or more components involved in the biogenesis of this network requires processing by TgASP5.
Despite these interesting data on the potential functions of the GRA proteins, the major question which addresses the role of the MNN within the PV and, later, within the cyst is not completely solved. Several hypotheses have been advanced:

i) the MNN could play a structural role within the PV to maintain the parasites immobile and organize them within the PV in order to allow their synchronous division (Magno *et al*., 2005a; Travier *et al*., 2008);

ii) during *in vitro* encystation, the GRA proteins associated with the MNN relocate close to the PVM, suggesting reorganization of the MNN close to the PVM during cyst development (Travier *et al.,* 2008; Magno *et al.,* 2005a; Lemgrüber *et al.,* 2011). The MNN could thus also play a crucial structural role to reinforce the cyst wall at the bradyzoite stage;

iii) the MNN could be implicated in the parasite virulence as it is more developed in the PV of virulent- rather than non-virulent strains (Sibley, 1989);

iv) The MNN could play a trophic role by Increasing the exchange surface with the host cell and it could thus be involved in the acquisition of host nutrients (Sibley, 1989; Mercier *et al.,* 1998a). Consistent with this hypothesis, it has been demonstrated that the deletion of *gra2* and the subsequent destabilization of the MNN decrease the rate at which parasites ingest host cytosolic proteins, suggesting an implication of the MNN in heterophagy (Dou *et al.,* 2014).

Independently of its function for the parasite's biology, the MNN structure was shown to be implicated in the adaptive immune response mounted by the infected host against *T. gondii.* During the infection, $CD8^{+}$T cells are activated by the recognition of a short antigenic peptide (HF10; 8-10 amino acids) located in the C-terminal region of GRA6 type II and presented at the surface of infected cells by MHC Cl I molecules (Blanchard *et al.,* 2008). In the PV formed by Δ*gra2* parasites, thus in absence of a normal MNN, GRA6 relocates to the PVM, which results in an increased MHC-Cl. I presentation of the HF10 peptide (Lopez *et al.,* 2015). Two hypotheses have been proposed to explain the implication of the MNN in antigen presentation:

i) exposure of the GRA6 C-terminal domain to the host cell cytoplasm (because of its insertion into the PVM instead of the MNN as a consequence of the deletion of *gra2*) may facilitate its cleavage and release into the host cell cytosol before being processed by the proteasome (Blanchard *et al.,* 2008; Lopez *et al.,* 2015);

ii) the proximity of GRA6 with a (still unknown) translocation machinery embedded in the PVM may facilitate the export of the HF10 peptide to the host cell cytosol and ER (Lopez *et al.,* 2015).

Interestingly, the existence of translocation channels in the PVM was recently demonstrated. GRA17, which is similar to PfEXP2, the Plasmodium PVM translocon that allows the transport of PEXEL-containing proteins into the erythrocyte cytoplasm (de Koning-Ward *et al.,* 2009), was shown to allow the transport of small molecules <3,000 daltons across the PV into the host cell cytoplasm, when associated with GRA23. GRA17 was proposed to function in conjunction with its paralog GRA23 at the PVM, as either hetero- or homo-multimeric complexes, not to translocate proteins into the host cell cytoplasm but to allow the transport of small molecules across the PVM (Gold *et al.,* 2015).

c) Dense granule proteins and lipid metabolism

Targeted deletion of either the *gra38* or the *gra40* gene did not highlight any particular phenotype. By contrast, type II Δ*gra39* parasites exhibited reduced parasite growth and tissue cyst burdens in infected mice, coupled to the appearance of many amylopectin granules in their cytoplasm (likely reflecting parasite stress) and the deposit of neutral lipids within their PV (Nadipuram *et al.,* 2016). This approach thus confirmed that many GRA proteins, because of their location in the PV, are directly or indirectly linked to the Toxoplasma lipid metabolism.

TgLCAT was shown to use phosphatidylcholine as substrate to form lysophosphatidylcholine (LPC). Knowing that LPC has the potential to disrupt membranes, TgLCAT could thus tune the parasite lipid metabolism to facilitate Toxoplasma egress (Pszenny *et al*., 2016).

III-5.2) Functions related to the infected host cell

a) GRA proteins and formation of thin PV extensions into the host cell cytoplasm

These thin membranous projections of the PV into the host cell cytoplasm were first described as being immune-reactive to GRA3 (Dubremetz *et al.,* 1993). They were more recently shown to be also decorated by GRA7 and GRA14 (Coppens *et al.,* 2006; Rome *et al.,* 2008; Romano *et al.,* 2013a). In particular, Rome *et al*. (2008) showed that antibodies specific to GRA3, GRA7 and GRA14 recognize the same extensions, that there is no precise localization of these proteins along the extensions, and that the 3 fluorescently labeled antibodies revealed similar puncta (**Figure 20A**). Moreover, GRA14-positive extensions were also shown to link two different vacuoles, leading to the suggestion that these PVM extensions may allow exclusive transport of GRA proteins from one PV to another within the same infected cell (Rome *et al*., 2008).

Numerous studies have shown that host cell lipids are scavenged and delivered into the PV to allow parasites' growth and maturation of the PVM and MNN (Coppens *et al.,* 2000; Coppens *et al.,* 2006; Caffaro and Boothroyd, 2011). The HOSTs have been proposed as conduits for the internalization into the PV of host-derived endosomal vesicles enriched in cholesterol (Coppens *et al.,* 2006) and GRA7, as a major component of these HOSTs, could be involved in lipids acquisition from the host cell. However, interestingly, GRA7 also decorates the PVM extensions that can sometimes be very long and target the host Golgi (Romano *et al.,* 2013b) (**Figure 20B**). Knowing that Toxoplasma scavenges shingolipids from its host cell *via* the host Golgi using Rab14- Rab30- and Rab46-associated vesicles (de Melo and de Souza, 1996; Bisanz *et al.,* 2006) and that early after infection, the host Golgi is attracted to the PV (to be later fragmented), it has been proposed that the close association between the Golgi stacks and the PV would facilitate scavenging of sphingolipids. GRA7, which decorates these PV extensions, could thus also be involved in shingolipids acquisition from the host cell through this second route.

To date, even if the PV extensions are known to be decorated with PVM-associated proteins such as GRA3, GRA7 or GRA14, nothing is known about the genesis of these structures and their exact function(s) at the host/parasite interface.

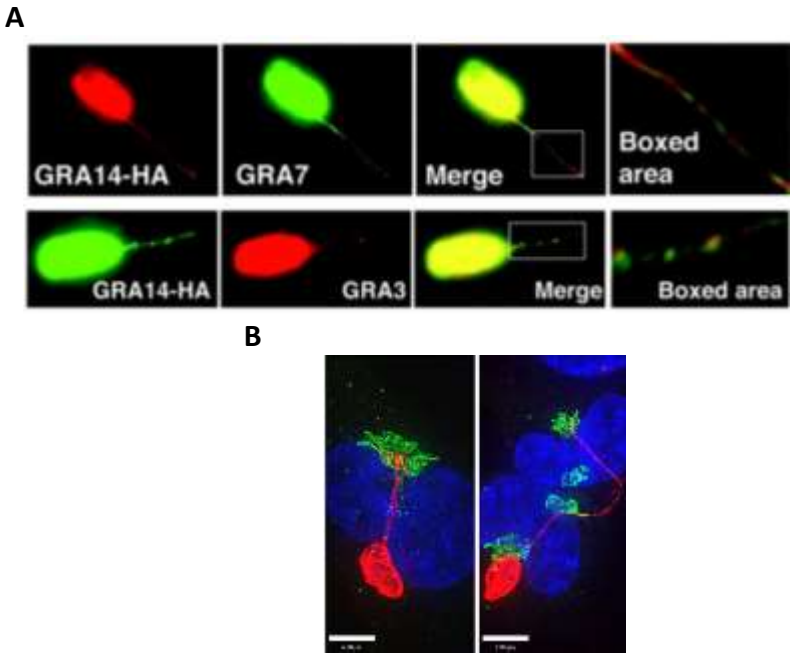

Figure 20. Immunofluorescence assays showing the detection of GRA proteins at the thin membranous extensions that run from the Toxoplasma parasitophorous vacuole membrane into the host cell cytoplasm. **A-**GRA3, GRA7 and GRA14 decorate the same extension without a precise co-localization of the proteins along the extension (Boxed area). **B**- GRA7 positive extensions target the distant host Golgi. From Rome *et al*., 2008 (**A**) and Romano *et al*., 2013b (**B**).

b) Dense granule proteins of the parasitophorous vacuole membrane: interactions with host cell proteins or host organelles

Three dense granule proteins have so far been demonstrated to have a direct impact on host organelles (MAF1) or host cell proteins (GRA6 and GRA7):

i) MAF1b is expressed by types I and III parasites and spans the PVM following its secretion into the PV. Both the types I and III parasites were shown to exhibit PVs that recruit a 3-fold higher number of host mitochondria. The molecular mechanism sustaining this increased interaction of the PVM with host mitochondria remains currently unknown (Pernas *et al.,* 2014; Adomako-Ankomah *et al.,* 2016);

ii) direct interaction between FLAG-tagged GRA6 and human influenza hemagglutinin (HA)-tagged calcium signal-modulating cyclophilin ligand (CAMLG, an integral membrane protein of the host ER), both transiently expressed in human epithelial kidney T cells, was demonstrated by co-immunoprecipitation (Ma, *et al.,* 2014). In a similar manner, a yeast

two-hybrid assay performed in HeLa cDNA expression library, resulted in the interaction of GRA3 with CAMLG (Kim *et al.,* 2008). However, whether the same kind of interactions between GRA3 or GRA6 with CALMG is established *in vivo,* remains to be determined;

iii) GRA7 has been shown to be part of a protein complex localized at the external face of the PVM, and which includes the rhoptry kinase ROP18 and the pseudo-kinases ROP8 and ROP2. ROP18 is known to be part of the major mechanism developed by virulent (type I) parasites to prevent the destruction of PVs by IRG proteins in mouse (not human) macrophages. By this mechanism, PVM-associated ROP5I/III sequesters IRG proteins and presents them to PVM-associated ROP18I/III for the phosphorylation on an essential Threonine residue in the N-terminal domain of IRGs, which in turn, prevents their assembly at the PVM for its further lysis (Etheridge *et al*., 2014). Specifically, GRA7 was shown to bind to one of the IRGs, *i.e.* immunity-related GTPase a6 (irga6), which led to its enhanced polymerization, rapid turnover, and eventual disassembly. The current understanding is thus that ROP18 and GRA7 act in a complex to target IRGs by distinct mechanisms that are synergistic and prevent the destruction of the PV (Alaganan *et al.,* 2014).

III-5.3) Dense granule proteins, efficient effectors that re-program the host cell

GRA15, GRA16, GRA24 and TgIST, once released into the PV, are targeted to the host cell nucleus, where they modulate the host cell expression in many ways which influence the quality of the immune response (sometimes in opposite directions) or the host cell cycle. Based on the current studies:

i) GRA15 type-II, in infected macrophages, induces the nuclear translocation of the NF-κB p65 factor, activating the transcription of pro-inflammatory genes such as IL12 (p40/p70) (Rosowski *et al*., 2011);

ii) GRA24 type-II induces prolonged auto-phosphorylation (and activation) of Thr180 and the nuclear translocation of host P38α mitogen-activated protein (MAP) kinase, thus increasing the production of pro-inflammatory cytokines (IL12 p40) in infected macrophages (Braun *et al.,* 2013);

iii) in the host cell nucleus TgIST binds to the gamma activated sequence (GAS) in place of STAT1, in the promoter of IFN-γ regulated genes, thus interacting with STAT1 and the Mi-2 nucleosome remodeling and deacetylase complex (Mi-2/NuRD complex), which, in turn, leads to the repression of the STAT1-mediated transcription of IFN-γ stimulated genes prior to IFN-γ priming. (Olias *et al*., 2016; Gay *et al*., 2016);

iv) GRA16 binds two host enzymes, the Herpes virus-associated ubiquitin specific protease deubiquitinase (HAUSP) and the PP2A phosphatase. Both exert several functions, including the

regulation of the p53 tumor suppressor pathway and the cell cycle. In a HAUSP-dependent manner, GRA16 alters p53 levels and induces nuclear translocation of the PP2A holoenzyme. GRA16 could thus control host cell arrest in the G2/M phase associated with Toxoplasma early infection (Bougdour *et al.,* 2013).

Even if they are not targeted to the host cell nucleus, some of the GRA proteins, in particular those which are targeted to the PVM, have been shown to efficiently contribute to the manipulation of the host cell. For examples,

i) GRA6 was shown to indirectly activate the transcription factor "nuclear factor of activated T cells 4" (NFAT4), likely *via* a direct interaction between its C-terminal domain and CAMLG (Ma *et al.,* 2014), which had been shown to be an activator of NFAT4 (Bram and Crabtree, 1994);

ii) recombinant GRA5 was shown to increase the migration of human CD34-DCs toward CCL19. A 29 amino acid synthetic peptide derived from the N-terminal region of GRA5 was found to be internalized by macropinocytosis and trigger *in vitro* migration of CD34-DCs *via* CCR7 expression and activation of the c-Jun N-terminal kinases pathway (Persat *et al*., 2012).

CHAPTER IV
FROM THE PARASITOPHOROUS VACUOLE TO THE CYST

Differentiation between stages is a crucial step of the life cycle of many protozoan parasites and for their transmission between hosts. In *Toxoplasma gondii,* interconversion between rapidly growing tachyzoites and latent encysted bradyzoites is an event accompanied by numerous morphological and metabolic adaptations resulting in long-term persistence in the host.
In this chapter, after a description of the mechanisms involved in tachyzoite to bradyzoite and PV to cyst differentiation, I will present the morphological features of both the bradyzoite cell and the cyst structure.

IV-1 DIFFERENTIATION OF TACHYZOITES TO BRADYZOITES RESULTS FROM STRESS

Before presenting the molecular mechanisms that sustain both the tachyzoite and the PV differentiation, one must remind the reader that one of the major differences between tachyzoites and bradyzoites is their rythmn of division. I will thus first briefly review below the various types of division processes that can be observed in Apicomplexa.

IV-1. 1) Toxoplasma tachyzoites divide by endodyogeny and exhibit a reduced cell cycle

Once inside their PV, tachyzoites start to multiply by a particular type of asexual binary division called endodyogeny. The molecular mechanisms involved in this particular division process are behind the scope of this review. I will just mention that it corresponds to an internal budding that gives rise to two daughter cells formed within the mother cell (**Figure 21A-B**).

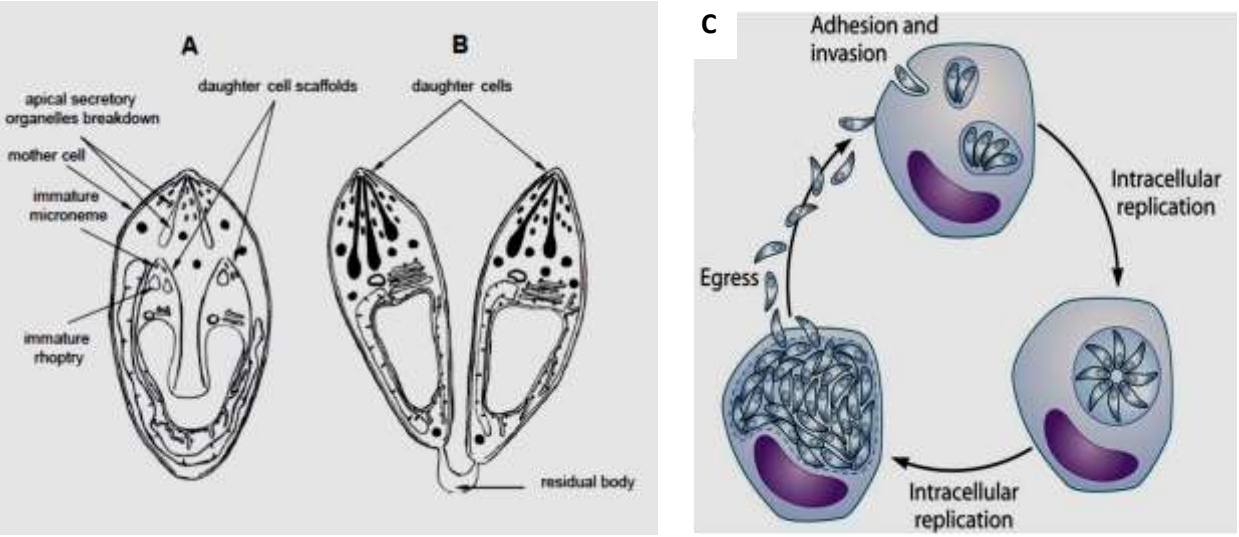

Figure 21. Schematic representation of tachyzoite division by endodyogeny.
A-Approximately four hours after the division process has begun, the volume of the mother cell has increased and the apical secretory organelles have begun to break down. The inner membrane complex scaffolds of the two daughter cells contain already the divided Golgi apparatus and apicoplast as wells as immature rhoptries and micronemes. The nucleus of the mother cell with its surrounding endoplasmic reticulum has branched and begun to invade the daughter cells scaffolds. The mitochondrion of the mother cell, which now encircles almost completely the daughter scaffolds, is one of the last organelles to divide. **B-** At the end of the endodyogeny process, the two daughter cells remain attached by a small residual body of division, which contains leftovers of the mother mitochondrion, endoplasmic reticulum, micronemes and rhoptries. From Mercier *et al*., 2010
C- Schematic representation of tachyzoite intracellular replication cycle. Adapted from Zhang *et al.,* 2013.

In *Toxoplasma gondii*, the time between two cell divisions depends on the parasite strain. It lasts between 5 and 10 hours (it is typically 8 hours for the RH strain) (Jones and Hirsch, 1972; Makioka and Ohtomo, 1995). One particularity of endodyogeny is that this is a synchronous process in all the tachyzoites of a given PV, which results in geometric expansion of clonal progenies until the host cell is lysed, ~48 h PI (Hu *et al.,* 2002a). At the time of host cell lysis, the PV occupies the entire space of the host cell cytoplasm and contains 128 or 256 tachyzoites, depending on the cytoplasm volume available in the host cell, and thus its shape. Following egress, free parasites infect adjacent cells (**Figure 21C**) or are transported in distant locations by the blood flow, ensuring parasite dissemination during the acute phase of infection (see chapter I).
Production of so numerous tachyzoites within the host cell in such a limited period of time is actually sustained by a cell cycle, which is particularly rapid, because of a lack of G2 phase and DNA synthesis being coupled to mitosis, as schematized on **Figure 22**.

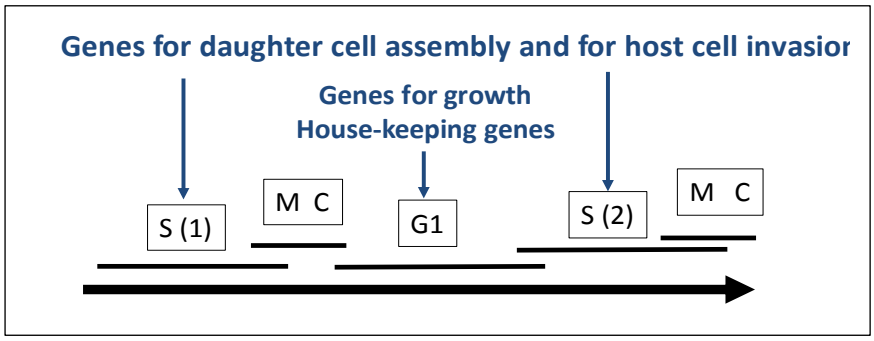

Figure 22. Schematization of the various phases of a tachyzoite cell cycle.
The scheme shows the lack of G2 phase and links the cell cycle phases to the two waves of transcription occurring respectively during the S (transcription of genes involved in daughter cell assembly and host cell invasion) and the G1 phases (transcription of the house-keeping genes).

IV-1.2) Bradyzoites, when dividing, proceed through alternative division processes

Endodyogeny differs from both the schizogony and the endopolyogeny processes, which are specific to closely related Apicomplexa parasites, namely *Plasmodium* and *Sarcocystis,* respectively (**Figure 23)**. In these division processes, cytokinesis and/or nuclear division are replaced by stages that are multinucleated or contain a single polyploid nucleus.
Interestingly, despite the fact that mature bradyzoites stop dividing (cell cycle arrested in G0/G1), these two modes of division are encountered in early bradyzoites (Dzierszinski *et al*., 2004; Striepen, 2007).

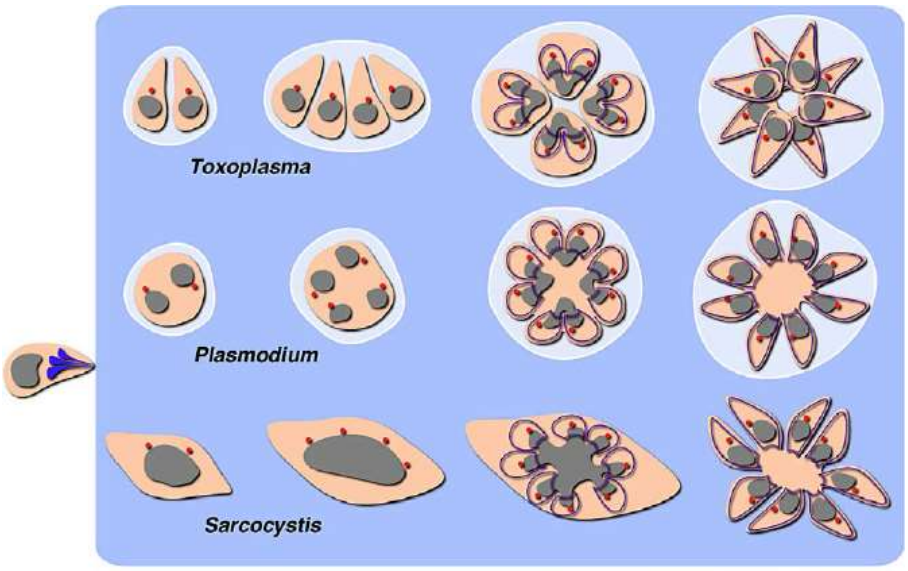

Figure 23. Schematic representation of the types of division processes encountered in Apicomplexa parasites.
Schematic outline of the cell division processes encountered in Toxoplasma tachyzoites (endodyogeny), Plasmodium merozoites (schizogony), and Sarcocystis (endopolygeny). Note that Sarcocystis develops directly within the host cell cytoplasm, while both Toxoplasma and Plasmodium are contained within a parasitophorous vacuole. DNA, grey; IMC, purple; centrosome, red. Adapted from Striepen *et al*., 2007.

IV-1. 3) Differentiation from tachyzoites to bradyzoites in response to stressing immune factors

During infection dissemination of tachyzoites is rapidly controlled by the host immune response (see chapter I). Although the development of bradyzoites occurs spontaneously in various tissues, cysts develop preferentially in neural and muscular tissues. It has been shown that host immunity factors play an important role in the cyst development and maintenance (Gross *et al.,* 1996; Denkers *et al*., 1998; Dupont *et al*., 2012). Very schematically, both activated $CD4^+$ and $CD8^+$ T cells that control *Toxoplasma* dissemination, also allow the development of a chronic infection by their production of INF-y, which:

i) triggers the production of nitric oxide (NO) and reactive oxygen species (ROS) by macrophages, astrocytes and microglia, thus reducing tachyzoite replication;
ii) activates IRG proteins such as IGTP and LRG-47, thus reducing parasite viability in activated murine macrophages and astrocytes (Butcher*, et al.*, 2005);
iii) triggers the production of host indoleamine 2,3 dioxygenase 1 and 2 in human brain endothelial cells, fibroblasts and macrophages, thus reducing the quantity of host tryptophan available for tachyzoite metabolism (Toxoplasma is auxotrophic for tryptophan).

The stress induced by the reduced quantity of nutrients and the development of intracellular mechanisms that aim at the destruction of the parasitophorous vacuole create the stress conditions required for the tahyzoites *i)* to slow down their cell cycle, *ii)* then progress through their cell cycle to reach a pre-mitotic checkpoint occurring at the S/M phase, where they engage their differentiation program (Croken *et al*., 2014b). Interestingly, analysis of the bradyzoite transcripts from the type II Me49 strain showed an enrichment of transcripts associated with ***i)*** ATP production via oxidative phosphorylation and the citric acid cycle; ***ii)*** transcription and translation machineries but ***iii)*** no difference in the genes related to invasion and formation of the PV (*mic*/*ron*/*rop*/*gra* genes) (Crocken *et al*., 2014a).

Furthermore, studies in humans and mice have revealed varying abilities to control infection and cyst burden, showing that the genetic background of the host is responsible for the development of latent infection (Brown*, et al.*, 1995; Suzuki*, et al.*, 1996; Mack*, et al.*, 1999; Suzuki, 2002). For example, BALB/c mice develop fewer brain cysts than other infected mice strains (such as CD1). This phenotype was linked to the quality of the $CD8^+$ T cells response, which eliminates brain cysts *via* perforin-mediated activity (Suzuki*, et al.*, 2010).

IV-1.4) Bradyzoite formation can be induced *in vitro* by the application of various stresses

Knowing that the conversion of tachyzoites into bradyzoites is stress-mediated (**Figure 24**), several methods have been developed to induce bradyzoite differentiation *in vitro*. The most commonly used method consists in incubating the infected cells in an alkaline medium for 3 or 4 days (Soëte *et al.,* 1994). Heat shock or treatment with sodium arsenite also trigger expression of bradyzoite antigens (Soëte*, et al.*, 1994), similarly to nutrient (ex: arginine) deprivation (Fox*, et al.*, 2004). The inhibition of parasite mitochondrion functions with sodium nitroprusside or other drugs cause oxidative stress (Bohne *et al.,* 1994; Tomavo and Boothroyd 1995) or alteration of ER (Narasimhan*, et al.*,2008), also inducing *in vitro* differentiation.

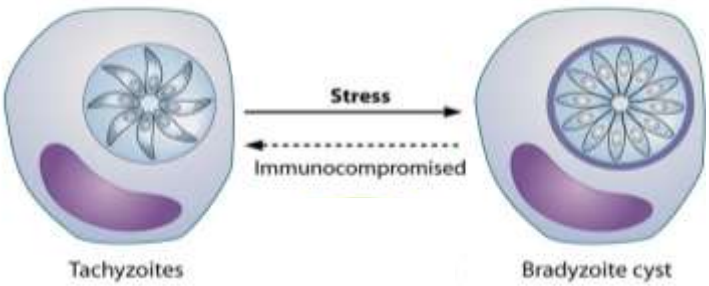

Figure 24: Conversion of *Toxoplasma* tachyzoites into latent bradyzoites and development of cyst structure results from the pressure of the host immune system *in vivo* or stress conditions *in vitro*. Adapted from Zhang *et al*., 2013.

IV-2. GENETIC AND EPIGENETIC REGULATION OF THE DIFFERENTIATION

Regulation of the differentiation occurs at the translational level, the transcriptional level and includes epigenetics regulation.

IV-2.1) Translational control of the differentiation

As in any eukaryotic cell, one the major Toxoplasma responses to cellular stress consists in the activation of various kinases, which leads to phosphorylation of the eukaryotic initiation factor 2 of translation TgeIF2α. The phosphorylation of this initiation factor is a conserved mechanism that eukaryotic cells use to repress global protein synthesis, while enhancing gene-specific translation of a subset of mRNAs (Zhang *et al.,* 2013). In *Toxoplasma*, high levels of TgIF2α–P are found in mature cysts induced *in vitro*, while the inhibition of TgIF2-dephosphorylation activates bradyzoite genes expression and cyst wall formation (Narasimhan *et al.*, 2008). *T. gondii* expresses 4 different kinases, TgIF2K-A, B, C, D, that could potentially phosphorylate TgIF2α. In particular, TgIF2K-C and D, which are homologous to the GCN2 mammalian kinase, that phosphorylates mammalian eIF2α kinase and facilitates adaptation to nutrient limitation, were very good candidates. Studies have shown that Toxoplasma uses both kinases: TgIF2K-D phosphorylates TgeIF2α to promote survival of tachyzoites following egress from host cells (Konrad *et al.,* 2011), while TgIF2K-C phosphorylates TgeIF2α to improve parasite viability during glutamine starvation (Konrad *et al.,* 2014). These studies suggested that the *Toxoplasma* GCN2-like kinases TgIF2K-C and TgIF2K-D evolved to have distinct roles, allowing the parasite to adapt to its environment (Konrad *et al.,* 2014).

IV-2.2) Transcriptional control of the differentiation

Despite the translational control that represses the translation of most mRNAs, translation of a subset of mRNAs coding for factors required to deal with stress still occurs. Studies showed that these mRNAs include those that code for the major family of plant-like transcription factors in Toxoplasma, the TgAP2 ("Apetala 2", because they contain an AP2 DNA binding-domain), which comprises 68 members in *T. gondii*.

High thoughput mRNA sequencing showed that some TgAP2 transcription factors are more specific of a particular Toxoplasma type:

i) steady state mRNA levels of TgAP2III-1 were shown to be significantly higher in PLK (type II) than in either RH (type I) or CTG (type III);

ii) expression of TgAP2IV-2 is higher in CTG tachyzoites (type III);

iii) RH tachyzoites (type I) express AP2IX-9 mRNA, a repressor of bradyzoite commitment, at significantly higher levels (Croken *et al*., 2014a).

Another study also based on high throughput mRNA sequencing showed that 11 TgAP2 transcription factors are up-regulated during bradyzoite differentiation:

i) TgAP2 XI-4 was shown to be involved in upregulation of bradyzoite specific genes after alkaline stress *in vitro*, while mice infected with TgAP2 XI-4 KO type II parasites have a defect in cyst formation;

ii) the expression of TgAP2 IX-9 was shown to peak in early stages of the alkaline stress response and to diminish in mature bradyzoite. This study also confirmed that TgAP2 IX-9 acts as a repressor of BZ differentiation (Walker *et al.,* 2013).

IV-2.3) Epigenetic regulation of the differentiation

As in any other eukaryotic cell, chromatin can be fashioned to be transcriptionally repressive or permissive, depending in part on histones post-translational modifications, which is usually referred to as the "histone code". Most of the studies so far have focused on the writers of this histone code, *i.e.* the enzymes that modify histones.

a) Histone acetylation

Chromatin immunoprecipitation (ChIP) experiments were used to study the regulation of bradyzoite conversion at the epigenetic level. The first studies demonstrated that the nucleosomes present in inactive bradyzoites-specific promoters are hypoacetylated at the tachyzoite stage, becoming acetylated under parasites differentiation (Saksouk *et al.,* 2005).

ChIP experiments performed on stressed parasite populations enriched for developing bradyzoites showed that the histones in the upstream sequence of bradyzoite-specific genes are acetylated by one of the two histone lysine acetyltransferases (KAT) expressed by *T. gondii*, *i.e*. TgGCN5a or histone deacetylase 3 (TgHDA3). TgGCN5a was shown to be required for increased expression of 74% of the genes which are up-regulated in response to alkaline pH (Naguleswaran *et al.,* 2010). TgHDA3 was found at the promoter region of bradyzoite-specific genes, which are silent at the tachyzoite stage. Drug inhibition of TgHDA3 induced histones acetylation and bradyzoite differentiation, confirming the role of TgHDA3 in the regulatory pathway driving parasite conversion (Bougdour *et al.,* 2009).

b) Histone methylation

While acetylation of histone lysine residues leads to gene activation, their methylation results in either gene activation or repression. The TgSET8 methyltransferase has been shown to monomethylate the lysine 20 on histone 4 (H4K20), promoting heterochromatin formation and gene silencing (Sautel *et al.,* 2009). In contrast, chemical inhibition of TgCARM1 histone methylase induced bradyzoite differentiation. TgCARM1 was shown to be associated with the promoter regions of tachyzoite-specific genes but enriched at bradyzoite-specific genes under induction of alkaline stress (Saksouk *et al.,* 2005).

To this date, even if the genetic mechanisms that lead to differentiation begin to be unraveled, important questions remain unsolved, such as what are the mechanism(s) that allow turning off the repressors of bradyzoite differentiation and importantly, does the same cascade take place in parasites that encyst *in vivo.*

IV-3 SPECIFIC FEATURES OF BRADYZOITES AND CYSTS

Morphological studies on encysted bradyzoites isolated from the brain or developed *in vitro* led to an increased knowledge of their biology.

IV-3.1) The bradyzoite cell

Bradyzoites differ from tachyzoites in different aspects:

(i) *their cell morphology*. Individual bradyzoites (7 × 1.5 µm) are a little shorter than tachyzoites (7 × 2 µm), with a more pronounced bow or crescent shape (Mehlhorn and Frenkel, 1980).

(ii) *their subcellular organization.* The nucleus appears more posterior, rhoptries more electron dense. The micronemes are more dispersed in the cytoplasm and more numerous. There are also less dense granules (Dubey *et al.,* 1998; Dzierszinski *et al*., 2004) (**Figure 25**).

(iii) *their accumulation of amylopectin granules*, that reflects glucose storage (Dubey *et al.,* 1998) (**Figure 25**);

(iv) *Changes in parasite cell division.* Dzierszinski *et al*. (2004) followed by time-lapse microscopy, the *in vitro* development of bradyzoites, demonstrating a growth rate reduction (cytokinesis of 12 h instead of 7 h) and asynchronous cycles of division that result in unusual numbers of parasites within a PV (*i.e.* the number of parasires it not a multiple of 2). Bradyzoites, metabolically quiescent, were indeed shown to replicate slowly within the tissue cysts by asynchronous endodyogeny but cycles of schizogony and endopolygeny were also observed (Dzierszinski *et al*., 2004) (see paragraph IV-1).

(v) *Changes in their metabolism.* Differentiation is accompanied by drastic changes in the expression profile (see paragraph IV-2), which results in progressive decrease in tachyzoite specific antigens such as SAG1, ENO2 (Enolase 2) or LDH1 (lactate dehydrogenase 1), while specific bradyzoite markers, such as HSP30/BAG1 (Heat Shock Protein/Bradyzoite Antigen 1), the membrane antigens SRS9/P36, SAG5A, SAG2C and SAG2D, and LDH2, ENO 1, are expressed. The differentiated parasites are also distinguished by the expression of the CST1 glycoprotein (SRS44, 116 kDa) at the cyst wall (Zhang *et al*., 2001; Lekutis *et al*., 2001; Ferguson, 2004; Van *et al*., 2007; Tomita *et al.,* 2013).

Many of these specific proteins favor the use of amylopectin and anaerobic glycolysis for the production of ATP (LDH2, Glucose 6 phosphate deshydrogenase, ENO1) and allow the parasite to cope with stress (HSPs). Together, these adaptations allow the parasite to remain dormant for extended periods of time.

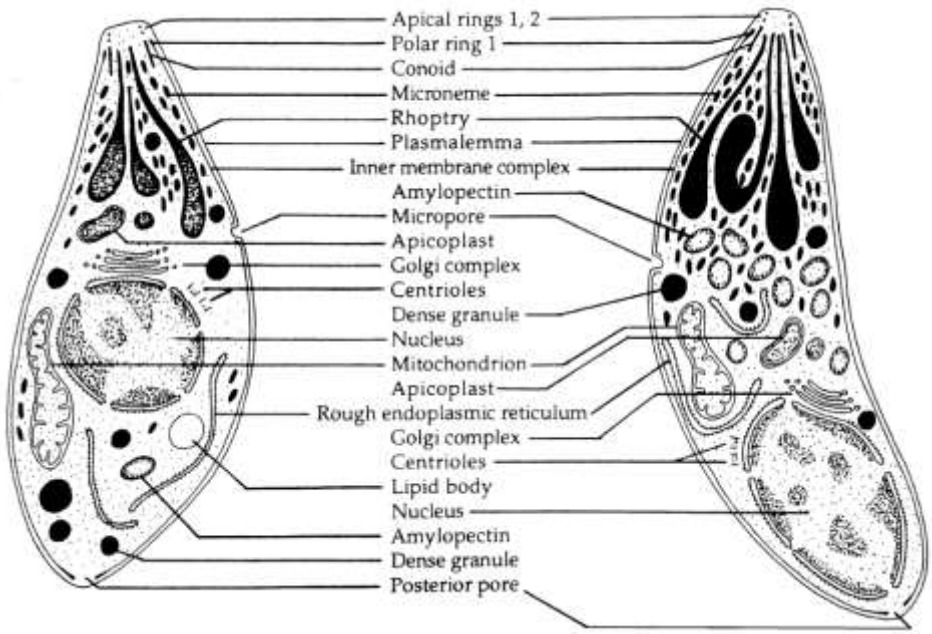

Figure 25. Schematic representation of a *T. gondii* tachyzoite (left) and a bradyzoite (right) showing their different subcellular reorganization. From Dubey *et al*., 1998.

IV-3.2) Specific features of the cyst

Cysts are intracellular structures that appear, in C57BL/6J mice infected IP with Me49 (type II) TK, as early as 1 day PI but they were readily detected in the brain during the 3rd week of infection (Afonso *et al*., 2012). In the routine of experimental protocols, cysts are usually recovered from the brain of infected mice after 7-8 weeks of infection. In mice, cysts can be detected in the brain, retina, skeletal and cardiac muscles, the testicles and in the central nervous system, more particularly in the medial- and basolateral amygdalae of the brain, and precisely in any kind of brain cells (neurons, astrocytes and microglial cells). Importantly, the cysts, which do develop intracellularly, do not trigger any inflammatory reaction.

Young cysts recovered from a mouse brain have a diameter of 5 μm, while a mature cyst can reach a diameter of 70-80 μm. It then contains 1,000-2,000 bradyzoites (**Figure 26**).

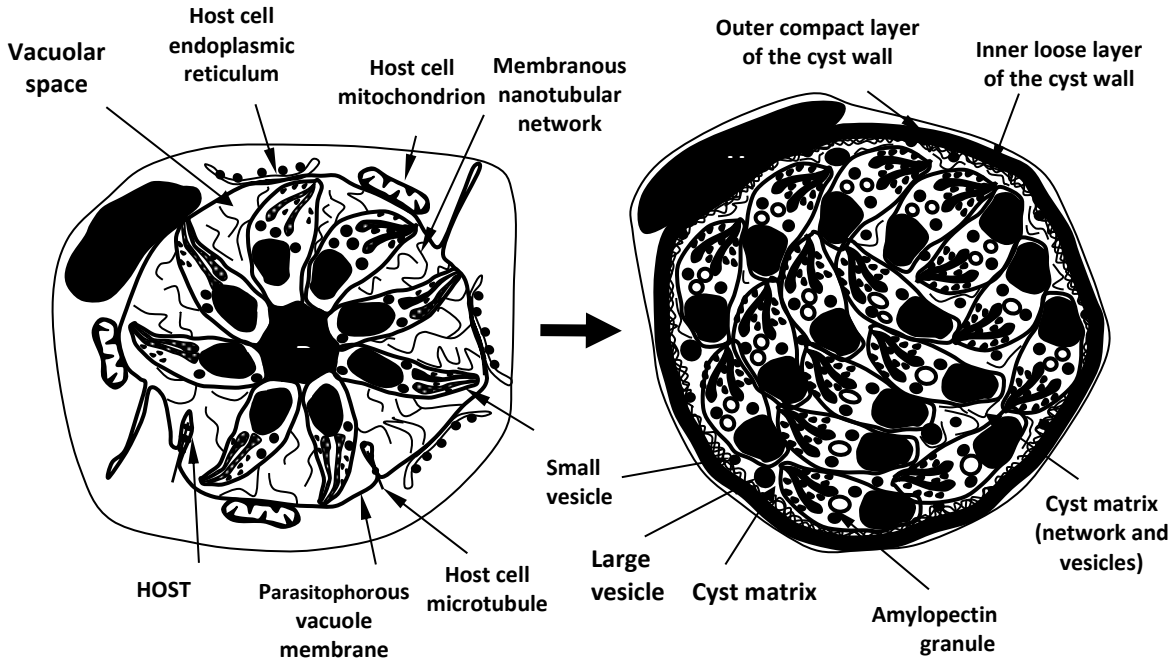

Figure 26. Transformation of the PV into an intracellular cyst.
On the left side of the figure, a PV containing eight tachyzoites. On the right side of the figure, the PV has transformed in an intracellular cyst. From Mercier *et al*., 2012

a) The cyst wall

The cyst wall develops from a modification of the PV membranes (PVM, MNNs, vesicles) and their associated proteins. Its average thickness is 240 nm. It is composed by two layers: an outer compact layer, which presents circular openings of 30-40 nm in diameter, and an inner thicker layer with a sponge appearance. The outer layer contains chitin, glycoproteins and glycolipids. (Boothroyd *et al*., 1997; Zhang *et al*., 2001; Tomita *et al.,* 2013) (**Figure 27**).

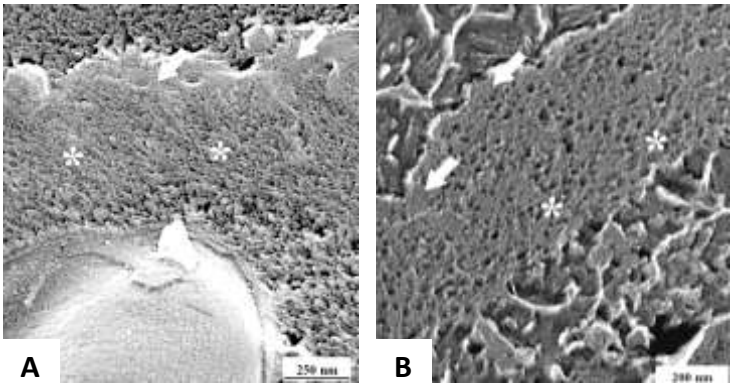

Figure 27. Composition of the cyst wall, as analyzed by Quick-Freezing, Freeze-Fracture, Deep-Etching and Rotary Replication (QF-FF-DE-RR). The two photos show the two layers of the cyst wall: one more compact (white arrows) facing the outer part of the cyst; and one looser (asterisks), with a sponge-like aspect facing the cyst matrix. From Lemgrüber, *et al*., 2011.

b) The cyst matrix

Inside the cysts the bradyzoites are surrounded by a matrix that contains a filamentous material, vesicles of different sizes and tubular structures (**Figure 27**) (Lemgrüber *et al.,* 2011).
Similar to the PV the tubular structures (diameter of 30-50 nm) connect the bradyzoites inside the cyst and to the cyst wall. The vesicles are of different sizes: large ones, L-vesicles, (diameter: 512 nm) and smaller ones, S-vesicles (diameter: 67 nm). The L-vesicles have a lumen granularity and density similar to that of the cyst wall. They contain glycoconjugates and unsaturated lipids and they are observed budding from the bradyzoite's posterior end and in the vicinity of the cyst wall (Lemgrüber *et al.,* 2011). Together, these observations, suggest that the L-vesicle could contribute to the cyst wall formation (Mercier and Delauw, 2012.)

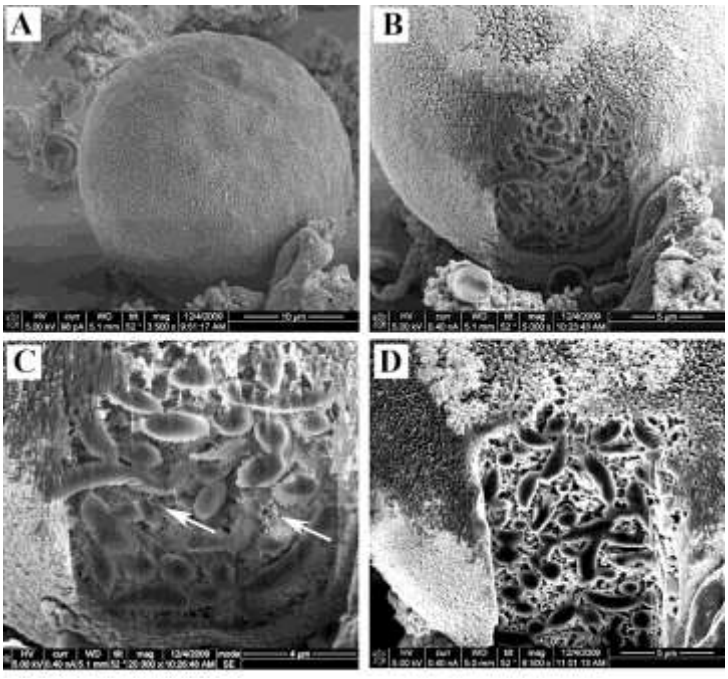

Figure 28: Scanning Electron Microscopy (SEM) of an isolated cyst.
A- The aspect of a cyst before cyst wall removal. **B-D** Matrix visualization after cyst wall milling: tubular structures (white arrows) are visible surrounding the bradyzoites inside the cyst. From Lemgrüber, *et al*., 2011.

IV-4) CONTRIBUTION OF THE DENSE GRANULE PROTEINS TO THE CYST FORMATION

Similar to their multiple roles in the PV, the dense granule proteins could also play several roles in the cyst.

IV-4.1) Structural role in the formation of the cyst wall?

Several features suggest the involvement of dense granule proteins in the formation of the cyst wall:

i) dense granules are organelles restricted to the Apicomplexa parasites that are able to form cysts;

ii) most of the canonical GRA are part of the cyst wall (Ferguson, 2004), an observation that correlates with their gene expression being maintained during the bradyzoite stage (Mercier and Cesbron-Delauw, 2015).

iii) Moreover, TEM associated to immunogold labeling allowed the observation of the localization of GRA1, GRA2, GRA3, GRA5, GRA6 and GRA7 in cysts: their localization is in agreement with their location in the PV. GRA3, GRA5, GRA7, which are indeed associated with the PVM at the tachyzoite stage, were associated with the outer membrane; GRA2, GRA3, GRA6 and GRA7, which were associated with the MNN of the tachyzoite PV, were

located to the inner membrane; GRA3 and GRA7 were also described as parts of the cyst matrix, associated with its vesicles and tubular network. GRA1, which is soluble in the tachyzoite PV compartment, was detected in the cyst matrix only (Torpier *et al*., 1993; Ferguson, 2004; Lemgrüber *et al*., 2011) (**Figure 29)**.

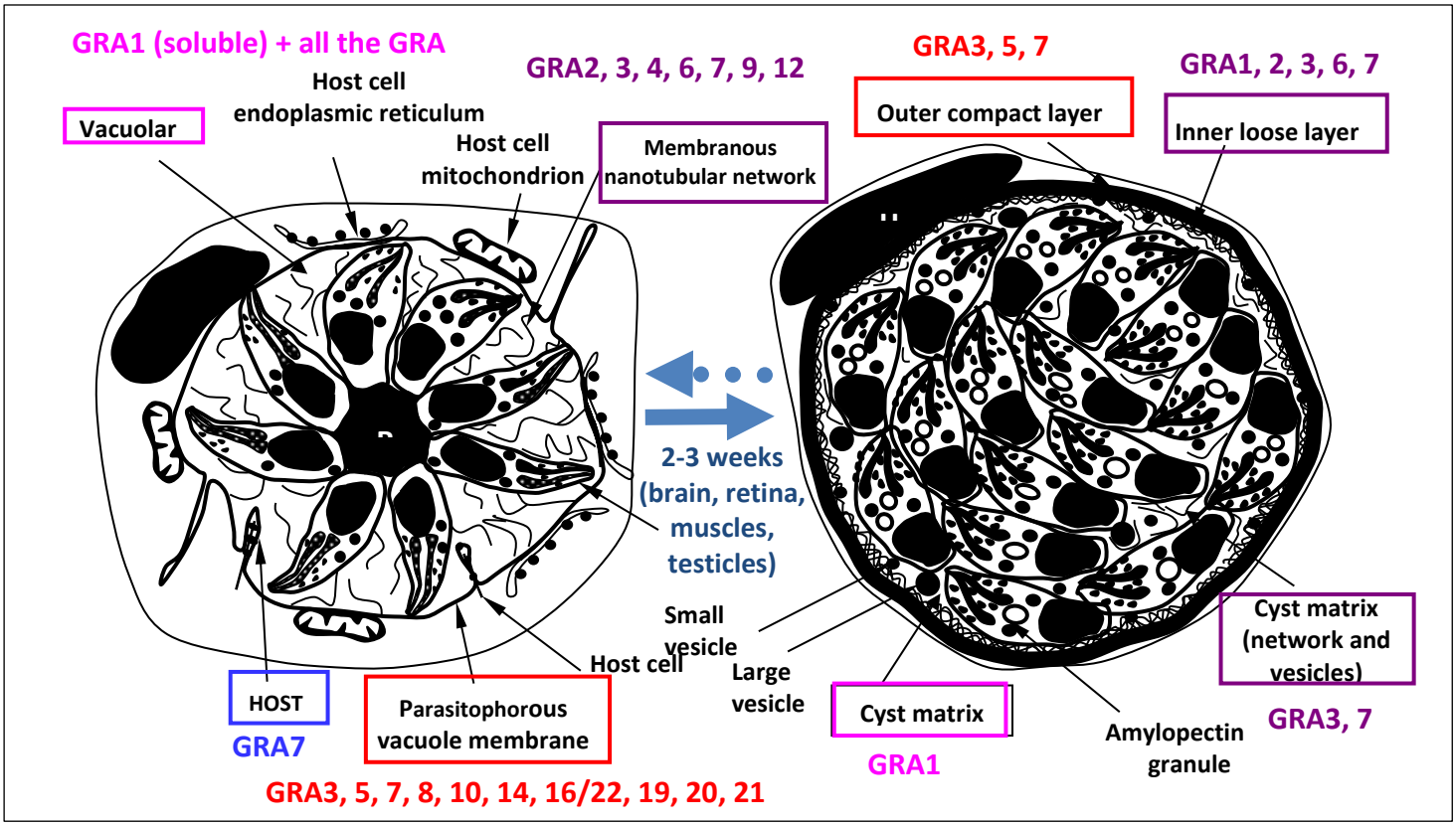

Figure 28. Schematic localization of the GRA proteins in the cyst.
Adapted from Mercier and Delauw, 2012

The location of the GRA proteins in the cyst wall is thus in agreement with their structural role in the cyst formation.

IV-4.2) Role(s) of the dense granule proteins in the host cell-cyst interaction?

The large majority of the studies performed to investigate the interactions between *T. gondii* and the host cell were performed *in vitro* using tachyzoites of the type I strain. Little is known about the interactions established between the host cell and bradyzoites and sporozoite stages.

The involvement of the dense granule proteins in host cell communication should of course not be excluded. The circular openings observed in the cyst wall **(Figure 27**) could be involved in nutrient

acquisition or in the export of vesicles into the host cytoplasm. The dense granule proteins are in the right location to be involved in the formation of these circular openings.
Studies performed *in vitro* showed that host ER accumulates around the PVM during the first 48 h of differentiation, while this phenotype disappears in more mature cysts (Guimarães *et al.,* 2009). Whether the dense granule proteins contribute to this recruitment, was not known when I began my PhD.
The two above possibilities are just examples of the potential roles of the dense granule proteins in the cyst. These questions will likely open the door to investigations in the future years.

IV-4.3) The GRA proteins are crucial for cyst burden *in vivo*

Similar to the studies that did investigate the role of the GRA proteins during acute infection, several studies did investigate their role during the chronic infection. To this aim, mice were infected with type II Prugniaud (PRU) strains deleted of one or several *gra* genes, this KO mutants having been constructed in the PRU*Δku80*Δ*hxgprt* strain, which is amenable to homologous recombination at a targeted locus (Fox *et al*., 2011). Infection of mice with PRU parasites KO for *gra4* and/or *gra6* (PRUΔ*ku80* Δ*gra4*::*hxgprt*, PRUΔ*ku80*Δ*gra6*::*hxgprt*, PRUΔ*ku80*Δ*gra6*Δ*gra4* strains) showed that the ability of these mutants to form brain cysts was reduced by 91% to 99% (Fox *et al.,* 2011).
A recent study showed that a Δ*gra39* KO mutant (Nadipuram *et al.,* 2016) was also less able to form brain cysts. However, the failure of this mutant to establish a chronic infection is likely due to its inability to replicate at a normal rate, limiting the quantity of parasites that reach the brain.

To date, only GRA4 and GRA6 (Fox *et al.,* 2011) have been shown to be involved the cyst formation *in vivo,* but nothing is known about the role of the other dense granule proteins in this process. Furthermore, the data collected to date confirmed the importance of the GRA proteins in the cyst formation but the molecular mechanisms that allow the development and the maintenance of cyst structures have, to our knowledge, never been investigated.

AIMS OF MY PhD PROJECT

Dense granule proteins (GRA) have been described as major components of both the PV and the cyst wall. Since they are involved in the PV maturation, numerous GRA proteins have been characterized at the tachyzoite stage and little is known about their role(s) in the parasite life cycle. The aim of my PhD project was to increase this knowledge focusing on the GRA5 protein, which had been previously characterized by the team of M.F Delauw.

GRA5 (21 kDa) is a 120 amino acid small protein predicted to contain a N-terminal hydrophobic signal peptide, a central hydrophobic alpha-helix, bordered by two hydrophilic regions (Lecordier *et al.,* 1993). Stored as a soluble protein within the dense granules, it is secreted into the PV following invasion. In this compartment, it traffics to the PVM, spans it and exposes its N-terminal region to the host cytosol (Gendrin et al., 2008; Lecordier *et al.,* 1999). During the chronic phase of infection GRA5 as well as GRA3 and GRA7 were found to localize in the outer membrane of the cyst wall (Torpier *et al*., 1993; Ferguson, 2004; Lemgrüber *et al*., 2011). In addition to its structural role, GRA5 was described as a modulator of human dendritic cells' migration, suggesting its possible involvement in the parasite dissemination *in vivo* (Persat *et al.,* 2012).

A collaboration with the team of David Bzik (Geisel School of Medicine at Dartmouth, Lebanon NH, USA) allows the access of our team to a collection of *T. gondii* type I (RH) and type II (*Prugniaud*) Δ*gra* null mutants ($GRA1_{II}$, $GRA2_{I,II}$-$GRA14_{I,II}$). These mutants were obtained after the generation of Δ*ku80* knockout strains in both the RH and the Prugniaud strains (Fox *et al.,* 2009; 2011). Loss of the non-homologous end-joining DNA repair pathway in these strains increases the efficiency of double-crossover homologous recombination at any given locus (as long as it is not vital) and allows rapid construction of knock-out mutants (Fox *et al.,* 2009; 2011).

Using Δ*gra* knockout *T. gondii* parasites and *in vitro* models, the aim of my PhD was to answer to the two following questions:

1/ are there some GRA proteins, including GRA5, which are important for the parasite invasion and proliferation?

2/ is GRA5 involved in the biogenesis of cysts?

In collaboration with the team of David Bzik, we performed a systematic comparative analysis of the behavior (invasion, proliferation, virulence) of Δ*gra* null mutants constructed in the virulent type I RH strain. This work was published in PLoS One, in July 2016: Rommereim, L*., **Bellini V.***, *et al.,* 2016, PLoS One, **11**(7): e0159306 (*, equal contributions)

Using the cyst-forming type II *Prugniaud strain,* I investigated the role of GRA5 in parasite invasion/proliferation and in the PV differentiation into a cyst-like structure (Bellini *et al*., in preparation).

During this work, I also collaborated with people of M.F. Delauw's team on the validation of a protocol for the collection of mouse and rat brains and their use for the quantification of Toxoplasma cysts. This work was published in the web publication BioProtocol, in April 2015:

Bellini, V. *et al*., bio-protocol.org/e1439, *Apr 05, 2015. Vol 5, Iss 7.*
Note: all the BioProtocols will be soon referenced in PubMedCentral.

The three papers to which I have contributed during my PhD will be presented in the above order in the following "Results" section.

RESULTS

Phenotypes Associated with Knockouts of Eight Dense Granule Gene Loci (GRA2-9) in Virulent *Toxoplasma gondii*

Leah M. Rommereim[1]*, Valeria Bellini[2,3]*, Barbara A. Fox[1], Graciane Pètre[2,3], Camille Rak[2,3], Bastien Touquet[2,3,4], Delphine Aldebert[2,3], Jean-François Dubremetz[5,6], Marie-France Cesbron-Delauw[2,3], Corinne Mercier[2,3], David J. Bzik[1]

1 Department of Microbiology and Immunology, The Geisel School of Medicine at Dartmouth, Lebanon, NH, United States of America,
2 Laboratoire Adaptation et Pathogénie des Micro-organismes, Université Grenoble Alpes, Université Joseph Fourier, Grenoble, France,
3 Centre National de la Recherche Scientifique, Unité Mixte de Recherche 5163, Grenoble, France,
4 Station de Cytométrie en Images en Microbiologie (SCIMI plateforme), Grenoble, France,
5 Université Montpellier 2, Place Eugène Bataillon, Montpellier, France,
6 Centre National de la Recherche Scientifique, Unité Mixte de Recherché 5235, Montpellier, France

***** These authors contributed equally to this work.

*July 26, 2016. PloS One. **11**: e0159306.*

During host cell invasion *T. gondii* forms a parasitophorous vacuole, an important compartment that ensures its replication and survival. The dense granule proteins have been characterized as major components of the PV: secreted during invasion they are massively accumulated at the PV membranes and within the PV lumen. To date several GRAs have been described, but the role of most of them remains unknown. This work, performed in collaboration with Leah Rommereim and David Bzik, from the Geisel School of Medicine at Dartmouth, Lebanon, NH, USA, aimed to study the essentiality and the involvement of 10 GRA proteins (GRA1-GRA10) in parasite infection, replication and virulence.

The Δ*gra* mutants were generated by Bzik and collaborators in the virulent type I RH strain. Specifically, they obtained 8 single Δ*gra* knockouts (Δ*gra2* to Δ*gra9*) and 5 double knocked-out parasite lines, respectively Δ*gra2*Δ*gra4*, Δ*gra2*Δ*gra6*, Δ*gra4*Δ*gra6*, Δ*gra*3Δ*gra*5, and Δ*gra*3Δ*gra*7. Their failure to generate Δ*gra1* and Δ*gra10* mutants suggested an essential role of these two proteins. All the other single gene knockouts were obtained. The infection and replication abilities of this set of Δ*gra* knocked-out parasites were observed using *in vitro* models. The first results did show that none of these mutants exhibited any particular replication defect. To confirm this phenotype, we performed a high throughput immunofluorescence analysis of cells infected with these mutants in order to screen larger samples of more than 5,000 PVs. We detected both the host-cell- and the parasite nuclei using Hoechst 33342, while both the vacuolar space and the parasites were labeled with anti-GRA1 antibody. The entire surface of each well was scanned with an Olympus IX8 inverted microscope equipped with a black and white Orca ER Camera and a LUCPLLN 20xPH1 objective and images of all the vacuoles were acquired. The ScanR software was used to count the total number of vacuoles (based on their GRA1 labeling) and the number of intracellular parasites per vacuole (based on their nuclear staining). The proliferation rate was calculated as the percentage of vacuoles containing 1, 2, 4, 8, or 16 parasites, while the invasion rate was calculated as the total number of vacuoles divided by the number of analyzed cells (counted on the basis of their nuclear staining).

This systematic analysis of the 8 Δ*gra* mutants demonstrated that the absence of any of these single GRA protein does not affect parasite replication. In contrast, Δ*gra2*, Δ*gra4*, Δ*gra5*, Δ*gra6,* Δ*gra7* and Δ*gra9* exhibited a decreased rate of invasion. Importantly, the study performed on the double *gra* knocked-out parasites showed a significant reduced replication rate for the Δ*gra4*Δ*gra6*, Δ*gra*3Δ*gra*5, and Δ*gra*3Δ*gra*7 strains, suggesting that some GRA proteins could play redundant roles.

During intracellular development of the vacuole, a stable and functional MNN dependent on both GRA2 and GRA6 (Mercier *et al.,* 2002) develops within the PV, while GRA7 is involved in the formation of HOST structures for host lipids import (Coppens *et al.,* 2006). To study the morphology of the vacuoles formed by these Δ*gra* mutants, transmission electron microscopy was performed on infected cells cultured either in complete- or lipid-free medium. No particular change was observed for the mutants, except for Δ*gra2*, Δ*gra6* and Δ*gra7* parasites. Confirming the phenotypes previously

described (Mercier *et al.,* 2002), the vacuoles formed by the Δ*gra2* and Δ*gra6* mutants showed destabilization of the MNN tubular structures into aggregated material and small vesicles, respectively. In contrast, we showed, for the first time, that vacuoles depleted in GRA7 displayed hyper-formation of the MNN. This result suggested that GRA7, in association with GRA2 and GRA6, could have a role in the regulation of the MNN formation and/or functions.

The GRA proteins are heavily expressed at the tachyzoite stage and they play important roles for the parasite virulence during the acute stage of infection. *In vivo* studies on CD1 mice were performed using single- and double Δ*gra* knocked-out parasites. All the mice infected by the Δ*gra* mutants died 10 days (more or less) post-infection, revealing no difference between the mutants. These results contrasted with previous studies published on Δ*gra*,2 Δ*gra6* and Δ*gra7* (Mercier *et al.,* 1998b; Alaganan *et al.,* 2014; Shastri *et al.,* 2014), and which showed that the quantity of injected tachyzoites as well as the site of infection have to be considered for this kind of *in vivo* test of parasite virulence. Together, these observations demonstrated that, during acute infection, individual GRA2-9 do not have particular functions but that, in complexes, they could play redundant and necessary roles.

PLOS | ONE

RESEARCH ARTICLE

Phenotypes Associated with Knockouts of Eight Dense Granule Gene Loci (*GRA2-9*) in Virulent *Toxoplasma gondii*

Leah M. Rommereim[1☯¤a], Valeria Bellini[2,3☯¤b], Barbara A. Fox[1], Graciane Pètre[2,3], Camille Rak[2,3], Bastien Touquet[2,3,4], Delphine Aldebert[2,3], Jean-François Dubremetz[5,6], Marie-France Cesbron-Delauw[2,3¤b], Corinne Mercier[2,3¤b], David J. Bzik[1]*

1 Department of Microbiology and Immunology, The Geisel School of Medicine at Dartmouth, Lebanon, NH, United States of America, **2** Laboratoire Adaptation et Pathogénie des Micro-organismes, Université Grenoble Alpes, Université Joseph Fourier, Grenoble, France, **3** Centre National de la Recherche Scientifique, Unité Mixte de Recherche 5163, Grenoble, France, **4** Station de Cytométrie en Images en Microbiologie (SCIMI platform), Grenoble, France, **5** Université Montpellier 2, Place Eugène Bataillon, Montpellier, France, **6** Centre National de al Recherché Scientifique, Unité Mixte de Recherché 5235, Montpellier, France

☯ These authors contributed equally to this work.
¤a Current address: Institute for Systems Biology, Seattle, WA, United States of America
¤b Current address: Laboratoire Techniques de l'Imagerie Médicale et de la Complexité Informatique, Mathématiques et Applications (TIMC-IMAG), CNRS UMR 5525, Université Grenoble Alpes, Grenoble, France
* David.J.Bzik@dartmouth.edu

OPEN ACCESS

Citation: Rommereim LM, Bellini V, Fox BA, Pètre G, Rak C, Touquet B, et al. (2016) Phenotypes Associated with Knockouts of Eight Dense Granule Gene Loci (*GRA2-9*) in Virulent *Toxoplasma gondii*. PLoS ONE 11(7): e0159306. doi:10.1371/journal.pone.0159306

Editor: Ira J Blader, University at Buffalo, UNITED STATES

Received: February 28, 2016

Accepted: June 30, 2016

Published: July 26, 2016

Data Availability Statement: All relevant data are within the paper and its Supporting Information files.

Funding: The authors acknowledge the contribution of J. Surre and P. Girard (Bachelor internships). This work was supported by National Institutes of Health (NIH), USA, Grants AI108489, AI105563, AI104514, and AI097018 to David J. Bzik; Labex Parafrap (ANR-11-LABX-0024) and Fondation pour la Recherche Médicale to Marie-France Cesbron-Delauw; Cluster 10, Région Rhône-Alpes and ANR 11 EMMA 03201 to Corinne Mercier. Leah M. Rommereim was a trainee on NIH training grants

Abstract

Toxoplasma gondii actively invades host cells and establishes a parasitophorous vacuole (PV) that accumulates many proteins secreted by the dense granules (GRA proteins). To date, at least 23 GRA proteins have been reported, though the function(s) of most of these proteins still remains unknown. We targeted gene knockouts at ten *GRA* gene loci (*GRA1-10*) to investigate the cellular roles and essentiality of these classical GRA proteins during acute infection in the virulent type I RH strain. While eight of these genes (*GRA2-9*) were successfully knocked out, targeted knockouts at the *GRA1* and *GRA10* loci were not obtained, suggesting these GRA proteins may be essential. As expected, the Δ*gra2* and Δ*gra6* knockouts failed to form an intravacuolar network (IVN). Surprisingly, Δ*gra7* exhibited hyper-formation of the IVN in both normal and lipid-free growth conditions. No morphological alterations were identified in parasite or PV structures in the Δ*gra3*, Δ*gra4*, Δ*gra5*, Δ*gra8*, *or* Δ*gra9* knockouts. With the exception of the Δ*gra3* and Δ*gra8* knockouts, all of the GRA knockouts exhibited defects in their infection rate *in vitro*. While the single GRA knockouts did not exhibit reduced replication rates *in vitro*, replication rate defects were observed in three double *GRA* knockout strains (Δ*gra4*Δ*gra6*, Δ*gra3*Δ*gra5* and Δ*gra3*Δ*gra7*). However, the virulence of single or double GRA knockout strains in CD1 mice was not affected. Collectively, our results suggest that while the eight individual GRA proteins investigated in this study (GRA2-9) are not essential, several GRA proteins may provide redundant and potentially important functions during acute infection.

5T32AI007363 and 2T32AI007519. Valeria Bellini was supported by a PhD fellowship from the Parafrap Labex. The funders had no role in study design, data collection and analysis, decision to publish, or preparation of the manuscript.

Competing Interests: The authors have declared that no competing interests exist.

Introduction

Toxoplasma gondii is an obligate intracellular protozoan pathogen capable of infecting any living nucleated cell [1]. As one of the most successful protozoan parasites in the group of cyst-forming *Apicomplexa*, *Toxoplasma* is estimated to chronically infect at least a third of the world's population [2]. Infections in immune-competent individuals are typically asymptomatic, though toxoplasmosis can cause severe pathological effects in immune privileged areas such as the eye or developing fetus [3], and toxoplasmosis is life-threatening in immunocompromised patients [4].

Toxoplasma enters host cells via a rapid active invasion mechanism [5] and utilizes the host cell plasma membrane to form, within the host cytosol, a distinct compartment termed the parasitophorous vacuole (PV), in which it replicates and divides [6–8]. *Toxoplasma* invasion and PV formation require three *Apicomplexa*-specific organelles: the micronemes, rhoptries and dense granules. The secreted microneme proteins (MICs) [9] aid in adhesion to the host cell and, with the secreted rhoptry neck proteins (RONs) [10], in formation of a moving junction through which the motile parasite penetrates the host cell. The rhoptry organelles also release rhoptry bulb proteins (ROPs) into the host cell cytosol during invasion. Many ROP proteins re-localize to the non-fusogenic [11] PV membrane (PVM), while other ROP proteins remain in the host cytoplasm or gain access to the host cell nucleus where they contribute to reprograming host gene expression [12].

Shortly after the formation of the PV, the dense granule proteins (GRAs) that are defined by their localization in electron dense granule organelles are massively secreted into the PV lumen [13–17]. A few proteins secreted by the dense granules exhibit homologies to proteins of known function such as cathepsin C [18], nucleoside triphosphate hydrolases (NTPases) [19, 20], an osteopontin-like protein [21], protease inhibitors [22, 23] and a lipolytic lecithin:cholesterol acyltransferase [24]. Yet, most GRA proteins do not have any identifiable gene homologues in species other than cyst-forming coccidians. Within the PV lumen, GRA2 initiates the formation of the membranous tubules that compose the intravacuolar network (IVN) and GRA6 stabilizes this network [25, 26], which is proposed to provide a scaffold for parasite replication [27, 28]. GRA7 aids in the formation of host organelle sequestering tubular structures (HOSTs), which are deep PVM invaginations that entrap single shortened host microtubules to direct host endocytic vacuoles to the PV for nutrient acquisition [29]. GRA7 also interacts with ROP2 and ROP4 [30] and acts in complex with ROP18 to bind host Immunity-related GTPase a6 (Irga6) [31], mediating resistance to a major interferon-γ (IFN-γ) triggered macrophage killing mechanism [32]. GRA22 was recently proposed to play a role in parasite egress [33]. GRA17 and GRA23 were identified as PVM-localized GRAs that mediate passive transport of small molecules [34]. Polymorphic type I GRA6 was recently shown to manipulate the host cell by activating the host transcription factor nuclear factor of activated T cells 4 (NFAT4) [35]. GRA5 increases the expression of CCR7 [36] and GRA25 induces the expression of CCL2 and C-X-C motif ligand 1 (CXCL1) [37]. Other GRA proteins are exported from the PV into the host cell cytosol and/or nucleus where they modify host cell signaling pathways [38]. This exported GRA protein class includes GRA15 [39], GRA16 [40], and GRA24 [41].

Genes encoding several GRA proteins identified in antigen-mapping studies have been previously deleted in virulent type I strains (GRA2, GRA5, GRA6, GRA7, GRA14 and GRA22) [25, 29, 31, 33, 42–44], or in low-virulence type II strains (GRA3, GRA4 and GRA6) [45, 46]. However, previous gene deletion studies in non-Δ*ku80* strains are complicated by frequent off-site mutation that could influence observed phenotypes [47].

In this study, we utilized the virulent type I Δ*ku80* strain that enables highly efficient and precise development of gene knockouts [46–48] or gene tagging [49] to target gene deletions at the

first ten *GRA* gene loci (*GRA1-10*). We isolated 8 of the 10-targeted knockouts (Δ*gra2-9*) and investigated invasion, growth, morphology and virulence phenotypes. Overall, our findings validate phenotypes associated with several previously reported *GRA* knockouts, and suggest that while GRA proteins (GRA2-9) are individually not essential, several of these GRA proteins are likely to provide redundant and potentially crucial functions during acute infection.

Materials and Methods

Primers

All oligonucleotide primers used in the development of plasmids for targeting gene deletions (S1 Table) and primers used in the validation of targeted gene deletions (S2 Table) are shown in the supplementary material. Sequences for primer design and validation of targeting plasmids were obtained from ToxoDB [www.toxodb.org] [50].

Plasmid Construction

Plasmids were developed using yeast recombination cloning that fused a ~1-kb 5' target flank, a ~2-kb hypoxanthine-xanthine-guanine-phosphoribosyltransferase (*HXGPRT*) selectable marker cassette and a ~1-kb 3' target flank with pRS416 by homologous crossovers at recombination junctions [48]. DNA elements for yeast recombination were amplified from type I RH (EP; ATCC 40050) genomic DNA. All targeting plasmids were validated by restriction enzyme digests and by DNA sequencing. The sequenced and fully annotated type I GT1 strain [www.toxodb.org] was used to identify GRA gene loci and type I sequences for targeting plasmid assembly. Plasmid pΔGRA1 was constructed by fusing the *HXGPRT* minigene cassette between a 1,095-bp 5' *GRA1* genomic target flank and a 940-bp 3' *GRA1* genomic target flank to delete nucleotides 5308191 to 5309090 of the *GRA1* locus on chromosome VIII annotated as TGGT1_270250. Plasmid pΔGRA2 was constructed by fusing the *HXGPRT* minigene cassette between a 1,136-bp 5' *GRA2* genomic target flank and a 1,025-bp 3' *GRA2* genomic target flank to delete nucleotides 814572 to 812564 of the *GRA2* locus on chromosome X annotated as TGGT1_227620. Plasmid pΔGRA2C was constructed by digesting pΔGRA2 with *Spe*I, followed by self-ligation to remove the *HXGPRT* minigene cassette. Plasmid pΔGRA3 was constructed by fusing the *HXGPRT* minigene cassette between a 950-bp 5' *GRA3* genomic target flank and a 860-bp 3' *GRA3* genomic target flank to delete nucleotides 988787 to 989625 of the *GRA3* locus on chromosome X annotated as TGGT1_227280. Plasmid pΔGRA3C was constructed by digesting pΔGRA3 with *Spe*I, followed by self-ligation to remove the *HXGPRT* minigene cassette. Plasmid pΔGRA4 was constructed by fusing the *HXGPRT* minigene cassette between a 1,130-bp 5' *GRA4* genomic target flank and a 988-bp 3' *GRA4* genomic target flank to delete nucleotides 1201331 to 1200129 of the *GRA4* locus on chromosome XI annotated as TGGT1_310780. Plasmid pΔGRA4C was constructed by digesting pΔGRA4 with *Spe*I, followed by self-ligation to remove the *HXGPRT* minigene cassette. Plasmid pΔGRA5 was constructed by fusing the *HXGPRT* minigene cassette between a 1,095-bp 5' *GRA5* genomic target flank and a 956-bp 3' *GRA5* genomic target flank to delete nucleotides 1753723 to 1754102 of the *GRA5* locus on chromosome V annotated as TGGT1_286450. Plasmid pΔGRA6 was constructed by fusing the *HXGPRT* minigene cassette between a 1,057-bp 5' *GRA6* genomic target flank and a 975-bp 3' *GRA6* genomic target flank to delete nucleotides 7195269 to 7194367 of the *GRA6* locus on chromosome X annotated as TGGT1_275440. Plasmid pΔGRA7 was constructed by fusing the *HXGPRT* minigene cassette between a 1,164-bp 5' *GRA7* genomic target flank and a 954-bp 3' *GRA7* genomic target flank to delete nucleotides 2582896 to 2585701 of the *GRA7* locus on chromosome VIIa, annotated as TGGT1_203310. Plasmid pΔGRA8 was constructed by fusing the *HXGPRT* minigene cassette between a 1,151-bp 5' *GRA8* genomic target flank and a 1,015-bp 3' *GRA8* genomic target flank

to delete nucleotides 1894848 to 1895699 of the *GRA8* locus on chromosome III annotated as TGGT1_354720. Plasmid pΔGRA9 was constructed by fusing the *HXGPRT* minigene cassette between a 1,110-bp 5' *GRA9* genomic target flank and a 971-bp 3' *GRA9* genomic target flank to delete nucleotides 5508787 to 5510441 of the *GRA9* locus on chromosome XII annotated as TGGT1_251540. Plasmid pΔGRA10 was constructed by fusing the *HXGPRT* minigene cassette between a 1,170-bp 5' *GRA10* genomic target flank and a 967-bp 3' *GRA10* genomic target flank to delete nucleotide 6215048 to 6217010 of the *GRA10* locus on chromosome VIII annotated as TGGT1_268900.

Cell and Parasite Cultures

All parasites cultures were maintained *in vitro* by serial passages in human foreskin fibroblast (HFF) monolayers (ATCC SCRC-1041.1) in Eagle's modified essential medium (EMEM) supplemented with 1% fetal bovine serum (FBS) at 36°C [51]. As specified in the text, certain experiments were performed using Dulbelcco's modified Eagle's medium (DMEM) supplemented with 10% FBS and 1% sodium pyruvate (D10 medium) or using lipid-free D10 medium (lfD10).

Gene Replacements and Deletions

All strains used or developed in this study are listed in Table 1. Parasites were transformed following previously described methods [47]. Gene replacements using the *HXGPRT* marker were selected in 25 μg/mL mycophenolic acid (MPA) and 50 μg/mL xanthine (MPA+X). *HXGPRT* deletion was selected using 200 μg/mL 6-thioxanthine (6TX). Genotype verification of precisely targeted gene replacement and deletion events was performed by PCR as previously described [47, 48].

Western Blots

Parasites were isolated from freshly lysed cultures and resuspended in Laemmli buffer. Proteins were separated by 13% SDS-PAGE (non-reduced conditions), transferred to nitrocellulose membranes and detected using the following primary antibodies: mAb TG17.179 anti-GRA2

Table 1. Strains used or developed in this study.

Strain	Parent Strain	Genotype
RHΔ*ku80Δhxgprt [48]*	RHΔ*ku80::HXGPRT [48]*	*Δku80Δhxgprt*
RHΔ*ku80Δgra2::HXGPRT*	RHΔ*ku80Δhxgprt*	*Δku80Δgra2::HXGPRT*
RHΔ*ku80Δgra3::HXGPRT*	RHΔ*ku80Δhxgprt*	*Δku80Δgra3::HXGPRT*
RHΔ*ku80Δgra4::HXGPRT*	RHΔ*ku80Δhxgprt*	*Δku80Δgra4::HXGPRT*
RHΔ*ku80Δgra5::HXGPRT*	RHΔ*ku80Δhxgprt*	*Δku80Δgra5::HXGPRT*
RHΔ*ku80Δgra6::HXGPRT*	RHΔ*ku80Δhxgprt*	*Δku80Δgra6::HXGPRT*
RHΔ*ku80Δgra7::HXGPRT*	RHΔ*ku80Δhxgprt*	*Δku80Δgra7::HXGPRT*
RHΔ*ku80Δgra8::HXGPRT*	RHΔ*ku80Δhxgprt*	*Δku80Δgra8::HXGPRT*
RHΔ*ku80Δgra9::HXGPRT*	RHΔ*ku80Δhxgprt*	*Δku80Δgra9::HXGPRT*
RHΔ*ku80Δgra2Δhxgprt*	RHΔ*ku80Δgra2::HXGPRT*	*Δku80Δgra2Δhxgprt*
RHΔ*ku80Δgra3Δhxgprt*	RHΔ*ku80Δgra3::HXGPRT*	*Δku80Δgra3Δhxgprt*
RHΔ*ku80Δgra4Δhxgprt*	RHΔ*ku80Δgra4::HXGPRT*	*Δku80Δgra4Δhxgprt*
RHΔ*ku80Δgra2Δgra4::HXGPRT*	RHΔ*ku80Δgra2Δhxgprt*	*Δku80Δgra2Δgra4::HXGPRT*
RHΔ*ku80Δgra2Δgra6::HXGPRT*	RHΔ*ku80Δgra2Δhxgprt*	*Δku80Δgra2Δgra6::HXGPRT*
RHΔ*ku80Δgra4Δgra6::HXGPRT*	RHΔ*ku80Δgra4Δhxgprt*	*Δku80Δgra4Δgra6::HXGPRT*
RHΔ*ku80Δgra3Δgra5::HXGPRT*	RHΔ*ku80Δgra3Δhxgprt*	*Δku80Δgra3Δgra5::HXGPRT*
RHΔ*ku80Δgra3Δgra7::HXGPRT*	RHΔ*ku80Δgra3Δhxgprt*	*Δku80Δgra3Δgra7::HXGPRT*

doi:10.1371/journal.pone.0159306.t001

(1:15,000) [16], mAb T6.2H11 anti-GRA3 (1:10,000) [52], rabbit anti-GRA4 (1:10,000) [53], mAb TG17.113 anti-GRA5 (1:5,000) [16], rabbit anti-GRA6 (1:20,000) [53], mAb BATO 214 anti-GRA7 (1:15,000) [54], mAb 3.2 anti-GRA8 (1:10,000) [55], rabbit anti-GRA9 (1:2,500) [56], rabbit anti-actin (1:10,000) [57] or mAb TG054 anti-SAG1 (1:15,000) [58] (antibodies purchased from the Biotem company, Apprieu, France or kindly provided by L. D. Sibley, Washington University School of Medicine, Saint-Louis, MO; D. Jacobs, Innogenetics-Fujirebio Europe N.V., Ghent, Belgium; G.E. Ward, University of Vermont College of Medicine, Burlington, VT; W. Daübener, Heinrich Heine Universität, Düsseldorf, Germany). Proteins were detected with horseradish peroxidase (HRP)-conjugated secondary antibodies (1:20,000; Jackson Immunoresearch Laboratories) and the peroxidase activity was visualized by chemiluminescence using the Supersignal ECL system (Pierce Chemical).

Indirect immunofluorescence

Confluent HFFs were grown on glass coverslips and infected overnight with parasites. For experiments using lipid free medium, HFFs were equilibrated in lfD10 and parasites were passed three times in lfD10 prior to infection experiments. Infected cells were fixed in 5% formaldehyde, permeabilized with 0.002% saponin and blocked in 5% goat serum-5% FBS (in Phosphate Buffered Saline (PBS)). Cells were then incubated with primary antibodies for 1 hr in 1% FBS, 0.002% saponin. Primary antibodies used in this study included mAbTG17.179 anti-GRA2 (1:500), mAb T6.2H11 anti-GRA3 (1:500), rabbit anti-GRA4 (1:500), rabbit anti-GRA6 (1:500), mAb BATO 214 anti-GRA7 (1:500), mAb 3.2 anti-GRA8 (1:500), rabbit anti-GRA9 (1:500), and mAb TG 05.54 anti-SAG1 (1: 500). Infected cells were washed and incubated for 1 h with the following secondary antibodies: goat anti-mouse IgG (H+L)-Alexa 488 (1:500, Jackson) or goat anti-mouse IgG (H+L) Alexa 594 (1:500, Jackson) or goat anti-rabbit IgG (H+L) Alexa 488 (1:500, Jackson). Coverslips were then incubated with 5 μg/mL Hoechst 33342 for 10 min to stain nuclei, mounted in Mowiol and observed using a 100X objective on an Axioplan II microscope (Zeiss). Images were acquired using a Zeiss black and white camera and the Axio Vision software (release 4.7.1).

Transmission Electron Microscopy (TEM)

Monolayers of HFFs were grown to confluence on Permanox slides, infected for 24 h in D10- or in lfD10 medium, rinsed with PBS, fixed for 2 h with glutaraldehyde diluted in 0.2 M $NaPO_4$ pH 7.4 and processed for TEM, as previously described [25]. To allow preservation of the IVN, the infected cells were flat embedded and sectioned en face.

Intracellular Replication and Infectivity Assays

The intracellular growth rate was determined in HFFs in a 30-hr growth assay. Freshly lysed parasites were filtered through a Nuclepore filter to remove host cell debris and used to infect HFFs at a multiplicity of infection (MOI) of ~ 0.1. An hour after infection the monolayer was washed with PBS and fresh medium was added to the culture. Cultures were prepared in duplicate. At 30 h post-infection the number of parasites/vacuole was scored from 250 PVs per parasite strain to determine the average number of parasites per vacuole in an HFF cell with a single PV. Samples were represented as the average number of parasite(s) per PV (± SEM). Replication rates were compared between parental and knockout strains using a Student's *t*-test, with significance being represented as a P value <0.05.

For high throughput replication and infectivity assays, HFF cells were plated in 96 well plates (10,000 cells per well). Cells were grown for 48 h, rinsed with PBS and 40,000 parasites of each strain (MOI ~1–2) were deposited into the wells (250 μL per well). Plates were spun at

400 rpm for 1 min, then incubated for 2 h to allow parasite invasion. After 3 washes in PBS, fresh D10 medium was added to each well and the plates were returned to culture for 24 h. The infected monolayers were washed with PBS, incubated with 5 μg/mL Hoechst 33342 for 10 min, rinsed, saturated and permeabilized for 15 min with 5% goat serum– 0.1% triton-X100 (PBS-T), and incubated for 45 min with mAb TG17.043 anti-GRA1 (1:500, Biotem) in PBS-T. After washes, cells were incubated with goat anti-mouse IgG-Alexa 488 (1:500, Jackson), washed again, and analyzed by high content screening microscopy using an Olympus IX8 inverted microscope equipped with a black and white Orca ER Camera, and a LUCPLLN 20xPH1 objective. Images of the entire surface of each well were analyzed using the ScanR software. The percentage of infected cells, the total number of parasites per PV as well as the percentage of PVs containing 1, 2, 4, 8, 16 parasites was determined for >5,000 PVs per strain. Statistical analyses were performed using a Student's *t*-test, with significance being represented as a *P*-value <0.05.

Ethics Statement

All animal experiments were performed in strict accordance with the U.S.A. Public Health Service Policy on Humane Care and Use of Laboratory Animals. Animals experiments were conducted in an AAALAC approved facility. All animal protocols (protocol bzik.dj2) were approved by the Institutional Animal Care and Use Committee (Dartmouth College: Animal Welfare Assurance Number #A3259-01). The humane endpoint of weight loss was used to determine when animals were euthanized ($\geq$ 17% body weight loss). Animals were monitored daily until weight loss occurred then animals were monitored at least twice a day. If the humane endpoint was reached, animals were euthanized using CO_2 and additionally by cervical dislocation. All efforts, including providing diet gel recovery to mice with weight loss, were made to minimize suffering.

Acute infection

Adult female CD1 mice were obtained from Charles River Laboratory and mice were maintained in Techniplast Seal Safe mouse cages on vent racks and provided with enrichment materials at the Dartmouth-Hitchcock Medical Center (Lebanon, NH) mouse facility. Acute virulence was determined by a single intraperitoneal injection of the indicated numbers of tachyzoites into groups of four to eight week old female CD-1 mice (17-21g) per experiment. Studies were done in a blinded manner to minimize subjective bias. No unexpected deaths occurred during experiments. Survival was monitored for 30 days and the percentage of surviving animals was determined by the number of animals that survived / the total number of animals that were infected x 100. In all experiments, plaque forming units (PFUs) to tachyzoite ratios were determined at the time of parasite inoculation to verify infectivity of parasite preparations. Survival was analyzed by the Kaplan-Meier method and curves were compared using the log rank (Mantel-Cox) test in GraphPad Prism.

Results

Targeted deletion of GRA2, GRA3, GRA4, GRA5, GRA6, GRA7, GRA8, and GRA9 gene loci

To further investigate the role of the first 10 historically identified GRA proteins (*GRA1-10*), we precisely targeted knockouts at each of these unique *GRA* gene loci using the virulent type I genetic background deficient in nonhomologous end-joining [48]. Gene knockout targeting plasmids were constructed according to the representative pΔGRA targeting plasmid shown in

Fig 1A. These targeting plasmids position the *HXGPRT* selectable marker between the 5' and 3' DNA flanks of the *GRA* gene of interest, thereby replacing the GRA protein coding sequence with the *HXGPRT* selectable marker [59].

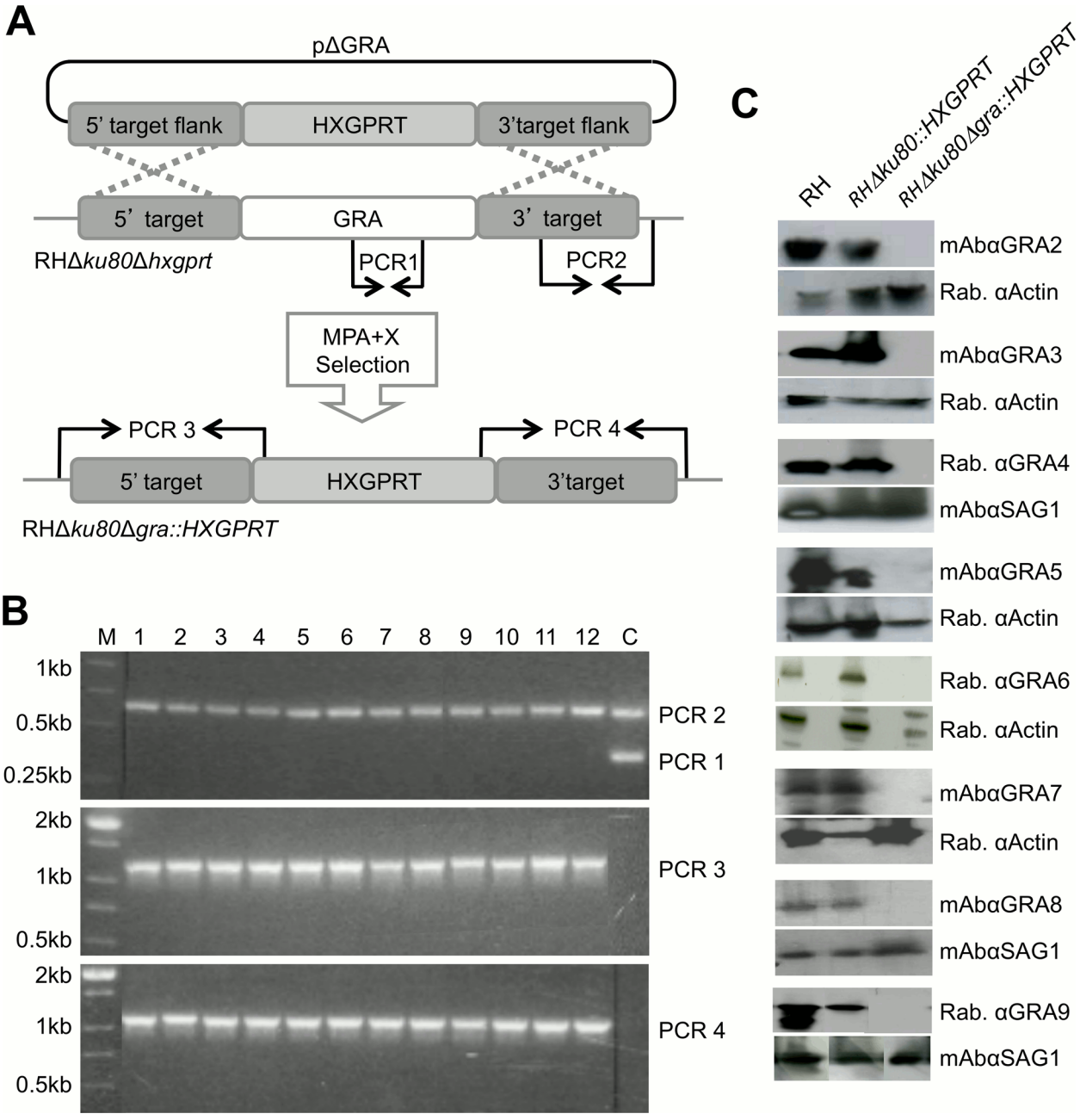

Fig 1. Construction and validation of the single *GRA2-9* knockout strains. A) Strategy for disruption of a *GRA* gene locus by double crossover homologous recombination in type I RHΔ*ku80*Δ*hxgprt* using a plasmid, pΔGRA, engineered to contain the 5' and 3' target flanks surrounding the *HXGPRT* selectable marker. Successful recombination events were selected by mycophenolic acid plus xanthine (MPA+X). This strategy is representative of each of the gene knockout attempts. B) Validation of the Δ*gra4* targeted gene deletion by PCR. The control parental strain is positive for PCR 1 (~ 380 bp) and PCR 2 (~ 670 bp) but negative for PCR 3 (~ 1,100 bp) and PCR4 (~ 1,200 bp). Clones 1–12 exhibit the banding pattern of a targeted Δ*gra4* gene knockout,. M: DNA size ladder. C) Western blot validation of the deletion of GRA2-9. Cell lysates from the equivalent of 2 x 10^7 parasites were loaded per lane, separated on a 13% SDS-PAGE (non-reduced conditions), probed with primary antibodies (indicated on the side of the gels), then with goat anti-mouse IgG or goat anti-rabbit IgG, both coupled to peroxidase and visualized by chemiluminescence.

doi:10.1371/journal.pone.0159306.g001

Following transfection into the RHΔ*ku80*Δ*hxgprt* parental strain [48] and MPA+X selection, we isolated knockout strains deleted for *GRA2* (Δ*gra2*), *GRA3* (Δ*gra3*), *GRA4* (Δ*gra4*), *GRA5* (Δ*gra5*), *GRA6* (Δ*gra6*), *GRA7* (Δ*gra7*), *GRA8* (Δ*gra8*), and *GRA9* (Δ*gra9*). Knockouts at the *GRA1* and *GRA10* loci were not obtained despite repeated transfection-selection attempts. The genotypes of the Δ*gra2-9* knockout strains (Table 1) were validated by PCR as shown in Fig 1B for the Δ*gra4* strain. The deletion of each GRA protein was also confirmed by western blot (Fig 1C), and also by indirect immunofluorescence in HFFs infected overnight (Fig 2).

The loss of single GRA genes does not affect the replication rate

GRA proteins have been proposed to facilitate interactions with the host cell and to potentially mediate nutrient acquisition [60]. We used two different methodologies to investigate whether GRA2-9 are necessary for parasite growth *in vitro*. First, we infected HFFs with each of the knockout strains and monitored the parasite replication rate by directly counting the number of parasites per PV in 250 PVs at 30 h post-infection by light microscopy. Using this direct method, we did not observe any significant defect in replication rates determined by scoring the number of parasites per PV (Table 2).

To extend this analysis and potentially detect subtle growth defects by analyzing a larger sample size of more than 5,000 PVs, we used a high throughput automated immunofluorescence method to quantify the percentage of PVs containing 1, 2, 4, 8, 16 parasites and determine the average number of parasites per vacuole (replication rate), as well as the number of infected HFF cells (infection rate). The results confirmed the data shown in Table 2 revealing there was no significant reduction in the replication rate of single GRA knockout strains (Fig 3A), though the Δ*gra7* knockout did exhibit a slight increase in the percentage of PVs containing only 1 or 2 parasites. In contrast, a significant decrease in the infection rate was observed for the Δ*gra2*, Δ*gra4*, Δ*gra5*, Δ*gra6*, Δ*gra7*, and Δ*gra9* knockout strains (Fig 3B).

Alteration of the intravacuolar network after deletion of GRA2, GRA6 and GRA7

To test whether the absence of lipids in growth medium would reveal any distinct morphologic changes in the Δ*gra2-9* knockout strains, we infected HFFs in normal D10 medium or HFFs that were pre-equilibrated in lfD10 medium. Each of the *GRA* knockout strains developed normal appearing PVs in both D10 (Fig 2) and in lfD10 media as assessed by indirect immunofluorescence assays (Fig 4).

Therefore, we assessed the morphology of the parental and *GRA* knockout strains cultured *in vitro* in D10 or lfD10 media by transmission electron microscopy (TEM). In the Δ*gra2* (Fig 5A) and Δ*gra6* (data not shown) knockout strains the parasites, their dense granules and PVM appeared normal; however, no IVN was observed in mature PVs grown in normal D10 medium (Fig 5A and data not shown), confirming previously reported phenotypes [25]. The absence of IVN in the mature PV of Δ*gra2* and Δ*gra6* strains was also observed in lfD10 medium (Fig 5A and data not shown). Interestingly, the Δ*gra7* knockout exhibited an increase in the density of membranous tubules and vesicles that form the IVN of parasites grown both in D10 and lfD10 media (Fig 5A and 5B). No major morphologic changes in the parasites or their PV were observed in other *GRA* knockout strains cultured in normal D10 or delipidated lfD10 conditions (Fig 5 and data not shown).

Targeted double deletions of dense granule genes

We generated several double *GRA* knockout strains for GRA proteins that were previously reported to associate or co-localize [61] to assess whether these GRA proteins may provide

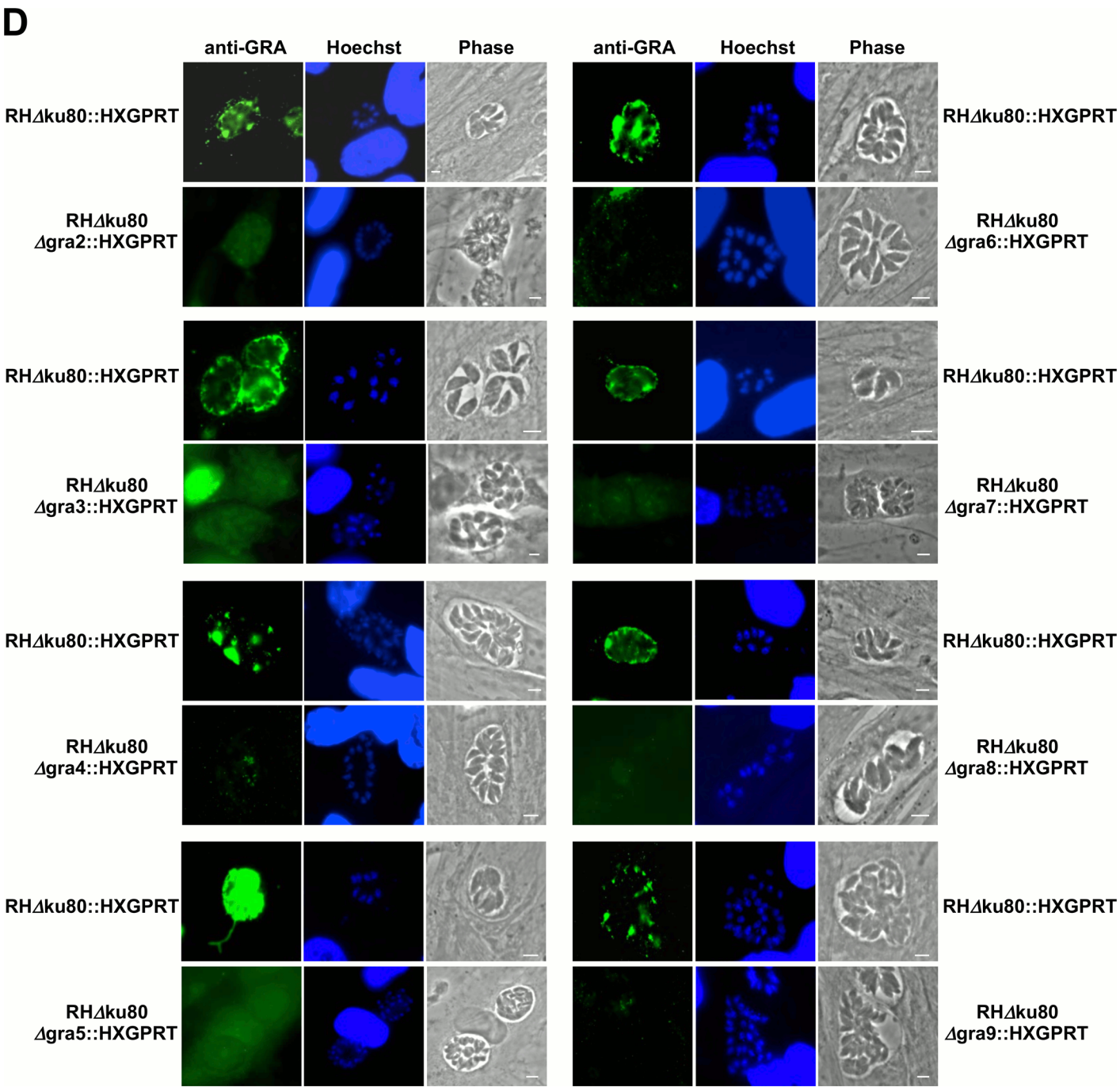

Fig 2. Indirect immunofluorescence assay verifies deletion of GRA proteins. IFA validation of the deletion of GRA2-9. HFFs were infected overnight with Δ*gra* knockout strains or with the parental strain. Infected cells were fixed, permeabilized with 0.002% saponin and incubated with the appropriate primary antibodies (see Material and Methods), followed by Alexa 488-coupled goat anti-mouse IgG or goat anti-rabbit IgG secondary antibodies. After labeling both the host- and parasite nuclei were revealed with Hoechst 33342; coverslips were mounted in Mowiol and observed by epifluorescence. To distinguish the shape of Δgra mutants' vacuoles in the absence of fluorescent signal, we chose to artificially increase their exposure time, which may lead to some artificial background noise. Scales: 5 μm.

doi:10.1371/journal.pone.0159306.g002

redundant functions. The *HXGPRT* marker present in the disrupted *GRA* locus was excised using the pΔGRAc plasmid and selection in 6-thioxanthine to generate the corresponding Δ*gra*Δ*hxgprt* strain (Fig 6A), and genotypes were validated by PCR (Fig 6B). The Δ*gra*Δ*hxgprt*

Table 2. Intracellular replication rate of single Δ*gra* knockout parasite strains.

Strain	Mean number of parasites per vacuole[a] (±SEM)	*P* (compared to the control strain)[b]	
		Significance	Control strain genotype
RHΔ*ku80::HXGPRT [48]*	19.85 ± 0.76		
RHΔ*ku80*Δ*gra2*::*HXGPRT*	19.06 ± 1.29	NS	RHΔ*ku80*::*HXGPRT*
RHΔ*ku80*Δ*gra3*::*HXGPRT*	17.12 ± 1.81	NS	RHΔ*ku80*::*HXGPRT*
RHΔ*ku80*Δ*gra4*::*HXGPRT*	18.94 ± 1.63	NS	RHΔ*ku80*::*HXGPRT*
RHΔ*ku80*Δ*gra5*::*HXGPRT*	22.44 ± 0.83	NS	RHΔ*ku80*::*HXGPRT*
RHΔ*ku80*Δ*gra6*::*HXGPRT*	20.82 ± 0.12	NS	RHΔ*ku80*::*HXGPRT*
RHΔ*ku80*Δ*gra7*::*HXGPRT*	23.38 ± 0.34	NS	RHΔ*ku80*::*HXGPRT*
RHΔ*ku80*Δ*gra8*::*HXGPRT*	19.72 ± 2.23	NS	RHΔ*ku80*::*HXGPRT*
RHΔ*ku80*Δ*gra9*::*HXGPRT*	21.60 ± 1.78	NS	RHΔ*ku80*::*HXGPRT*

[a] The number of parasites per vacuole was scored at 30 h PI in HFF cells containing a single PV.

[b] *P* value was determined by a Student's *t*-test. NS, not significant at $P \leq 0.05$.

doi:10.1371/journal.pone.0159306.t002

knockout strains were then used to generate double *GRA* knockout strains following the forward strategy illustrated in Fig 1A using MPA + X selection. Five double *GRA* knockout mutants were generated: Δ*gra2*Δ*gra4*, Δ*gra2*Δ*gra6*, Δ*gra4*Δ*gra6*, Δ*gra3*Δ*gra5* and Δ*gra3*Δ*gra7* (Table 1). Interestingly, despite several attempts, we failed to isolate a Δ*gra2*Δ*gra4*Δ*gra6* triple knockout strain even though each of the three corresponding double *GRA* knockout gene combinations was successfully isolated (Table 1).

Double GRA knockout strains display defects in replication rate

We measured the *in vitro* replication rates of the double *GRA* knockout strains via direct counting of parasites in > 250 PVs 30 h post-infection. The Δ*gra4*Δ*gra6*, Δ*gra3*Δ*gra5* and Δ*gra3*Δ*gra7* knockout strains exhibited mild defects in their *in vitro* replication rate (Table 3). No growth replication defects were observed for the Δ*gra2*Δ*gra4* or Δ*gra2*Δ*gra6* knockout strains (Table 3).

Deletion of GRA2-9 does not affect acute infection or virulence in vivo

Previous work identified several GRA proteins (GRA2, GRA6, and GRA7) as playing a role in type I parasite virulence during acute infection [25, 31, 37, 42]. To examine the virulence of the Δ*gra2*-9 knockout strains, we infected CD-1 female mice intraperitoneally with 100 tachyzoites (parental RH strain LD_{100} = 1 parasite) and monitored their survival. Absence of these individual GRA proteins (Fig 7A and 7B) or multiple GRA proteins (Fig 7C) did not increase or decrease virulence during acute infection. All mice succumbed to the infection within 8–12 days.

Discussion

The aim of this study was to apply a more systematic and reliable genetic approach using the virulent type I strain Δ*ku80* genetic background to examine or re-examine phenotypes associated with the absence of the dense granule proteins GRA1-10. Previously, only one of these ten GRA proteins (GRA7, [31]) was knocked out in a background that eliminates off-target mutations that could influence phenotypes in non-Δ*ku80* strains [47]. Using the virulent type I Δ*ku80* genetic model that enables efficient and precise targeted deletion [46–48], we successfully generated parasite strains containing single and double deletions of the *GRA* loci *GRA2-9*

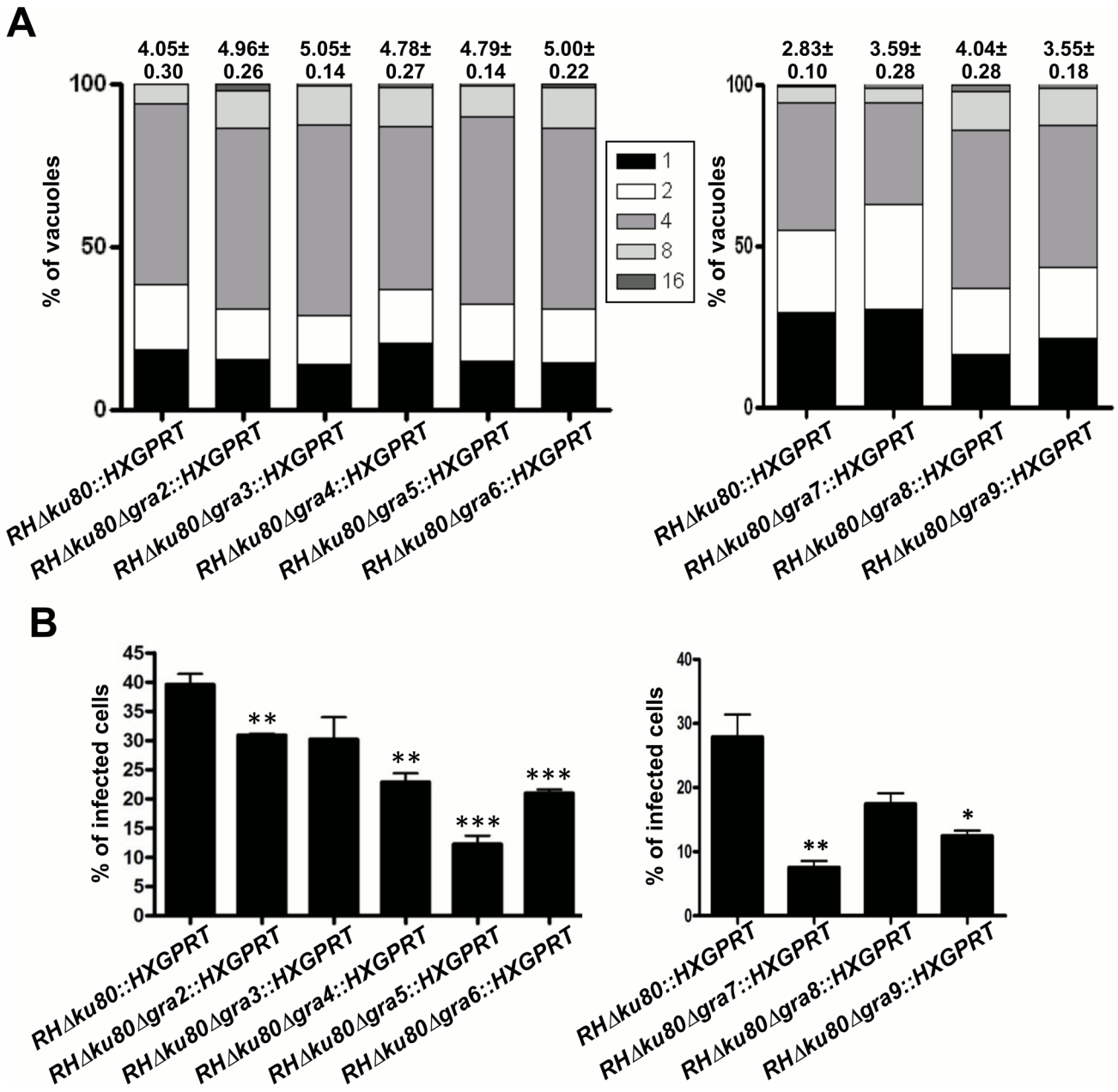

Fig 3. Replication and infection rates of single Δ*gra2*-9 gene knockout strains calculated by high throughput microscopy. A) Replication rate of each of the Δ*gra2*-9 strains compared to that of the parental strain. The percentage of PVs containing 1, 2, 4, 8 or 16 parasites per vacuole was calculated from three coverslips of infected HFFs. The numbers above each bar represent the average number of parasites per vacuole calculated from the total number obtained the three coverslips. The values are representative of one experiment out of three, which provided similar results. B) Percentage of HFFs infected by each Δ*gra2-9* knockout strain *versus* the parental Δ*ku80* strain. The infection rate was calculated from the number of PVs observed on three coverslips. Comparisons between the parental strain and each of the knockout strains were performed using a Student's *t*-test and asterisks indicate significant differences. *: $p = 0.0128$ for Δ*gra9*; **: $p = 0.0099$ for Δ*gra2*, 0.0022 for Δ*gra4*, 0.0051 for Δ*gra7*; ***: $p = 0.0003$ for Δ*gra5* and 0.0007 for Δ*gra6*. The values are representative of one experiment out of three, which provided similar results. The total number of PVs observed in A and B are respectively: parental Δ*ku80* strain, 5,757 (left panel) and 5,206 (right panel); Δ*gra2*, 5,200; Δ*gra3*, 5,173; Δ*gra4*, 6,176; Δ*gra5*, 5,845; Δ*gra6*, 6,311; Δ*gra7*, 5,165; Δ*gra8*, 5,177; Δ*gra9*, 5,065.

doi:10.1371/journal.pone.0159306.g003

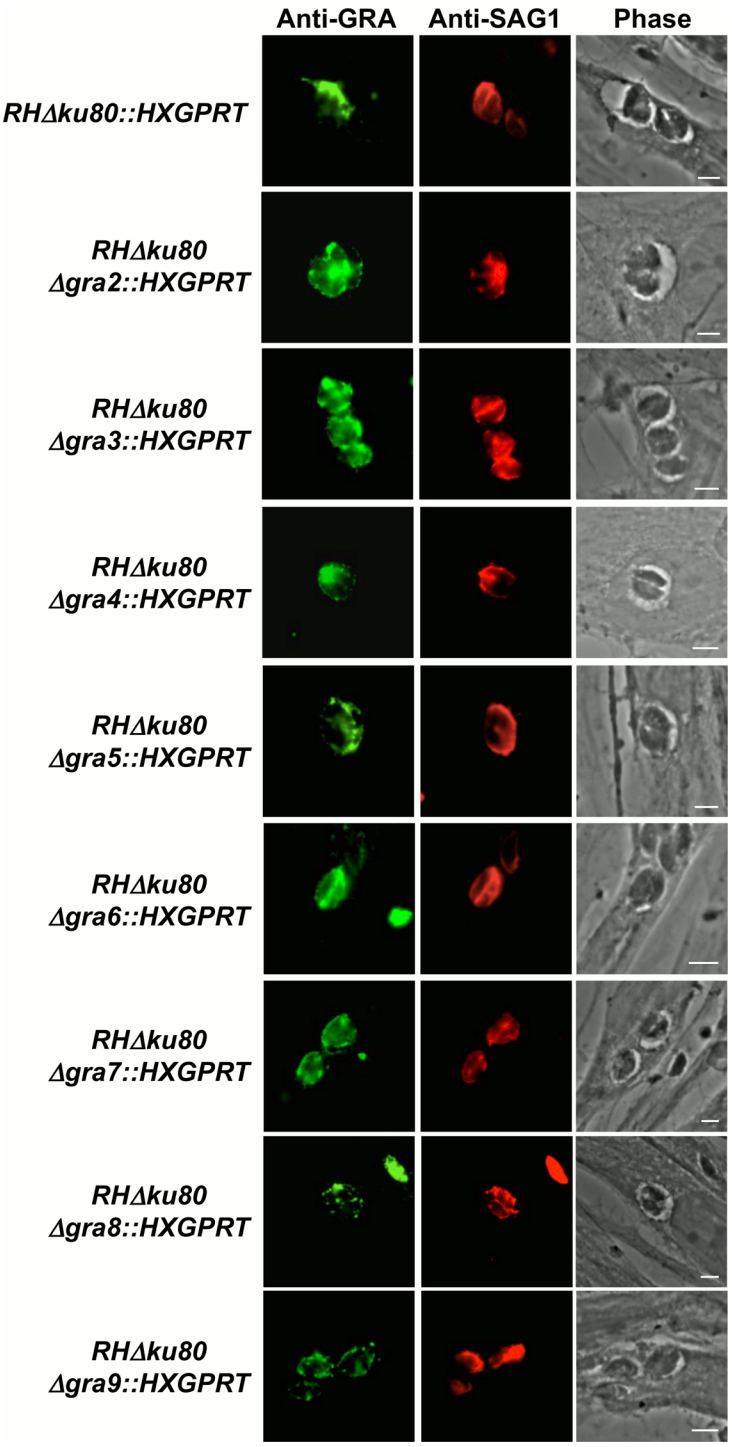

Fig 4. PV formation by Δ*gra2-9* single knockout strains in normal and lipid-free media. HFFs were pre-equilibrated in lipid-free D10 media (lfD10), then infected overnight with a single Δ*gra* knockout parasite strain or the Δ*ku80* parental strain. All parasite strains were passaged 3 times in lfD10 medium prior to infecting HFFs. Infected cells were fixed, permeabilized with 0.002% saponin, incubated with rabbit serum anti-GRA6 (all strains but Δ*gra6*) or with rabbit serum anti-GRA4 (Δ*gra6*) and with mAb anti-SAG1, visualized with goat anti-rabbit IgG coupled to Alexa 488 and goat anti-mouse IgG coupled to Alexa 594, mounted in Mowiol and observed by epifluorescence. To distinguish the shape of Δgra mutants' vacuoles in the absence of fluorescent signal, we chose to artificially increase their exposure time, which may lead to some background noise. Scales: 5 μm.

doi:10.1371/journal.pone.0159306.g004

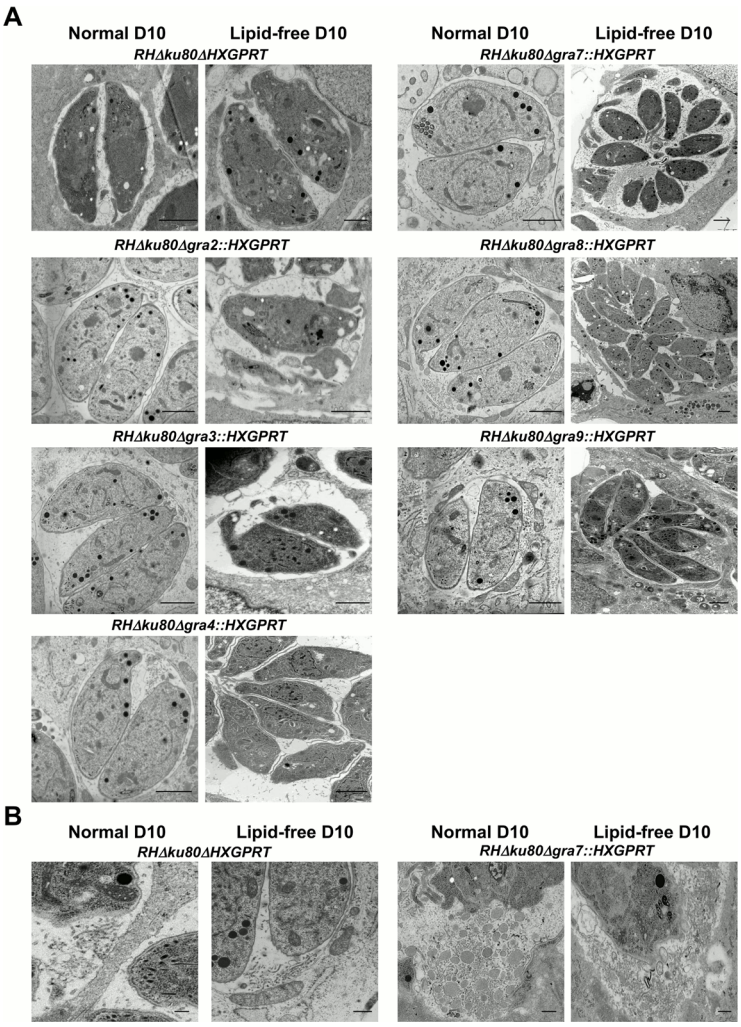

Fig 5. Visualization of the Δ*gra2-9* knockout parasites and PV morphology by transmission electron microscopy. A) HFFs and parasites were cultured in D10 medium ("Normal D10") or pre-equilibrated in lipid-free D10 medium ("Lipid-free D10"). Host cells were infected overnight with Δ*gra2-9* knockout or parental strains, fixed, and then processed for transmission electron microscopy. Scale: 2 μm. B) Magnification of the posterior end of an intracellular Δ*gra7* knockout parasite in "Normal D10" and in "Lipid-free D10" showing the hyper-formation of the IVN. Scales: 2 μm.

doi:10.1371/journal.pone.0159306.g005

(Table 1). This study is the first to report results on knockouts at the *GRA3*, *GRA4*, *GRA8* and *GRA9* loci, as well as results on the double *GRA* knockouts Δ*gra2*Δ*gra4*, Δ*gra4*Δ*gra6*, *gra3*Δ*gra5* and Δ*gra3*Δ*gra7* in the virulent type I RH genetic background.

While knockouts were readily isolated at the *GRA2-9* loci, we could not isolate a Δ*gra1* or a Δ*gra10* knockout, suggesting the possibility that these *GRA* genes are required for parasite growth or survival, though additional experiments would be necessary to validate this conclusion. Previously, RNA-knockdown of *GRA10* expression severely inhibited growth of the parasite *in vitro* [62]. *GRA1* encodes a GRA protein that localizes to the PV lumen as a calcium-binding [63], soluble protein [13]. This unique localization and the inability to knockout these genes in a type I strain suggests that GRA1 and GRA10 may participate in essential growth functions. The potential essentiality of the *GRA1* and *GRA10* genes could be further addressed in the future using either an inducible type I deletion scheme such as Cre-recombinase [64], an

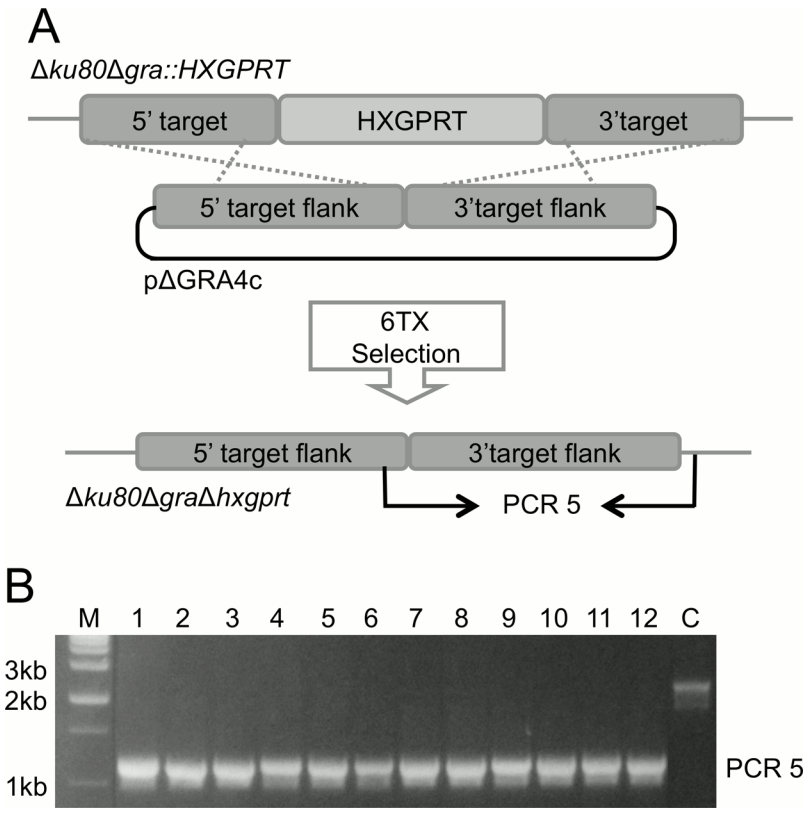

Fig 6. Strategy for removal of the *HXGPRT* selectable marker from a *GRA* gene locus. A) Removal of the *HXGPRT* selectable marker from RHΔ*ku80*Δ*gra*::*HXGPRT*. This strategy is representative of each of the *HXGPRT* removal attempts. Following transfection with an *HXGPRT*-excised plasmid, clones lacking *HXGPRT* but containing the 5' and 3' flanking regions of the original *GRA* locus were generated by double-crossover homologous recombination, using 6TX selection. B) Validation of the *HXGPRT* removal from the *gra4* gene locus. The parental strain exhibits a PCR5 amplicon of ~ 2,300 bp, corresponding to a DNA fragment that includes the *HXGPRT* coding sequence. Clones 1–12 exhibit a PCR5 amplicon of ~ 1,100 bp, which corresponds to the removal of *HXGPRT*. M: DNA size ladder; C: control parental strain.

doi:10.1371/journal.pone.0159306.g006

inducible type I expression scheme [65], the CRISPR (clustered regularly interspaced short palindromic repeats)/CAS9 technology [66], or alternatively to apply the recently developed type II Δ*ku80* genetic model [46] which exhibits extremely rare or undetectable off-site targeting in comparison to type I Δ*ku80* genetic models [47].

Table 3. Intracellular replication rate of double Δ*gra* knockout parasite strains.

Strain	Mean number of parasites per vacuole[a] (±SEM)	*P* (compared to the control strain)[b]	
		Significance	Control strain genotype
RHΔ*ku80*::*HXGPRT (48)*	19.85 ± 0.76		
RHΔ*ku80*Δ*gra2*Δ*gra4*::*HXGPRT*	16.89 ± 1.12	NS	RHΔ*ku80*::*HXGPRT*
RHΔ*ku80*Δ*gra2*Δ*gra6*::*HXGPRT*	18.97 ± 0.56	NS	RHΔ*ku80*::*HXGPRT*
RHΔ*ku80*Δ*gra4*Δ*gra6*::*HXGPRT*	15.53 ± 0.68	S	RHΔ*ku80*::*HXGPRT*
RHΔ*ku80*Δ*gra3*Δ*gra5*::*HXGPRT*	14.14 ± 0.75	S	RHΔ*ku80*::*HXGPRT*
RHΔ*ku80*Δ*gra3*Δ*gra7*::*HXGPRT*	14.85 ± 0.60	S	RHΔ*ku80*::*HXGPRT*

[a] The number of parasites per vacuole was scored at 30 h post-infection in HFF cells containing a single PV.

[b] *P* value was determined by a Student's T-test. S, significant at $P \leq 0.05$; NS, not significant.

doi:10.1371/journal.pone.0159306.t003

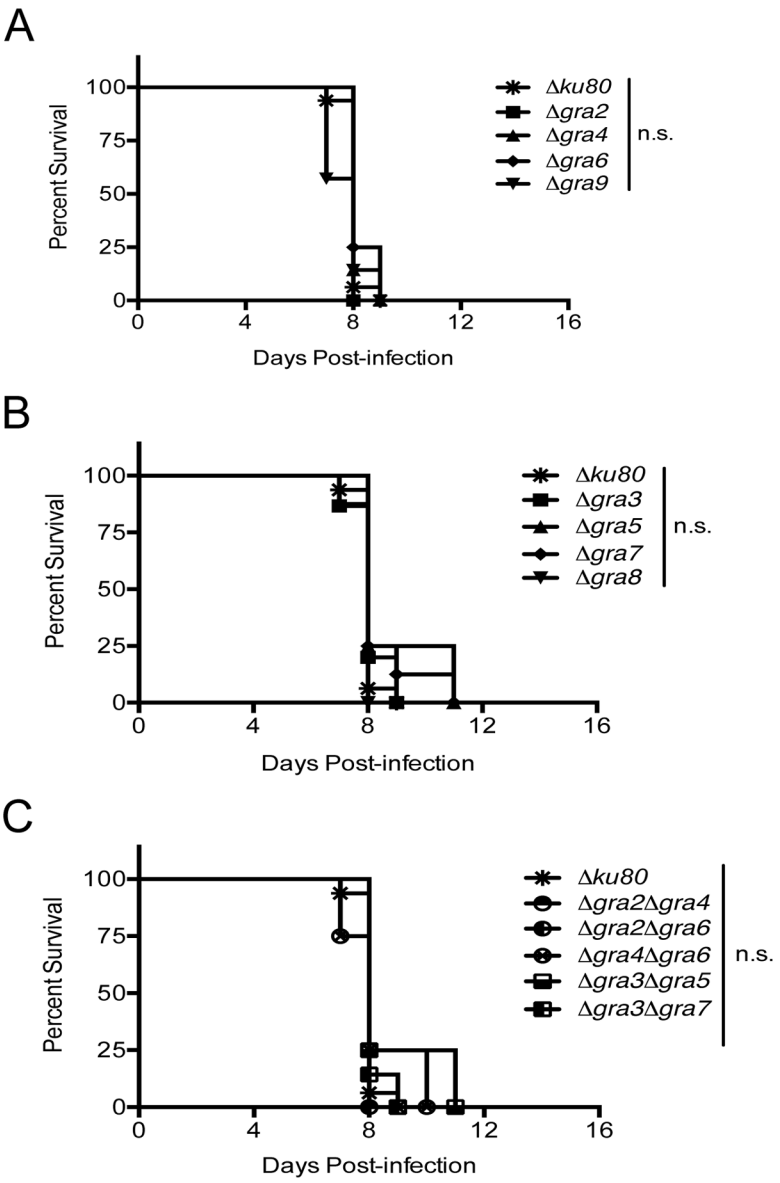

Fig 7. Virulence of single and double *GRA* knockout strains in CD1 mice. One hundred tachyzoites of the parental (Δ*ku80*) or knockout (Δ*gra)* strains were injected intraperitoneally (i.p.) into 8 week old female CD1 mice and survival was followed for 30 days (n = 8 for Δ*gra3*, Δ*gra4*, Δ*gra7*, Δ*gra9*, Δ*gra3*Δ*gra5* and Δ*gra3*Δ*gra7*, n = 4 for Δ*gra2*, Δ*gra5*, Δ*gra6*, Δ*gra8*, Δ*gra2*Δ*gra4*, Δ*gra2*Δ*gra6*, and Δ*gra4*Δ*gra6*). A) Survival of mice infected with parasites containing single *GRA* knockouts for IVN-localized GRA proteins. B) Survival of mice infected with parasites containing single *GRA* knockouts for PVM-localized GRA proteins. C) Survival of mice infected with parasites containing double *GRA* knockouts. Significance was determined by a Student's t-test comparing the knockout strain with the parental.

doi:10.1371/journal.pone.0159306.g007

Each of the GRA2-9 proteins contains either a transmembrane hydrophobic alpha-helix or amphipathic alpha-helices [67] that allow for insertion into and localization at the PVM and/or the IVN membranes. In addition, GRA2 and GRA6 induce formation and maturation of the IVN [25, 26] GRA7 was previously identified as a GRA protein possessing the ability to tubulate membranes *in vitro* [29]. We examined the parasite and PV morphologies of single *GRA* knockout strains cultured in both normal D10- and lipid free lfD10 media by indirect

immunofluorescence and TEM. Interestingly, any phenotype observed in the D10 medium was also present in the delipidated lfD10 medium. For all single *GRA* knockout strains the parasites, their dense granules and their PVM appeared normal in D10 as well as in lfD10 medium. Any morphological differences in the knockouts occurred only in the IVN structures, reinforcing the importance of certain GRA proteins as key regulators of the formation and maintenance of the IVN. In corroboration with previous reports [25], the Δ*gra2* and the Δ*gra6* knockout strains lacked an IVN in D10 and in delipidated lfD10 media. In contrast, the Δ*gra7* knockout strain exhibited a hyper-formation of the IVN in both D10 and lfD10 media. TEM images of a previously reported Δ*gra7* knockout strain [31] also suggests the possibility of hyper-formation of the IVN, although additional studies are necessary to conclusively determine the magnitude and significance of this phenotype. While GRA2 and GRA6 are associated with the IVN membranes, GRA7 associates with the PVM but not directly with the IVN membranes [68]. GRA7 was previously shown to deform liposomes into tubular membranes [29], as well as interact with GRA2 and GRA6 [61]. Collectively, these observations suggest that GRA7 may coordinately regulate IVN functions in conjunction with GRA2 and GRA6. The IVN membranes were also recently implicated in heterophagy since deletion of GRA2 and subsequent loss of the IVN decreased the rate at which parasites ingest host cytosolic proteins [69]. The complex relationship of GRA protein functions in the context of PV membrane functions and IVN membrane functions merits further investigation.

The high throughput growth assay revealed significant defects in the infection rate in the Δ*gra2*, Δ*gra4*, Δ*gra5*, Δ*gra6*, Δ*gra7*, and Δ*gra9* knockout strains. However, with the exception of a slight increase in percentage of Δ*gra7* parasite vacuoles with only 1 or 2 parasites, we did not detect any significant replication rate defect in any of the single *GRA* knockout strains by direct scoring of PVs or by automated high-throughput microscopy. GRA proteins traffic as soluble protein complexes with other GRA proteins to the IVN and PVM [61]. Once inserted into the membranes they can interact with similarly localized GRA [61] and ROP proteins [30, 31]. Therefore, to determine if GRA proteins could play redundant roles, we generated double *GRA* knockout strains of GRA proteins reported to reside in GRA complexes or of GRA proteins which share similar localization: Δ*gra2*Δ*gra4*, Δ*gra2*Δ*gra6*, Δ*gra4*Δ*gra6*, Δ*gra3*Δ*gra5* and Δ*gra3*Δ*gra7*. Of these double *GRA* knockout strains, we found that the Δ*gra4*Δ*gra6*, Δ*gra3*Δ*gra5* and Δ*gra3*Δ*gra7* knockouts displayed significant replication defects *in vitro*, though the corresponding single knockouts did not. These results suggest that certain GRA proteins most likely serve redundant function(s) during the tachyzoite stage, or potentially function in a similar pathway.

Though the canonical GRA proteins are heavily expressed during tachyzoite stages [70], they appear to be dispensable for acute virulence in type I strains. None of the single or double deletion strains that we tested exhibited any significant defects in virulence following intraperitoneal infection of CD-1 mice. In contrast, several type I *GRA* knockout strains were previously reported to exhibit detectable defects in acute virulence: Δ*gra2* [42], Δ*gra6* [25, 37], and Δ*gra7* [31]. In our virulence assays we injected mice with a dose of 100 tachyzoites using the intraperitoneal route. Previously, Mercier *et. al* injected many mice with 10 parasites to detect a minor defect in Δ*gra2* virulence [42]. In addition, the decreased virulence phenotype of type I Δ*gra6* and Δ*gra7* mutants was previously observed following the infection of mice at atypical sites (sub-cutaneously or in the footpad) [31, 37].

Based on their pattern of secretion and their localization at the PVM as well as at the IVN, the GRA2-9 proteins may play a role in host-pathogen interactions, nutrient acquisition or vacuole integrity. While we could isolate double GRA knockouts of any double combination of Δ*gra2*, Δ*gra4*, and Δ*gra6*, we could not isolate the triple Δ*gra* knockout—Δ*gra2*Δ*gra4*Δ*gra6*. Collectively, our results suggest that while GRA2-9 individually provide non-essential

functions for acute infection, some of these GRA proteins in complexes are likely to play redundant but necessary roles during acute infection. Additional experiments are still necessary to further define these functions.

The *GRA2-9* genes characterized in this study may play essential roles during transition to or growth in other life stages such as the development of tissue cysts that establish chronic infection. Most of the GRA2-9 proteins are expressed not only at the tachyzoite stage but also in the encysted bradyzoite stage [71–74]. Furthermore, a significant role for several of these GRA proteins (GRA3, GRA4, and GRA6) in type II strains has been reported [45, 46]. These findings suggest that a key role of PVM- and IVN-localized GRAs may be to prepare the PV for cyst formation or to provide essential functions during the encysted tissue stages [68]. Though the function of a large number of GRA proteins remains elusive, our study 1) has reported for the first time the *GRA3*, *GRA4*, *GRA8 and GRA9* knockouts as well as double knockouts for *GRA2-9* in the type I RH background and 2) has determined that GRA2-9 are not required for acute virulence following intraperitoneal infection of mice. Additionally we have identified that a subset of GRA proteins, which cooperate in complexes, appear to provide key functions associated with IVN formation or function.

Supporting Information

S1 Table. Primers used for generating Δ*gra* knockout strains.
(DOC)

S2 Table. Primers used for validating Δ*gra* knockout strains.
(DOC)

Acknowledgments

The authors acknowledge the following persons for sharing antibodies: L. D. Sibley, Washington University School of Medicine, Saint-Louis, MO; G.E. Ward, University of Vermont College of Medicine, Burlington, VT; W. Daübener, Heinrich Heine Universität, Düsseldorf, Germany; and D. Jacobs, Innogenetics-Fujirebio Europe N.V., Ghent, Belgium. They acknowledge the contribution of J. Surre and P. Girard (Bachelor internships). This work was supported by National Institutes of Health (NIH), USA, Grants AI108489, AI105563, AI104514, and AI097018 to D.J.B.; Labex Parafrap (ANR-11-LABX-0024) and Fondation pour la Recherche Médicale to M.F.C.D.; Cluster 10, Région Rhône-Alpes and ANR 11 EMMA 03201 to C. M. L.M.R. was a trainee on NIH training grants 5T32AI007363 and 2T32AI007519. V.B. was supported by a PhD fellowship from the Parafrap Labex.

Author Contributions

Conceived and designed the experiments: LMR BAF DJB CM. Performed the experiments: LMR BAF VB GP CR BT DA. Analyzed the data: LMR BAF VB JFD MFCD CM DJB. Wrote the paper: LMR VB BAF CM MFCD DJB.

References

1. Dubey JP. Advances in the life cycle of Toxoplasma gondii. International journal for parasitology. 1998; 28(7):1019–24. Epub 1998/09/02. PMID: 9724872.
2. Montoya JG, Liesenfeld O. Toxoplasmosis. Lancet. 2004; 363(9425):1965–76. Epub 2004/06/15. doi: 10.1016/S0140-6736(04)16412-X PMID: 15194258.
3. Montoya JG, Remington JS. Management of Toxoplasma gondii infection during pregnancy. Clin Infect Dis. 2008; 47(4):554–66. PMID: 18624630 doi: 10.1086/590149

4. Hill DE, Chirukandoth S, Dubey JP. Biology and epidemiology of Toxoplasma gondii in man and animals. Anim Health Res Rev. 2005; 6(1):41–61. PMID: 16164008.
5. Carruthers V, Boothroyd JC. Pulling together: an integrated model of Toxoplasma cell invasion. Current opinion in microbiology. 2007; 10(1):83–9. Epub 2006/07/14. doi: 10.1016/j.mib.2006.06.017 PMID: 16837236.
6. Hakansson S, Charron AJ, Sibley LD. Toxoplasma evacuoles: a two-step process of secretion and fusion forms the parasitophorous vacuole. The EMBO journal. 2001; 20(12):3132–44. Epub 2001/06/19. doi: 10.1093/emboj/20.12.3132 PMID: 11406590; PubMed Central PMCID: PMC150190.
7. Charron AJ, Sibley LD. Host cells: mobilizable lipid resources for the intracellular parasite Toxoplasma gondii. Journal of cell science. 2002; 115(Pt 15):3049–59. Epub 2002/07/16. PMID: 12118061.
8. Charron AJ, Sibley LD. Molecular partitioning during host cell penetration by Toxoplasma gondii. Traffic. 2004; 5(11):855–67. Epub 2004/10/14. doi: 10.1111/j.1600-0854.2004.00228.x PMID: 15479451.
9. Carruthers VB, Tomley FM. Microneme proteins in apicomplexans. Sub-cellular biochemistry. 2008; 47:33–45. Epub 2008/06/03. PMID: 18512339; PubMed Central PMCID: PMC2847500.
10. Besteiro S, Dubremetz JF, Lebrun M. The moving junction of apicomplexan parasites: a key structure for invasion. Cellular microbiology. 2011; 13(6):797–805. Epub 2011/05/04. doi: 10.1111/j.1462-5822.2011.01597.x PMID: 21535344.
11. Mordue DG, Hakansson S, Niesman I, Sibley LD. Toxoplasma gondii resides in a vacuole that avoids fusion with host cell endocytic and exocytic vesicular trafficking pathways. Experimental parasitology. 1999; 92(2):87–99. Epub 1999/06/15. PMID: 10366534.
12. Boothroyd JC, Dubremetz JF. Kiss and spit: the dual roles of Toxoplasma rhoptries. Nat Rev Microbiol. 2008; 6(1):79–88. PMID: 18059289.
13. Sibley LD, Niesman IR, Parmley SF, Cesbron-Delauw MF. Regulated secretion of multi-lamellar vesicles leads to formation of a tubulo-vesicular network in host-cell vacuoles occupied by Toxoplasma gondii. J Cell Sci. 1995; 108 (Pt 4):1669–77. PMID: 7615684.
14. Carruthers VB, Sibley LD. Sequential protein secretion from three distinct organelles of Toxoplasma gondii accompanies invasion of human fibroblasts. Eur J Cell Biol. 1997; 73(2):114–23. PMID: 9208224.
15. Dubremetz JF, Achbarou A, Bermudes D, Joiner KA. Kinetics and pattern of organelle exocytosis during Toxoplasma gondii/host-cell interaction. Parasitology research. 1993; 79(5):402–8. Epub 1993/01/01. PMID: 8415546.
16. Charif H, Darcy F, Torpier G, Cesbron-Delauw MF, Capron A. Toxoplasma gondii: characterization and localization of antigens secreted from tachyzoites. Experimental parasitology. 1990; 71(1):114–24. Epub 1990/07/01. PMID: 2191870.
17. Mercier C, Adjogble KD, Daubener W, Delauw MF. Dense granules: are they key organelles to help understand the parasitophorous vacuole of all apicomplexa parasites? International journal for parasitology. 2005; 35(8):829–49. Epub 2005/06/28. doi: 10.1016/j.ijpara.2005.03.011 PMID: 15978597.
18. Que X, Engel JC, Ferguson D, Wunderlich A, Tomavo S, Reed SL. Cathepsin Cs are key for the intracellular survival of the protozoan parasite, Toxoplasma gondii. The Journal of biological chemistry. 2007; 282(7):4994–5003. Epub 2006/12/14. doi: 10.1074/jbc.M606764200 PMID: 17164247.
19. Bermudes D, Peck KR, Afifi MA, Beckers CJ, Joiner KA. Tandemly repeated genes encode nucleoside triphosphate hydrolase isoforms secreted into the parasitophorous vacuole of Toxoplasma gondii. J Biol Chem. 1994; 269(46):29252–60. PMID: 7961894.
20. Asai T, Miura S, Sibley LD, Okabayashi H, Takeuchi T. Biochemical and molecular characterization of nucleoside triphosphate hydrolase isozymes from the parasitic protozoan Toxoplasma gondii. J Biol Chem. 1995; 270(19):11391–7. PMID: 7744775.
21. Cortez E, Stumbo AC, Saldanha-Gama R, Villela CG, Barja-Fidalgo C, Rodrigues CA, et al. Immunolocalization of an osteopontin-like protein in dense granules of Toxoplasma gondii tachyzoites and its association with the parasitophorous vacuole. Micron. 2008; 39(1):25–31. Epub 2007/10/13. doi: 10.1016/j.micron.2007.08.007 PMID: 17931871.
22. Pszenny V, Ledesma BE, Matrajt M, Duschak VG, Bontempi EJ, Dubremetz JF, et al. Subcellular localization and post-secretory targeting of TgPI, a serine proteinase inhibitor from Toxoplasma gondii. Molecular and biochemical parasitology. 2002; 121(2):283–6. Epub 2002/05/30. PMID: 12034464.
23. Morris MT, Coppin A, Tomavo S, Carruthers VB. Functional analysis of Toxoplasma gondii protease inhibitor 1. The Journal of biological chemistry. 2002; 277(47):45259–66. Epub 2002/09/14. doi: 10.1074/jbc.M205517200 PMID: 12228242.
24. Pszenny V, Ehrenman K, Romano JD, Kennard A, Schultz A, Roos DS, et al. A Lipolytic Lecithin:Cholesterol Acyltransferase Secreted by Toxoplasma Facilitates Parasite Replication and Egress. The

Journal of biological chemistry. 2016; 291(8):3725–46. Epub 2015/12/24. doi: 10.1074/jbc.M115.671974 PMID: 26694607; PubMed Central PMCID: PMC4759155.

25. Mercier C, Dubremetz JF, Rauscher B, Lecordier L, Sibley LD, Cesbron-Delauw MF. Biogenesis of nanotubular network in Toxoplasma parasitophorous vacuole induced by parasite proteins. Molecular biology of the cell. 2002; 13(7):2397–409. Epub 2002/07/23. doi: 10.1091/mbc.E02-01-0021 PMID: 12134078; PubMed Central PMCID: PMC117322.

26. Lopez J, Bittame A, Massera C, Vasseur V, Effantin G, Valat A, et al. Intravacuolar Membranes Regulate CD8 T Cell Recognition of Membrane-Bound Toxoplasma gondii Protective Antigen. Cell reports. 2015; 13(10):2273–86. Epub 2015/12/03. doi: 10.1016/j.celrep.2015.11.001 PMID: 26628378.

27. Magno RC, Lemgruber L, Vommaro RC, De Souza W, Attias M. Intravacuolar network may act as a mechanical support for Toxoplasma gondii inside the parasitophorous vacuole. Microscopy research and technique. 2005; 67(1):45–52. Epub 2005/07/19. doi: 10.1002/jemt.20182 PMID: 16025490.

28. Sibley LD, Krahenbuhl JL, Adams GM, Weidner E. Toxoplasma modifies macrophage phagosomes by secretion of a vesicular network rich in surface proteins. The Journal of cell biology. 1986; 103(3):867–74. Epub 1986/09/01. PMID: 3528173; PubMed Central PMCID: PMC2114290.

29. Coppens I, Dunn JD, Romano JD, Pypaert M, Zhang H, Boothroyd JC, et al. Toxoplasma gondii sequesters lysosomes from mammalian hosts in the vacuolar space. Cell. 2006; 125(2):261–74. PMID: 16630815.

30. Dunn JD, Ravindran S, Kim SK, Boothroyd JC. The Toxoplasma gondii dense granule protein GRA7 is phosphorylated upon invasion and forms an unexpected association with the rhoptry proteins ROP2 and ROP4. Infection and immunity. 2008; 76(12):5853–61. Epub 2008/09/24. doi: 10.1128/IAI.01667-07 PMID: 18809661; PubMed Central PMCID: PMC2583583.

31. Alaganan A, Fentress SJ, Tang K, Wang Q, Sibley LD. Toxoplasma GRA7 effector increases turnover of immunity-related GTPases and contributes to acute virulence in the mouse. Proceedings of the National Academy of Sciences of the United States of America. 2014; 111(3):1126–31. Epub 2014/01/07. doi: 10.1073/pnas.1313501111 PMID: 24390541; PubMed Central PMCID: PMC3903209.

32. Fentress SJ, Behnke MS, Dunay IR, Mashayekhi M, Rommereim LM, Fox BA, et al. Phosphorylation of immunity-related GTPases by a Toxoplasma gondii-secreted kinase promotes macrophage survival and virulence. Cell Host Microbe. 2010; 8(6):484–95. Epub 2010/12/15. doi: 10.1016/j.chom.2010.11.005 PMID: 21147463; PubMed Central PMCID: PMC3013631.

33. Okada T, Marmansari D, Li ZM, Adilbish A, Canko S, Ueno A, et al. A novel dense granule protein, GRA22, is involved in regulating parasite egress in Toxoplasma gondii. Molecular and biochemical parasitology. 2013; 189(1–2):5–13. Epub 2013/04/30. doi: 10.1016/j.molbiopara.2013.04.005 PMID: 23623919.

34. Gold DA, Kaplan AD, Lis A, Bett GC, Rosowski EE, Cirelli KM, et al. The Toxoplasma Dense Granule Proteins GRA17 and GRA23 Mediate the Movement of Small Molecules between the Host and the Parasitophorous Vacuole. Cell host & microbe. 2015; 17(5):642–52. Epub 2015/05/15. doi: 10.1016/j.chom.2015.04.003 PMID: 25974303; PubMed Central PMCID: PMC4435723.

35. Ma JS, Sasai M, Ohshima J, Lee Y, Bando H, Takeda K, et al. Selective and strain-specific NFAT4 activation by the Toxoplasma gondii polymorphic dense granule protein GRA6. The Journal of experimental medicine. 2014; 211(10):2013–32. Epub 2014/09/17. doi: 10.1084/jem.20131272 PMID: 25225460; PubMed Central PMCID: PMC4172224.

36. Persat F, Mercier C, Ficheux D, Colomb E, Trouillet S, Bendridi N, et al. A synthetic peptide derived from the parasite Toxoplasma gondii triggers human dendritic cells' migration. Journal of leukocyte biology. 2012; 92(6):1241–50. Epub 2012/10/04. doi: 10.1189/jlb.1211600 PMID: 23033174.

37. Shastri AJ, Marino ND, Franco M, Lodoen MB, Boothroyd JC. GRA25 is a novel virulence factor of Toxoplasma gondii and influences the host immune response. Infection and immunity. 2014; 82(6):2595–605. Epub 2014/04/09. doi: 10.1128/IAI.01339-13 PMID: 24711568; PubMed Central PMCID: PMC4019154.

38. Bougdour A, Tardieux I, Hakimi MA. Toxoplasma exports dense granule proteins beyond the vacuole to the host cell nucleus and rewires the host genome expression. Cellular microbiology. 2014; 16(3):334–43. Epub 2014/01/01. doi: 10.1111/cmi.12255 PMID: 24373221.

39. Rosowski EE, Lu D, Julien L, Rodda L, Gaiser RA, Jensen KD, et al. Strain-specific activation of the NF-kappaB pathway by GRA15, a novel Toxoplasma gondii dense granule protein. J Exp Med. 2011; 208(1):195–212. Epub 2011/01/05. doi: 10.1084/jem.20100717 PMID: 21199955; PubMed Central PMCID: PMC3023140.

40. Bougdour A, Durandau E, Brenier-Pinchart MP, Ortet P, Barakat M, Kieffer S, et al. Host Cell Subversion by Toxoplasma GRA16, an Exported Dense Granule Protein that Targets the Host Cell Nucleus and Alters Gene Expression. Cell Host Microbe. 2013; 13(4):489–500. Epub 2013/04/23. doi: 10.1016/j.chom.2013.03.002 PMID: 23601110.

41. Braun L, Brenier-Pinchart MP, Yogavel M, Curt-Varesano A, Curt-Bertini RL, Hussain T, et al. A Toxoplasma dense granule protein, GRA24, modulates the early immune response to infection by promoting a direct and sustained host p38 MAPK activation. The Journal of experimental medicine. 2013; 210 (10):2071–86. Epub 2013/09/18. doi: 10.1084/jem.20130103 PMID: 24043761; PubMed Central PMCID: PMC3782045.

42. Mercier C, Howe DK, Mordue D, Lingnau M, Sibley LD. Targeted disruption of the GRA2 locus in Toxoplasma gondii decreases acute virulence in mice. Infect Immun. 1998; 66(9):4176–82. PMID: 9712765.

43. Mercier C, Rauscher B, Lecordier L, Deslee D, Dubremetz JF, Cesbron-Delauw MF. Lack of expression of the dense granule protein GRA5 does not affect the development of Toxoplasma tachyzoites. Molecular and biochemical parasitology. 2001; 116(2):247–51. Epub 2001/08/28. PMID: 11522359.

44. Rome ME, Beck JR, Turetzky JM, Webster P, Bradley PJ. Intervacuolar transport and unique topology of GRA14, a novel dense granule protein in Toxoplasma gondii. Infection and immunity. 2008; 76 (11):4865–75. Epub 2008/09/04. doi: 10.1128/IAI.00782-08 PMID: 18765740; PubMed Central PMCID: PMC2573327.

45. Craver MP, Knoll LJ. Increased efficiency of homologous recombination in Toxoplasma gondii dense granule protein 3 demonstrates that GRA3 is not necessary in cell culture but does contribute to virulence. Molecular and biochemical parasitology. 2007; 153(2):149–57. Epub 2007/04/10. doi: 10.1016/j.molbiopara.2007.02.013 PMID: 17418907.

46. Fox BA, Falla A, Rommereim LM, Tomita T, Gigley JP, Mercier C, et al. Type II Toxoplasma gondii KU80 knockout strains enable functional analysis of genes required for cyst development and latent infection. Eukaryot Cell. 2011; 10(9):1193–206. Epub 2011/05/03. doi: 10.1128/EC.00297-10 PMID: 21531875; PubMed Central PMCID: PMC3187049.

47. Rommereim LM, Hortua Triana MA, Falla A, Sanders KL, Guevara RB, Bzik DJ, et al. Genetic manipulation in Deltaku80 strains for functional genomic analysis of Toxoplasma gondii. J Vis Exp. 2013;(77:): e50598. Epub 2013/07/31. doi: 10.3791/50598 PMID: 23892917; PubMed Central PMCID: PMC3735270.

48. Fox BA, Ristuccia JG, Gigley JP, Bzik DJ. Efficient gene replacements in Toxoplasma gondii strains deficient for nonhomologous end joining. Eukaryot Cell. 2009; 8(4):520–9. PMID: 19218423 doi: 10.1128/EC.00357-08

49. Huynh MH, Carruthers VB. Tagging of endogenous genes in a Toxoplasma gondii strain lacking Ku80. Eukaryot Cell. 2009; 8(4):530–9. PMID: 19218426 doi: 10.1128/EC.00358-08

50. Gajria B, Bahl A, Brestelli J, Dommer J, Fischer S, Gao X, et al. ToxoDB: an integrated Toxoplasma gondii database resource. Nucleic Acids Res. 2008; 36(Database issue):D553–6. PMID: 18003657.

51. Gigley JP, Fox BA, Bzik DJ. Cell-mediated immunity to Toxoplasma gondii develops primarily by local Th1 host immune responses in the absence of parasite replication. J Immunol. 2009; 182(2):1069–78. PMID: 19124750.

52. Achbarou A, Mercereau-Puijalon O, Sadak A, Fortier B, Leriche MA, Camus D, et al. Differential targeting of dense granule proteins in the parasitophorous vacuole of Toxoplasma gondii. Parasitology. 1991; 103 Pt 3:321–9. PMID: 1780169.

53. Labruyere E, Lingnau M, Mercier C, Sibley LD. Differential membrane targeting of the secretory proteins GRA4 and GRA6 within the parasitophorous vacuole formed by Toxoplasma gondii. Mol Biochem Parasitol. 1999; 102(2):311–24. PMID: 10498186.

54. Saavedra R, De Meuter F, Herion P. Monoclonal antibodies identify new Toxoplasma gondii soluble antigens. Hybridoma. 1990; 9(5):453–63. PMID: 2258184.

55. Carey KL, Donahue CG, Ward GE. Identification and molecular characterization of GRA8, a novel, proline-rich, dense granule protein of Toxoplasma gondii. Molecular and biochemical parasitology. 2000; 105(1):25–37. PMID: 10613696.

56. Adjogble KD, Mercier C, Dubremetz JF, Hucke C, Mackenzie CR, Cesbron-Delauw MF, et al. GRA9, a new Toxoplasma gondii dense granule protein associated with the intravacuolar network of tubular membranes. International journal for parasitology. 2004; 34(11):1255–64. doi: 10.1016/j.ijpara.2004.07.011 PMID: 15491588.

57. Dobrowolski JM, Sibley LD. Toxoplasma invasion of mammalian cells is powered by the actin cytoskeleton of the parasite. Cell. 1996; 84(6):933–9. PMID: 8601316.

58. Rodriguez C, Afchain D, Capron A, Dissous C, Santoro F. Major surface protein of Toxoplasma gondii (p30) contains an immunodominant region with repetitive epitopes. European journal of immunology. 1985; 15(7):747–9. doi: 10.1002/eji.1830150721 PMID: 2408905.

59. Donald RG, Carter D, Ullman B, Roos DS. Insertional tagging, cloning, and expression of the Toxoplasma gondii hypoxanthine-xanthine-guanine phosphoribosyltransferase gene. Use as a selectable marker for stable transformation. J Biol Chem. 1996; 271(24):14010–9. PMID: 8662859.

The role of GRA5 in the differentiation of Type II *Prugniaud* parasites

GRA5 regulates the recruitment of host organelles around the vacuole formed by cystogenic Toxoplasma parasites

Valeria Bellini[1], Corinne Loeuillet[1], Jean-Michel Saliou[2], Cordiela Bisanz[1], Catherine Lemaire[1], Delphine Jublot[1], Salima Kamche[1], Barbara A. Fox[3], David J. Bzik[3], Eugenio Paccagnini[4], Bastien Touquet[5], Delphine Aldebert[5,] Pietro Lupetti[4], Yves Usson[1], Pierre Cavailles[1], Corinne Mercier[1*] and Marie-France Delauw[1*]

1 Techniques de l'Ingénierie Médicale et de la Complexité Informatique, Mathématiques et Applications, Grenoble (TIMC-IMAG), CNRS UMR 5525, Université Grenoble Alpes, Grenoble, France

2 Centre d'Infection et d'Immunité de Lille, CNRS UMR 8204, INSERM U1019, Institut Pasteur de Lille, Centre Hospitalo-Universitaire de Lille, Université de Lille, Lille, France

3 Department of Microbiology and Immunology, The Geisel School of Medicine at Dartmouth, Lebanon, NH, United States of America,

4 Department of Life Science, University of Siena, Siena, Italy

5 Automated Microscopy Facility, CNRS UMR 5525, Université Grenoble Alpes, Grenoble, France

***** These authors contributed equally to this work.

Summary

During the acute infection, *Toxoplasma gondii* replicates, within its host cell, inside a parasitophorous vacuole (PV), which is an interface compartment between the parasite and the host cell. The PV rapidly evolves into an intracellular cyst, which contains slow dividing parasites and persists in the brain. The molecular mechanisms which underlie this differentiation process are poorly understood. The proteins secreted from the parasite dense granules are major components of both the PV and the cyst wall. Using an *in vitro* model to induce parasite differentiation of the type II cystogenic strain *Prugniaud*, in which the *gra5* gene had been knocked-out (PRUΔ*gra*5), we demonstrated a novel and crucial role for the GRA5 protein during the cyst wall development. Compared to both the parental and the complemented strains, PRUΔ*gra*5 parasites differentiated earlier an uncompleted cyst wall. Transmission electron microscopy and immunofluorescence analyses of differentiated cultures revealed a destabilization of these cyst-like structures and a peculiar interaction with host cell organelles. The cyst wall of PRUΔ*gra*5 indeed lost typical association with host endoplasmic reticulum elements and interacted instead with host microtubules, while attracting host mitochondria in a mitochondrion association factor 1 (MAF1)-independent manner. Proteomic analyses showed that the loss of GRA5 hampered the expression of other cyst wall components such as the matrix antigen 1 (MAG1) and proteins with redox functions including the protein disulfure isomerase (*Tg*PDI). In addition, PRUΔ*gra*5- infected cells displayed an increased expression of proteins involved in cell adhesion, cytoskeleton organization and DNA repair, contrasting with the metabolic pattern of proteins expressed in host cells infected by the parental- or complemented strains. For the first time, we demonstrated that GRA5 is likely to interact with parasite components of the PV membrane and the cyst wall to ensure integrity of the PV membrane, which is necessary to form stable *in vitro* cyst-like structures, suggesting a pivotal role of GRA5 in the biogenesis and maintenance of brain cysts *in vivo*.

Introduction

Intracellular pathogens most often reside in a safe membrane-bound compartment in which they replicate. The vacuole membrane, while protecting the pathogen from the host defense mechanisms, acts as an interacting platform between the pathogen and its host cell. In particular, the vacuole membrane is the site of interaction with host structures and recruitment of host organelles. The protozoan parasite *Toxoplasma gondii* is well adapted to its obligate intracellular life style. During acute infection, the tachyzoite stage can virtually infect any kind of nucleated cells in which it multiplies and differentiates. Host cell invasion is an active process leading to the formation of a membrane-bound compartment named the parasitophorous vacuole (PV). The Toxoplasma PV is characterized by an internal membranous nanotubular network (MNNs) that connects the parasites together and to the PV limiting membrane (Sibley *et al*., 1995). The PV-surrounding membrane (PVM) derives from the host plasma membrane but it is rapidly modified by parasite secreted proteins. Located at the interface with the host cell, the PVM protects Toxoplasma from host cell defense mechanisms and provides the parasite with nutrients to allow parasite replication (Mercier and Delauw, 2012).

In response to stress signals such as the host immune response, tachyzoites differentiate into slow-growing bradyzoites and form intracellular cysts. These are PV-derived structures which comprise *(i)* a cyst wall composed of two layers and covered by a rough membrane and *(ii)* an internal matrix that contains filaments and vesicles which connect the bradyzoites together and to the cyst wall (Lemgrüber *et al.,* 2011). Preferentially located in the brain and in muscle tissues, the cysts represent a "safe home" for the parasites that can remain latent for extended periods of time in the host.

The dense granule proteins (GRAs) have been shown to be main components of the PV compartment. They are synthesized as soluble proteins, stored within the dense granules, and they are secreted into the newly formed PV, where they become membrane-associated either to *(i)* the PVM (GRA3, GRA5, GRA7, GRA8, GRA10, GRA14, GRA17, GRA19, GRA20, GRA21, GRA22, GRA23, MAF1) and its long and thin extensions that plunge into the host cytoplasm; *(ii)* the MNN (GRA2, GRA4, GRA6, GRA9, GRA12); *(iii)* the vacuolar host sequestering tubulostructures (HOSTs) (GRA7); or they remain soluble in the vacuolar space (GRA1, GRA38, GRA39, GRA40) (Mercier and Cesbron-Delauw., 2015; Gold *et al.,*2015; Nadipuram *et al*., 2016; Pernas *et al.*, 2014). During the cyst formation the proteins, which were

located at the PV membrane (as for examples GRA3, GRA5 and GRA7), become part of the outer membrane of the cyst wall, while the MNN-associated proteins (GRA2 and GRA6) relocate to the inner layer of the cyst wall. GRA1, which remained soluble in the vacuolar space, is located in the cyst matrix (Torpier *et al*., 1993; Ferguson, 2004; Lemgrüber *et al*., 2011; Mercier and Delauw 2012; Mercier and Cesbron-Delauw, 2015).

Apart from their described structural role, the functions of the GRA proteins in the parasite life cycle and their interactions with the host cell are increasingly investigated. A systematic study performed on a series of Δ*gra* knock-outs (KO) constructed in the type I virulent strain RH analyzed the implication of ten GRA proteins (GRA1-10) in parasite infection, proliferation and virulence (Rommereim *et al.,* 2016). Except for GRA1 and GRA10 which appeared to be essential, some of these GRA proteins in complex (*i.e.* GRA7, in association with GRA2 and GRA6, Braun *et al*., 2007) were shown to play pivotal roles during the acute infection (Mercier *et al*., 1998; Ma *et al*., 2014, Alaganan *et al*., 2014) to regulate the MNN formation (Rommereim *et al*., 2016), while multiple KOs such as Δ*gra4*Δ*gra6,* Δ*gra3*Δ*gra5*, Δ*gra3*Δ*gra7* showed replication rate defects. GRA7 had also been characterized as playing important roles in the nutrients' uptake by its involvement in the formation of PV extensions into the host cell cytoplasm as well as HOSTs, which sequester host endocytic organelles, host lipids and cholesterol into the vacuolar space (Coppens *et al.,* 2006; Romano *et al.,* 2013). Moreover, the PVM-associated GRA17 and GRA23 were recently characterized as playing a coordinated role to ensure the active transport of small molecules from the host cell cytosol into the PV (Gold *et al*., 2015). Shortly after invasion, parasites of the types I and III recruit host mitochondria and endoplasmic reticulum (ER) elements to the PV and this recruitment was shown to be dependent on the expression of the dense granule protein MAF1, which is targeted to the PVM (Pernas *et al.,* 2014). Finally, *T. gondii* parasites also use GRA proteins to subvert the host cell responses. GRA6 was for example shown to activate the Nuclear Factor of Activated T cells 4 (*i.e.* the transcription factor NFAT4) (Ma, *et al.,* 2014), while a T epitope located in the C-terminal region of $GRA6_{II}$ was implicated in antigen presentation (Blanchard *et al.,* 2008). In mouse macrophages GRA7 was shown to bind and sequester one of the immunity-related GTPases (IRGs) to prevent PV lysis (Alaganan *et al*., 2014). GRA5 was shown to increase the migration of human dendritic cells (Persat *et al.,* 2012), while the dense-granule like proteins GRA15, GRA16, GRA24 and inhibitor of Signal Transducer and Activator of Transcription 1 (STAT1)-dependent transcription (TgIST) were shown to be targeted to the host cell

nucleus, where they re-program host cell expression (Rosowski *et al*., 2011; Bougdour *et al.,* 2013; Braun *et al.,* 2013; Olias *et al.,* 2016; Gay *et al.,* 2016).

While the functions played by the GRA proteins during the acute infection continue to be studied using the type I virulent strain RH, limited attention has so far been given to the roles played by the GRA proteins in parasite/host cell interactions of type II strains and during the chronic phase of infection. The aim of this study was thus to better characterize the role of GRA proteins in the invasion and proliferation of type II parasites as well as in their differentiation into bradyzoites and cyst development. Specifically, we used the *Prugniaud*-derived PRUΔ*ku80*Δ*hxgprt* (PRUΔ*hx*) parental strain (Fox *et al*., 2011) and the recently constructed PRUΔ*ku80*Δ*gra5*::*hxgprt* (PRUΔ*gra5*) *gra5* KO mutant to focus on the GRA5 protein. Composed of 120 amino acids (aa) (21 kDa), at the tachyzoite stage, GRA5 is stably associated with the PVM via a central transmembrane domain, while its N-terminus extends into the host cytoplasm and its C-terminus remains in the PV lumen (Lecordier *et al.,* 1999). As mentioned before GRA5 increases the migration of human DCs during the acute infection (Persat *et al.,* 2012), and it is exposed at the outer membrane of the cyst during the chronic phase (Lane *et al.,* 1996). From its functions at the tachyzoite stage, its particular localization at the PV and its persistent expression at the cyst wall outer membrane, we hypothesized that GRA5 would play an important role in cyst biogenesis, such as GRA6 and GRA4 (Fox *et al.,* 2011). Using an *in vitro* model of cyst formation, we described in this study how GRA5 is implicated in the regulation of the PVM differentiation.

Results

Construction of both the Tg∆*gra5* knocked-out- and the PRU∆*gra5*::*gra5* complemented strains in the cyst-forming strain Pru∆*ku80*∆*hxgprt*

In order to explore the role of the GRA5 protein in parasite differentiation and cyst development, a *gra5* knocked-out (KO) mutant was constructed in the type II cyst-forming Prugniaud strain (**Fig. 1**). Deletion of the single copy gene *gra5* was achieved by a double homologous recombination event replacing the *gra5* coding sequence with the hypoxanthine-xanthine-guanine phosphoribosyl transferase (*hxgprt*) selectable marker at the *gra5* locus of the parental PRU∆*ku80*∆*hxgprt* (PRU ∆*hx*) strain described previously (Fox *et al.,* 2011) (**Fig. 1A)**. Screening of the transfected population for the presence of parasites lacking GRA5 using an immunofluorescence assay (IFA) with mAb anti-GRA5, and subsequent cloning led to the isolation of the Pru∆*ku80*∆GRA5::*hxgprt* (Pru∆*gra5*) KO strain.

The Pru∆*gra5* strain was then complemented with *gra5* placed under the control of its native promoter by single homologous recombination using the pLic-3HA-DHFR plasmid (Huynh *et al*., 2009) to express the 1.6 Kb region upstream from the GRA5 predicted start codon and the whole *gra5* coding sequence (plasmid pGRA5.3HA-DHFR shown in **Fig. 1B**). To avoid expression of the HA tag carried by pLic-3HA-DHFR, the stop codon of GRA5 was maintained. PRU∆*gra5* parasites were transfected with pGRA5.3HA-DHFR and selected with pyrimethamine before cloning. Both the complemented PRU∆*ku80*∆*gra5*::*gra5-hxgprt* (PRU∆*gra5*::*gra5*) and the KO PRU∆*gra5* strains were validated by immunofluorescent assay (IFA) and immunoblot (**Fig. 1C-D**). The IFA showed a clear co-staining of both the GRA5 and the GRA6 proteins in both PRU∆*hx* and PRU∆*gra5*::*gra5* parasite dense granules and vacuoles after 24 h of development within host cells, contrary to Pru∆*gra5*, in which GRA6 could only be detected (**Fig. 1C**). Immunoblot confirmed the lack of expression of GRA5 (21 kDa) in PRU∆*gra5*, contrary to both the parental- and the complemented strains. The SAG1 protein (30 kDa) was used as an internal control of the quantity of parasite lysate loaded in each lane (**Fig. 1D**).

Lack of *gra5* does not hamper infection and intracellular proliferation of type II tachyzoites

To investigate whether GRA5 is involved in parasite infection and proliferation, we used a high throughput automated IFA that allows the scanning and the analysis of large samples (~ 1,000 cells

and > 500 PV) (Rommereim *et al*., 2016). Parasite infection was analyzed after 4 h of HFFs inoculation with the parental-, the KO- or the complemented strains. In order to discriminate the extracellular- from the intracellular parasites, infected cells were fixed, permeabilized and labelled with both SAG1 and GRA1. Parasite proliferation was analyzed 36 h post-infection (PI) by the determination of the percentage of PV containing respectively 1, 2, 4, 8 or 16 parasites. The 3 strains PRUΔ*hx*, PRUΔ*gra5* and PRUΔ*gra5*::*gra5* exhibited infection rates, which were not significantly different: they were indeed comprised between 28 and 39% (**Fig. 2A**). Surprisingly, compared with parental PRUΔ*hx*, both PRUΔ*gra5* and PRUΔ*gra5*:: *gra5* showed an increased mean number of parasites per vacuole: 41% of vacuoles in both PRUΔ*gra5* and PRUΔ*gra5*:: *gra5* contained 1 parasite; 20% and 21% of vacuoles in these strains contained 4 and 8 parasites, respectively, while 55% of the PRUΔ*hx* vacuoles contained 1 parasite and respectively 14% and 11% of vacuoles of this strain contained 4 and 8 parasites (**Fig. 2B**). The lack of significant difference between the growth rates of the PRUΔ*gra5* KO and PRUΔ*gra5*::*gra5* complemented strains indicated that the increased proliferation rate observed in the PRUΔ*gra5* KO compared to the PRUΔ*hx* parental strain was not due to the lack of GRA5. A plaque assay confirmed the differences observed 36 h PI in the proliferation rates between PRUΔ*gra5* and PRUΔ*gra5*::*gra5 vs* PRUΔ*hx* (**Fig. 2C-2D**).

PRUΔ*gra5* parasites exhibit a higher basal level of differentiation

GRA5 has been characterized as a component of both the PV membrane and the cyst wall (Charif *et al*., 1990; Lecordier *et al*., 1993; Torpier *et al*., 1993; Ferguson, 2004; Lemgrüber *et al*., 2011). We thus examined whether deletion of *gra5* would affect *in vitro* differentiation of PVs into cyst-like structures, when infected cells were switched to alkaline medium and incubated without CO_2 (Soëte *et al*., 1993). Differentiation of PV membranes into cyst walls was monitored by the quantification of PV-cyst structures expressing the CST1 (also called SAG1-Related-Sequence 44 (SRS44); Tomita *et al.*, 2013) glycoprotein, which is expressed at the PV-cyst membrane early during the conversion of tachyzoites into bradyzoites and which can be easily detected using a specific lectin extracted from *Dolichos biflorus* and coupled to a fluorochrome (Zhang *et al.,* 2001; Bellini et al., 2015). Differentiation of tachyzoites to bradyzoites was monitored by quantification of the cyst-like structures expressing the SRS9 bradyzoite marker (Kim *et al*., 2007; Van *et al.,* 2007) (**Fig. 3A**). The

results showed that, 36 h PI without alkaline stress, the basal (spontaneous) rate of differentiation of PRUΔ*gra5* parasites was significantly higher than that of the parental parasites and was also higher (although not significantly) than that of the complemented parasites (**Fig. 3B-C**). Both the parental- and the complemented strains exhibited indeed respectively 14 and 19% of CST1-positive vacuoles, compared to 40% in PRUΔ*gra5* (**Fig. 3B**). Similarly, 2.8 and 7% of CST1 and SRS9 double positive vacuoles were detected in PRUΔ*hx* and PRUΔ*gra5*::*gra5,* respectively, compared to 13% in PRUΔ*gra5* (**Fig. 3C**). Similar differences between the strains were observed 24 h after having switched the cultures to alkaline conditions (**Fig. 3D-E**). Interestingly, while the number of CST1-positive vacuoles-cyst-like structures increased between 24 and 48 h of incubation in alkaline medium for PRUΔ*gra5*::*gra5*, it did not increase for PRUΔ*gra5* parasites over this time lapse (**Fig. 3D**), most probably because of cell lysis and subsequent parasite re-invasion. Altogether, these results indicate that deletion of *gra5* accelerates the differentiation process, in particular that of PV membranes into cyst walls. The differentiation process of PRUΔ*gra5* parasites was initiated *in vitro* during normal conditions of culture, suggesting that these KO parasites might be more sensitive to the stress inherent to *in vitro* culture.

Lack of GRA5 results in increased recruitment of both host mitochondria and microtubules around the PV membrane during *in vitro* differentiation

Having observed that PRUΔ*gra5* parasites display earlier differentiation of their PV membrane into cyst wall-like structures *in vitro* (**Fig. 3**), we next examined by Transmission Electron Microscopy (TEM), the morphology of vacuoles-cysts formed by PRUΔ*gra5* parasites after 36 h of *in vitro* stressed culture. We chose this timing *i)* to optimize the number of differentiated vacuoles in the parental strain and *ii)* to avoid too much host cell lysis by PRUΔ*gra5* parasites, which grow faster than the parental ones (**Fig. 2D**). As described earlier (Guimarães *et al.,* 2009), the PV membrane of PRUΔ*hx* parental parasites, which were differentiating into cysts, appeared as two dense layers separated by a thin clearer space, and was decorated with elements of the Host rough Endoplasmic Reticulum (HER), the ribosomes of which being exposed to the host cell cytoplasm, while the smooth face of the HER was tightly associated with the PV membrane (**Fig. 4A-4B**). In contrast, the PV membrane of PRUΔ*gra5* parasites was fuzzier (the two dense layers could not be observed), and closely surrounded by many Host Mitochondria (HM) (**Fig. 4C**) and Host Microtubules (HMTs), which were organized in

dense arrays perpendicularly to the PV membrane surface (**Fig. 4D**). Interestingly, HER elements were not often observed in close association with the PV-cyst membrane of PRUΔ*gra5* parasites but they were instead observed scattered in the host cell cytoplasm (**Fig. 4D**). Tomography was then performed on the PV-cyst membrane of PRUΔ*gra5* KO parasites to investigate in more detail the possible fusion between the external membrane of host mitochondria and the PV-cyst membrane. Tomographic sequences as that presented in **Fig. 4E** showed that, in all the sections of the preparations, both the external membrane of the mitochondria and the membrane of the PV were distinguished, excluding the possibility of a membrane fusion between both organelles.

To refine these observations and compare the relative distances between the host cell organelles recruited to the PV membrane and this membrane in the various Toxoplasma strains, HFFs which had been infected for 36 h with PRUΔ*hx,* PRUΔ*gra5* or PRUΔ*gra5*::*gra5*, were switched to alkaline medium and further incubated for 36 h without CO_2. PV membrane differentiation was monitored by the labeling of CST1, while host microtubules and host mitochondria were revealed by IFA using anti-α tubulin and anti-cytochrome C antibodies, respectively. To quantify the distance between the PV membrane and the host cell mitochondria/microtubules, the slides were observed by confocal microscopy. The algorithm "fluorescence intensity as a function of distance" was developed to quantify the fluorescence intensity of a marker associated with host mitochondria/microtubules detected from the PV membrane. This fluorescence intensity was related to a distance (in μm). With this algorithm, the highest the intensity, the shortest the distance between the PV membrane and the host cell organelle/cytoskeleton element would be (**Fig. 5A**). Averaging the summed fluorescence intensities on the number of stacks and plotting these numbers for each strain revealed that, after 36 h of culture under stress conditions, the average distance between the limiting membrane of PRUΔ*gra5* vacuoles-cyst-like structures and host mitochondria was 1.6 and 1.75 fold shorter than that calculated for both PRUΔ*hx* and PRUΔ*gra5::gra5* (0.8 μm *versus* 1.3 μm and 1.4 μm, respectively) (**Fig. 5B**). Similarly, the average distance between the limiting membrane of PRUΔ*gra5* vacuoles-cyst-like structures and host microtubules was 2.4 and 2.2 fold shorter than that calculated for both PRUΔ*hx* and PRUΔ*gra5::gra5* (0.5 μm *versus* 1.2 μm and 1.1 μm, respectively) (**Fig. 5C**). The shorter distance calculated between the PRUΔ*gra5* limiting membrane and host cell mitochondria could suggest potential functional interaction between the two organelles.

The tighter recruitment of host mitochondria to the membrane of Pru∆*gra5* vacuoles-cyst-like structures does not rely on MAF1b

The PV formed by parasites from both type I and III *T. gondii* lineages differs from that formed by type II strains in their capacity to recruit host mitochondria (Pernas *et al.,* 2014). The high level of expression of the TgMAF1RHb paralog at the PV membrane of type I tachyzoites was indeed associated with their attraction of host mitochondria. In contrast, the low level of transcription of *TgMAF1RHb* correlated with the lack of detection of the MAF1b protein at the PV membrane of type II tachyzoites, was linked to their failure to recruit host mitochondria (Adomako-Ankomah *et al.,* 2016). Having observed a closer association of host mitochondria with the membrane of Pru∆*gra5* cyst-like structures (**Fig. 5B**), we investigated the potential expression of MAF1b by PRU∆*gra5* parasites. While the PV of RH tachyzoites showed an intense MAF1b fluorescence signal (**Fig. 6A, top line**), the PV and cyst-like structures of PRU∆*hx* failed to detect the protein (**Fig. 6A-B, middle lines**), thus validating the experimental protocol for the detection of MAF1b and confirming the results previously published (Pernas *et al.,* 2014). MAF1b could not be detected in either the PV or the cyst-like structures formed by PRU∆*gra5* parasites (**Fig. 6A-B, bottom lines**), indicating that the recruitment of host mitochondria to the membrane of PV/cyst-like structures in this strain would be independent of the expression of MAF1b. To confirm these results and exclude the possibility of a lack of MAF1b (PRU) detection by the antibodies raised against the type I protein, the specific mRNA encoding MAF1b type II was quantified by qRT-PCR 8 h after inoculation of the parasites onto HFFs cells as well as after another 24 h of culture under stress conditions. The amounts of *MAFPRU1b* mRNA expressed in PRU∆*hx* as well as in PRU∆*gra5* parasites were respectively 2.5 and 1.3 times lower than that detected in RH parasites after 8 h of culture with CO_2. They were also respectively 8.3 and 10 times lower than that detected in RH parasites after 24 h of culture under stress conditions (**Fig. 6C**). Note that, for an easy comparison, all the mRNA levels were compared to the level of *MAFRH1b* mRNA quantified in RH after 8 h of culture with CO_2 and normalized to the arbitrary value of 1 (**Fig. 6C**). These results thus confirmed that the ability of PRU∆*gra5* parasites to attract host mitochondria is not linked to their expression of the MAF1b paralog.

The loss of GRA5 does not increase the expression of other parasite proteins

To investigate whether the loss of GRA5 would alter the expression of other parasite proteins, we performed a proteomic analysis on different fractions of infected HFFs incubated for 24 h under normal- (+ CO_2) or stressing (- CO_2) conditions. Briefly, after mechanical lysis of infected cells, the fraction containing intact parasites (Low Speed Pellet, LSP) was separated from that containing the vacuole and the host cell components (Low Speed Supernatant, LSS). Proteins from each fraction were separated by SDS-PAGE and analyzed by mass spectrometry. The parasite proteins (those from the LSP and those localized within the PV or injected into the host cell cytoplasm, LSS) were identified in ToxoDB.org using a semi-quantitative analysis method that proceeded in two steps. We first compared the proteins expressed by PRUΔ*gra5::gra5* (selected because of a higher amount of protein in the sample) to those expressed by PRUΔ*gra5*. We selected the parasite proteins which had more than 3 peptides mapped in the complemented strain and, in the same time, showed a fold increase expression over PRUΔ*gra5* that was >4 (this corresponds to the ratio between the spectra of the two parasite lines). The resulting list of proteins was compared, in a second step, to that of the PRUΔ*hx* parental strain and we set again the limit of detection to a 4-fold increased spectra ratio, when compared with PRUΔ*gra5*. Conversely, we repeated this two -step-analysis method while selecting the proteins more expressed in 1) PRUΔ*gra5*, as compared to PRUΔ*gra5::gra5* and 2) comparing this first list of proteins to the proteins expressed by PRUΔ*hx*.

As an internal positive control, GRA5 was detected only in the LSP +CO_2 fraction (purified parasites) of both the complemented- and the parental strains (**Table 4**), confirming the *gra5* deletion in PRUΔ*gra5* and its restauration in PRUΔ*gra5*::*gra5*, as compared to PRUΔ*hx*. Out of the 17 proteins identified in cultures under differentiation (-CO_2), 16 (including GRA5) were found to be over-expressed in tachyzoites (LSP) and the vacuoles/host cell cytoplasm (LSS) of both the wild-type and the complemented strain (**Table 4**). In contrast, comparison of PRUΔ*gra5* parasites (LSP) to PRUΔ*hx* and PRUΔ*gra5*::*gra5* did not reveal any protein over-expressed, when the parasites were cultured under stressing conditions (-CO_2), and only 1 protein, the dense granule protein DG32, was found to be over-expressed in the vacuole/host cell cytoplasm of PRUΔ*gra5*, as compared to PRUΔ*hx* and PRUΔ*gra5*::*gra5* (LSS, -CO_2) (**Table 5**). Surprisingly and in agreement with the above results of over-expression, only 6 parasite proteins were found to depend on the presence of GRA5 in the

vacuole/host cell cytoplasm (LSS, -CO_2) (**Table 4**). These proteins included the protein disulfide isomerase (PDI), a putative alkyl hydroperoxide reductase, the phosphofructokinase (PFKII), MAG1, the tryptophanyl-tRNA synthetase (TrpRS2), and the glyceraldehyde-3-phosphate dehydrogenase (GAPDH1). Interestingly, 3 of them, PDI, PFKII and MAG1, were commonly secreted during normal culture conditions and during parasite differentiation (compare the results of the **Tables 4**).

The loss of GRA5 alters the expression profile of infected cells and the diversity of host proteins is dramatically reduced under stressing conditions

Analysis of human (host cell) protein expression (using UniProt.org database) generated 5,285 proteins. To take into account the response of non-infected host cells submitted to the alkaline stress, we removed the proteins identified in the (LSS, -CO_2, non-infected HFFs) fraction from the lists of proteins. The results were then analyzed using the semi-quantitative analysis method described above. In a similar manner to what had been performed for the LSP fraction, proteins were selected 1) if they were represented by more than 3 detected peptides and 2) if their spectra ratio (LSS -CO_2 / LSS +CO_2) was >4 (data not shown). This strategy allowed the determination of the response of the host cells, when infected respectively by PRUΔ*hx*, PRUΔ*gra5::gra5* or PRU*Δgra5* parasites (LSS +CO_2) and when parasites had begun their differentiation process (LSS -CO_2). To better highlight the differences of the host cells in response to the infection by the 3 different strains, the human proteins were divided into 9 "families" according to their functions (Gene Ontology). The relative percentages of expression of these 9 families are shown in **Figure 7**. When infected in normal conditions of culture (+CO_2) by PRUΔ*gra5* parasites, as compared to PRUΔ*hx* and PRUΔ*gra5::gra5*, the HFFs 1) stopped expressing proteins related to transcription and folding activities, 2) expressed instead proteins involved in the reorganization of their cytoskeleton and 3) increased their expression of proteins involved in cell-cell adhesion. One can also notice that, when infected by PRUΔ*hx* and PRUΔ*gra5::gra5,* the cells did not express proteins related to lysosome binding, proteolysis, and cytoskeleton organization (**Fig. 7, upper panels**). Consecutively to the culture switch to stressing conditions (**Fig. 7B, lower panels**), HFFs infected with PRUΔ*hx* and PRUΔ*gra5::gra5* increased the variety of expressed protein families but stopped their expression of proteins related to intracellular transport or transport across membranes. The families of proteins the most abundantly expressed were the proteins related to metabolic processes and transcription or folding. By contrast, when

infected by PRUΔ*gra5*, HFFs dramatically reduced the number of protein families expressed, limiting them to proteins related to 1) cell-cell adhesion, 2) organization of the cytoskeleton and 3) nucleotide binding and DNA repair.

Discussion

The parasitophorous vacuole and the tissue cyst are the "safe homes" of *Toxoplasma gondii* during the acute and the chronic infections, respectively. These structures protect the parasites from the host, ensuring, at the same time, its proliferation or latency, and nutrient acquisition. The dense granule proteins, which are major components of both the PV and the cyst wall, have been described not only as having a structural role but also as effectors that interact with the host. However, to date, while the functions of GRA proteins are increasingly documented for the type I virulent strain, much less attention has been given to the type II parasites forming-cysts. Here, using the *Prugniaud* type II strain, we demonstrated a novel role of GRA5 during parasite and vacuole differentiation, an important step to develop the cyst structure. The depletion in *gra5* altered the stability of the PVM leading to an early but incomplete cyst wall differentiation, which modifies the interaction with host cell organelles.

In this study, we first observed that, unlike the RHΔ*gra5* strain which displayed a defect in parasite host cell invasion (3 fold less invasion, when compared to the WT) (Rommereim *et al.,* 2016), the PruΔ*gra5* strain did not present any significant difference in its invasion rate, when compared to the parental and the complemented strains. Although this tends to suggest that GRA5 behaves differently in type I *vs* type II parasites, the reason for this difference remains to be explored more carefully. Indeed, the first generated RHΔ*gra5* mutant (Mercier *et al*., 2001) was not found to have a defect in an invasion assay that was quantified by manual counting, whereas the assay developed by Rommereim and collaborators (2016) used a more sensitive high throughput immunofluorescence assay to count the infected cells. Unexpectedly, compared with the PruΔ*gra5* strain, the control strain used in our study displayed a significantly slower rate of multiplication, while the complemented strain Δ*gra5::gra5* exhibited a similar infection rate as that of Δ*gra5*. Even if this phenotype would require further clarifications by complementing PRUΔ*hx*, the similar growth observed between PRUΔ*gra5* and the complemented strain demonstrates that GRA5 is dispensable for the parasite proliferation in both the PRU type II strain and, as reported previously (Mercier *et al*., 2001; Rommereim *et al*., 2016), the RH type I strain.

GRA5 is one of the proteins associated with the PV membrane (PVM) and which accumulates in the outer membrane of the cyst wall, suggesting a role during latent infection (Torpier *et al.,* 1993; Lane *et al.,* 1996). Using an *in vitro* model, we showed that parasites lacking GRA5 have a higher basal level of differentiation. The CST1 marker (a glycoprotein of the cyst wall) (Tomita *et al.,* 2013) was indeed more easily detected in the vacuoles of PRUΔ*gra5* parasites than in those of both the parental- and the complemented strains after 36 h of culture without any environmental stress. This difference was maintained when the alkaline stress was applied to induce parasite differentiation. A similar, however lower, effect was obtained for the expression of SRS9 (a bradyzoite-specific antigen), probably due to the delay required for its expression. The CST1 glycoprotein was indeed originally described as being expressed at the cyst wall after 24 h only of stress induction (Zhang *et al.,* 2001), suggesting that PVM modifications may appear before subsequent bradyzoite differentiation. Both the PVM and the cyst wall provide a physical barrier against host cell attacks. Accordingly, our results suggest that the deletion of *gra5* in the Prugniaud strain alters the stability of the PVM, increasing the natural cyst wall differentiation, important to protect the parasites from harsh environmental conditions.

However, although PVM modifications started earlier in PRUΔ*gra5* vacuoles, their ultrastructural analysis under alkaline stress revealed an abnormal cyst wall differentiation. Hence, while the parental strain exhibited regular vacuoles with a thick PV-cyst like structure membrane consisting in two dark layers bordering a lighter one, and surrounded by elements of the HER (Guimarães *et al.,* 2009), the PV-cyst like structure membrane of PRUΔ*gra5* parasites was less regular, fuzzier and no association with HER was observed. In addition, this vacuolar destabilization was associated with an increased interaction with HMTs and an increased recruitment of host mitochondria. The quantification of these two phenotypes by IFA and image analysis allowed to demonstrate the restoration of the parental phenotype in the PRUΔ*gra5*::*gra5* complemented strain, confirming that the interaction of the PRUΔ*gra5* differentiating vacuoles with host cell organelles and cytoskeleton is a consequence of the depletion in GRA5. Further analysis of the Host Mitochondria Association (HMA) by tomography demonstrated that the recruitment resulted in a close contact between the PVM and the external face of the mitochondria envelope, but not a fusion.

The HMA phenomenon is considered to be important for the uptake of host nutrients. It is not specific to *T. gondii* but was also described for the coccidian parasites *Hammondia hammondi* and other intracellular pathogens such as *Chlamydia pittaci* and *Legionella pneumophila* (Matsumoto *et al.,*

1991; Scalon *et al.,* 2004). While, for these pathogens, the molecular mechanism sustaining this recruitment remains unknown, in *T. gondii*, a dense granule protein targeted to the PVM, *i.e*. Mitochondrial Associated Factor 1 (MAF1), has been characterized as the HMA effector (Pernas *et al.,* 2014; Adomako-Ankomah *et al.,* 2016). Specifically, HMA is mediated by the MAF1b1 paralog, which is more abundantly transcribed in types I and III- than in type II strains. The polyclonal antibody raised against the C-terminus of MAF1b1 type I protein (amino acids 134-443) did not reveal expression of the protein in type II parasites, confirming that HMA is exclusively expressed at the PVM of type I and III strains (Pernas *et al.,* 2014). Our results showed that the loss of the PVM stability consecutive to the *gra5* deletion, and associated with parasite differentiation, induces HMA in a *Prugniaud* type II strain. The possible expression of MAF1b1 by PRUΔ*gra5* parasites was tested by IFA under normal culture conditions or during differentiation. Confirming the previous results, we found MAF1 positive vacuoles in RH but not in PRU parasites nor in the PRUΔ*gra5*. More recently, a polymorphism in a proline-rich region (amino acids 152-164) was detected between the MAF1b1 paralogs of the RH type I *vs* Me49 type II strains (Adomako-Ankomah *et al.,* 2016). To confirm that the non-detection of MAF1 in type II vacuoles by IFA was not caused by an inefficient recognition of the type II protein by the antibody raised against the type I protein, we performed a quantitative RT-PCR to analyze the protein transcription. Similar to a previous study (Adomako-Ankomah *et al.,* 2016), we detected a lower expression of the *MAF1b1* paralog in both the parental PRU and the *gra5* knockout than in RH parasites. Moreover, when the parasites were submitted to alkaline stress, the *MAF1b1* mRNA level increased in the RH strain, while it continued to decrease in the PRU strain. These observations confirmed that the HMA detected in PRUΔ*gra5* parasites is not likely to be mediated by MAF1 and would involve other(s) mechanism(s), such as reorganization of the host cytoskeleton. This reorganization has been characterized in *T. gondii* type I parasites. Occurring at the beginning of the infection (1 h post-infection), it was described to play a role in the positioning of the PV near the host nucleus and the microtubule organizing centers (Walker *et al.,* 2008).

Another important host organelle, normally associated with the PVM, is the HER which, with mitochondria, represents a source of nutrients (lipids, calcium and amino-acids) for intracellular parasites (Sinai *et al.,* 1997; Magno *et al.,* 2005). Based on a yeast double-hybrid approach, GRA3 and GRA5 were proposed as possible candidates to HER recruitment via their binding to the integral membrane protein Calcium Modulating Ligand (CALMG) (Ahn *et al.,* 2006). Although this interaction

needs to be proven *in cellulo*, the hypothesis fits with our observation that the depletion in GRA5 causes a looser association between the PVM and the HER during parasite differentiation *in vitro.*

Proteomic analysis of *in vitro* parasite cultures, submitted or not to alkaline stress, was useful to clarify PRUΔ*gra5* phenotypes. Six Toxoplasma proteins were found specifically associated to the vacuolar fraction of both the parental and the complemented strains, while they were missing from the PRUΔ*gra5* fraction. Among them, only three proteins behaved like GRA5 because they were found to be similarly abundant in the presence or absence of stress. Interestingly, they were detected in the parasites fraction of the three strains PRUΔ*hx*, PRUΔ*gra5* and PRUΔ*gra5::gra5*, demonstrating that their transcription is not modified by the absence of GRA5. This observation, which contrasts with their absence in the vacuole-containing fractions, supports a possible loss of a partner like GRA5 and/or substrates normally present within the PV. These three candidates correspond to the protein disulfide isomerase (PDI) (TGME49_211680), the phosphofructokinase (PFKII), (TGME49_226960), and the matrix antigen MAG1 (TGME49_270240).

PDI is a member of the thioredoxin superfamily of redox proteins. Specifically, TgPDI is a protein disulfide isomerase. It belongs to a family of proteins which are conserved and known to be multifunctional. TgPDI (52 kDa) is composed of 470 amino acids, including a signal peptide (the first 24 amino acids) and four domains, *i. e*. the two active sites (cysteine residues) separated by two substrate binding sites (hydrophobic domains) (Moncada *et al*., 2016). TgPDI was recently described as important for parasite invasion; probably due to its capacity to reduce disulfide bonds. This reduction of disulfide bridges is indeed crucial to activate host cell surface integrins, promoting parasite adhesion (Stolf *et al*., 2011). Interestingly, PDI is also known to have a chaperone activity involved in protein folding to form or brake disulfide bounds. As described for the mammalian PDI (Ali Khan and Mutus 2014), in *Toxoplasma gondii* this protein exhibits a C-terminal KDEL ER-retention sequence (Moncada *et al*., 2016), which could interact with the HER. According to its multiple roles, locations and the presence of a signal peptide, we can speculate that TgPDI is also secreted into the PV in order to ensure protein folding and PVM stability, necessary for the parasite development. In addition, the presence of GRA5 correlating with a more stable association between the HER and the PVM during vacuole differentiation, it can be speculated that the loss of TgPDI, together with the loss of GRA5, would destabilize the HER-PVM interaction.

Like TgPDI, MAG1 is another interesting candidate. Composed of 425 amino acids, MAG1 is a 65 kDa protein which also bears a 25 residue-signal peptide and a predicted transmembrane domain, both features being typical of a dense granule protein (Weiss and Kim, 2011). Originally detected in the cyst matrix and the cyst wall, it was first characterized as a protein exclusively expressed at the bradyzoite stage (Parmley *et al.,* 1994). However, Ferguson and collaborators (2002) further showed that MAG1 is also expressed at the tachyzoite stage. Staining of liver and brain sections of both RH (virulent)- and RRA (avirulent)- infected mice, indeed revealed the presence of MAG1 in both the vacuoles and the cyst walls (Ferguson *et al.,* 2002), strengthening the possible partnership between MAG1 and GRA5 in the PVM for cyst wall development.

The other proteins over-expressed in vacuole fractions of the parental and complemented strains are enzymes implicated in both redox and metabolic processes. Among them, PKII, which regulates the metabolism of glucose (glycolysis or gluconeogenesis), is expressed in presence or absence of alkaline stress, suggesting a regulatory function important for parasite energy in both the tachyzoite and the bradyzoite stages. Interestingly, the major representation of metabolic enzymes (PKII, GADPH1, tryptophanyl-tRNA synthetase (TrpRS2) in the vacuoles under alkaline stress most probably reflects an increased metabolic activity of the parasites during differentiation. Indeed, differentiation requires the activation of pathways to produce energy stores (amylopectine granules) or cyst wall components (protein glycosylation). In addition, the expression of enzymes implicated in the redox functions (TgPDI, Putative alkyl hydroperoxide reductase/Thiol specific antioxidant) are prevalent in vacuoles without stress application, supporting the idea of a higher vacuolar homeostasis and higher stability of the PVM in both parental and GRA5 complemented strains.

The host cytoskeleton reorganization, first revealed by TEM and confocal analysis, in the PRUΔ*gra5*-infected cells, was confirmed by the pattern of protein expression in host cells (UniProt database). While cells infected with the parental and complemented strains showed a typical phenotype of active cells going through signal transduction, protein transcription (or folding) and metabolic processes (or proteolysis), a different profile was detected in PRUΔ*gra5*-infected cells, in which proteins implicated in cell adhesion, cytoskeleton organization and DNA repair started to be expressed during normal culture conditions, becoming prevalent with the stress application that induced parasite differentiation.

Our results pave the way to further analysis that will investigate the interactions between GRA5 and the selected candidates. Importantly, they also suggested that the integrity of the PVM, which we showed here to be crucial to ensure cyst and parasite differentiation, has an impact on the host cell response and that this response is important to maintain the homeostasis required by the intracellular parasites to persist in a host cell.

Material and Methods

Culture of both the host cells and parasites

Human Foreskin Fibroblasts (HFF; ATCC-CRL 1634) were maintained in D10 medium (Dulbecco's Modified Eagle's Medium (DMEM, Gibco) supplemented with 10% heat-inactivated fetal bovine serum (FBS), 1 mM glutamine, 500 units/mL penicillin and 50 mg/mL streptomycin) (Gibco), at 37°C, in a humidified atmosphere containing 5% CO_2.

Tachyzoites of the Prugniaud or RH strain (**Table 1**) were maintained by serial passage into HFF monolayers in D10 medium, at 37°C, in a humidified atmosphere containing 5% CO_2.

Construction of the PRUΔ*gra5* knocked-out- and the PRUΔ*gra5::gra5* complemented parasite strains

Construction of the pΔGRA5 plasmid and its transfection into the parental strain PruΔ*ku80*Δ*hxgprt* were performed as previously described (Fox *et al.,* 2011; Rommereim *et al.,* 2016). Replacement of the *gra5* coding sequence by the *hxgprt* selectable marker was achieved by culture of the transfected parasites in D10 supplemented with 25 μg/mL mycophenolic acid (MPA; Sigma) and 50 μg/mL xanthine (MPA+X; Sigma), leading to the isolation of PruΔ*ku80*Δ*gra5::hxgprt* (abbreviated PruΔ*gra5)* knocked-out parasites. Their subsequent cloning led to the isolation of the particular parasite line described in this article.

For the complementation of the PruΔ*gra5* knocked-out parasites, a 2 Kb genomic fragment containing 1.6 Kb upstream of the GRA5 start codon and the entire *gra5* coding sequence was amplified from Prugniaud genomic DNA (extracted from Prugniaud parasites using the PureLink DNA genomic extraction Minikit from Life-technologies) using the LIC primers COMP-F and COMP-R described in **Table 2**, and cloned into the pLic-3HA-DHFR plasmid (gift from Dr Maryse Lebrun, CNRS UMR 5235, Université de Montpellier, France) (Huynh *et al*., 2009), leading to the pLic-GRA5.3HA-DHFR complementation plasmid (**Fig. 1A**). Fifty million of freshly harvested tachyzoites of the PRUΔ*gra5* strain were resuspended in 0.4 mL of electroporation buffer (10 mM KPO_4, pH 7.6; 120 mM KCl; 0.15 mM $CaCl_2$; 5 mM MgCl-6H_2O; 25 mM HEPES, 2 mM EDTA) with 100 μg of circular pLic- GRA5.3HA-DHFR plasmid. The electroporation was performed using a BTX-ECM630 electroporator (1 pulse at

2,000 V, 25 Ω, 25 µF). Parasites were then cultured in D10, at 37°C, until lysis before being selected for 4 serial passages in D10 supplemented with 1 µM pyrimethamine and sub-cloned by limiting dilution.

Confirmation of Pru∆*gra5* knocked-out parasites by immunoblot

1 x 10^7 freshly isolated tachyzoites were solubilized in 1X Laemmli Buffer (in absence of reducing agent). Proteins were separated in 13% SDS-PAGE, transferred to a nitrocellulose membrane and detected using the primary monoclonal antibodies (mAbs) TG17.113 anti-GRA5 (Biotem, Apprieu, France) and TG054 anti-SAG1 (Rodriguez *et al*., 1985) (**Table 3**) followed by goat serum anti-mouse IgG conjugated to horseradish peroxidase (HRP) (**Table 3**). The peroxidase activity was revealed by chemiluminescence using the Supersignal ECL system (Pierce Chemical) (2 min, Room Temperature (RT)).

Confirmation of Pru∆*gra5* knocked-out parasites by immunofluorescence assay

HFFs grown to confluency on glass coverslips in 4 well-plates (in D10, at 37°C and 5% of CO_2) were infected with 10 µL of freshly harvested tachyzoites of different selected clones, and incubated for 36 h, at 37°C, and 5% of CO_2. Infected cells were washed 3 times with PBS and fixed in 4% methanol-free formaldehyde (Polyscience) for 20 min at room temperature (RT). The cells were permeabilized for 15 min in 0.1% Triton X-100 (in PBS) at RT, and saturated for 40 min in 5% FBS-5% Goat Serum (GS) at RT. Using PBS-1% GS, a co-staining to detect both the GRA5 and GRA6 proteins was performed using mAb anti-GRA5 and rabbit anti-GRA6 serum (**Table 3**) (1 h incubation) followed by 1 h incubation in goat serum anti-mouse IgG conjugated to Alexa-594 and goat serum anti-rabbit IgG conjugated to Alexa-488. The cells and parasites' nuclei were revealed with Hoechst 33258 (MoleculaProbes) (15 min incubation at RT, 1:30,000). After 3 washes with PBS 1X, the coverslips were mounted onto glass slides using mowiol (Invitrogen). The images were acquired using an Axioplan 2 (Zeiss) microscope equipped for phase contrast, epifluorescence, and an Axiocam HRm camera.

Infection assay

For infection assays, HFF cells were plated in 96 well plates (20,000 cells per well) in D10. After 24 h of culture, the cells were rinsed with PBS and 40,000 parasites of each strain (MOI 2:1) were loaded into

each well (250 µL per well). Plates were spun at 400 rpm for 1 min. After 3 washes in PBS, both host cells and parasites' nuclei were stained with 5 µg/mL Hoechst 33342 for 20 min at RT. The stained cells were rinsed with PBS 3 times and fixed for 15 min, at 37°C, with 3.7% methanol-free formaldehyde. After a 40 min saturation step with 5% goat serum (GS) (in PBS) at RT, extracellular parasites were stained for 45 min at RT with mAb anti-SAG1, followed by goat serum-anti mouse IgG conjugated to Alexa-488 idem (45 min, RT). The cells were washed 3 times in PBS and permeabilized for 15 min with PBS 5% GS in 0.1% triton-X100 at RT. The intracellular parasites were detected in the same conditions using mAb anti-GRA1 (45 min, RT) followed by goat serum anti mouse IgG conjugated to Alexa-594 (45 min, RT). The images were acquired by high content screening microscopy using an Olympus IX8 inverted microscope equipped with a black and white Orca ER Camera, and a LUCPLLN 20xPH1 objective. Images of the entire surface of each well were analyzed using the ScanR software. The percentage of infected cells was determined by calculating the number of intracellular parasites divided by the number of analyzed cells (> 1,000).

Intracellular proliferation assay

For intracellular proliferation assays, HFF cells were plated in 96 well plates (20,000 cells per well) in D10. After 24 h of culture the cells were rinsed with PBS and 40,000 parasites of each strain (MOI 2:1) were loaded into each well (250 µL per well). Plates were spun at 400 rpm for 1 min and incubated for 4 h to allow parasite invasion. Infected cells were washed 3 times with PBS and 250 µL of fresh D10 were added into the wells, followed by 36 h of culture at 37°C, 5% CO_2. Cells were then rinsed in PBS, stained with 5 µg/mL Hoechst 33342 for 20 min at 37°C, and fixed for 15 min at 37°C in 3.7% methanol-free formaldehyde. After 3 washes in PBS, a saturation-permeabilization step was performed for 15 min with PBS 5% GS in 0.1% triton-X100 at RT. The vacuoles and parasites were stained using mAb anti-GRA1 (45 min, RT), followed by goat serum anti-mouse IgG conjugated to Alexa-488 (45 min, RT). Analyses were performed as described above for the infection assay. The total number of parasites per PV as well as the percentage of PVs containing 1, 2, 4, 8, or 16 parasites were determined for >5,000 PVs per strain.

Spontaneous differentiation assay

HFFs grown to confluency on glass coverslips in 4 well-plates (in D10, at 37°C and 5% of CO_2) were infected with 100,000 freshly harvested tachyzoites per well and incubated for 4 h to allow parasite invasion. After 3 washes in PBS, fresh D10 was added to each well and the plates were returned to culture for 36 h at 37°C, 5% of CO_2. The cells were then washed 3 times in PBS, fixed and processed for IFA as detailed below.

Alkaline stress-induced differentiation

HFFs grown to confluency in 24 well-plates were infected with 20,000 freshly harvested tachyzoites per well and incubated for 36 h, at 37°C, in fresh D10 and with 5% of CO_2 to allow the formation of intracellular PVs. To induce the differentiation of tachyzoites into bradyzoites and PVs into cyst-like structures, the D10 medium was replaced by RPMI 1640 (Gibco) supplemented with 1% FBS, 2 mM glutamine, 50 µg/mL penicillin/streptomycin, 2 g/L $NaCOH_3$ and buffered with 50 mM HEPES to pH 8.2 (referred to "alkaline medium"). The cells were then maintained for 24 h or 48 h, at 37°C, in absence of CO_2, and the alkaline medium was renewed once a day. Infected cells were fixed and processed for IFA as detailed below.

Differentiated vacuoles and host organelles interaction assay

40,000 HFFs were seeded onto glass coverslips in 24 wells plates incubated with D10, at 37°C, and 5% of CO_2. After 16 to 24 h of culture the cells were infected with 40,000 freshly harvested tachyzoites (MOI, 1:1) and incubated for 4 h to allow parasite invasion. After 3 washes in PBS, fresh D10 was added to each well and the plates were returned to culture for 36 h. To induce parasites and vacuoles' differentiation the D10 was replaced by alkaline medium and the infected cells were incubated for 36 h, at 37°C, and in absence of CO_2. Differentiated cultures were fixed and stained to detect differentiated vacuoles as well as host mitochondria or host microtubules by IFA as explained below.

Indirect Immunofluorescence Assay (IFA)

To detect spontaneous- or induced-differentiation in parasites and vacuoles, infected cells were washed 3 times with PBS and fixed in 4% methanol-free formaldehyde (20 min, RT). Infected cells were permeabilized for 15 min with PBS in 0.1% Triton X-100, and saturated for 40 min in PBS 5% FBS-

5% GS. Using PBS-1% GS, the bradyzoites were detected using mAb anti-SRS9 (incubated for 1h, RT) (**Table 3**) followed by a 1 h incubation in goat serum anti-mouse IgG conjugated to Alexa-594. Then, the cyst walls were revealed using *Dolichos biflorus* lectin-FITC (**Table 3**) (1 h incubation, RT), and the cells- and parasites' nuclei were revealed with Hoechst 33258 (15 min incubation, RT, 1:30,000). The coverslips were mounted onto glass slides using mowiol. The percentage of differentiated vacuoles was calculated out of 200 vacuoles scanned in a given well, using an Axioplan 2 (Zeiss) microscope equipped for phase contrast, epifluorescence, and an Axiocam HRm camera. An Olympus IX8 inverted microscope was used to screen the entire surface of each well of infected cells cultured in 24 well plates and let to differentiate.

To study the potential recruitment of host cell mitochondria or microtubules to differentiating PV membranes, infected cells were fixed for 15 min at 37°C in 4% methanol-free formaldehyde or in PFA-Sucrose-NaOH (PBS, 4% Formaldheyde, 4% Sucrose, 0.1M NaOH) solution, respectively. Infected cells were permeabilized for 15 min with PBS in 0.1% Triton X-100, saturated for 40 min in PBS 5% FBS-5% GS, and incubated for 1 h with mAb anti-cytochrome C (**Table 3**) or mAb anti-α tubulin (**Table 3**) diluted in 1% GS (in PBS). The bound specific mAbs were revealed by a 1h incubation in goat serum anti-mouse IgG conjugated to Alexa-594, while *Dolichos biflorus* lectin-FITC was used as a marker of differentiated vacuoles. Host cells and parasites' nuclei were revealed by a 15 min incubation in Hoechst 33258. Coverslips were mounted onto glass slides using mowiol and infected cells were observed using a Zeiss LSM710 confocal microscope (immersed objective 63x NA 1.3). Z stacks were acquired and the analyses were performed using the ImageJ software and the algorithm "Intensity as a function of Distance" explained below.

Quantitative analysis with the algorithm "Intensity as a function of Distance"

To quantify the recruitment of host mitochondria and microtubules to the PV-cyst-like structures, we used the algorithm "Intensity as a function of Distance". This algorithm functions via user input (*e.g*. drawing the boundary of an object) and a shell-pixel counting method (*e.g*. generating concentric 1-pixel wide layers around the object) (Nolan *et al.,* 2015). As depicted on **Fig. 5A**, the user thus *i)* draws the boundary (in yellow) of an object (cyst-like structure, in green), *ii)* selects the channel in which the intensity of fluorescence must be quantified (Alexa-594), and *iii)* selects the maximum distance through which the intensity of fluorescence must be calculated (in this experiment: 25 pixels (or

layers in white), representing 6.5 μm, a physiologically relevant distance). The algorithm then sums the average fluorescence intensity of each pixel within a layer, thus leading to the identification of the layer where the maximum fluorescence intensity can be detected and which corresponds to the layer, where most of the host cell elements (mitochondria or microtubules) can be detected. Multiplying the position of this layer by its corresponding width provides the distance from the boundary (in μm) (*e.g.* 0.26 μm for pixel 1 or 1.38 μm for pixel 3). This quantification is applied to each stack. The distance from the boundary of the defined cyst-like structure and the maximum concentration in host cell elements (mitochondria or microtubules) calculated for each stack is finally averaged on the number of stacks, which leads to the formula:

$$\text{Average distance (in } \mu\text{m)} = \frac{\Sigma\,[(\text{layer rank of the MAX intensity signal}) \times \text{size of the pixel}]}{\text{number of stacks}}$$

The analyses were performed in a 6.5 μm-radius from the PV membrane boundary and on 50 different events from two different experiments.

Transmission Electron Microscopy (TEM)

HFF monolayers were grown on 4 wells labteks (ThermoFisher) in D10, 37°C, 5% CO_2 until confluency, and incubated with 20,000 freshly harvested tachyzoites for 36 h in D10, at 37°C, and with 5% of CO_2 in order to obtain vacuoles containing 4 parasites. To induce parasite differentiation infected cells were washed once in PBS and switched to alkaline medium before being returned to culture for 36 h at 37°C, in absence of CO_2. Infected cells were fixed with 2.5% glutaraldehyde in 0.1 M cacodylate buffer (pH 7.2) for 2 h at 4°C, rinsed in PBS, post-fixed in 1% osmium tetroxide-PBS (1 h, 4°C), dehydrated in a graded series of alcohol percentages, and embedded in a mixture of epon–araldite resins. The samples were sectioned with a Reichert ultra-microtome, stained with uranyl acetate and lead citrate and observed at 100 kV using a Fei Tecnai G2 spirit.

Electron Tomography

280-nm-thick sections were decorated on both faces with 10 nm colloidal gold particles before being observed using a Philips CM200 FEG tomograph operating at 200 kV, and equipped with a 2048 x 2048 CCD TVIPS TemCam-F224HD camera and with TVIPS EM menu 4 and EM-Tools software packages. Tomographic tilt series of images were recorded in double tilt axis geometry,

at the 27,500x magnification (pixel size: 0.66 nm), with a maximum tilt range of about -60° +60° and tilt increment of 1°. 3D tomograms were reconstructed and visualized using the IMOD software package (http://bio3d.colorado.edu/imod/).

Plaque assay

For plaque assay, HFFs were plated into 24 wells plates and cultured to form a confluent monolayer. 40,000 parasites were introduced into each well and incubated for 4 h to allow parasite invasion. After 3 washes in PBS, fresh D10 was added and plates were incubated at 37°C for 36 h. Infected cells were washed once in PBS and returned to culture in alkaline medium for 12, 36 or 48 h, at 37°C, and in absence of CO_2. Infected cells were scraped off and collected into 5 mL of PBS. Their plasma membrane was disrupted by 3 passages through a 27 *g* needle mounted onto a 5 mL syringe to release the intracellular parasites. After a centrifugation (10 min; 1,000 g) the parasites were dispersed into 2 mL of D10, serial-diluted (dilution rate: 1 to 4), and the parasite dilutions were seeded into a 24 well plate containing confluent HFFs. Plates were incubated without disturbance for 7 days, at 37°C, with 5% CO_2, to allow the formation of visible lysis plaques in the host cell monolayers. The infected cells were fixed for 5 min with cold methanol (-20°C) and stained (35 min) with 20% methanol-0,5% crystal violet solution (Sigma). After 3 washes with PBS, the plates were dried before being imaged and the plaques generated by each parasite dilution were counted.

Statistical analyses

Non-parametric Mann-Whitney *t*-tests were used to calculate the statistical significant differences ($P < 0.05$) using the GraphPad Prism 6 software.

Quantitative real-time RT-PCR

MAF1b expression was assessed in both RH and PRU (parental and Δ*gra*5) strains by RT-PCR. For samples preparation HFFs were cultured in T25 flasks to reach confluency. Freshly lysed parasites were loaded for 8 h onto the monolayers in fresh D10, at 37°C, under 5% of CO_2. After 1 wash in PBS, incomplete alkaline RPMI (1%, FBS, pH 8.2) was added to induce parasite differentiation and the flasks were returned to culture in absence of CO_2 for 24 h. At each time point, the intracellular parasites were isolated by 3 passages in a 10 mL syringe mounted on a 2.7 *g* needle. After a centrifugation (10

min; 1,000 g) total RNA was prepared using Pure link RNA Mini-Kit (Life-technologies), while the iScript Reverse Transcriptase Supermix for RT-qPCR (BIORAD) was used for cDNA preparation. Samples were analyzed by real-time quantitative PCR using primers specific for MAF1b (GeneBank ref: KU761340.1 (Me49)) or *Tg* ACTIN (ToxoDB ref: 219290 (Me49)) as control (**Table 2**). The reaction was performed using Fast Syber Green Master Mix (Applied Biosystem) and StepOnePlus (Applied Biosystem) and quantified with the delta-delta CT ($\Delta\Delta$CT) method.

Cell-fractionation

Two T175 flasks of confluent HFFs were infected with each strain for 12 h to allow parasite invasion. After a wash in PBS to eliminate the extracellular parasites, fresh D10 or incomplete alkaline RPMI was added and the cells were returned to culture for 12 h, at 37°C, and in presence or absence of CO_2. After 2 washes in PBS, infected HFFs were scraped and both the host cell and the PV membranes were mechanically disrupted by passing the cells through 20 *g* (X3) and 25 *g* (X3) needles. Released parasites were then collected by serial centrifugations: 5 min at 2,000 g (4°C), followed by 10 min at 2,000 g (4°C). The two resulting pellets (Low-Speed Pellet, LSP) were resuspended in 150 µL of PBS completed with protease inhibitors (cOmplete EDTA-free, Roche) and Laemmli loading buffer (Bio-Rad). The PV and host cells components collected from the two supernatants (Low-Speed Supernatant, LSS) were precipitated in 4 volumes of cold Acetone (1h; -20°C). After a 10 min centrifugation at 10,000 g (4°C), the pellets were dried (30 min; RT) and solubilized in 100 µL of PBS - protease inhibitors - Laemmli loading buffer (Bio-Rad) before protein denaturation and fractionation, as described below.

Protein preparation and Mass Spectometry

After denaturation for 3 min at 100°C, protein samples were fractionated on a 10% acrylamide SDS-PAGE. The electrophoretic migration was stopped as soon as the protein sample progressed for 1 cm into the separating gel. The gel was briefly stained with Coomassie Blue, and five bands, containing the whole sample, were cut out. Digestion of gel slices was performed as previously described (Miguet *et al.,* 2009). An UltiMate 3000 RSLCnano System (Thermo Fisher Scientific) was used for separation of the protein digests. Peptides were automatically fractionated onto a commercial C18 reversed phase column (75 µm × 150 mm, 2 µm particle, PepMap100 RSLC column, Thermo Fisher

Scientific, temperature 35 °C). Trapping was performed during 4 min at 5 µL/min, with solvent A (98 % H_2O, 2% Acetonitrile (ACN) and 0.1 % Formic Acid (FA)). Elution was performed using two solvents, A (0,1 % FA in water) and B (0,1 % FA in ACN), respectively, at a flow rate of 300 nL/min. Gradient separation was 3 min at 5% B, 37 min from 5 % B to 30% B, 5 min to 80% B, and maintained for 5 min. The column was equilibrated for 10 min with 5% buffer B prior to the next sample analysis.

The eluted peptides from the C18 column were analyzed by Q-Exactive instruments (Thermo Fisher Scientific). The electrospray voltage was 1.9 kV, and the capillary temperature was 275 °C. Full MS scans were acquired in the Orbitrap mass analyzer over m/z 300–1200 range with resolution 35,000 (m/z 200). The target value was 5.00E+05. Ten most intense peaks with charge state between 2 and 4 were fragmented in the HCD collision cell with normalized collision energy of 27%, and tandem mass spectrum was acquired in the Orbitrap mass analyzer with resolution 17,500 at m/z 200. The target value was 1.00E+05. The ion selection threshold was 5.0E+04 counts, and the maximum allowed ion accumulation times were 250 ms for full MS scans and 100 ms for tandem mass spectrum. Dynamic exclusion was set to 30 s.

Proteomic data analysis

Raw data collected during nano LC-MS/MS analysis were processed and converted into *.mgf peak list format with Proteome Discoverer 1.4 (Thermo Fisher Scientific). MS/MS data was interpreted using the search engine Mascot (version 2.4.0, Matrix Science, London, UK) installed on a local server. Searches were performed with a tolerance on mass measurement of 0.2 Da for precursor and 0.2 Da for fragment ions, against two different composite target decoy databases: 1) the ToxoDB database (50,620 total entries) built from 3 strains of *Toxoplasma gondii* (ToxoDB.org database: strains ME49, GT1 and VEG; release 12.0, December 2016; 25,192 entries) and 2) the human UniProt database (156,639 total entries; taxo number 9606). Both databases are fused with the sequences of recombinant trypsin and a list of classical contaminants (118 entries). Cysteine carbamidomethylation, methionine oxidation, protein N-terminal acetylation and cysteine propionamidation were searched as variable modifications. Up to one trypsin missed cleavage were allowed. For each sample, peptides were filtered out according to the cutoff set for proteins hits with 1 or more peptides longer than 9 residues, ion score > 35, identity score > 9, corresponding to 1% false positive rate.

A second filter was applied to select the candidates. Only the data with a requirement of three (or more than three) unique peptide identifications per protein were considered.

Acknowledgements

This work was financially supported by the “Labex Paradrap” (ANR-11-LABX-0024) and the “Fondation pour la Recherche Médicale” to MFCD. The authors acknowledge Annie Andrieux (INSERM U216, Université Grenoble Alpes, France), Nicolas Blanchard (INSERM U1043, CNRS, UMR 5282, Université de Toulouse, Toulouse, France), John C. Boothroyd (Department of Microbiology and Immunology, Stanford University School of Medicine, Stanford, CA, USA), Maryse Lebrun (CNRS UMR 5235, Université de Montpellier, France) for sharing reagents, the help of Mashal Ahmed, Amélie Donchet and Julie Védel (internship students). VB was supported by a PhD fellowship from the Parafrap Labex.

Bibliographic References

Adomako-Ankomah, Y., English, E.D., Danielson, J.J., Pernas, L.F., Parker, M.L., Boulanger, M.J., Dubey, J.P., and Boyle, J.P. (2016). Host Mitochondrial Association Evolved in the Human Parasite Toxoplasma gondii via Neofunctionalization of a Gene Duplicate. Genetics *203*, 283–298.

Alaganan, A., Fentress, S.J., Tang, K., Wang, Q., and Sibley, L.D. (2014). Toxoplasma GRA7 effector increases turnover of immunity-related GTPases and contributes to acute virulence in the mouse. Proc. Natl. Acad. Sci. U.S.A. *111*, 1126–1131.

Ali Khan, H., and Mutus, B. (2014). Protein disulfide isomerase a multifunctional protein with multiple physiological roles. Front Chem *2*, 70.

Ahn, H.-J., Kim, S., Kim, H.-E., and Nam, H.-W. (2006). Interactions between secreted GRA proteins and host cell proteins across the paratitophorous vacuolar membrane in the parasitism of Toxoplasma gondii. Korean J. Parasitol. *44*, 303–312.

Bellini, V., Loeuillet, C., Massera, C., Cesbron-Delauw, M. and Cavaillès, P. (2015). Cyst Detection in *Toxoplasma gondii* Infected Mice and Rats Brain. *Bio-protocol* 5(7): e1439. DOI: 10.21769/BioProtoc.1439.

Blanchard, N., Gonzalez, F., Schaeffer, M., Joncker, N.T., Cheng, T., Shastri, A.J., Robey, E.A., and Shastri, N. (2008). Immunodominant, protective response to the parasite Toxoplasma gondii requires antigen processing in the endoplasmic reticulum. Nat. Immunol. *9*, 937–944.

Bougdour, A., Durandau, E., Brenier-Pinchart, M.-P., Ortet, P., Barakat, M., Kieffer, S., Curt-Varesano, A., Curt-Bertini, R.-L., Bastien, O., Coute, Y., et al. (2013). Host cell subversion by Toxoplasma GRA16, an exported dense granule protein that targets the host cell nucleus and alters gene expression. Cell Host Microbe *13*, 489–500.

Braun, L., Brenier-Pinchart, M.-P., Yogavel, M., Curt-Varesano, A., Curt-Bertini, R.-L., Hussain, T., Kieffer-Jaquinod, S., Coute, Y., Pelloux, H., Tardieux, I., et al. (2013). A Toxoplasma dense granule protein, GRA24, modulates the early immune response to infection by promoting a direct and sustained host p38 MAPK activation. J. Exp. Med. *210*, 2071–2086.

Braun, L., Travier, L., Kieffer, S., Musset, K., Garin, J., Mercier, C., and Cesbron-Delauw, M.-F. (2007). Purification of Toxoplasma dense granule proteins reveals that they are in complexes throughout the secretory pathway. Mol. Biochem. Parasitol. *157*, 13–21.

Charif, H., Darcy, F., Torpier, G., Cesbron-Delauw, M.F., and Capron, A. (1990). Toxoplasma gondii: characterization and localization of antigens secreted from tachyzoites. Exp. Parasitol. *71*, 114–124.

Coppens, I., Dunn, J.D., Romano, J.D., Pypaert, M., Zhang, H., Boothroyd, J.C., and Joiner, K.A. (2006). Toxoplasma gondii sequesters lysosomes from mammalian hosts in the vacuolar space. Cell *125*, 261–274.

Ferguson, D.J.P. (2004). Use of molecular and ultrastructural markers to evaluate stage conversion of Toxoplasma gondii in both the intermediate and definitive host. Int. J. Parasitol. *34*, 347–360.

Ferguson, D.J.P., and Parmley, S.F. (2002). Toxoplasma gondii MAG1 protein expression. Trends Parasitol. *18*, 482.

Fox, B.A., Falla, A., Rommereim, L.M., Tomita, T., Gigley, J.P., Mercier, C., Cesbron-Delauw, M.-F., Weiss, L.M., and Bzik, D.J. (2011). Type II Toxoplasma gondii KU80 knockout strains enable functional analysis of genes required for cyst development and latent infection. Eukaryotic Cell *10*, 1193–1206.

Gay, G., Braun, L., Brenier-Pinchart, M.-P., Vollaire, J., Josserand, V., Bertini, R.-L., Varesano, A., Touquet, B., De Bock, P.-J., Coute, Y., et al. (2016). Toxoplasma gondii TgIST co-opts host chromatin repressors dampening STAT1-dependent gene regulation and IFN-γ-mediated host defenses. J. Exp. Med. *213*, 1779–1798.

Guimarães, E.V., Carvalho, L. de, and Barbosa, H.S. (2009). Interaction and cystogenesis of Toxoplasma gondii within skeletal muscle cells in vitro. Mem. Inst. Oswaldo Cruz *104*, 170–174.

Gold, D.A., Kaplan, A.D., Lis, A., Bett, G.C.L., Rosowski, E.E., Cirelli, K.M., Bougdour, A., Sidik, S.M., Beck, J.R., Lourido, S., et al. (2015). The Toxoplasma dense granule proteins GRA17 and GRA23 mediate the movement of small molecules between the host and the parasitophorous vacuole. Cell Host Microbe. *17*, 642–652.

Huynh, M.-H., and Carruthers, V.B. (2009). Tagging of endogenous genes in a Toxoplasma gondii strain lacking Ku80. Eukaryotic Cell *8*, 530–539.

Kim, S.-K., Karasov, A., and Boothroyd, J.C. (2007). Bradyzoite-specific surface antigen SRS9 plays a role in maintaining Toxoplasma gondii persistence in the brain and in host control of parasite replication in the intestine. Infect. Immun. *75*, 1626–1634.

Lane, A., Soete, M., Dubremetz, J.F., and Smith, J.E. (1996). Toxoplasma gondii: appearance of specific markers during the development of tissue cysts in vitro. Parasitol. Res. *82*, 340–346.

Lecordier, L., Mercier, C., Torpier, G., Tourvieille, B., Darcy, F., Liu, J.L., Maes, P., Tartar, A., Capron, A., and Cesbron-Delauw, M.F. (1993). Molecular structure of a Toxoplasma gondii dense granule antigen (GRA 5) associated with the parasitophorous vacuole membrane. Mol. Biochem. Parasitol. *59*, 143–153.

Lecordier, L., Mercier, C., Sibley, L.D., and Cesbron-Delauw, M.F. (1999). Transmembrane insertion of the Toxoplasma gondii GRA5 protein occurs after soluble secretion into the host cell. Mol. Biol. Cell *10*, 1277–1287.

Lemgrüber, L., Lupetti, P., Martins-Duarte, E.S., De Souza, W., and Vommaro, R.C. (2011). The organization of the wall filaments and characterization of the matrix structures of Toxoplasma gondii cyst form. Cell. Microbiol. *13*, 1920–1932.

Ma, J.S., Sasai, M., Ohshima, J., Lee, Y., Bando, H., Takeda, K., and Yamamoto, M. (2014). Selective and strain-specific NFAT4 activation by the Toxoplasma gondii polymorphic dense granule protein GRA6. J. Exp. Med. *211*, 2013–2032.

Magno, R.C., Straker, L.C., de Souza, W., and Attias, M. (2005). Interrelations between the parasitophorous vacuole of Toxoplasma gondii and host cell organelles. Microsc. Microanal. *11*,166–174.

Matsumoto, A., Bessho, H., Uehira, K., and Suda, T. (1991). Morphological studies of the association of mitochondria with chlamydial inclusions and the fusion of chlamydial inclusions. J Electron Microsc (Tokyo) *40*, 356–363.

Mercier, C., and Cesbron-Delauw, M.-F. (2015). Toxoplasma secretory granules: one population or more? Trends Parasitol. *31*, 60–71.

Mercier, C. and Delauw, M. F. (2012) Safe living within a parasitophorous vacuole: the recipe of success by *Toxoplasma gondii*. *Pathogen Interaction.* At the Frontiers of Cellular Microbiology (Ghigo, E. ed.) pp. 1-18, *Transworld Research Network.*

Mercier C, Howe DK, Mordue D, Lingnau M, Sibley LD. (1998). Targeted disruption of the GRA2 locus in Toxoplasma gondii decreases acute virulence in mice. Infect. Immun. *66*, 4176-4182.

Mercier, C., Rauscher, B., Lecordier, L., Deslée, D., Dubremetz, J.F., and Cesbron-Delauw, M.F. (2001). Lack of expression of the dense granule protein GRA5 does not affect the development of Toxoplasma tachyzoites. Mol. Biochem. Parasitol. *116*, 247–251.

Miguet, L., Béchade, G., Fornecker, L., Zink, E., Felden, C., Gervais, C., Herbrecht, R., Van Dorsselaer, A., van Dorsselaer, A., Mauvieux, L., et al. (2009). Proteomic analysis of malignant B-cell derived microparticles reveals CD148 as a potentially useful antigenic biomarker for mantle cell lymphoma diagnosis. J. Proteome Res. *8*, 3346–3354.

Moncada, D., Arenas, A., Acosta, A., Molina, D., Hernández, A., Cardona, N., Gomez-Yepes, M., and Gomez-Marin, J.E. (2016). Role of the 52 KDa thioredoxin protein disulfide isomerase of Toxoplasma gondii during infection to human cells. Exp. Parasitol. *164*, 36–42.

Nadipuram, S.M., Kim, E.W., Vashisht, A.A., Lin, A.H., Bell, H.N., Coppens, I., Wohlschlegel, J.A., and Bradley, P.J. (2016). In Vivo Biotinylation of the Toxoplasma Parasitophorous Vacuole Reveals Novel Dense Granule Proteins Important for Parasite Growth and Pathogenesis. MBio *7*.

Nolan, S.J., Romano, J.D., Luechtefeld, T., and Coppens, I. (2015). Neospora caninum recruits host cell structures to its parasitophorous vacuole and salvages lipids from organelles. Euk. Cell *14*, 454–473.

Olias, P., Etheridge, R.D., Zhang, Y., Holtzman, M.J., and Sibley, L.D. (2016). Toxoplasma Effector Recruits the Mi-2/NuRD Complex to Repress STAT1 Transcription and Block IFN-γ-Dependent Gene Expression. Cell Host Microbe *20*, 72–82.

Parmley, S.F., Yang, S., Harth, G., Sibley, L.D., Sucharczuk, A., and Remington, J.S. (1994). Molecular characterization of a 65-kilodalton Toxoplasma gondii antigen expressed abundantly in the matrix of tissue cysts. Mol. Biochem. Parasitol. *66*, 283–296.

Pernas, L., Adomako-Ankomah, Y., Shastri, A.J., Ewald, S.E., Treeck, M., Boyle, J.P., and Boothroyd, J.C. (2014). Toxoplasma effector MAF1 mediates recruitment of host mitochondria and impacts the host response. PLoS Biol. *12*, e1001845.

Persat, F., Mercier, C., Ficheux, D., Colomb, E., Trouillet, S., Bendridi, N., Musset, K., Loeuillet, C., Cesbron-Delauw, M.-F., and Vincent, C. (2012). A synthetic peptide derived from the parasite Toxoplasma gondii triggers human dendritic cells' migration. J. Leukoc. Biol. *92*, 1241–1250.

Rodriguez C, Afchain D, Capron A, Dissous C, Santoro F. (1985). Major surface protein of Toxoplasma gondii (p30) contains an immunodominant region with repetitive epitopes. Eur J Immunol. 1985 Jul;15(7):747-749.

Romano, J.D., Sonda, S., Bergbower, E., Smith, M.E., and Coppens, I. (2013). Toxoplasma gondii salvages sphingolipids from the host Golgi through the rerouting of selected Rab vesicles to the parasitophorous vacuole. Mol. Biol. Cell *24*, 1974–1995.

Rommereim, L.M., Bellini, V., Fox, B.A., Pètre, G., Rak, C., Touquet, B., Aldebert, D., Dubremetz, J.-F., Cesbron-Delauw, M.-F., Mercier, C., et al. (2016). Phenotypes Associated with Knockouts of Eight Dense Granule Gene Loci (GRA2-9) in Virulent Toxoplasma gondii. PLoS ONE *11*, e0159306.

Rosowski, E.E., Lu, D., Julien, L., Rodda, L., Gaiser, R.A., Jensen, K.D.C., and Saeij, J.P.J. (2011). Strain-specific activation of the NF-kappaB pathway by GRA15, a novel Toxoplasma gondii dense granule protein. J. Exp. Med. *208*, 195–212.

Scanlon, M., Leitch, G.J., Visvesvara, G.S., and Shaw, A.P. (2004). Relationship between the host cell mitochondria and the parasitophorous vacuole in cells infected with Encephalitozoon microsporidia. J. Eukaryot. Microbiol. *51*, 81–87.

Sibley, L.D., Niesman, I.R., Parmley, S.F., and Cesbron-Delauw, M.F. (1995). Regulated secretion of multi-lamellar vesicles leads to formation of a tubulo-vesicular network in host-cell vacuoles occupied by Toxoplasma gondii. J. Cell. Sci. *108 (Pt 4)*, 1669–1677.

Sinai, A.P., Webster, P., and Joiner, K.A. (1997). Association of host cell endoplasmic reticulum and mitochondria with the Toxoplasma gondii parasitophorous vacuole membrane: a high affinity interaction. J. Cell. Sci. *110 (Pt 17)*, 2117–2128.

Soëte, M., Fortier, B., Camus, D., and Dubremetz, J.F. (1993). Toxoplasma gondii: kinetics of bradyzoite-tachyzoite interconversion in vitro. Exp. Parasitol. *76*, 259–264.

Stolf, B.S., Smyrnias, I., Lopes, L.R., Vendramin, A., Goto, H., Laurindo, F.R.M., Shah, A.M., and Santos, C.X.C. (2011). Protein disulfide isomerase and host-pathogen interaction. Scientific World Journal *11*, 1749–1761.

Tomita T, Bzik DJ, Ma YF, Fox BA, Markillie LM, Taylor RC, Kim K, Weiss LM (2013). The Toxoplasma gondii cyst wall protein CST1 is critical for cyst wall integrity and promotes bradyzoite persistence. PLoS Pathog. *9*, e1003823.

Torpier, G., Charif, H., Darcy, F., Liu, J., Darde, M.L., and Capron, A. (1993). Toxoplasma gondii: differential location of antigens secreted from encysted bradyzoites. Exp. Parasitol. *77*, 13–22.

Van, T.T., Kim, S.-K., Camps, M., Boothroyd, J.C., and Knoll, L.J. (2007). The BSR4 protein is up-regulated in Toxoplasma gondii bradyzoites, however the dominant surface antigen recognized by the P36 monoclonal antibody is SRS9. Int. J. Parasitol. *37*, 877–885.

Walker, M.E., Hjort, E.E., Smith, S.S., Tripathi, A., Hornick, J.E., Hinchcliffe, E.H., Archer, W., and Hager, K.M. (2008). Toxoplasma gondii actively remodels the microtubule network in host cells. Microbes Infect. *10*, 1440–1449.

Weiss, L.M., and Kim, K. (2011). The development and biology of bradyzoites of Toxoplasma gondii. Front. Biosci. *5*, D391-405.

Zhang, Y.W., Halonen, S.K., Ma, Y.F., Wittner, M., and Weiss, L.M. (2001). Initial characterization of CST1, a Toxoplasma gondii cyst wall glycoprotein. Infect. Immun. *69*, 501–507.

Legend of figures

Figure1. Construction and characterization of both the Pru∆*ku80*∆*gra5*::*hxgprt* (Pru∆*gra5*) knocked-out- and the PRU∆*gra5*::*gra5-hxgprt* (PRU∆*gra5*::*gra5*) complemented type II strains

A) Schematic representation of the strategy used to generate the Pru∆*ku80*∆*gra5*::*hxgprt* (Pru∆*gra5*) knocked-out strain. The *gra5* gene was deleted from the Pru∆*ku80*∆*hxgprt* parental strain and replaced by the *hxgprt* selectable marker (provided by the p∆GRA5 plasmid that allows expression of *hxgprt* under the 5' and 3' regulatory sequences of *gra5*) by double cross-over homologous recombination at the *gra5* locus. Parasite recombinants having integrated *hxgprt* were positively selected by the combination of mycophenolic acid and xanthine (MPA+X). **B)** Schematic representation of the strategy that led to the construction of the PRU∆*gra5*::*gra5-hxgprt* (PRU∆*gra5*::*gra5*) complemented strain. The pLic-3HA-DHFR plasmid was modified to insert 1.6 Kb of the *gra5* 5' upstream region (5' PRUGRA5) and the *gra5* coding sequence (including its stop codon) (GRA5 CDS) in order to generate the pLic-GRA5.3HA-DHFR plasmid. In pLic-GRA5.3HA-DHFR the GRA5 expression cassette is followed by the triplicated sequence of the HA epitope tag (x3HA) and the 3' untranslated region of *hxgprt* (3'UTR). The DHFR selectable marker is shown in yellow. After transfection the parasites were selected with pyrimethamine and cloned. **C)** The parental, knocked-out and complemented strains were respectively inoculated onto HFF monolayers for 36 h. After fixation, permeabilization and saturation, infected cells were incubated with monoclonal antibody anti-GRA5 (mAb αGRA5), washed, and further incubated with goat anti-mouse IgG coupled to Alexa-594 (red). To verify the specificity of the GRA5 signal, co-labeling of GRA6 was performed using rabbit anti-GRA6 serum followed by goat anti-rabbit IgG coupled to Alexa-488 (green). Both host and parasite nuclei were revealed with Hoechst 33258 (blue). "Merge" shows the co-localization of both the GRA proteins in the parasites. **D)** Immunoblot of both GRA5 (21 kDa, revealed with mAb anti-GRA5) and SAG1 (30 kDa, revealed with mAb αSAG1) in parasite protein lysates. Cell lysate equivalent to $1x10^7$ parasites was loaded per lane.

<u>Figure 2.</u> The lack of GRA5 does not hamper infection and proliferation of type II tachyzoites

A) To compare their infection rates HFF monolayers were infected with PRUΔ*hx*, PRUΔ*gra5* or PRUΔ*gra5*::*gra5* tachyzoites at a MOI of 2:1 for 4 h. Extra- and intracellular parasites were discriminated by IFA. Monoclonal antibody to SAG1 followed by goat anti-mouse IgG coupled to Alexa-488 (green) were used to detect the extracellular parasites. After further permeabilization of the infected cells the intracellular vacuoles and parasites were revealed using monoclonal antibody to GRA1 followed by goat anti-mouse IgG conjugated to Alexa-594. The nuclei of both host cells and parasites were revealed by Hoechst 33342. The percentage of infected cells was calculated by dividing the number of intracellular parasites by the number of analyzed HFFs (~ 1,000) and multiplying by 100. The Mann Whitney statistical *t*-test performed on 3 different experiments did not reveal significant differences between the 3 strains. **B)** Parasite proliferation was quantified 36 h p.i. by staining of boh the intracellular vacuoles and parasites with monoclonal antibody anti-GRA1 followed by goat serum anti-mouse IgG conjugated to Alexa-594. The nuclei of both host cells and parasites (detected with Hoechst 33342) allowed the quantification of the percentage of vacuoles containing 1, 2, 4, 8 or 16 parasites formed in each type of infected cells. The percentages were calculated from more than 500 analyzed vacuoles observed in a total of 3 experiments. **C)** Intracellular growth on the long term by plaque assays. 40,000 parasites of each strain were loaded onto HFFs grown to confluency in 24 well-plates. After 36 h of culture extra- and intracellular parasites were collected, serial diluted, loaded onto novel HFF monolayers, led to proliferate for 7 days and stained with crystal violet. **D)** The total number of parasites was calculated by multiplying the number of plaques observed for a given parasite dilution by the dilution factor and this number was averaged on 2 experiments performed in similar conditions.

<u>Figure 3.</u> Deletion of *gra5* induces earlier *in vitro* differentiation

A) Schematic representation of the experimental protocol used to quantify the differentiation of parental- (PRU Δ*hx*), KO- (PRUΔ*gra5*) and complemented (PRU Δ*gra5*::*gra5*) parasites. HFF monolayers were infected with parasites and cultured for 36 h in presence of CO_2 (before stress). To induce the differentiation infected cells were washed and further incubated for 24 or 48 h in alkaline medium (1% FBS, pH 8.2) and in absence of CO_2 (after stress). Before and after stress differentiating parasites were detected using monoclonal antibody to SRS9, followed by goat serum-anti mouse IgG

conjugated to Alexa-594 (red), while PV membranes differentiating into cyst walls were monitored using *Dolichos bifluorus* lectin recognizing the CST1 glycoprotein and conjugated to fluorescein isothiocyanate (FITC, green). The nuclei of both the cells and the parasites were revealed using Hoechst 33258 (grey). The photos show HFF cells, which have been infected by PRUΔ*gra5*::*gra5* parasites grown for 48 h under stress conditions. The parasites which developed in HFF cells (grown on glass coverslips) without alkaline stress were analyzed using an Axioplan 2 microscope (Zeiss) equipped for phase contrast and epifluorescence and coupled to an Axiocam HRm camera. After 24 or 48 h of culture under stress conditions, images of the entire surface of each well from the 24 well-plates (without coverslips) were acquired with an Olympus IX8 inverted microscope equipped with a black and white Orca ER Camera, and the total number of vacuoles-cysts was determined. Quantification of CST1-positive **(B)** or SRS9 and CST1-positive **(C)** vacuoles-cysts after 36 h of culture, followed by 24 or 48 h of culture under stress conditions **(D-E).** Statistical analyses were performed using the Mann-Whitney *t*-test to compare the differences between the strains in each culture condition. *P < 0.05; **P ≤ 0.008 indicates significant differences.

<u>Figure 4.</u> Host mitochondria and host microtubules are recruited to the membrane of Pru*Δgra5* cyst-like structures

All the presented images were acquired after 36 h of *in vitro* culture in stress conditions. **A)** Transmission Electron Micrograph of a PRUΔ*hx* vacuole showing close association between the PV membrane and elements of the HER. **B)** Magnification of the **A)** inset. The black arrows delineate the PV membrane while black arrowheads point out the ribosomes of the HER. **C)** Transmission electron micrograph of a PRUΔ*gra5* vacuole showing its close association with host mitochondria (HM). **D)** High magnification of a PRUΔ*gra5* vacuole showing the dense array of host microtubules (HMT, black arrows) aligned perpendicularly to the PV membrane surface (black arrowheads). AG, amylopectin granule; P, parasite; PV, parasitophorous vacuole; PVM, parasitophorous vacuole membrane. **E)** The outer membrane of host mitochondria does not fuse with the PV membrane of PruΔ*gra5.* Tomographic analysis of the association between a PRUΔ*gra5* vacuole (PV) and a host mitochondrion (HM) showing the close association, but not the fusion, between the HM external membrane (black arrows) and the PV membrane (black arrowheads). The analysis was performed on 280 nm thick

sections. Images were recorded in double tilt axis geometry, at the 27,500x magnification (nominal pixel size 0.66 nm). The reconstructed structures were visualized in 2D as tomographic slices.

Figure 5. Host mitochondria are at a shorter distance to the membrane of cyst-like structures in PruΔ*gra5*

PRUΔ*hx*, PRUΔ*gra5* and PRUΔ*gra5::gra5* parasites were cultured for 36 h in D10 and in presence of 5% CO_2 before being switched to alkaline medium and further incubated for 36 h without CO_2. Infected cells were processed for IFA and incubated with anti-cytochrome C or anti α-tubulin followed by goat serum anti-mouse IgG conjugated to Alexa-594 (Red). Differentiation of the PV membrane was detected using *Dolichos bifluorus* lectin-FITC. **A)** The left panel shows one example of a boundary (yellow circle), as defined by the algorithm "Intensity as a function of Distance". In this case, the boundary delineates a selected differentiated PV membrane (in green) chosen on one image acquired from PRUΔ*hx*-infected HFFs. The anti-cytochrome C antibody was used to label the host mitochondria in red. The right panel shows the pixels (or layers), which were analyzed by the algorithm (with a maximum of 25 layers). The white layers super-impose the host cell cytoplasm area (left panel), where host mitochondria were detected. **B)** The left panel exemplifies the closer association of host cell mitochondria with the limiting membrane of differentiating PV-cyst-like structures in PRUΔ*gra5*. The graph on the right represents the averaged distance between the membrane of the differentiating PV-cyst-like structures and the region of the maximal host mitochondria fluorescence in PruΔ*hx*, PRUΔ*gra5* and PRUΔ*gra5::gra5*. **C)** The left panel shows the closer association of host cell microtubules with the limiting membrane of differentiating PV-cyst-like structures in PRUΔ*gra5*. The graph on the right represents the averaged distance between the membrane of the differentiating PV-cyst-like structures and the region of the maximal host microtubules' fluorescence in PruΔ*hx*, PRUΔ*gra5* and PRUΔ*gra5::gra5*. 50 events from two different experiments were analyzed by confocal microscopy and analyzed with the ImageJ software. Significant differences ** $P \leq 0.009$; *** $P = 0.0005$.

Figure6. The recruitment of host mitochondria to the membrane of PV-cyst-like structures in Pru∆*gra5* does not rely on the expression of *MAF1RHb1*

40,000 tachyzoites of RH, PRU∆*hx* or PRU∆*gra5* were inoculated onto confluent HFFs and cultured for 8 h under 5% of CO_2, before being switched to alkaline stress for 24 h. **A)** After 8 h of culture with CO_2 GRA7 and MAF1 were respectively labeled using rabbit serum anti-GRA7 and mouse monoclonal antibody to MAF1b1 followed by the corresponding goat sera anti- rabbit or mouse IgG respectively conjugated to Alexa-488 or Alexa-594 (Red). **B)** After 24 h of culture under stress conditions differentiating vacuoles were labeled using *Dolichos biflorous* lectin conjugated to FITC and mouse monoclonal antibody to MAF1b1 followed by goat serum anti-mouse IgG conjugated to Alexa-488 (green). Parasites and cell nuclei were stained by Hoechst 33258. **C)** *MAF1b1*(PRU) mRNA levels in RH, PRU∆*hx* and PRU∆*gra5* parasites after 8 h of culture with CO_2 and after 24 h of culture under stress conditions. The primers used to amplify *MAF1b* were designed from the MAF1ME49b1 gene sequence. The mRNA levels were analyzed by real-time quantitative PCR, using the TgACTIN mRNA as an internal control of steady state expression. The quantification was performed using the delta-delta CT (∆∆CT) method and the data were represented as compared to the MAF1ME49b1 mRNA (to which the 1 value was arbitrarily attributed) detected in RH after 8 h of culture with CO_2 (red arrow). Statistical analyses were performed using Mann Whitney *t*-tests. Significant differences: *P < 0.05

Figure 7. Schematic representation of the host cells proteins expression during parasite infection and differentiation.

The selection of proteins (UniProt.org) was perfomed using a semiquantitative analysis. On the left, proteins which were represented by more than 3 peptides in the PRU∆*gra5::gra5* strain and which exhibited more than a 4-fold-increased detection in both the complementated- and the parental strains, compared with the PRU∆*gra5* strain. On the right, proteins which were represented by more than 3 peptides in the PRU∆*gra5* strain and which exhibited more than a 4-fold-increased detection in PRU∆gra5, compared to both the complementated- and the parental strains. Sorted proteins were divided into 9 different families according to their function (Gene Ontology). The pies represent their relative expression in each sample (LSS, vacuoles and host cells fraction) and for each culture condition: 24 h of infection (+CO_2) or 12 h after stress (-CO_2).

Table 1. Strains used or developed in this work

Strain	Parent strain	Genotype	References
PRUΔ*ku*80Δ*hxgprt* (PRUΔ*hx*)	PRUΔ*ku80*::*hxgprt*	Δ*ku80*Δ*hxgprt*	*Fox et al., 2011*
PruΔ*ku80Δgra5*:.*hxgprt* (PruΔ*gra5*)	PruΔ*ku80*Δ*hxgprt*	Δ*ku80*Δ*gra5*:.*hxgprt*	This study
PruΔ*ku80*Δ*gra5*::*gra5* (PruΔ*gra5*::*gra5*)	PruΔ*ku80*Δ*gra5*::*hxgprt*	Δ*ku80*::*hxgprt*	This study
RHΔ*ku80*::*hxgprt*	RH	Δ*ku80*::*hxgprt*	*Fox et al., 2009*
RHΔ*ku80*Δ*gra5*::*hxgprt*	RHΔ*ku80*Δ*hxgprt*	Δ*ku80*Δ*hxgprt*	*Fox et al., 2009*

Table 2. List of primers used in this work

Forward primers[a]	Reverse primers[a]	Purpose
COMP-F: 5'- TACTTCCAATCCAATTTAATGCCAACGGTG CCAGCTCCTGTGTACA-3'	COMP-R: 5'- TCCTCCACTTCCAATTTTAGCTTACTCTTCCT CGGCAACTTCTTC-3'	GRA5 complementation
MAF1b-F: 5'-TACGGCAACCTGAACAACAACGTC-3'	MAF1b-R: 5'-AATGACGCCGGCAATCGTTG-3'	MAF1 quantitative RT-PCR
TgActin-F: 5'-AACGGTGATGATGTTGCCATCG-3'	TgActin-R: 5'-TGCTACATCGCCCTCGAGTTC-3'	Actin control in MAF1 quantitative RT-PCR

[a], underlined sequences were used for ligation-independent cloning.

Table 3. List of antibodies used in this work

PRIMARY ANTOBODIES			
Type of antibody	**IFA dilution**	**Immunoblot dilution**	**References**
Anti-SAG1 mouse monoclonal antibody TG054	1/500	1/1,000	Rodriguez *et al*., 1985
Anti-SRS9 mouse monoclonal antibody T84A12_IC3	1/500	NA	Kim and Boothroyd, 2007
Anti-GRA1 mouse monoclonal antibody TG17-43	1/500	NA	Biotem, Apprieu, France Charif *et al*., 1990
Anti-GRA5 mouse monoclonal antibody TG17.113	1/500	1/1,000	Biotem, Apprieu, France Charif *et al*., 1990
Rabbit serum anti-GRA7	1/1,000	NA	J.C. Boothroyd, Standford University School of Medicine
Rabbit serum anti-HF10 ($GRA6_{II}$)	1/500	NA	Blanchard *et al*., 2008
anti-MAF1 mouse monoclonal antibody	1/500	NA	Pernas *et al*., 2014
Rabbit serum anti-MAF1	1/500	NA	Pernas *et al.*, 2014
Anti-α-tubulin mouse monoclonal antibody	1/4,000	NA	A. Andrieux, Grenoble Institute of Neurosciences
Anti-cytochrome C monoclonal mouse antibody CTC03(2B5)	1/500	NA	Thermo Fisher Scientific
SECONDARY ANTIBODIES			
Type of antibody	***IF dilution***	***Immunoblot dilution***	***References***
Goat anti-mouse IgG (H+L) conjugated to Alexa-594	1/1,000	NA	Alexa Fluor (A-11005) Thermo Fisher Scientific
Goat anti-mouse IgG (H+L) conjugated to Alexa-488	1/1,000	NA	Alexa Fluor (A-11001) Thermo Fisher Scientific
Goat anti-rabbit IgG (H+L) conjugated to Alexa-594	1/1,000	NA	Alexa Fluor (A-11012) Thermo Fisher Scientific
Goat anti-rabbit IgG (H+L) conjugated to Alexa-488	1/1,000	NA	Alexa Fluor (A-11008) Thermo Fisher Scientific
Goat anti-Mouse IgG (H+L) conjugated to HRP	NA	1/10,000	A-16084 Thermo Fisher Scientific
FLUORESCENT PROBE			
Type of probe	***IF dilution***	***Immunoblot dilution***	***Reference***
Dolichos biflorus lectin (DBL) conjugated to FITC	1/500	NA	Vector Laboratories

NA: does not apply

Table 4

List of proteins identified in the LSP fraction (tachyzoites only) of PRUΔ*hx* and PRUΔ*gra5::gra5* infected cells after 24 h of culture (+CO_2) or 12 h of culture under stress conditions (-CO_2).

LSP fraction (parasites only) of PRUΔhx and PRUΔgra5::gra5 infected cells after 24 h of culture (+CO_2)					
Protein name[a]	**MW (Da)**	**Accession number**	**Number of peptides (spectra)[b]**		
			Δhx	***Δgra5::gra5***	***Δgra5***
Dense granule protein GRA5	12.8	TGME49_286450	4 (20)	3 (5)	NA[c]

LSP fraction (parasites only) of PRUΔhx and PRUΔgra5::gra5 infected cells after 12 h of culture with stress (-CO_2)					
Protein name[a]	**MW (Da)**	**Accession number**	**Number of peptides (spectra)[b]**		
			Δhx	***Δgra5::gra5***	***Δgra5***
Putative alkyl hydroperoxide reductase/ Thiol specific antioxidant/ Mal allergen	21.7	TGME49_217890	3(5)	7 (14)	NA[c]
Rhoptry protein ROP15	36.5	TGME49_211290	3 (3)	5 (10)	2 (2)
Phospholipase/ carboxylesterase	52	TGME49_228290	1 (2)	5 (8)	NA
Dense granule protein GRA5	12.8	TGME49_286450	5 (14)	3 (6)	NA
Putative vacuolar ATP synthase sub.b	56.6	TGME49_219800	2 (2)	5 (5)	NA
Fructose-bisphospatase II	42.3	TGME49_247510	2 (2)	4 (5)	NA
Peptidase M16, alpha subunit, putative	62.2	TGME49_202680	2 (4)	4 (5)	NA
Hypothetical protein	40.2	TGME49_247440	3 (5)	7 (10)	1 (1)
GAP45	27.3	TGME49_223940	4 (5)	5 (5)	NA
DnaK family protein	90.14	TGME49_219310	8 (8)	11 (19)	1 (1)
Dense granule protein DG32	24.15	TGME49_297880	5 (6)	5 (7)	1 (1)

LSS fraction (vacuoles, host cells) of PRUΔhx and PRU Δgra5::gra5 infected cells after 24 h of culture (+CO_2)					
Protein name[a]	**MW (Da)**	**Accession number**	**Number of peptides (spectra)[b]**		
			Δhx	***Δgra5::gra5***	***Δgra5***
Protein disulfide isomerase	52.8	TGME49_211680	5 (5)	10 (11)	NA[c]
Putative alkyl hydroperoxide reductase/ Thiol specific antioxidant/ Mal allergen	21.7	TGME49_217890	2 (2)	4 (5)	NA
Phosphofructokinase PFKII	13.3	TGME49_226960	2 (2)	4 (4)	NA
MAG1 protein	49.2	TGME49_270240	2 (2)	3 (5)	NA

LSS fraction (vacuoles, host cells) of PRUΔhx and PRUΔgra5::gra5 infected cells after 12 h of culture with stress (-CO_2)					
Protein name[a]	**MW (Da)**	**Accession number**	**Number of peptides (spectra)[b]**		
			Δhx	***Δgra5::gra5***	***Δgra5***
Protein disulfide isomerase	52.8	TGME49_211680	2 (2)	10 (13)	NA[c]

Tryptophanyl-tRNA synthetase (TrpRS2)	77	TGME49_288360	3 (3)	7 (8)	NA
Glyceraldehyde-3-phosphate dehydrogenase GAPDH1	53.4	TGME49_289690	3 (3)	4 (6)	NA
Phosphofructokinase PFKII	13.3	TGME49_226960	2 (2)	5 (5)	NA
MAG1 protein	49.2	TGME49_270240	2 (2)	5 (5)	NA

[a]The list of protein candidates (ToxoDB.org) was sorted using the semi-quantitative analysis method: proteins which had more than 3 peptides mapped in the PRUΔ*gra5::gra5* strain and more than a 4-fold-increased detection in both the complemented and parental strains over PRUΔ *gra5* were retained.

[b]The number of peptides (number of spectra) in each sample was detected by mass spectrometry.

[c]NA, no count detected in PRUΔ*gra5*.

Table 5. List of proteins identified in the LSP fraction (tachyzoites only) of PRUΔ*gra5*-infected cells after 24 h of culture (+CO_2) or 12 h of culture under stress (-CO_2)

LSP fraction (parasites only) of PRUΔgra5 infected cells after 24 h of culture (+CO_2)					
Protein name[a]	**MW (Da)**	**Accession number**	**Number of peptides (spectra)[b]**		
			Δhx	***Δgra5::gra5***	***Δgra5***
Cyclophilin	19.6	TGME49_221210	1(2)	NA[c]	5 (8)
Putative eukaryotic porin	50	TGME49_218280	1 (2)	NA	5 (8)
Putative cyclophilin1	26.2	TGME49_230520	1 (1)	NA	4 (6)
Putative ATP synthase	19.4	TGME49_226000	1 (1)	NA	4 (6)
Ribosomal protein RPS13	17	TGME49_270380	1 (1)	NA	5 (5)
Ribosomal protein RPL30	11.6	TGME49_232230	NA	NA	5 (5)
Hypothetical protein	13.2	TGME49_218240	1 (1)	NA	5 (5)
Ribosomal protein RPL11	20.2	TGME49_309820	1 (1)	1 (1)	4 (5)
Ribosomal protein RPS24	30.3	TGME49_215460	1 (1)	1 (1)	5 (5)

LSS fraction (vacuoles, host cells) of PRUΔgra5 infected cells after 12 h of culture under stress (-CO_2)					
Protein name[a]	**MW (Da)**	**Accession number**	**Number of peptides (spectra)[b]**		
			Δhx	***Δgra5::gra5***	***Δgra5***
Dense granule protein DG32	24	TGME49_297880	2 (2)	1 (1)	6 (6)

[a]The list of protein candidates (ToxoDB.org) was sorted using the semi-quantitative analysis method: proteins which had more than 3 peptides mapped in the PRUΔ*gra5* strain and more than a 4-fold-increased detection in PRUΔ*gra5* over PRU*Δh and* PRU*Δgra5::gra5* were retained.

[b]The number of peptides (number of spectra) in each sample was detected by mass spectrometry.

[c]NA, no count detected in PRUΔ*gra5::gra5 or* PRUΔ*hx*

Figure 1

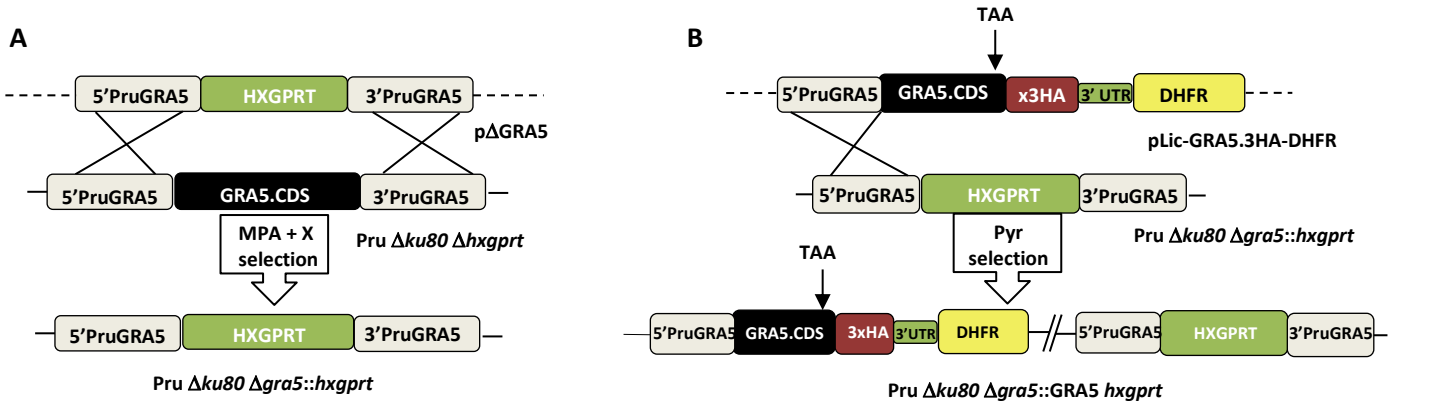
A
5'PruGRA5
HXGPRT
3'PruGRA5
pΔGRA5
5'PruGRA5
GRA5.CDS
3'PruGRA5
MPA + X selection
Pru Δku80 Δhxgprt
5'PruGRA5
HXGPRT
3'PruGRA5
Pru Δku80 Δgra5::hxgprt
B
TAA
5'PruGRA5
GRA5.CDS
x3HA
3' UTR
DHFR
pLic-GRA5.3HA-DHFR
5'PruGRA5
HXGPRT
3'PruGRA5
Pru Δku80 Δgra5::hxgprt
Pyr selection
TAA
5'PruGRA5
GRA5.CDS
3xHA
3'UTR
DHFR
5'PruGRA5
HXGPRT
3'PruGRA5
Pru Δku80 Δgra5::GRA5 hxgprt

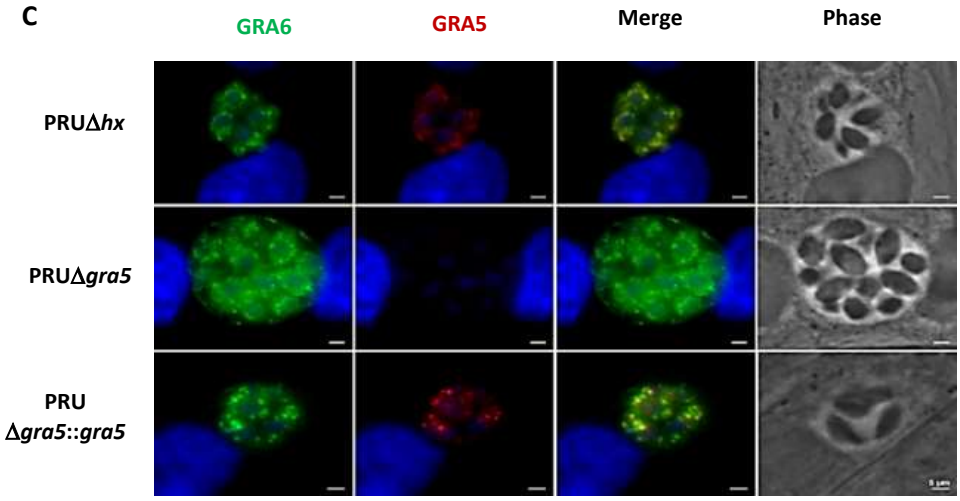
C
GRA6
GRA5
Merge
Phase
PRUΔhx
PRUΔgra5
PRU Δgra5::gra5

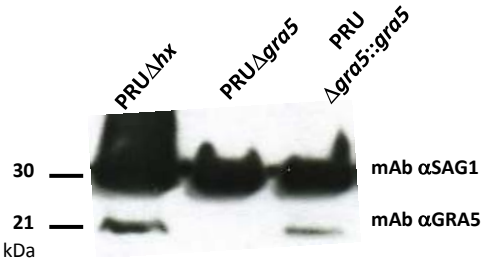
D
PRUΔhx
PRUΔgra5
PRU Δgra5::gra5
30
21
kDa
mAb αSAG1
mAb αGRA5

Figure 2

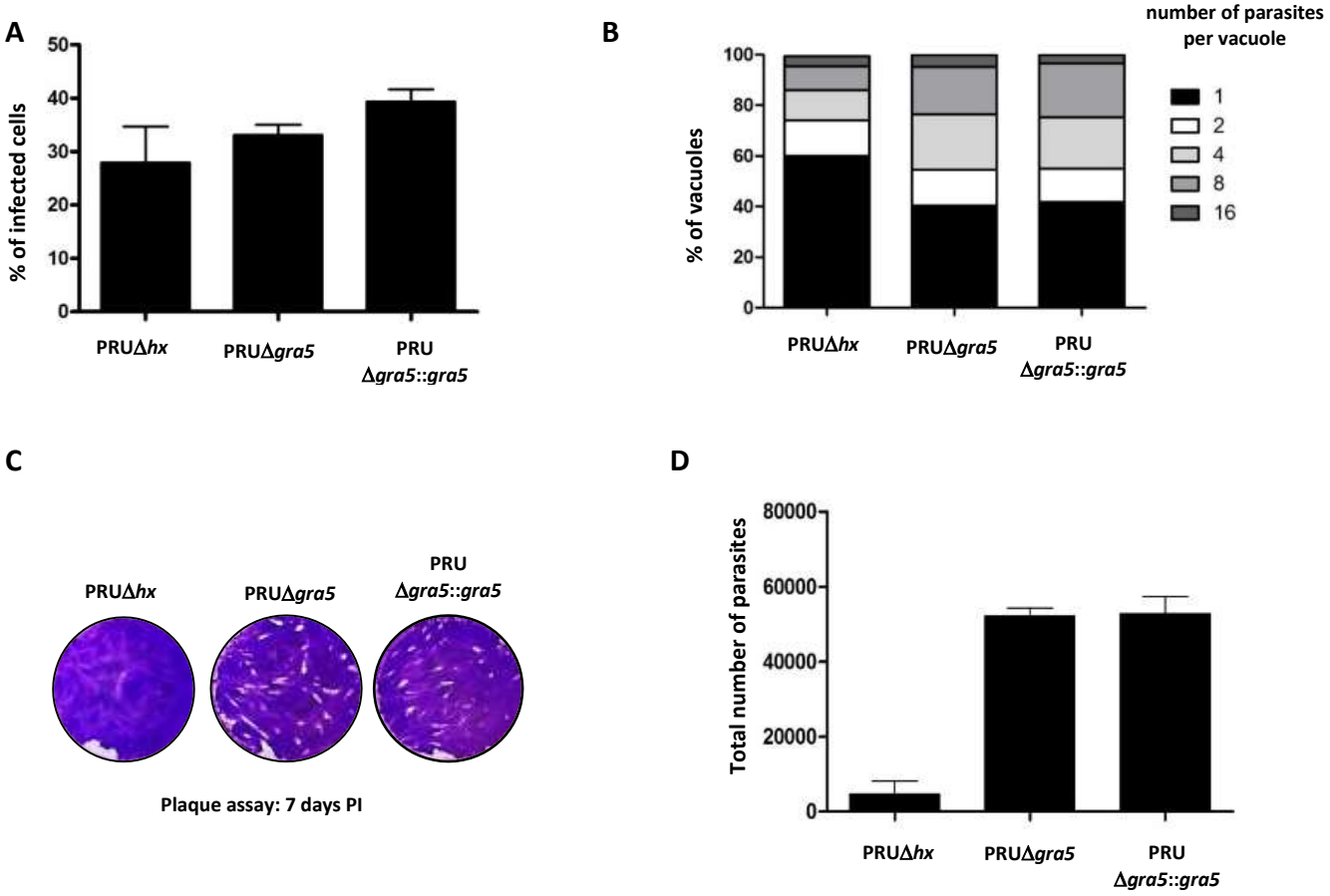
A
% of infected cells
50
40
30
20
10
0
PRUΔhx
PRUΔgra5
PRU Δgra5::gra5
B
number of parasites per vacuole
% of vacuoles
100
80
60
40
20
0
1
2
4
8
16
PRUΔhx
PRUΔgra5
PRU Δgra5::gra5
C
PRUΔhx
PRUΔgra5
PRU Δgra5::gra5
Plaque assay: 7 days PI
D
Total number of parasites
80000
60000
40000
20000
0
PRUΔhx
PRUΔgra5
PRU Δgra5::gra5

Figure 3

A

36 h incubation of confluent HFFs with *T. gondii*

culture at 37°C, without CO_2, in alkaline medium

before stress

24 h or 48 h (after stress)

Incubation of parasites with
mAb αSRS9 (bradyzoite Ag)
+
Staining of the cyst wall with
Dolichos biflorus lectin
(CST1 protein)-FITC
+
Staining of nuclei:
Hoechst 33258 (grey)

Number of vacuoles:
Axioplan2 (Zeiss) (epifluorescence microscopy)

Number of vacuoles:
Olympus IX8 inverted microscope

B

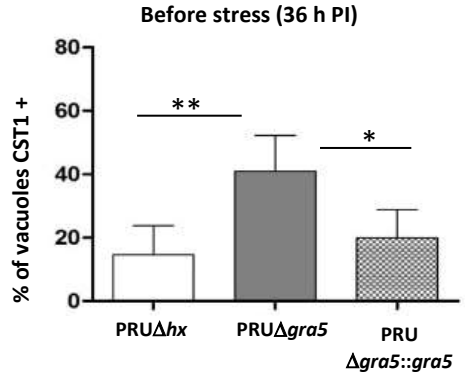

C

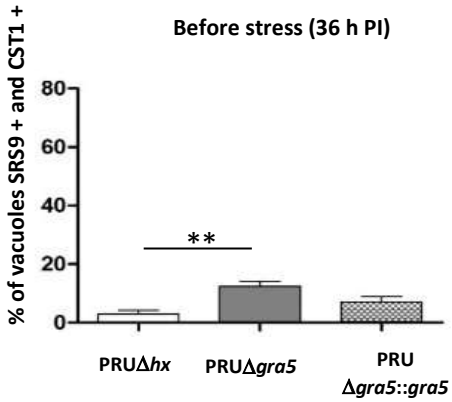

D

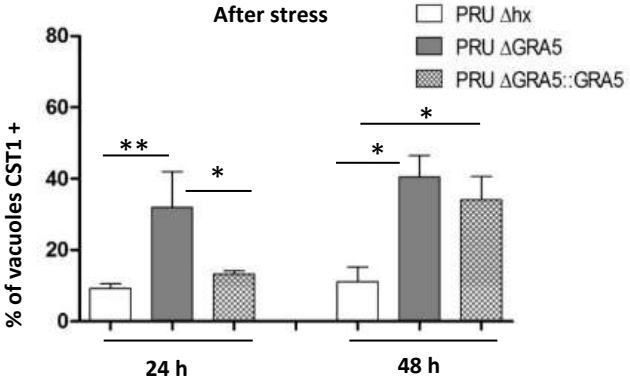

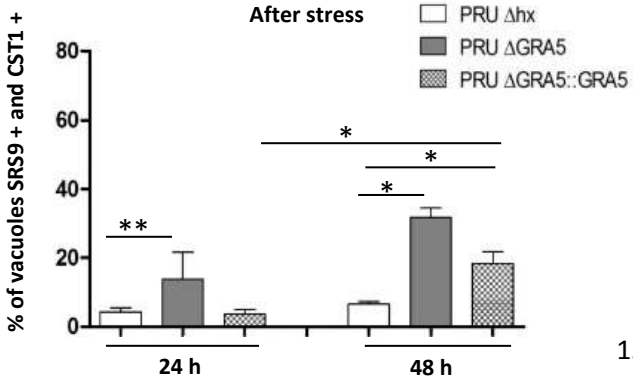

Figure 4

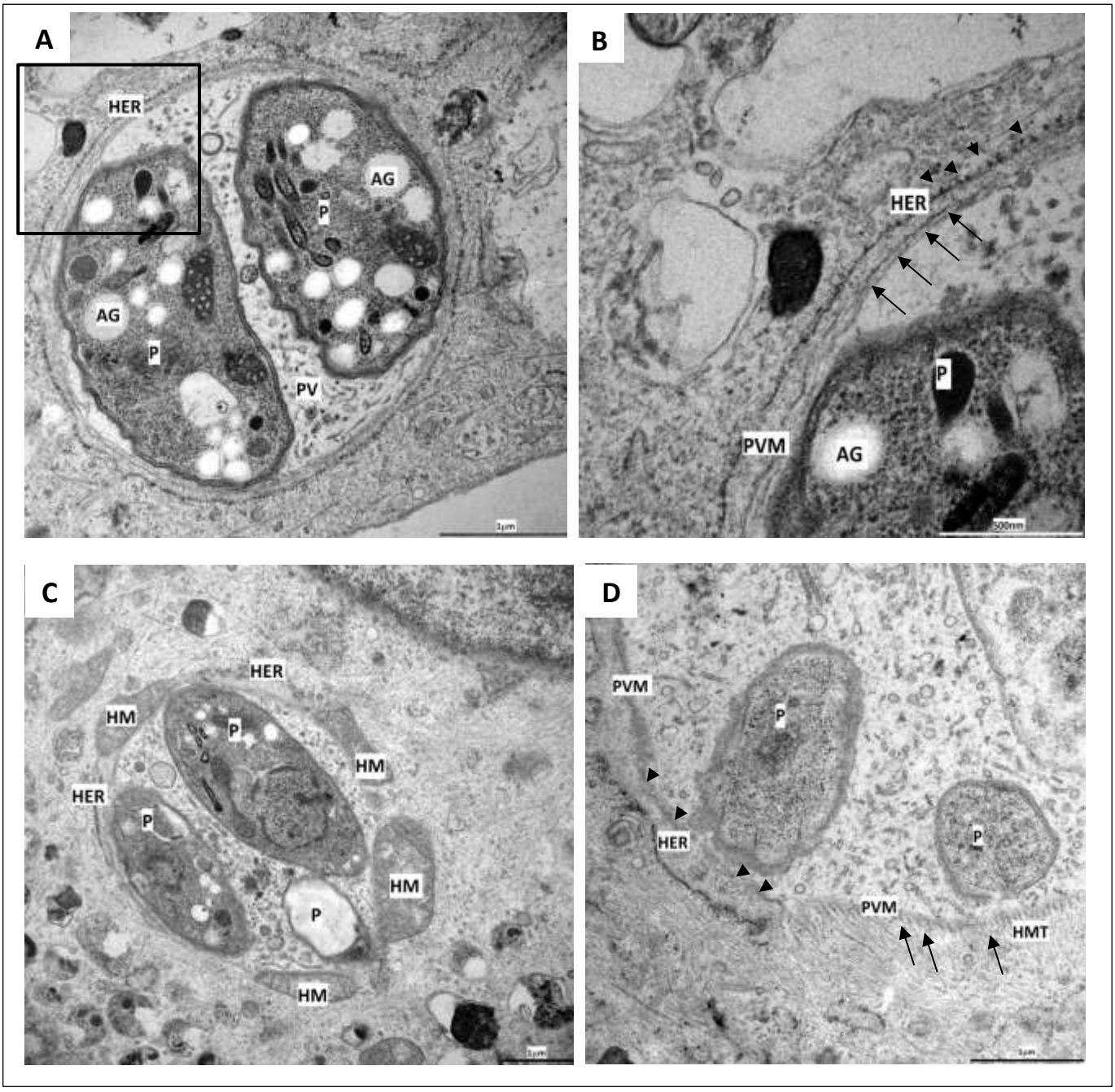
A
HER
AG
P
AG
P
PV
B
HER
P
PVM
AG
C
HER
HM
P
HM
HER
P
HM
P
HM
D
PVM
P
HER
P
PVM
HMT

E

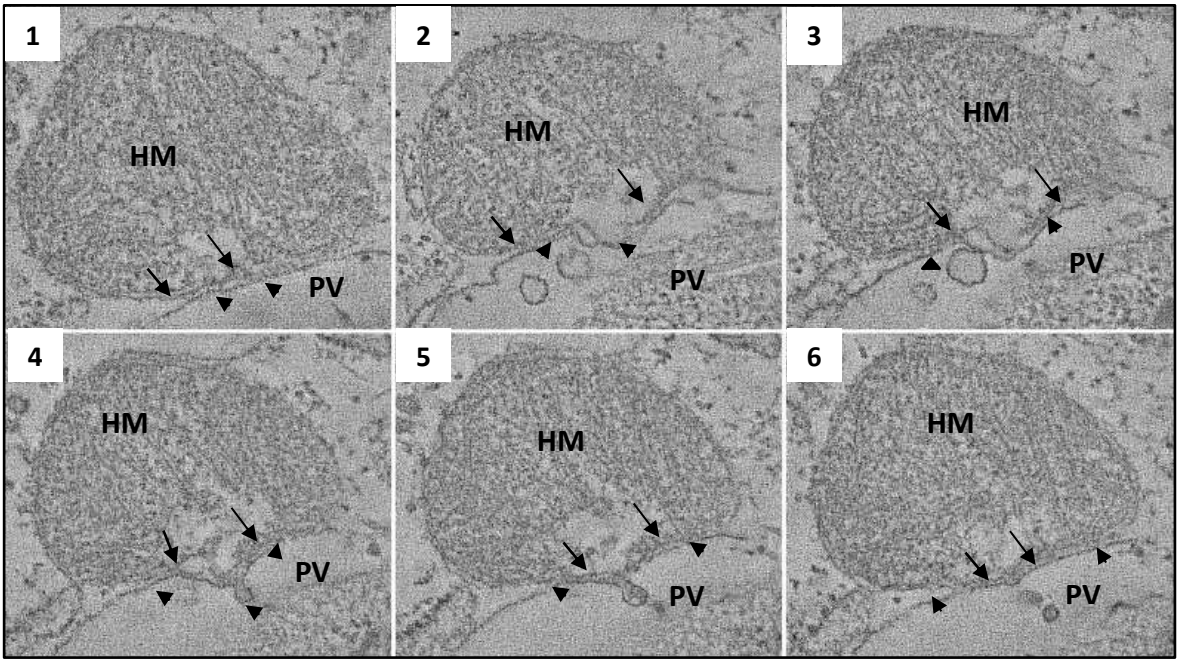

Figure5

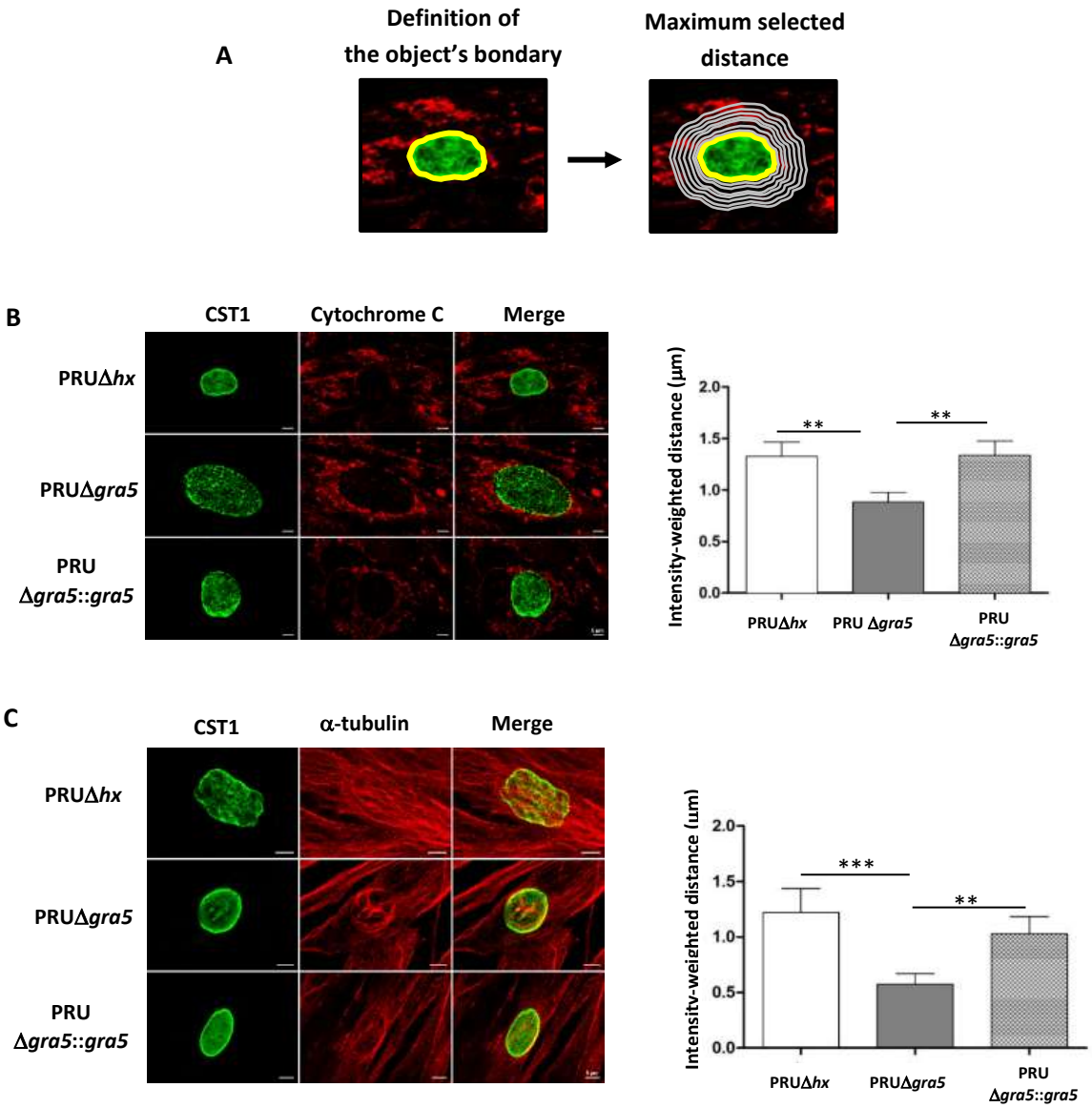
A
Definition of
the object's bondary
Maximum selected
distance
B
CST1
Cytochrome C
Merge
PRUΔhx
PRUΔgra5
PRU
Δgra5::gra5
Intensity-weighted distance (μm)
2.0
1.5
1.0
0.5
0.0
**
**
PRUΔhx
PRU Δgra5
PRU
Δgra5::gra5
C
CST1
α-tubulin
Merge
PRUΔhx
PRUΔgra5
PRU
Δgra5::gra5
Intensity-weighted distance (μm)
2.0
1.5
1.0
0.5
0.0
***
**
PRUΔhx
PRUΔgra5
PRU
Δgra5::gra5

Figure 6

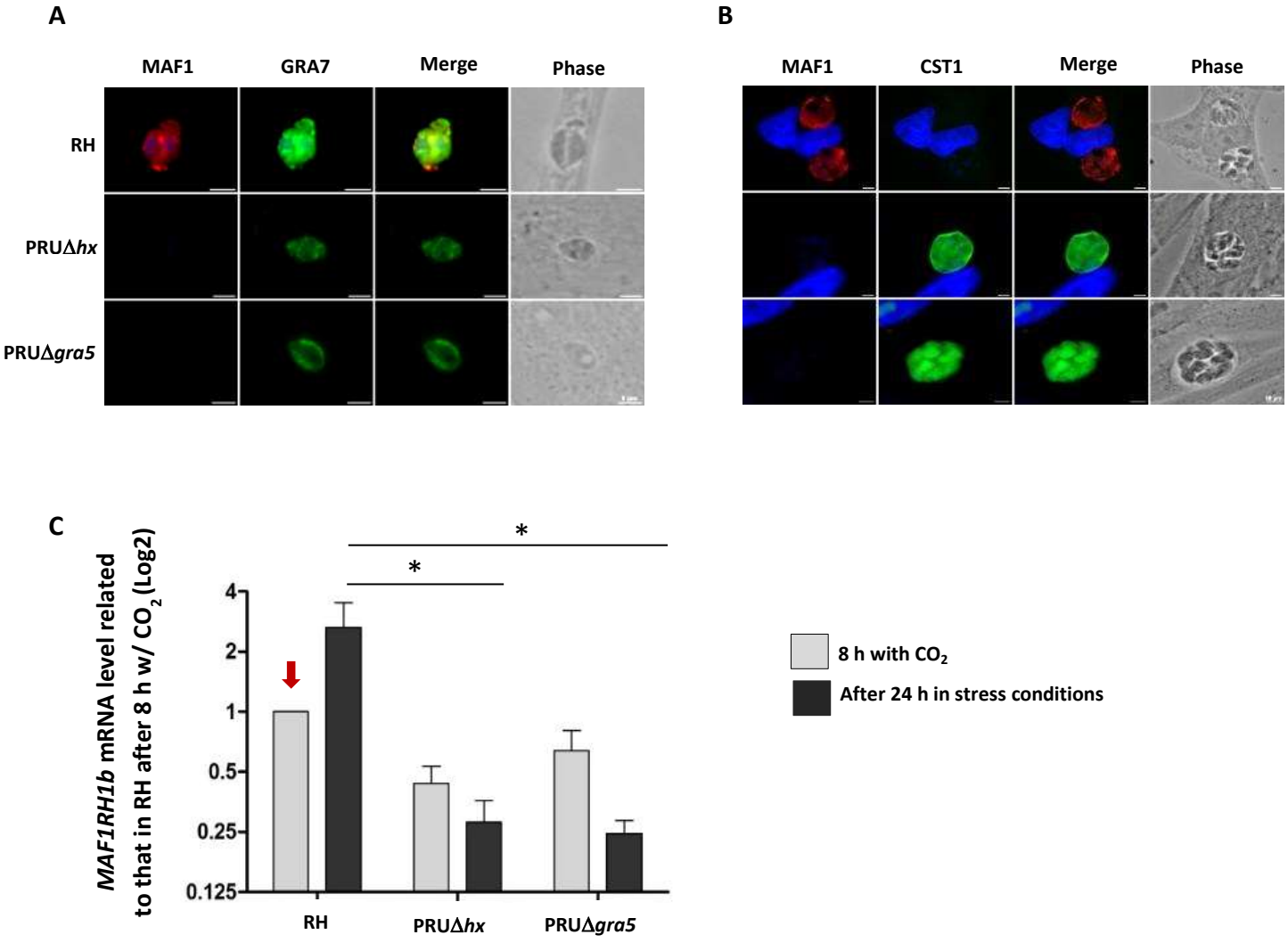
A
MAF1
GRA7
Merge
Phase
RH
PRUΔhx
PRUΔgra5
B
MAF1
CST1
Merge
Phase
C
MAF1RH1b mRNA level related to that in RH after 8 h w/ CO2 (Log2)
4
2
1
0.5
0.25
0.125
*
*
RH
PRUΔhx
PRUΔgra5
8 h with CO2
After 24 h in stress conditions

Figure 7

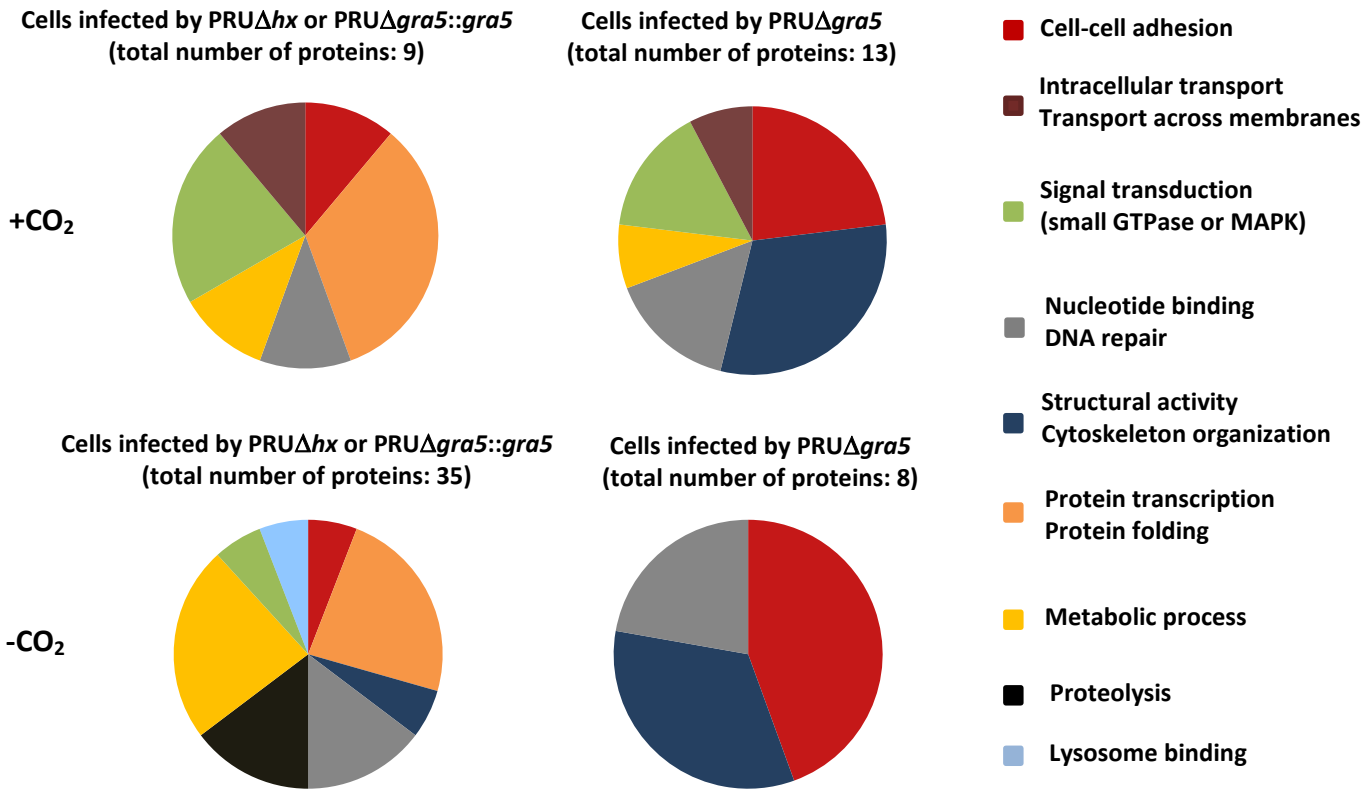
Cells infected by PRUΔhx or PRUΔgra5::gra5
(total number of proteins: 9)
Cells infected by PRUΔgra5
(total number of proteins: 13)
+CO2
Cells infected by PRUΔhx or PRUΔgra5::gra5
(total number of proteins: 35)
Cells infected by PRUΔgra5
(total number of proteins: 8)
-CO2
Cell-cell adhesion
Intracellular transport
Transport across membranes
Signal transduction
(small GTPase or MAPK)
Nucleotide binding
DNA repair
Structural activity
Cytoskeleton organization
Protein transcription
Protein folding
Metabolic process
Proteolysis
Lysosome binding

Cyst Detection in *Toxoplasma gondii*-Infected Mice and Rats Brain

Valeria Bellini[1, 2], Corinne Loeuillet[1, 2], Céline Massera[1, 2], Marie-France Cesbron-Delauw[1, 2]* and Pierre Cavaillès[1, 2*]

1 Laboratoire Adaptation et Pathogénie des Microorganismes (LAPM), Grenoble, France;
2 Université Joseph Fourier Grenoble 1, Grenoble, France

*For correspondence: Marie-France Cesbron-Delauw, marie-france.cesbron@ujf-grenoble.fr
Pierre Cavaillès, pierre.cavailles@ujf-grenoble.fr

http://www.bio-protocol.org/e1439 *Apr 05, 2015. Vol 5, Iss 7.*

Toxoplasma gondii infects all warm-blooded animals (including humans) causing toxoplasmosis, a life-long chronic infection. At the first contact with the parasite, the host develops an inflammatory response necessary to control parasite replication. However, during this acute phase of infection, *T. gondii* disseminates readily into the whole infected host and rapidly crosses the blood-brain barrier. Together with muscles, the eyes and the testicles, the brain constitutes one of the preferred organs in which the parasite differentiates and forms intracellular cysts, where *T. gondii* safely persists during the entire life of the infected organism or individual.

Rodents (mice and rats) represent the most commonly used models to study the chronic infection *in vivo*. In these sensitive animals the parasite dissemination that follows an intraperitoneal injection is rapid and the parasite invades the brain 8 to 10 days post-infection (Saeij *et al.,* 2005). However, it takes 4 to 8 weeks to observe well-developed brain cysts.

The quantification of brain cysts is an important parameter to reveal the ability of a specific *T. gondii* strain to form cysts *in vivo*. Since the quantification of cysts from an entire infected brain is not an easy task, the routine technique consists in counting the cysts from a brain section only (usually $1/10^{th}$ of a rat brain or $¼^{th}$ of a mouse brain), leading to an estimation- rather than a real cyst quantification- in the infected brain. To improve the precision of these counts, a previous study from our laboratory (Aldebert *et al.,* 2011) had allowed the development of a method for the scanning an entire infected brain and the automatic counting of all the cysts observed in the brain. This epifluorescence-based microscopy technique allowed faster analysis of the infected brain and a more accurate determination of the cyst number.

During my PhD, I revised the protocol developed by Aldebert *et al.* (2011) in order to improve the labelling of these brain cysts, while reducing the amount of brain material lost during the preparation of the brain material. The revised protocol is briefly described below.

The brains of infected mice are homogenized to be further treated with proteinase K (PK) in order to digest the excess of brain tissue, thus increasing the fluidity of the suspension. The homogenates are incubated with *Dolichos bifluorus* lectin conjugated to FITC. This lectin does recognize the CST1 glycoprotein, which is a component of the cyst wall. The fluorescently labelled brains are plated into 6 well-plates (1 brain per plate), and analyzed by high content screening microscopy (Scan^R Olympus). Images of the entire surface of each well are acquired in order to count the total number of cysts present in each brain.

The published “Bio-protocol” describes in details all the reagents and material required to set up the experiment as well as the sequential steps, from the brain collection to the cyst numbering. This method was validated using 8 week-infected mice and rats.

Category by field: Microbiology > Microbe-host interactions > In vivo model > Mammal
Category by field: Cell Biology > Cell imaging > Fluorescence
Category by organism: Protozoans > Toxoplasma > Toxoplasma gondii > Physiology

"Cyst Detection in *Toxoplasma gondii*-infected mice and rats brain."

Valeria Bellini[1,2], Corinne Loeuillet[1,2], Céline Massera[1,2], Marie-France Cesbron-Delauw[1,2] and Pierre Cavaillès[1,2]
1: Laboratoire Adaptation et Pathogénie des Microorganismes (LAPM). CNRS UMR 5163
2: Université Joseph Fourier Grenoble 1, Grenoble, France
Corresponding authors: Marie-France Cesbron-Delauw, marie-france.cesbron@ujf-grenoble.fr
Pierre Cavaillès, pierre.cavailles@ujf-grenoble.fr

[Abstract] Toxoplasmosis caused by the intracellular parasite *Toxoplasma gondii*, is characterized by a life-long chronic infection. The parasite is an efficient neurotropic infectious agent that establishes its "safe" life by forming intracellular cysts in chronically infected animals and humans. This protocol describes the specific recipes and method to stain brain cysts from infected mice and rats for further quantification using epifluorescence microscopy. This method provides the possibility to scan the entire brain and thus to numerate all cysts.

Materials and Reagents

1. Human foreskin fibroblasts (HFFs) cells culture (ATTC, catalog number: SCRC-1042)
2. Dulbecco's modified Eagle medium (DMEM) (Life Technologies, catalog number: 41966-029/052)
3. Fetal bovine serum (FBS) (Eurobio®, catalog number: CVFSVF0001)
4. Penicillin/streptomycin (PAN Biotech GmbH, catalog number: P0607-100)
5. L-Glutamine 200mM (Life-Technologies, catalog number: 25030-024)
6. Dulbecco's phosphate-buffered saline (DPBS) (Life Technologies, catalog number: 14190-094/069)
7. Proteinase K (molecular biology grade) (Biolab, catalog number: P8107S, Lot: 0051310)
8. TRIS (Euromedex, catalog number: 26-128-3094-B)
9. EDTA (Euromedex, catalog number: E013)
10. SDS (Euromedex, catalog number: EU0660)
11. NaCl (Euromedex, catalog number: 1112-A)
12. HCl (ACS reagent 37%, Sigma-Aldrich, catalog number: 258148-2.5ML)
13. Phenylmethylsulfonylfluoride (PMSF) (EUROMEDEX, catalog number: 1111-C)
14. Hoescht 33258 (Life Technologies, Molecular Probes®, catalog number: H-3569)
15. Formaldehyde Methanol free (Polysciences, catalog number: 04018)
16. *Dolichos biflorus* lectin coupled to fluorescein isothiocyanate (FITC) (Clinisciences, catalog number: FL-1031)
17. Complete DMEM medium (see Recipes)
18. Phenylmethylsulfonylfluoride (PMSF) solution (see Recipes)

19. Lysis buffer (see Recipes)

Equipment

1. 37°C/5% CO_2 cell culture incubator
2. 6-well plates
3. Scissors and forceps
4. Glass homogenizers (Potter-Elvehjem PTFE, 15 ml, Dutscher, catalog numbers: 057009 and 057021)
5. 15 ml polystyrene tubes
6. Epifluorescence microscope

Procedure

A. Preparation of Human Foreskin Fibroblasts cell culture in 6-well plates

Plate HFFs cells in complete DMEM medium and culture them for 4 days at 37°C in presence of CO_2. HFFs have to be at 100% confluence in each well (8.10^5 cells) before staining.

B. Staining of HFFs

1. Wash twice the cells culture with 1ml DPBS 1x.
2. Fix cells with 1 ml formaldehyde diluted at 2.5% in DPBS 1x for 20 min at 4°C.
3. Incubate 20 min, in the dark and at RT, the cells with 1 ml of Hoescht diluted 1/50,000 in DPBS 1x.
4. Wash twice the cells culture with 1ml DPBS 1x.
5. Add 1 ml DPBS 1x.
6. Stored at 4 °C until addition of the stained homogenized brain.

Note: The stained cells are stored at 4°C for a maximum of 24h.

C. Isolation of brains from infected mice or rats

1. Anesthesize animal with isofluoran and euthanize it by cervical dislocation.
2. Soak the head with 70% (v/v) ethanol.
3. Cut the skin at the base of skull and remove it as much as possible.
4. Cut with scissors the dorsal and lateral part of the skull and take the top off.
5. Collect the brain tissue in 5 ml DPBS 1x solution.

D. Brains homogenization

Put each mouse brain in 2 ml DPBS 1x into a glass homogenizer, homogenize at RT and adjust final volume to 4 ml. For rat brain, homogenize in 4 ml and adjust to 8 ml final.

Note: Brains can be stored at 4 °C until the staining for no more than 2 days.

E. Brains staining

1. Prepare 5x lysis buffer and proteinase K at 8 U/ml (stock at 800 U/ml, 1/100 dilution in 5x lysis buffer just before use).
2. For mice, take 1 ml of homogenized brain (¼ brain), add 398 µl of 5x lysis buffer, 2 µl of proteinase K (see step E-1, so final concentration at 0.008 U/ml) and 600 µl of 1x DPBS (final volume of 2 ml).
   For rats, take 2 ml of homogenized brain (¼ brain), add 995 µl of 5x lysis buffer, 5 µl of proteinase K (see step E-1, so final concentration at 0.008 U/ml) and 2 ml of 1x DPBS (final volume of 5 ml).
3. Incubate at 56 °C for 15 min, homogenize every 5 min by vortexing.
4. Stop the proteinase K activity by adding PMSF to a final concentration of 2 mM (stock at 200 mM), homogenize and incubate at RT for 5 min.
5. Centrifuge the sample for 15 min at 1,250 *x g* (RT).
6. Gently eliminate the supernatant by pipetting.
7. Resuspend in 1 ml of *Dolichos biflorus* lectin diluted at 1/250 in DPBS 1x (996 µl 1x DPBS + 4 µl of *Dolichos biflorus* lectin).
8. Incubate 30 min at RT in a mechanical wheel placed in the dark.
9. Add 3 ml DPBS 1x and homogenize to wash the sample.
10. Centrifuge 15 min at 1,250 *x g* (RT).
11. Gently eliminate the supernatant by pipetting.
12. Resuspend each sample in 1 ml in DPBS 1x and transfer onto Hoescht-stained HFFs (see part A and B of the procedure) by pipetting (1 ml/well).

Note: it is important to transfer the homogenized brain pellet onto HFF cells to facilitate microscope focus when there are no or very few cysts.

F. Count the cysts using epifluorescence microscopy (Representative data).

Note: *Samples can be stored at 4 °C until microscope observation for no more than 10 days.*

To know the cysts quantity in entire brain, multiply the counted number by 4.

Representative data

A) **B)** **C)**

Representative cysts staining from uninfected and infected CBA mice brain with *Toxoplasma gondii* parasites. Two months after i.p. infection of CBA mice with 1,000 ΔKu80-ΔHXGPRT (PRU) tachyzoïtes, brains were collected, homogenized in 4 mL of PBS and ¼ of each brain suspension was used for the labeling of cyst walls with the *D. biflorus*-FITC lectin and analyzed by high content screening microscopy (Scan^R Olympus). A) Photo (4X objective) of a CBA infected mouse brain. Three stained cysts are present in this field. B) Uninfected CBA mouse brain (4X objective) no cysts are visible but only brain debris. C) Representative panel of stained cysts obtained from infected CBA mouse and detected by (4X objective) microscopy. Cysts are zoomed to detect potential false positive as in A6.

Recipes

1. Complete DMEM medium
   10% (v/v) FBS
   0.5% (v/v) penicillin/streptomycin
   2 mM glutamine
2. Phenylmethylsulfonylfluoride (PMSF) solution (stock concentration of 200mM)
   0.35 g of PMSF powder to dissolve in 10 ml of isopropanol
   Stored at -20 °C in 1 ml aliquots
   NB: PMSF will take some time to dissolve.
3. Lysis buffer (500 ml)
   10 M TRIS: 2.5 ml of 2 M TRIS at pH 8.0 (60 g in 250 ml H_2O, adjust pH)
   1 mM EDTA: 2 ml of 250 mM EDTA at pH 8.0 (23.27 g in 250 ml H_2O, adjust pH)
   0.2% (w/v) SDS: 5 ml of 20% (w/v) SDS
   100 mM NaCl (1.165 g)
   Up to 500 ml H_2O
   NB: The 8.0 pH is adjusted using HCl 3M. (HCl 3M: 25ml HCl 37% added to 75ml of H_2O)

Acknowledgments

This work was supported by the ANR grants Nu 05-MIIM-020-02 and Nu 07-MIME-013-01, the Lyonbiopole competitiveness cluster and the French Parasitology consortium ParaFrap (ANR-11-LABX0024).

This protocol was adapted from the following articles:

1. Aldebert, D., Hypolite, M., Cavailles, P., Touquet, B., Flori, P., Loeuillet, C. and Cesbron-Delauw, M. F. (2011). Development of high-throughput methods to quantify cysts of *Toxoplasma gondii*. *Cytometry A* 79(11): 952-958.
2. Cavailles, P., Flori, P., Papapietro, O., Bisanz, C., Lagrange, D., Pilloux, L., Massera, C., Cristinelli, S., Jublot, D., Bastien, O., Loeuillet, C., Aldebert, D., Touquet, B., Fournie, G. J. and Cesbron-Delauw, M. F. (2014). A highly conserved Toxo1 haplotype directs resistance to toxoplasmosis and its associated caspase-1 dependent killing of parasite and host macrophage. *PLoS Pathog* 10(4): e1004005.

CONCLUSION-PERSPECTIVES

Conclusions

Together, these results show a novel role for GRA5 during the parasitophorous vacuole differentiation *in vitro* in regulating host cell organelles around the PVM. GRA5 is not involved in tachyzoite invasion or replication. It is instead crucial to maintain the PVM stability, ensuring parasite survival *via* nutrients' acquisition and cyst differentiation. Here, we demonstrated that the depletion in GRA5 in the cyst-forming type II *Prugniaud* strain led to PVM destabilization, which subsequently induced an earlier but incomplete cyst wall differentiation. The depletion in GRA5 was correlated with the absence of MAG1 in the vacuole. MAG1 is one of the components of the cyst wall. It was also shown to accumulate at the PVM during the cyst wall differentiation *in vitro* (Lane *at al.,* 1996). In our proteomic analyses, MAG1 was found associated with the loss of PVM-HER association and the loss of the TgPDI vacuolar protein, which may be involved in the maintenance of a stable PVM by its redox functions.

The HER represents an important source of nutrients, particularly during parasite differentiation, during which energy is required. This request results in the recruitment of host mitochondria, independently on MAF1. Host microtubules, which are rearranged in dense arrays around the PVM could help in this recruitment. Alternatively, the higher density of host microtubules around the PVM could reinforce the structural integrity of the PV/cyst-like structure.

Together, these phenotypes described for PRUΔ*gra5* demonstrate that molecular adaptation of the parasitophorous vacuole is crucial for the cyst formation, suggesting a pivotal role of GRA5 in the biogenesis and maintenance of brain cysts *in vivo.*

Perspectives

To validate the proposed model, several experiments need to be further undertaken, as follows.

1/ My experiments revealed a higher level of spontaneous cyst wall differentiation in PRUΔ*gra5*, suggesting a loss of PVM stability during the acute infection. To confirm that the PVM destabilization induces the recruitment of host mitochondria and the reorganization of the host cytoskeleton even in absence of any external stress, new immunofluorescence assays and image analyses will be performed in infected cells after 36 h of culture at 37°C and 5% of CO_2.

2/We have confirmed that HMA is not dependent on MAF1 in type II parasites, suggesting the involvement of another mechanism, such as reorganization of the host cytoskeleton. Treatment of infected cells with nocodazole, which would induce depolymerization of host microtubules, or taxol, which would stabilize host microtubules, could be performed to validate this hypothesis.

3/ Using a proteomic approach, we discovered the absence of MAG1 in the vacuoles of PRUΔ*gra5* parasites, suggesting a possible interaction between MAG1 and GRA5.
A previous two hybrid study in yeast described GRA5, together with GRA3, as possible effectors to mediate the binding of the host ER to the PVM via their binding to the host ER integral membrane protein CALMG. Subcellular-fractionation of infected cells, followed by immunoprecipitation of GRA5, and identification of its potential partners by mass spectrometry will be performed to investigate this hypothesis.

4/Here, we described the structural role of GRA5 in cyst wall development during *in vitro* differentiation. In this model no cytokines nor host immune response were present to modify the activity of the infected cells. To confirm that GRA5 is also involved in *in vivo* cyst development and maintenance, we recently infected CBA mice, which are sensitive to *T. gondii* infection to follow the formation of brain cysts 4 and 8 weeks post-infection. The differences, if any, between the parental-, the GRA5 KO mutant, and the complemented strains will be important to conclude about the ability of PRUΔ*gra5* parasites to form cysts. Furthermore, differences in the number of cysts between differente time points will help us understand the kinetics of cyst formation and maintenance *in vivo.*

On a longer term, investigations on the role of TgPDI could provide information on the redox process and whether it is necessary to maintain the intravacuolar homeostasis, and if it is involved in the association of the host ER with the PV.

Finally, another aspect that requires more attention is the possible difference in the behaviors of $GRA5_I$ and $GRA5_{II}$. **Figure30** shows the GRA5 polymorphism between the different Toxoplasma strains. Although $GRA5_I$, $GRA5_{II}$ and $GRA5_{III}$ share high levels of similarity (100% of similarity in their signal peptide and their transmembrane domain), different functions cannot be excluded. Complementation of the PRUΔ*gra5* strain with $GRA5_I$ (and *vice versa*) could be performed to investigate whether this polymorphism could change the protein functions.

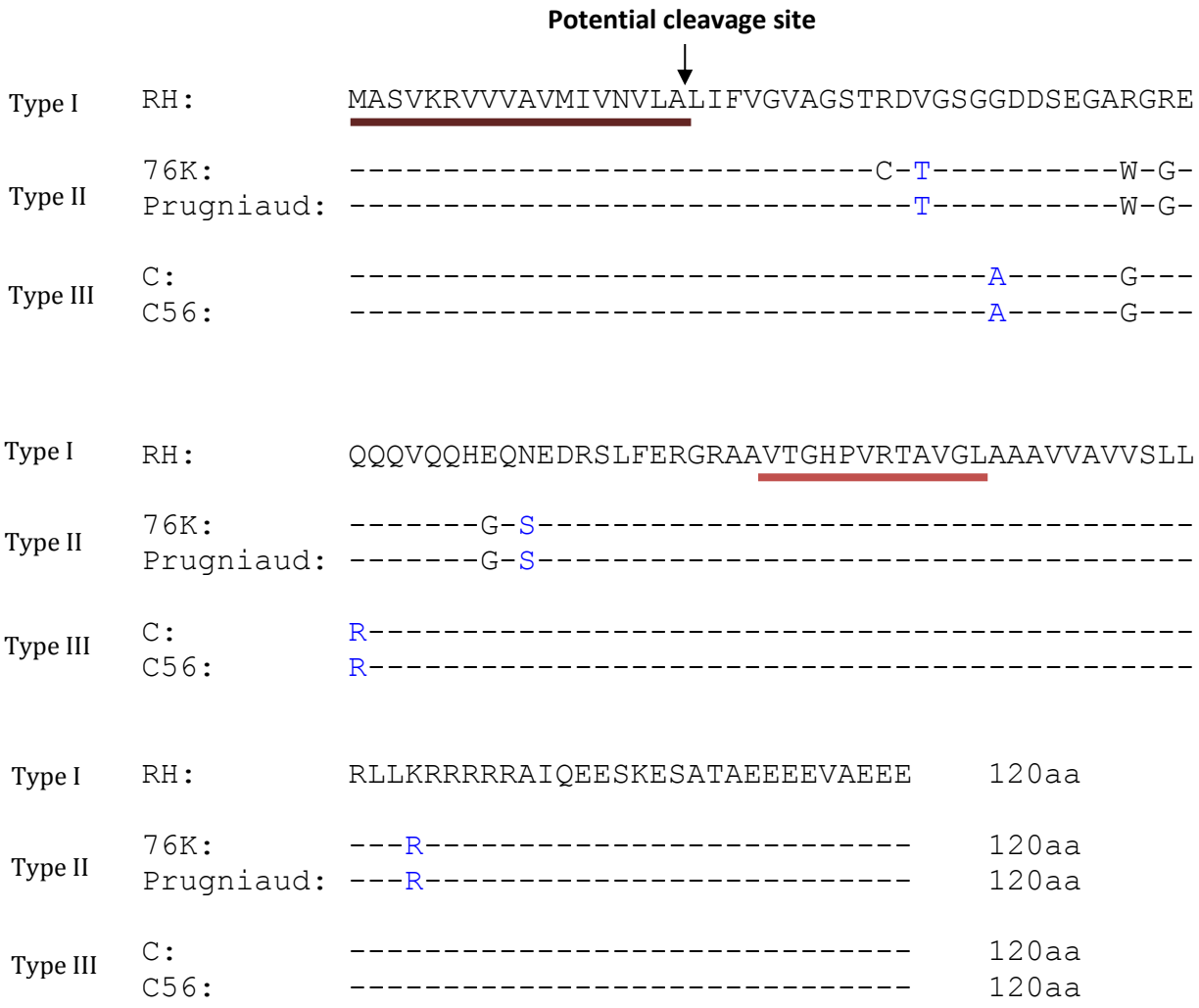

Figure 30. Alignment of the GRA5 types I, II, III amino acid sequences

Alignment of the GRA5 amino acid sequences from various *T. gondii* strains, namely RH (type I), PRU and 76K (type II), C and C56 (type III).

The protein of 120 amino acid shows a high level of similarity between the different strains. The signal peptide is underlined in brown, while the transmembrane domain is underlined in dark red. The arrow indicates the potential cleavage site of the signal peptide.

Résumé en français

Toxoplasma gondii : approches moléculaires (analyse de mutants « knocked-out ») pour l'étude de la fonction de protéines de granules denses dans l'interaction hôte-parasite

Toxoplasma gondii est un parasite appartenant au phylum des Apicomplexa. Il est responsable de la toxoplasmose, une infection chronique qui touche plus d'1/3 de la population mondiale. Contrairement aux autres Apicomplexa, *T. gondii* est capable d'infecter tous les animaux à sang chaud (carnivores, herbivores et les oiseaux, l'homme compris), qui constituent les hôtes intermédiaires chez lesquels se déroule le cycle asexué du parasite. Chez les hôtes définitifs, le chat et les autres félidés, le parasite peut développer son cycle vital complet, sexué et asexué. A l'exception des infections congénitales, la transmission du parasite se fait par voie orale, suite à l'ingestion de viande crue ou peu cuite, de légumes ou d'eau contaminés par les formes de résistance du parasite. Ces formes infectieuses comprennent *i)* les bradyzoïtes, stade quiescent ou à prolifération lente, se développant dans des structures kystiques et *ii)* les sporozoïtes présents dans les oocystes émis dans les feces des félidés. L'ingestion de kystes ou d'oocystes aboutit à la libération de formes infectieuses et à leur transformation en tachyzoïtes, stade parasitaire à prolifération rapide, capable de disséminer dans l'organisme et d'infecter tous les types cellulaires. Lors des premières semaines de l'infection (infection aiguë), les tachyzoïtes sont éliminés par la réponse immunitaire innée de l'hôte mais certains y échappent et s'enkystent dans le cerveau et dans les tissus musculaires. Cette infection chronique persiste à vie chez l'individu et est corrélée au développement d'une protection à la réinfection. Chez les sujets immunocompétents, la toxoplasmose est généralement asymptomatique. Il existe 3 situations au cours desquelles la toxoplasmose peut être mortelle. Chez les sujets immunodéficients, la réactivation des kystes cérébraux peut être fatale, si elle n'est pas traitée rapidement. L'infection d'une femme non immunisée pendant le 1er trimestre de sa grossesse peut conduire à une infection congénitale se traduisant par des troubles neurologiques très graves, voire la mort du fœtus *in utero*. Enfin, il existe, principalement en Amérique du Sud, des souches hyper-virulentes qui génèrent des toxoplasmoses mortelles, même chez les sujets immunocompétents. Des traitements ne sont administrés qu'aux patients immunodéficients, aux femmes enceintes et aux enfants atteints de toxoplasmose congénitale. Ces traitements ciblent la réplication des tachyzoïtes et leur passage trans-placentaire. Malheureusement, il n'existe actuellement aucun traitement efficace permettant l'élimination des kystes. De même, il n'existe pas de vaccin administrable aux humains.

T. gondii est un parasite à développement intracellulaire obligatoire. Le tachyzoïte pénètre dans la cellule hôte en formant une vacuole parasitophore (VP), compartiment qui le protège des attaques du système endo-lysosomal, tout en lui permettant d'interagir avec la cellule pour la contrôler et acquérir des nutriments. Dans les situations de stress pour le parasite, comme lors de la mise en place de la réponse immunitaire, le tachyzoïte se transforme en bradyzoïte. Parallèlement, la VP se modifie en kyste intracellulaire qui est formé *i)* d'une paroi rigide composée par deux membranes, une externe et compacte et l'autre interne et spongieuse, en continuité avec *ii)* une matrice contenant des filaments et des vésicules qui connectent les parasites entre eux et à la paroi du kyste (Lemgrüber *et al.,* 2011).

Les mécanismes de différenciation du tachyzoïte en bradyzoïte et de la VP en kyste sont encore peu connus. Des travaux ont montré l'importance des protéines de granules denses (GRA) en tant que constituants de la VP, dans la formation de la paroi kystique et dans l'interaction avec la cellule hôte.

Les protéines GRA sont stockées dans les granules denses, organites de sécrétion spécifiques des parasites Apicomplexa formant des kystes. Au moment de l'infection de la cellule hôte, les GRA sont sécrétées dans la VP, où elles contribuent à rendre ce compartiment métaboliquement actif (Mercier and Cesbron-Delauw 2015). A ce jour, plus d'une vingtaine de protéines GRA ont été identifiées. La plupart d'entre elles possède un domaine hydrophobe transmembranaire impliqué dans leur association *i)* avec la membrane délimitant la VP (GRA3, GRA5, GRA7, GRA8, GRA10, GRA14, GRA17, GRA19, GRA20, GRA21, GRA22, GRA23, MAF1), *ii)* aux membranes du réseau de nanotubes intra-vacuolaire (GRA2, GRA4, GRA6, GRA9, GRA12) et *iii)* à des structures intra-vacuolaires, formées par les microtubules de la cellule hôte et appelées HOSTs (host sequestering tubulostructures) (GRA7). D'autres protéines GRA sont sous forme soluble à l'intérieur de l'espace vacuolaire (GRA1, GRA38, GRA39, GRA40) (Mercier and Cesbron-Delauw, 2015 ; Gold *et al.,*2015 ; Nadipuram *et al*., 2016 ; Pernas *et al.*, 2014). Ces structures vacuolaires jouent un rôle important dans le maintien et l'acquisition des métabolites de la cellule-hôte. GRA7, qui est présente au niveau des HOSTs, est impliquée dans l'acquisition d'organites endocytaires sources de lipides et de cholestérol (Coppens *et al.,* 2006 ; Romano *et al.,* 2014), tandis que GRA17 et GRA23 ont un rôle dans le transport actif de petites molécules du cytosol à l'intérieur de la VP (Gold *et al.,* 2015).
Le kyste est le résultat de la maturation de la VP : les protéines GRA de la membrane délimitant la VP restent associées à la membrane externe de la paroi kystique (GRA3, GRA5 and GRA7), tandis que les protéines GRA associées aux nanotubes intravacuolaires constituent la couche interne (GRA2 and GRA6). GRA1, qui est soluble dans la vacuole, reste dans la matrice du kyste (Torpier *et al*., 1993 ; Ferguson, 2004 ; Lemgrüber *et al*., 2011 ; Mercier and Delauw 2012 ; Mercier and Cesbron-Delauw, 2015). En plus de leur rôle structural dans la VP et la paroi kystique, les protéines GRA interviennent dans le contrôle de la cellule hôte. Au cours de l'infection aiguë, GRA6 intervient dans l'activation de la réponse immunitaire adaptative (Blanchard *et al.,* 2008) et plus récemment, elle a été montrée comme étant responsable de l'activation du facteur de transcription NFAT4 (nuclear factor of activated T cells 4) (Ma, *et al.,* 2014). GRA5 induit la migration des cellules dendritiques humaines, tandis que GRA15, GRA16, GRA24 et la protéine TgIST (inhibitor of *signal transducer and activator of transcription 1* (STAT1)-dependent transcription) sont détectées dans le noyau de la cellule hôte où elles jouent un rôle dans la modification de la réponse cellulaire (Rosowski *et al*., 2011 ; Bougdour *et al.,* 2013 ; Braun *et al.,* 2013 ; Olias *et al.,* 2016 ; Gay *et al.,* 2016).
Les interactions établies entre les protéines GRA et les organites de la cellule-hôte ainsi que son cytosquelette, et les fonctions des protéines GRA au stade chronique sont encore peu étudiées. Les études fonctionnelles des GRA basées sur l'étude de parasites invalidés pour un ou plusieurs gènes *gra* ont récemment connu un essor, suite à la construction de parasites invalidés pour le gène *ku80*, chez lesquels la double recombinaison homologue à un locus donné est optimisée, tant que ce locus n'est pas essentiel. A ce jour, ces études ont étés menées principalement au stade tachyzoïte, en utilisant la souche parasitaire de type I (RH) très virulente et incapable de développer une infection latente chez la souris.

Pour mieux comprendre le rôle des protéines GRA dans l'invasion, la prolifération et la virulence du parasite *T. gondii*, j'ai participé à une étude réalisée en collaboration avec une équipe américaine (L. Rommereim and D. Bzik, Geisel School of Medicine at Dartmouth, Lebanon, USA). Les résultats de ce travail ont étés récemment publiés (Rommerein*, Bellini* *et al.,* 2016 (*, co-auteurs)). Cette étude concerne l'analyse de 8 souches parasitaires de type I (RH) invalidées pour un seul gène *gra* (souches

Δ*gra2*-Δ*gra9*) et de 5 souches invalidées de deux gènes *gra* (Δ*gra2*Δ*gra4* ; Δ*gra2*Δ*gra6* ; Δ*gra4*Δ*gra6* ; Δ*gra3*Δ*gra5* ; Δ*gra3*Δ*gra7*). Dans un premier temps, la construction des parasites « knocked-out » (KO) par l'équipe américaine a montré le rôle essentiel des protéines GRA1 et GRA10, pour lesquelles le développement des souches mutantes n'a pas été possible. *Via* des études *in vitro,* les parasites KO GRA ont ensuite été analysés pour leur capacité d'invasion et de prolifération. Les premiers résultats n'avaient pas montré des différences significatives entre les souches KO pour une seule protéine GRA. Une méthode d'immunofluorescence à haut débit, plus sensible, a été réalisée dans notre laboratoire. Cette approche automatisée a permis d'analyser plus de 5000 VPs réparties sur toute la surface des échantillons, en utilisant le logiciel ScanR. Ces expériences ont montré que l'invasion des souches Δ*gra2*, Δ*gra4*, Δ*gra5*, Δ*gra6*, Δ*gra7* et Δ*gra9* diminue par rapport celle de la souche parentale. Ces expériences ont aussi confirmé que l'invalidation d'un seul gène *gra* n'induisait pas de modification de la capacité de prolifération des parasites type I. L'analyse des doubles KO GRA a révélé une diminution significative du taux de prolifération des souches Δ*gra4*Δ*gra6*, Δ*gra3*Δ*gra5* et Δ*gra3*Δ*gra7*, ce qui suggère un rôle redondant de ces protéines GRA. De plus, une analyse en microscopie électronique des vacuoles parasitaires a confirmé l'importance structurale des protéines GRA2 et GRA6 dans la formation du réseau intravacuolaire. Comme publié précédemment (Mercier *et al.,* 2002), une déstabilisation du réseau tubulaire en vésicules (Δ*gra2*) ou en matériel agrégé (Δ*gra6*) a en effet été observée. Par contre, une hyper-formation du réseau intravacuolaire a été observée dans les vacuoles des parasites Δ*gra7*, ce qui suggère une collaboration entre les protéines GRA2, GRA6 et GRA7 pour le maintien d'un réseau stable et structuré. Enfin, une étude *in vivo* a été effectuée pour analyser la virulence des différentes souches Δ*gra*. Contrairement aux travaux précédemment publiés qui montraient une diminution de la virulence des parasites Δ*gra2*, Δ*gra6* et Δ*gra7* (Mercier *et al.,* 1998 ; Alagan *et al.,* 2014 ; Shastri *et al.,* 2014), notre étude n'a pas révélé de différences significatives entre les souches parasitaires sauvage et invalidées, l'infection des souris conduisant à leur mort en 10 jours environ. Cette différence avec les résultats publiés était probablement due aux différences dans les quantités de parasites injectés et les lieux d'injection. L'ensemble de ces résultats a montré que les protéines GRA2-GRA9, seules, n'ont pas une influence importante pendant l'infection aiguë par le parasite de type I mais que, en complexe, ces protéines peuvent être nécessaires et jouer des rôles redondants pour un développement normal de la vacuole et la réplication du parasite.

Une seule étude concerne la souche de type II (*Prugniaud*) qui, par sa capacité à former des kystes intracérébraux, permet de générer un cycle parasitaire asexué complet. Cette souche représente donc un bon modèle pour l'étude du rôle des protéines GRA dans la différenciation de la VP. En utilisant un modèle *in vitro* d'induction de la différenciation de parasites *Prugniaud* type II (PRU*Δku80Δhx* et PRU*Δku80Δgra5::hxgprt*), mon projet principal de thèse visait à caractériser les fonctions de GRA5 à différents phases du cycle biologique de *T. gondii,* notamment lors du développement des kystes.

La protéine GRA5, stockée dans les granules denses du parasite, est d'abord secrétée sous forme soluble à l'intérieur de la vacuole pour être ensuite dirigée à la membrane délimitant la VP, avec son domaine N-terminal exposé dans le cytosol de la cellule hôte (Lecordier *et al.,* 1999). Sa position à la membrane vacuolaire lors de l'infection aiguë et à la membrane externe de la paroi kystique lors de l'infection chronique (Lane *et al.,* 1996), en plus de son implication dans la migration des cellules dendritiques humaines (Persat *et al.,* 2012), étaient des éléments suggérant un rôle possible de GRA5 dans la kystogenèse *via* des interactions de la protéine avec la cellule hôte.

Dans le précèdent travail (Rommerein *et al.,* 2016), nous avions montré que l'invalidation du gène *gra5* n'impacte pas la prolifération des parasites type I (RH) mais, qu'en association avec GRA3, GRA5 peut avoir un rôle dans la réplication parasitaire. L'étude d'un mutant délété de *gra5* dans une souche kystogène de type II m'a permis *i)* de découvrir une nouvelle fonction structurale de GRA5 dans le maintien de l'intégrité de la membrane de la VP et *ii)* de montrer que GRA5 est nécessaire à la formation de la paroi du kyste. Plus précisément, nos résultats ont montré que GRA5 n'est pas impliquée dans l'infection et la prolifération des parasites de type II. Par contre, les parasites PRU∆*gra*5 ont une différenciation plus précoce de la paroi de leurs kystes que les souches sauvages et complémentées. Visible après 36 h d'infection, cette différenciation plus précoce est maintenue suite à l'application d'un stress alcalin induisant la kystogenèse. L'analyse ultrastructurale et en microscopie confocale de cultures parasitaires sous stress a révélé une formation incomplète de la paroi du kyste associée à des modifications dans l'interaction du kyste en formation avec les organites de la cellule hôte. Alors que la VP de la souche parentale présente un contour régulier associé au reticulum endoplasmique (RE) de la cellule hôte, la VP formée par les parasites PRU∆*gra5* perd cette association, en recrutant les mitochondries et les microtubules de la cellule hôte au niveau de la membrane délimitant la VP.

Le recrutement des mitochondries de l'hôte au niveau de la membrane vacuolaire est un phénomène décrit pour le parasite *T. gondii* comme dépendant de l'expression d'une protéine « GRA-like » appelée MAF1 (mitochondrial associated factor 1) (Pernas *et al.,* 2014). Ce phénomène semble spécifique des souches de types I et III qui expriment majoritairement la forme MAF1b1 responsable de cette interaction (Adomako-Ankomah *et al.,* 2016). Le recrutement des mitochondries de l'hôte autour de la VP décrit dans notre étude, dans le cas des souches de type II, n'est pas lié à MAF1b1 mais est la conséquence de la délétion de *gra5* par un mécanisme qu'il reste à définir.

La réorganisation du cytosquelette de la cellule hôte autour de la VP est un autre phénomène connu et décrit pour le parasites de type I. Cette réorganisation qui apparaît 1 h après infection, est importante pour le positionnement de la vacuole contre le noyau de la cellule hôte et du centre d'organisation des microtubules (COMT) (Walker *et al.,* 2008). Un autre organite de l'hôte décrit pour être fortement associé à la VP est le RE qui, avec les mitochondries, représente une source de nutriments pour les parasites intra-vacuolaires. Dans le cas de *T. gondii,* les protéines GRA3 et GRA5 ont été précédemment caractérisées comme des facteurs possibles d'interaction avec le RE, *via* leur lien avec la calmoduline (CAMLG), une protéine intégrale de la membrane du RE (Ahn *et al.,* 2006). Même si cette hypothèse reste à être confirmée *in cellulo*, nos résultats montrent que la déplétion en GRA5 entraine une diminution de l'association du RE de l'hôte à la VP, ce qui suggère que cette interaction pourrait être fonctionnelle.

Des analyses protéomiques différencielles de cellules infectées par les souches PRU∆*gra5,* parentale et complémentée en différenciation ont ensuite montré que la délétion de *gra5* entraine, au niveau de la VP, la perte d'expression d'autres composants de la paroi en différenciation tels que TgMAG1, et des protéines impliquées dans le processus d'oxydo-réduction, comme la Protéine Disulfure Isomérase (TgPDI). MAG1 est une protéine abondante de la paroi kystique et du stade bradyzoïte (Pamley *et al.,* 1994). Elle est aussi sécrétée dans VP (Fergurson *et al*., 2002). L'absence de MAG1 dans des vacuoles ∆*gra5* peut donc être liée à une interaction possible entre les deux protéines nécessaires pour la stabilisation et la différenciation de la membrane vacuolaire en paroi kystique. L'autre protéine candidate potentiellement impliquée dans le maintien d'une membrane vacuolaire est TgPDI, précédemment caractérisée pendant le processus d'invasion (Moncada *et al*., 2016). Cette

enzyme, qui est capable de réduire des ponts disulfures, pourrait activer des intégrines de la membrane cellulaire de l'hôte, en permettant l'adhésion du parasite (Stolf *et al*., 2011). Toutefois, PDI a aussi une activité de chaperone. Par sa capacité à former et réduire des ponts disulfures, elle est impliquée dans le repliement des protéines. Toutes ces caractéristiques, en plus de sa localisation et de la présence d'un peptide signal, suggèrent que TgPDI pourrait être sécrétée dans la VP afin d'assurer la formation des protéines et le maintien d'une membrane vacuolaire stable. De plus, PDI possède aussi un domaine C-terminal KDEL (Moncada *et al.,* 2016) qui pourrait interagir avec le RE de l'hôte. L'absence de cette protéine, en plus de celle de GRA5 au niveau de la VP, pourrait être impliquée dans la diminution des interactions entre la VP et le RE de l'hôte. L'analyse protéomique de la réponse des cellules hôtes infectées par le mutant PRUΔ*gra5* a révélé une augmentation de l'expression des protéines impliquées dans des fonctions d'adhésion cellulaire, d'organisation du cytosquelette et de modification de l'ADN stress dépendante. Par contraste, après infection par les souches parentale et complémentée, les protéines les plus représentées sont impliquées dans des processus métaboliques et/ou de protéolyse. L'ensemble de ces résultats montrent que l'adaptation moléculaire de la VP est essentielle pour assurer 1/ les échanges avec le cytoplasme de la cellule hôte, qui est source de métabolites, 2/ l'homéostasie vacuolaire, 3/ la formation d'un kyste stable. Cette étude a donc permis de comprendre l'importance de GRA5 dans le maintien de cette adaptation, ses interactions possibles avec d'autres composants parasitaires au niveau de la membrane vacuolaire et de la paroi kystique, ainsi qu'avec le RE de la cellule hôte (de façon directe ou indirecte), toutes ces interactions permettant d'envisager un rôle essentiel de GRA5 dans la biogenèse et le maintien des kystes intracérébraux pendant une infection *in vivo.*

Pendant mon projet de thèse j'ai aussi eu la possibilité de participer à la mise au point d'un protocole de marquage des kystes intracérébraux, ce marquage étant nécessaire pour l'analyse des kystes formés *in vivo*. Une méthode développée au laboratoire (Aldebert *et al.,* 2011) et basée sur le marquage immunofluorescent des kystes présents dans un cerveau infecté, permet d'analyser l'ensemble du cerveau, donc d'obtenir une quantification assez précise des kystes *ex vivo*, ce qui est un avantage certain par rapport aux techniques classiques basées sur une estimation de ce nombre de kystes, en comptant les kystes à partir d'une partie du cerveau (1/10 ou ¼).
Ma contribution au développement de ce nouveau protocole a permis d'améliorer les conditions de détection des kystes dans le cerveau, tout en réduisant la perte d'échantillon lors des étapes du protocole. Le « bio-protocol » qui a été récemment publié (Bellini *et al.,* 2015) décrit en détail, toutes les phases du prélèvement des cerveaux, de leur marquage, de l'analyse et du comptage des kystes, étapes validées sur des modèles de souris (8 semaines) et de rats infectés.

Ma thèse présente donc 3 chapitres de résultats qui décrivent le rôle de certaines protéines GRA pendant la phase aigüe de l'infection parasitaire (souches de type I) et le rôle de GRA5 dans des souches de type II. Nous avons ainsi montré l'importance de cette protéine dans la formation d'un kyste stable, ce qui est nécessaire au maintien et à la transmission du parasite *in vivo*. Un point commun de ces travaux est le développement des nouvelles méthodologies : construction de souches KO pour les protéines GRA, analyses automatisées pour la quantification de différents phénotypes (invasion, prolifération, interaction avec les organites de la cellule hôte, énumération des kystes *ex vivo*). Ces approches plus sensibles et plus spécifiques que les méthodes classiques permettent donc des résultats plus fiables.

BIBLIOGRAPHIC REFERENCES

Achbarou, A., Mercereau-Puijalon, O., Sadak, A., Fortier, B., Leriche, M.A., Camus, D., and Dubremetz, J.F. (1991). Differential targeting of dense granule proteins in the parasitophorous vacuole of Toxoplasma gondii. Parasitology *103 Pt 3*, 321–329.

Adjogble, K.D.Z., Mercier, C., Dubremetz, J.-F., Hucke, C., Mackenzie, C.R., Cesbron-Delauw, M.-F., and Däubener, W. (2004). GRA9, a new Toxoplasma gondii dense granule protein associated with the intravacuolar network of tubular membranes. Int. J. Parasitol. *34*, 1255–1264.

Adomako-Ankomah, Y., English, E.D., Danielson, J.J., Pernas, L.F., Parker, M.L., Boulanger, M.J., Dubey, J.P., and Boyle, J.P. (2016). Host mitochondrial association evolved in the human parasite Toxoplasma gondii via neofunctionalization of a gene duplicate. Genetics *203*, 283–298.

Afonso, C., Paixão, V.B., and Costa, R.M. (2012). Chronic Toxoplasma infection modifies the structure and the risk of host behavior. PLoS One. *7*, e32489.

Ahn, H.-J., Kim, S., Kim, H.-E., and Nam, H.-W. (2006). Interactions between secreted GRA proteins and host cell proteins across the paratitophorous vacuolar membrane in the parasitism of Toxoplasma gondii. Korean J. Parasitol. *44*, 303–312.

Aikawa, M., Miller, L.H., Johnson, J., and Rabbege, J. (1978). Erythrocyte entry by malarial parasites. A moving junction between erythrocyte and parasite. J. Cell Biol. *77*, 72–82.

Ajzenberg, D., Bañuls, A.L., Tibayrenc, M., and Dardé, M.L. (2002). Microsatellite analysis of Toxoplasma gondii shows considerable polymorphism structured into two main clonal groups. Int. J. Parasitol. *32*, 27–38.

Ajzenberg, D., Collinet, F., Mercier, A., Vignoles, P., and Dardé, M.-L. (2010). Genotyping of Toxoplasma gondii isolates with 15 microsatellite markers in a single multiplex PCR assay. J. Clin. Microbiol. *48*, 4641–4645.

Alaganan, A., Fentress, S.J., Tang, K., Wang, Q., and Sibley, L.D. (2014). Toxoplasma GRA7 effector increases turnover of immunity-related GTPases and contributes to acute virulence in the mouse. Proc. Natl. Acad. Sci. U.S.A. *111*, 1126–1131.

Aldebert, D., Hypolite, M., Cavailles, P., Touquet, B., Flori, P., Loeuillet, C., and Cesbron-Delauw, M.F. (2011). Development of high-throughput methods to quantify cysts of Toxoplasma gondii. Cytometry A *79*, 952–958.

Alexander, D.L., Mital, J., Ward, G.E., Bradley, P., and Boothroyd, J.C. (2005). Identification of the moving junction complex of Toxoplasma gondii: a collaboration between distinct secretory organelles. PLoS Pathog. *1*, e17.

Aliberti J, Sher A. (2002). Role of G-protein-coupled signaling in the induction and regulation of dendritic cell function by Toxoplasma gondii. Microbes Infect. 4, 991-997.

Allahyari, M., Mohabati, R., Amiri, S., Esmaeili Rastaghi, A.R., Babaie, J., Mahdavi, M., Vatanara, A., and Golkar, M. (2016). Synergistic effect of rSAG1 and rGRA2 antigens formulated in PLGA

microspheres in eliciting immune protection against Toxoplasama gondii. Exp. Parasitol. *170*, 236–246.

Andrade, E.F., Stumbo, A.C., Monteiro-Leal, L.H., Carvalho, L., and Barbosa, H.S. (2001). Do microtubules around the Toxoplasma gondii-containing parasitophorous vacuole in skeletal muscle cells form a barrier for the phagolysosomal fusion? J. Submicrosc. Cytol. Pathol. *33*, 337–341.

Andrade, W.A., Souza, M. do C., Ramos-Martinez, E., Nagpal, K., Dutra, M.S., Melo, M.B., Bartholomeu, D.C., Ghosh, S., Golenbock, D.T., and Gazzinelli, R.T. (2013). Combined action of nucleic acid-sensing Toll-like receptors and TLR11/TLR12 heterodimers imparts resistance to Toxoplasma gondii in mice. Cell Host Microbe *13*, 42–53.

Arsenijevic, D., Bilbao, F.D., Giannakopoulos, P., Girardier, L., Samec, S., and Richard, D. (2001). A role for interferon-gamma in the hypermetabolic response to murine toxoplasmosis. Eur. Cytokine Netw. *12*, 518–527.

Baird, J.R., Fox, B.A., Sanders, K.L., Lizotte, P.H., Cubillos-Ruiz, J.R., Scarlett, U.K., Rutkowski, M.R., Conejo-Garcia, J.R., Fiering, S., and Bzik, D.J. (2013). Avirulent Toxoplasma gondii generates therapeutic antitumor immunity by reversing immunosuppression in the ovarian cancer microenvironment. Cancer Res. *73*, 3842–3851.

de Barros, J.L.V.M., Barbosa, I.G., Salem, H., Rocha, N.P., Kummer, A., Okusaga, O.O., Soares, J.C., and Teixeira, A.L. (2017). Is there any association between Toxoplasma gondii infection and bipolar disorder? A systematic review and meta-analysis. J Affect Disord *209*, 59–65.

Beck, H.-P., Blake, D., Dardé, M.-L., Felger, I., Pedraza-Díaz, S., Regidor-Cerrillo, J., Gómez-Bautista, M., Ortega-Mora, L.M., Putignani, L., Shiels, B., et al. (2009). Molecular approaches to diversity of populations of apicomplexan parasites. Int. J. Parasitol. *39*, 175–189.

Bellini, V., Loeuillet, C., Massera, C., Cesbron-Delauw, M. and Cavaillès, P. (2015). Cyst Detection in *Toxoplasma gondii* Infected Mice and Rats Brain. *Bio-protocol* 5(7): e1439. DOI: 10.21769/BioProtoc.1439.

Bermudes, D., Peck, K.R., Afifi, M.A., Beckers, C.J., and Joiner, K.A. (1994). Tandemly repeated genes encode nucleoside triphosphate hydrolase isoforms secreted into the parasitophorous vacuole of Toxoplasma gondii. J. Biol. Chem. *269*, 29252–29260.

Besteiro, S., Bertrand-Michel, J., Lebrun, M., Vial, H., and Dubremetz, J.-F. (2008). Lipidomic analysis of Toxoplasma gondii tachyzoites rhoptries: further insights into the role of cholesterol. Biochem. J. *415*, 87–96.

Besteiro, S., Michelin, A., Poncet, J., Dubremetz, J.-F., and Lebrun, M. (2009). Export of a Toxoplasma gondii rhoptry neck protein complex at the host cell membrane to form the moving junction during invasion. PLoS Pathog. *5*, e1000309.

Bichet, M., Touquet, B., Gonzalez, V., Florent, I., Meissner, M., and Tardieux, I. (2016). Genetic impairment of parasite myosin motors uncovers the contribution of host cell membrane dynamics to Toxoplasma invasion forces. BMC Biol. *14*, 97.

Bisanz, C., Bastien, O., Grando, D., Jouhet, J., Maréchal, E., and Cesbron-Delauw, M.-F. (2006). Toxoplasma gondii acyl-lipid metabolism: de novo synthesis from apicoplast-generated fatty acids versus scavenging of host cell precursors. Biochem. J. *394*, 197–205.

Blanchard, N., Gonzalez, F., Schaeffer, M., Joncker, N.T., Cheng, T., Shastri, A.J., Robey, E.A., and Shastri, N. (2008). Immunodominant, protective response to the parasite Toxoplasma gondii requires antigen processing in the endoplasmic reticulum. Nat. Immunol. *9*, 937–944.

Bliss, S.K., Butcher, B.A., and Denkers, E.Y. (2000). Rapid recruitment of neutrophils containing prestored IL-12 during microbial infection. J. Immunol. *165*, 4515–4521.

Bliss, S.K., Gavrilescu, L.C., Alcaraz, A., and Denkers, E.Y. (2001). Neutrophil depletion during Toxoplasma gondii infection leads to impaired immunity and lethal systemic pathology. Infect. Immun. *69*, 4898–4905.

de Boer, J., Wulffraat, N., and Rothova, A. (2003). Visual loss in uveitis of childhood. Br. J. Ophthalmol. *87*, 879–884.

Bohne, W., Heesemann, J., and Gross, U. (1994). Reduced replication of Toxoplasma gondii is necessary for induction of bradyzoite-specific antigens: a possible role for nitric oxide in triggering stage conversion. Infect. Immun. *62*, 1761–1767.

Bonhomme, A., Maine, G.T., Beorchia, A., Burlet, H., Aubert, D., Villena, I., Hunt, J., Chovan, L., Howard, L., Brojanac, S., et al. (1998). Quantitative immunolocalization of a P29 protein (GRA7), a new antigen of toxoplasma gondii. J. Histochem. Cytochem. *46*, 1411–1422.

Boothroyd, J.C., Black, M., Bonnefoy, S., Hehl, A., Knoll, L.J., Manger, I.D., Ortega-Barria, E., and Tomavo, S. (1997). Genetic and biochemical analysis of development in Toxoplasma gondii. Philos. Trans. R. Soc. Lond., B, Biol. Sci. *352*, 1347–1354.

Boucher, L.E., and Bosch, J. (2015). The apicomplexan glideosome and adhesins - Structures and function. J. Struct. Biol. *190*, 93–114.

Bougdour, A., Maubon, D., Baldacci, P., Ortet, P., Bastien, O., Bouillon, A., Barale, J.-C., Pelloux, H., Ménard, R., and Hakimi, M.-A. (2009). Drug inhibition of HDAC3 and epigenetic control of differentiation in Apicomplexa parasites. J. Exp. Med. *206*, 953–966.

Bougdour, A., Durandau, E., Brenier-Pinchart, M.-P., Ortet, P., Barakat, M., Kieffer, S., Curt-Varesano, A., Curt-Bertini, R.-L., Bastien, O., Coute, Y., et al. (2013). Host cell subversion by Toxoplasma GRA16, an exported dense granule protein that targets the host cell nucleus and alters gene expression. Cell Host Microbe *13*, 489–500.

Bougdour A, Tardieux I, Hakimi MA. (2014). Toxoplasma exports dense granule proteins beyond the vacuole to the host cell nucleus and rewires the host genome expression. Cell Microbiol. 16, 334-343.

Boulanger, M.J., Tonkin, M.L., and Crawford, J. (2010). Apicomplexan parasite adhesins: novel strategies for targeting host cell carbohydrates. Curr. Opin. Struct. Biol. *20*, 551–559.

Bradley, P.J., Ward, C., Cheng, S.J., Alexander, D.L., Coller, S., Coombs, G.H., Dunn, J.D., Ferguson, D.J., Sanderson, S.J., Wastling, J.M., et al. (2005). Proteomic analysis of rhoptry organelles reveals many novel constituents for host-parasite interactions in Toxoplasma gondii. J. Biol. Chem. *280*, 34245–34258.

Bram, R.J., and Crabtree, G.R. (1994). Calcium signalling in T cells stimulated by a cyclophilin B-binding protein. Nature *371*, 355–358.

Braun, L., Travier, L., Kieffer, S., Musset, K., Garin, J., Mercier, C., and Cesbron-Delauw, M.-F. (2007). Purification of Toxoplasma dense granule proteins reveals that they are in complexes throughout the secretory pathway. Mol. Biochem. Parasitol. *157*, 13–21.

Braun, L., Brenier-Pinchart, M.-P., Yogavel, M., Curt-Varesano, A., Curt-Bertini, R.-L., Hussain, T., Kieffer-Jaquinod, S., Coute, Y., Pelloux, H., Tardieux, I., et al. (2013). A Toxoplasma dense granule protein, GRA24, modulates the early immune response to infection by promoting a direct and sustained host p38 MAPK activation. J. Exp. Med. *210*, 2071–2086.

Brown, C.R., Hunter, C.A., Estes, R.G., Beckmann, E., Forman, J., David, C., Remington, J.S., and McLeod, R. (1995). Definitive identification of a gene that confers resistance against Toxoplasma cyst burden and encephalitis. Immunology. *85*, 419–428.

Brown, K.M., Lourido, S., and Sibley, L.D. (2016). Serum Albumin Stimulates Protein Kinase G-dependent Microneme Secretion in Toxoplasma gondii. J. Biol. Chem. *291*, 9554–9565.

Bullen, H.E., Jia, Y., Yamaryo-Botté, Y., Bisio, H., Zhang, O., Jemelin, N.K., Marq, J.-B., Carruthers, V., Botté, C.Y., and Soldati-Favre, D. (2016). Phosphatidic Acid-Mediated Signaling Regulates Microneme Secretion in Toxoplasma. Cell Host Microbe. *19*, 349–360.

Butcher, B.A., Greene, R.I., Henry, S.C., Annecharico, K.L., Weinberg, J.B., Denkers, E.Y., Sher, A., and Taylor, G.A. (2005). p47 GTPases regulate Toxoplasma gondii survival in activated macrophages. Infect. Immun. *73*, 3278–3286.

Buxton, D. (1998). Protozoan infections (Toxoplasma gondii, Neospora caninum and Sarcocystis spp.) in sheep and goats: recent advances. Vet. Res. *29*, 289–310.

Buxton, D., and Innes, E.A. (1995). A commercial vaccine for ovine toxoplasmosis. Parasitology. *110 Suppl*, S11-16.

Caffaro, C.E., and Boothroyd, J.C. (2011). Evidence for host cells as the major contributor of lipids in the intravacuolar network of Toxoplasma-infected cells. Euk. Cell. *10*, 1095–1099.

Capron, A., and Dessaint, J.P. (1988). Vaccination against parasitic diseases: some alternative concepts for the definition of protective antigens. Ann. Inst. Pasteur Immunol. *139*, 109–117.

Carey, K.L., Donahue, C.G., and Ward, G.E. (2000). Identification and molecular characterization of GRA8, a novel, proline-rich, dense granule protein of Toxoplasma gondii. Mol. Biochem. Parasitol. *105*, 25–37.

Carme, B., Bissuel, F., Ajzenberg, D., Bouyne, R., Aznar, C., Demar, M., Bichat, S., Louvel, D., Bourbigot, A.M., Peneau, C., et al. (2002). Severe acquired toxoplasmosis in immunocompetent adult patients in French Guiana. J. Clin. Microbiol. *40*, 4037–4044.

Carruthers, V., and Boothroyd, J.C. (2007). Pulling together: an integrated model of Toxoplasma cell invasion. Curr. Opin. Microbiol. *10*, 83–89.

Carruthers, V.B., and Sibley, L.D. (1997). Sequential protein secretion from three distinct organelles of Toxoplasma gondii accompanies invasion of human fibroblasts. Eur. J. Cell Biol. *73*, 114–123.

Carruthers, V.B., and Tomley, F.M. (2008). Microneme proteins in apicomplexans. Subcell. Biochem. *47*, 33–45.

Carruthers, V.B., Sherman, G.D., and Sibley, L.D. (2000). The Toxoplasma adhesive protein MIC2 is proteolytically processed at multiple sites by two parasite-derived proteases. J. Biol. Chem. *275*, 14346–14353.

Cesbron-Delauw, M.F., Guy, B., Torpier, G., Pierce, R.J., Lenzen, G., Cesbron, J.Y., Charif, H., Lepage, P., Darcy, F., and Lecocq, J.P. (1989). Molecular characterization of a 23-kilodalton major antigen secreted by Toxoplasma gondii. Proc. Natl. Acad. Sci. U.S.A. *86*, 7537–7541.

Cesbron-Delauw, M.-F., Gendrin, C., Travier, L., Ruffiot, P., and Mercier, C. (2008). Apicomplexa in mammalian cells: trafficking to the parasitophorous vacuole. Traffic. *9*, 657–664.

Charif, H., Darcy, F., Torpier, G., Cesbron-Delauw, M.F., and Capron, A. (1990). Toxoplasma gondii: characterization and localization of antigens secreted from tachyzoites. Exp. Parasitol. *71*, 114–124.

Chen, Z.W., Gao, J.M., Huo, X.X., Wang, L., Yu, L., Halm-Lai, F., Xu, Y.H., Song, W.J., Hide, G., Shen, J.L., et al. (2011). Genotyping of Toxoplasma gondii isolates from cats in different geographic regions of China. Vet. Parasitol. *183*, 166–170.

Chhabra, E.S., and Higgs, H.N. (2007). The many faces of actin: matching assembly factors with cellular structures. Nat. Cell Biol. *9*, 1110–1121.

Ching, X.T., Fong, M.Y., and Lau, Y.L. (2016). Evaluation of immunoprotection conferred by the subunit vaccines of GRA2 and GRA5 against acute toxoplasmosis in BALB/c mice. Front. Microbiol. *7*, 609.

Chtanova, T., Han, S.-J., Schaeffer, M., van Dooren, G.G., Herzmark, P., Striepen, B., and Robey, E.A. (2009). Dynamics of T cell, antigen-presenting cell, and pathogen interactions during recall responses in the lymph node. Immunity. *31*, 342–355.

Coffey, M.J., Sleebs, B.E., Uboldi, A.D., Garnham, A., Franco, M., Marino, N.D., Panas, M.W., Ferguson, D.J., Enciso, M., O'Neill, M.T., et al. (2015). An aspartyl protease defines a novel pathway for export of Toxoplasma proteins into the host cell. Elife *4*, pii: e10809.

Combe CL, Curiel TJ, Moretto MM, Khan IA. (2005). NK cells help to induce CD8(+)-T-cell immunity against Toxoplasma gondii in the absence of CD4(+) T cells. Infect Immun. *73*, 4913-21

Coppens, I., and Joiner, K.A. (2003). Host but not parasite cholesterol controls Toxoplasma cell entry by modulating organelle discharge. Mol. Biol. Cell. *14*, 3804–3820.

Coppens, I., Sinai, A.P., and Joiner, K.A. (2000). Toxoplasma gondii exploits host low-density lipoprotein receptor-mediated endocytosis for cholesterol acquisition. J. Cell Biol. *149*, 167–180.

Coppens, I., Dunn, J.D., Romano, J.D., Pypaert, M., Zhang, H., Boothroyd, J.C., and Joiner, K.A. (2006). Toxoplasma gondii sequesters lysosomes from mammalian hosts in the vacuolar space. Cell. *125*, 261–274.

Cortez, E., Stumbo, A.C., Saldanha-Gama, R., Villela, C.G., Barja-Fidalgo, C., Rodrigues, C.A., das Graças Henriques, M., Benchimol, M., Barbosa, H.S., Porto, L.C., et al. (2008). Immunolocalization of an osteopontin-like protein in dense granules of Toxoplasma gondii tachyzoites and its association with the parasitophorous vacuole. Micron. *39*, 25–31.

Cossart, P., and Helenius, A. (2014). Endocytosis of viruses and bacteria. Cold Spring Harb. Perspect Biol. *6*, pii: a016972.

Courret, N., Darche, S., Sonigo, P., Milon, G., Buzoni-Gâtel, D., and Tardieux, I. (2006). CD11c- and CD11b-expressing mouse leukocytes transport single Toxoplasma gondii tachyzoites to the brain. Blood. *107*, 309–316.

Cowper, B., Matthews, S., and Tomley, F. (2012). The molecular basis for the distinct host and tissue tropisms of coccidian parasites. Mol. Biochem. Parasitol. *186*, 1–10.

Crawford, M.J., Thomsen-Zieger, N., Ray, M., Schachtner, J., Roos, D.S., and Seeber, F. (2006). Toxoplasma gondii scavenges host-derived lipoic acid despite its de novo synthesis in the apicoplast. EMBO J. *25*, 3214–3222.

Croken, M.M., Ma, Y., Markillie, L.M., Taylor, R.C., Orr, G., Weiss, L.M., and Kim, K. (2014a). Distinct strains of Toxoplasma gondii feature divergent transcriptomes regardless of developmental stage. PLoS One. *9*, e111297.

Croken MM, Qiu W, White MW, Kim K. (2014b). Gene Set Enrichment Analysis (GSEA) of Toxoplasma gondii expression datasets links cell cycle progression and the bradyzoite developmental program. BMC Genomics. *15*, 515.

Curt-Varesano, A., Braun, L., Ranquet, C., Hakimi, M.-A., and Bougdour, A. (2016). The aspartyl protease TgASP5 mediates the export of the Toxoplasma GRA16 and GRA24 effectors into host cells.

Cell. Microbiol. *18*, 151–167.

Debierre-Grockiego, F., Campos, M.A., Azzouz, N., Schmidt, J., Bieker, U., Resende, M.G., Mansur, D.S., Weingart, R., Schmidt, R.R., Golenbock, D.T., et al. (2007). Activation of TLR2 and TLR4 by glycosylphosphatidylinositols derived from Toxoplasma gondii. J. Immunol. *179*, 1129–1137.

Del Carmen, M.G., Mondragón, M., González, S., and Mondragón, R. (2009). Induction and regulation of conoid extrusion in Toxoplasma gondii. Cell. Microbiol. *11*, 967–982.

Delorme-Walker, V., Abrivard, M., Lagal, V., Anderson, K., Perazzi, A., Gonzalez, V., Page, C., Chauvet, J., Ochoa, W., Volkmann, N., et al. (2012). Toxofilin upregulates the host cortical actin cytoskeleton dynamics, facilitating Toxoplasma invasion. J. Cell. Sci. *125*, 4333–4342.

Denkers, E.Y., and Gazzinelli, R.T. (1998). Regulation and function of T-cell-mediated immunity during Toxoplasma gondii infection. Clin. Microbiol. Rev. *11*, 569–588.

Derouin, F., Pelloux, H., and ESCMID Study Group on Clinical Parasitology (2008). Prevention of toxoplasmosis in transplant patients. Clin. Microbiol. Infect. *14*, 1089–1101.

Desai, S.A., and Rosenberg, R.L. (1997). Pore size of the malaria parasite's nutrient channel. Proc. Natl. Acad. Sci. U.S.A. *94*, 2045–2049.

Dou, Z., McGovern, O.L., Di Cristina, M., and Carruthers, V.B. (2014). Toxoplasma gondii ingests and digests host cytosolic proteins. MBio *5*, e01188-01114.

Dowse, T.J., and Soldati, D. (2005). Rhomboid-like proteins in Apicomplexa: phylogeny and nomenclature. Trends Parasitol. *21*, 254–258.

Drewry, L.L., and Sibley, L.D. (2015). Toxoplasma actin is required for efficient host cell invasion. MBio *6*, e00557.

Dubey, J.P., Miller, N.L., and Frenkel, J.K. (1970). Toxoplasma gondii life cycle in cats. J. Am. Vet. Med. Assoc. *157*, 1767–1770.

Dubey, J.P., Lindsay, D.S., and Speer, C.A. (1998). Structures of Toxoplasma gondii tachyzoites, bradyzoites, and sporozoites and biology and development of tissue cysts. Clin. Microbiol. Rev. *11*, 267–299.

Dubey JP, Zhu XQ, Sundar N, Zhang H, Kwok OC, Su C. (2007). Genetic and biologic characterization of Toxoplasma gondii isolates of cats from China. Vet Parasitol. *145*, 352-356.

Dubremetz JF. (1998). Host cell invasion by Toxoplasma gondii. Trends Microbiol. *6*, 27-30.

Dubremetz, J.F., Achbarou, A., Bermudes, D., and Joiner, K.A. (1993). Kinetics and pattern of organelle exocytosis during Toxoplasma gondii/host-cell interaction. Parasitol. Res. *79*, 402–408.

Dunay, I.R., Damatta, R.A., Fux, B., Presti, R., Greco, S., Colonna, M., and Sibley, L.D. (2008). Gr1(+) inflammatory monocytes are required for mucosal resistance to the pathogen Toxoplasma gondii. Immunity. *29*, 306–317.

Dupont, C.D., Christian, D.A., and Hunter, C.A. (2012). Immune response and immunopathology during toxoplasmosis. Semin. Immunopathol. *34*, 793–813.

Dziadek, B., and Brzostek, A. (2012). Recombinant ROP2, ROP4, GRA4 and SAG1 antigen-cocktails as possible tools for immunoprophylaxis of toxoplasmosis: what's next? Bioengineered. *3*, 358–364.

Dzierszinski, F., Nishi, M., Ouko, L., and Roos, D.S. (2004). Dynamics of Toxoplasma gondii differentiation. Euk. Cell. *3*, 992–1003.

Egarter, S., Andenmatten, N., Jackson, A.J., Whitelaw, J.A., Pall, G., Black, J.A., Ferguson, D.J.P., Tardieux, I., Mogilner, A., and Meissner, M. (2014). The Toxoplasma Acto-MyoA motor complex is important but not essential for gliding motility and host cell invasion. PLoS One. *9*, e91819.

Ehrenman, K., Sehgal, A., Lige, B., Stedman, T.T., Joiner, K.A., and Coppens, I. (2010). Novel roles for ATP-binding cassette G transporters in lipid redistribution in Toxoplasma. Mol. Microbiol. *76*, 1232–1249.

El Bissati, K., Chentoufi, A.A., Krishack, P.A., Zhou, Y., Woods, S., Dubey, J.P., Vang, L., Lykins, J., Broderick, K.E., Mui, E., et al. (2016). Adjuvanted multi-epitope vaccines protect HLA-A*11:01 transgenic mice against Toxoplasma gondii. JCI Insight. *1*, e85955.

El Hajj H, Demey E, Poncet J, Lebrun M, Wu B, Galéotti N, Fourmaux MN, Mercereau-Puijalon O, Vial H, Labesse G, Dubremetz JF. (2006). The ROP2 family of Toxoplasma gondii rhoptry proteins: proteomic and genomic characterization and molecular modeling. Proteomics. 6, 5773-5784.

El Hajj, H., Lebrun, M., Arold, S.T., Vial, H., Labesse, G., and Dubremetz, J.F. (2007a). ROP18 is a rhoptry kinase controlling the intracellular proliferation of Toxoplasma gondii. PLoS Pathog. *3*, e14.

Endeshaw MM[1], Li C, de Leon J, Yao N, Latibeaudiere K, Premalatha K, Morrissette N, Werbovetz KA. (2010). Synthesis and evaluation of oryzalin analogs against Toxoplasma gondii. Bioorg Med Chem Lett. *20*, 5179-5183.

Etheridge, R.D., Alaganan, A., Tang, K., Lou, H.J., Turk, B.E., and Sibley, L.D. (2014). The Toxoplasma pseudokinase ROP5 forms complexes with ROP18 and ROP17 kinases that synergize to control acute virulence in mice. Cell Host Microbe *15*, 537–550.

Farrell, A., Thirugnanam, S., Lorestani, A., Dvorin, J.D., Eidell, K.P., Ferguson, D.J.P., Anderson-White, B.R., Duraisingh, M.T., Marth, G.T., and Gubbels, M.-J. (2012). A DOC2 protein identified by mutational profiling is essential for apicomplexan parasite exocytosis. Science. *335*, 218–221.

Ferguson, D.J.P. (2004). Use of molecular and ultrastructural markers to evaluate stage conversion of Toxoplasma gondii in both the intermediate and definitive host. Int. J. Parasitol. *34*, 347–360.

Ferguson, D.J., Hutchison, W.M., and Siim, J.C. (1975). The ultrastructural development of the macrogamete and formation of the oocyst wall of Toxoplasma gondii. Acta Pathol. Microbiol. Scand. B *83*, 491–505.

Fernandes, M.C., and Andrews, N.W. (2012). Host cell invasion by Trypanosoma cruzi: a unique strategy that promotes persistence. FEMS Microbiol. Rev. *36*, 734–747.

Foussard, F., Leriche, M.A., and Dubremetz, J.F. (1991). Characterization of the lipid content of Toxoplasma gondii rhoptries. Parasitology. *102 Pt 3*, 367–370.

Fox, B.A., Gigley, J.P., and Bzik, D.J. (2004). Toxoplasma gondii lacks the enzymes required for de novo arginine biosynthesis and arginine starvation triggers cyst formation. Int. J. Parasitol. *34*, 323–331.

Fox, B.A., Ristuccia, J.G., Gigley, J.P., and Bzik, D.J. (2009). Efficient gene replacements in Toxoplasma gondii strains deficient for nonhomologous end joining. Euk. Cell. *8*, 520–529.

Fox, B.A., Falla, A., Rommereim, L.M., Tomita, T., Gigley, J.P., Mercier, C., Cesbron-Delauw, M.-F., Weiss, L.M., and Bzik, D.J. (2011). Type II Toxoplasma gondii KU80 knockout strains enable functional analysis of genes required for cyst development and latent infection. Euk. Cell *10*, 1193–1206.

Fox, B.A., Sanders, K.L., Rommereim, L.M., Guevara, R.B., and Bzik, D.J. (2016). Secretion of Rhoptry and Dense Granule Effector Proteins by Nonreplicating Toxoplasma gondii Uracil Auxotrophs Controls the Development of Antitumor Immunity. PLoS Genet. *12*, e1006189.

Franco, M., Panas, M.W., Marino, N.D., Lee, M.-C.W., Buchholz, K.R., Kelly, F.D., Bednarski, J.J., Sleckman, B.P., Pourmand, N., and Boothroyd, J.C. (2016). A Novel Secreted Protein, MYR1, Is Central to Toxoplasma's Manipulation of Host Cells. MBio. *7*, e02231-02215.

Frenkel, J.K., Dubey, J.P., and Miller, N.L. (1969). Toxoplasma gondii: fecal forms separated from eggs of the nematode Toxocara cati. Science. *164*, 432–433.

Frickel, E.-M., Sahoo, N., Hopp, J., Gubbels, M.-J., Craver, M.P.J., Knoll, L.J., Ploegh, H.L., and Grotenbreg, G.M. (2008). Parasite stage-specific recognition of endogenous Toxoplasma gondii-derived CD8+ T cell epitopes. J. Infect. Dis. *198*, 1625–1633.

Garnett, J.A., Liu, Y., Leon, E., Allman, S.A., Friedrich, N., Saouros, S., Curry, S., Soldati-Favre, D., Davis, B.G., Feizi, T., et al. (2009). Detailed insights from microarray and crystallographic studies into carbohydrate recognition by microneme protein 1 (MIC1) of Toxoplasma gondii. Protein Sci. *18*, 1935–1947.

Gay, G., Braun, L., Brenier-Pinchart, M.-P., Vollaire, J., Josserand, V., Bertini, R.-L., Varesano, A., Touquet, B., De Bock, P.-J., Coute, Y., et al. (2016). Toxoplasma gondii TgIST co-opts host chromatin repressors dampening STAT1-dependent gene regulation and IFN-γ-mediated host defenses. J. Exp. Med. *213*, 1779–1798.

Gazzinelli, R., Xu, Y., Hieny, S., Cheever, A., and Sher, A. (1992). Simultaneous depletion of CD4+ and CD8+ T lymphocytes is required to reactivate chronic infection with Toxoplasma gondii. J. Immunol.

149, 175–180.

Gendrin, C., Mercier, C., Braun, L., Musset, K., Dubremetz, J.-F., and Cesbron-Delauw, M.-F. (2008). Toxoplasma gondii uses unusual sorting mechanisms to deliver transmembrane proteins into the host-cell vacuole. Traffic. *9*, 1665–1680.

Gendrin, C., Bittame, A., Mercier, C., and Cesbron-Delauw, M.-F. (2010). Post-translational membrane sorting of the Toxoplasma gondii GRA6 protein into the parasite-containing vacuole is driven by its N-terminal domain. Int. J. Parasitol. *40*, 1325–1334.

Gold, D.A., Kaplan, A.D., Lis, A., Bett, G.C.L., Rosowski, E.E., Cirelli, K.M., Bougdour, A., Sidik, S.M., Beck, J.R., Lourido, S., et al. (2015). The Toxoplasma dense granule proteins GRA17 and GRA23 mediate the movement of small molecules between the host and the parasitophorous vacuole. Cell Host Microbe. *17*, 642–652.

Goldszmid RS, Bafica A, Jankovic D, Feng CG, Caspar P, Winkler-Pickett R, Trinchieri G, Sher A. (2007). TAP-1 indirectly regulates CD4+ T cell priming in Toxoplasma gondii infection by controlling NK cell IFN-gamma production.. J Exp Med. *204*, 2591-2602.

Golkar M, Shokrgozar MA, Rafati S, Musset K, Assmar M, Sadaie R, Cesbron-Delauw MF, Mercier C. (2007). Evaluation of protective effect of recombinant dense granule antigens GRA2 and GRA6 formulated in monophosphoryl lipid A (MPL) adjuvant against Toxoplasma chronic infection in mice. Vaccine. *25*, 4301-4311.

Gonzalez, V., Combe, A., David, V., Malmquist, N.A., Delorme, V., Leroy, C., Blazquez, S., Ménard, R., and Tardieux, I. (2009). Host cell entry by Apicomplexa parasites requires actin polymerization in the host cell. Cell Host Microbe. *5*, 259–272.

Gormley, P.D., Pavesio, C.E., Minnasian, D., and Lightman, S. (1998). Effects of drug therapy on Toxoplasma cysts in an animal model of acute and chronic disease. Invest. Ophthalmol. Vis. Sci. *39*, 1171–1175.

Graindorge, A., Frénal, K., Jacot, D., Salamun, J., Marq, J.B., and Soldati-Favre, D. (2016). The conoid-associated motor MyoH is indispensable for Toxoplasma gondii entry and exit from host cells. PLoS Pathog. *12*, e1005388.

Grigg, M.E., Bonnefoy, S., Hehl, A.B., Suzuki, Y., and Boothroyd, J.C. (2001). Success and virulence in Toxoplasma as the result of sexual recombination between two distinct ancestries. Science. *294*, 161–165.

Gross, U., Bohne, W., Lüder, C.G., Lugert, R., Seeber, F., Dittrich, C., Pohl, F., and Ferguson, D.J. (1996). Regulation of developmental differentiation in the protozoan parasite Toxoplasma gondii. J. Eukaryot. Microbiol. *43*, 114S–116S.

Guimarães, E.V., Carvalho, L. de, and Barbosa, H.S. (2009). Interaction and cystogenesis of Toxoplasma gondii within skeletal muscle cells in vitro. Mem. Inst. Oswaldo Cruz *104*, 170–174.

Gupta, N., Zahn, M.M., Coppens, I., Joiner, K.A., and Voelker, D.R. (2005). Selective disruption of phosphatidylcholine metabolism of the intracellular parasite Toxoplasma gondii arrests its growth. J. Biol. Chem. *280*, 16345–16353.

Håkansson, S., Morisaki, H., Heuser, J., and Sibley, L.D. (1999). Time-lapse video microscopy of gliding motility in Toxoplasma gondii reveals a novel, biphasic mechanism of cell locomotion. Mol. Biol. Cell. *10*, 3539–3547.

Håkansson S, Charron AJ, Sibley LD. (2001) Toxoplasma evacuoles: a two-step process of secretion and fusion forms the parasitophorous vacuole. EMBO J. *20*, 3132-3144.

Hall, A.O., Beiting, D.P., Tato, C., John, B., Oldenhove, G., Lombana, C.G., Pritchard, G.H., Silver, J.S., Bouladoux, N., Stumhofer, J.S., et al. (2012). The cytokines interleukin 27 and interferon-γ promote distinct Treg cell populations required to limit infection-induced pathology. Immunity. *37*, 511–523.

Halonen SK, Weidner E. (1994). Overcoating of Toxoplasma parasitophorous vacuoles with host cell vimentin type intermediate filaments. J Eukaryot Microbiol. 41, 65-71.

Hammoudi, P.-M., Jacot, D., Mueller, C., Di Cristina, M., Dogga, S.K., Marq, J.-B., Romano, J., Tosetti, N., Dubrot, J., Emre, Y., et al. (2015). Fundamental roles of the Golgi-associated Toxoplasma aspartyl protease, ASP5, at the host-parasite interface. PLoS Pathog. *11*, e1005211.

Hampton MM. (2015). Congenital Toxoplasmosis: A Review. Neonatal Netw. *34*, 274-278.

He, X., Grigg, M.E., Boothroyd, J.C., and Garcia, K.C. (2002). Structure of the immunodominant surface antigen from the Toxoplasma gondii SRS superfamily. Nat. Struct. Biol. *9*, 606–611.

Heaslip, A.T., Nelson, S.R., and Warshaw, D.M. (2016). Dense granule trafficking in Toxoplasma gondii requires a unique class 27 myosin and actin filaments. Mol. Biol. Cell. *27*, 2080–2089.

Henriquez, F.L., Nickdel, M.B., McLeod, R., Lyons, R.E., Lyons, K., Dubremetz, J.F., Grigg, M.E., Samuel, B.U., and Roberts, C.W. (2005). Toxoplasma gondii dense granule protein 3 (GRA3) is a type I transmembrane protein that possesses a cytoplasmic dilysine (KKXX) endoplasmic reticulum (ER) retrieval motif. Parasitology. *131*, 169–179.

High, K.P., Joiner, K.A., and Handschumacher, R.E. (1994). Isolation, cDNA sequences, and biochemical characterization of the major cyclosporin-binding proteins of Toxoplasma gondii. J. Biol. Chem. *269*, 9105–9112.

Hill, D., and Dubey, J.P. (2002). Toxoplasma gondii: transmission, diagnosis and prevention. Clin. Microbiol. Infect. *8*, 634–640.

Hiller, N.L., Bhattacharjee, S., van Ooij, C., Liolios, K., Harrison, T., Lopez-Estraño, C., and Haldar, K. (2004). A host-targeting signal in virulence proteins reveals a secretome in malarial infection. Science. *306*, 1934–1937.

Hiszczyńska-Sawicka, E., Olędzka, G., Holec-Gąsior, L., Li, H., Xu, J.B., Sedcole, R., Kur, J., Bickerstaffe, R., and Stankiewicz, M. (2011). Evaluation of immune responses in sheep induced by DNA immunization with genes encoding GRA1, GRA4, GRA6 and GRA7 antigens of Toxoplasma gondii. Vet. Parasitol. *177*, 281–289.

Howard, J.C., Hunn, J.P., and Steinfeldt, T. (2011). The IRG protein-based resistance mechanism in mice and its relation to virulence in Toxoplasma gondii. Curr. Opin. Microbiol. *14*, 414–421.

Howe, D.K., and Sibley, L.D. (1995). Toxoplasma gondii comprises three clonal lineages: correlation of parasite genotype with human disease. J. Infect. Dis. *172*, 1561–1566.

Hsiao, C.-H.C., Hiller, L.N., Haldar, K., and Knoll, L.J. (2013). A HT/PEXEL motif in Toxoplasma dense granule proteins is a signal for protein cleavage but not export into the host cell. Traffic. *14*, 519–531.

Hu, K., Mann, T., Striepen, B., Beckers, C.J.M., Roos, D.S., and Murray, J.M. (2002a). Daughter cell assembly in the protozoan parasite Toxoplasma gondii. Mol. Biol. Cell. *13*, 593–606.

Hu, K., Roos, D.S., and Murray, J.M. (2002b). A novel polymer of tubulin forms the conoid of Toxoplasma gondii. J. Cell Biol. *156*, 1039–1050.

Hunter, C.A., and Sibley, L.D. (2012). Modulation of innate immunity by Toxoplasma gondii virulence effectors. Nat. Rev. Microbiol. *10*, 766–778.

Hunter, C.A., Subauste, C.S., Van Cleave, V.H., and Remington, J.S. (1994). Production of gamma interferon by natural killer cells from Toxoplasma gondii-infected SCID mice: regulation by interleukin-10, interleukin-12, and tumor necrosis factor alpha. Infect. Immun. *62*, 2818–2824.

Hutchison, W.M. (1965). Experimental transmission of Toxoplasma gondii. Nature. *206*, 961–962.

Ibrahim HM, Xuan X, Nishikawa Y. (2010). Toxoplasma gondii cyclophilin 18 regulates the proliferation and migration of murine macrophages and spleen cells. Clin. Vaccine Immunol. *17*, 1322-1329.

Innes, E.A., Bartley, P.M., Maley, S., Katzer, F., and Buxton, D. (2009). Veterinary vaccines against Toxoplasma gondii. Mem. Inst. Oswaldo Cruz. *104*, 246–251.

Johnson, L.L., and Sayles, P.C. (2002). Deficient humoral responses underlie susceptibility to Toxoplasma gondii in CD4-deficient mice. Infect. Immun. *70*, 185–191.

Jones, T.C., Yeh, S., and Hirsch, J.G. (1972). The interaction between Toxoplasma gondii and mammalian cells. I. Mechanism of entry and intracellular fate of the parasite. J. Exp. Med. *136*, 1157–1172.

Jongert, E., Melkebeek, V., De Craeye, S., Dewit, J., Verhelst, D., and Cox, E. (2008). An enhanced GRA1-GRA7 cocktail DNA vaccine primes anti-Toxoplasma immune responses in pigs. Vaccine. *26*, 1025–1031.

Katlama, C., Mouthon, B., Gourdon, D., Lapierre, D., and Rousseau, F. (1996). Atovaquone as long-term suppressive therapy for toxoplasmic encephalitis in patients with AIDS and multiple drug intolerance. Atovaquone Expanded Access Group. AIDS. *10*, 1107–1112.

Keeley, A., and Soldati, D. (2004). The glideosome: a molecular machine powering motility and host-cell invasion by Apicomplexa. Trends Cell Biol. *14*, 528–532.

Khan, A., Fux, B., Su, C., Dubey, J.P., Darde, M.L., Ajioka, J.W., Rosenthal, B.M., and Sibley, L.D. (2007). Recent transcontinental sweep of Toxoplasma gondii driven by a single monomorphic chromosome. Proc. Natl. Acad. Sci. U.S.A. *104*, 14872–14877.

Khan, A., Dubey, J.P., Su, C., Ajioka, J.W., Rosenthal, B.M., and Sibley, L.D. (2011). Genetic analyses of atypical Toxoplasma gondii strains reveal a fourth clonal lineage in North America. Int. J. Parasitol. *41*, 645–655.

Khan, I.A., Smith, K.A., and Kasper, L.H. (1988). Induction of antigen-specific parasiticidal cytotoxic T cell splenocytes by a major membrane protein (P30) of Toxoplasma gondii. J. Immunol. *141*, 3600–3605.

Kim JY, Ahn HJ, Ryu KJ, Nam HW. (2008). Interaction between parasitophorous vacuolar membrane-associated GRA3 and calcium modulating ligand of host cell endoplasmic reticulum in the parasitism of Toxoplasma gondii. Korean J Parasitol. 46, 209-216.

Kim SK, Fouts AE, Boothroyd JC. (2007). Toxoplasma gondii dysregulates IFN-gamma-inducible gene expression in human fibroblasts: insights from a genome-wide transcriptional profiling. J Immunol. *178*, 5154-5165.

de Koning-Ward, T.F., Gilson, P.R., Boddey, J.A., Rug, M., Smith, B.J., Papenfuss, A.T., Sanders, P.R., Lundie, R.J., Maier, A.G., Cowman, A.F., et al. (2009). A newly discovered protein export machine in malaria parasites. Nature. *459*, 945–949.

Konrad, C., Wek, R.C., and Sullivan, W.J. (2011). A GCN2-like eukaryotic initiation factor 2 kinase increases the viability of extracellular Toxoplasma gondii parasites. Euk. Cell. *10*, 1403–1412.

Konrad, C., Wek, R.C., and Sullivan, W.J. (2014). GCN2-like eIF2α kinase manages the amino acid starvation response in Toxoplasma gondii. Int. J. Parasitol. *44*, 139–146.

Kugler, D.G., Flomerfelt, F.A., Costa, D.L., Laky, K., Kamenyeva, O., Mittelstadt, P.R., Gress, R.E., Rosshart, S.P., Rehermann, B., Ashwell, J.D., et al. (2016). Systemic Toxoplasma infection triggers a long-term defect in the generation and function of naive T lymphocytes. J. Exp. Med. *213*, 3041–3056.

Labruyère, E., Lingnau, M., Mercier, C., and Sibley, L.D. (1999). Differential membrane targeting of the secretory proteins GRA4 and GRA6 within the parasitophorous vacuole formed by Toxoplasma gondii. Mol. Biochem. Parasitol. *102*, 311–324.

Lamarque, M.H., Papoin, J., Finizio, A.-L., Lentini, G., Pfaff, A.W., Candolfi, E., Dubremetz, J.-F., and Lebrun, M. (2012). Identification of a new rhoptry neck complex RON9/RON10 in the Apicomplexa

parasite Toxoplasma gondii. PLoS One. *7*, e32457.

Lambert, H., Hitziger, N., Dellacasa, I., Svensson, M., and Barragan, A. (2006). Induction of dendritic cell migration upon Toxoplasma gondii infection potentiates parasite dissemination. Cell. Microbiol. *8*, 1611–1623.

Lane, A., Soete, M., Dubremetz, J.F., and Smith, J.E. (1996). Toxoplasma gondii: appearance of specific markers during the development of tissue cysts in vitro. Parasitol. Res. *82*, 340–346.

Lebrun, M., Michelin, A., El Hajj, H., Poncet, J., Bradley, P.J., Vial, H., and Dubremetz, J.F. (2005). The rhoptry neck protein RON4 re-localizes at the moving junction during Toxoplasma gondii invasion. Cell. Microbiol. *7*, 1823–1833.

Lecordier, L., Mercier, C., Torpier, G., Tourvieille, B., Darcy, F., Liu, J.L., Maes, P., Tartar, A., Capron, A., and Cesbron-Delauw, M.F. (1993). Molecular structure of a Toxoplasma gondii dense granule antigen (GRA 5) associated with the parasitophorous vacuole membrane. Mol. Biochem. Parasitol. *59*, 143–153.

Lecordier, L., Moleon-Borodowsky, I., Dubremetz, J.F., Tourvieille, B., Mercier, C., Deslée, D., Capron, A., and Cesbron-Delauw, M.F. (1995). Characterization of a dense granule antigen of Toxoplasma gondii (GRA6) associated to the network of the parasitophorous vacuole. Mol. Biochem. Parasitol. *70*, 85–94.

Lecordier, L., Mercier, C., Sibley, L.D., and Cesbron-Delauw, M.F. (1999). Transmembrane insertion of the Toxoplasma gondii GRA5 protein occurs after soluble secretion into the host cell. Mol. Biol. Cell *10*, 1277–1287.

Lee, D.-H., Kim, A.-R., Lee, S.-H., and Quan, F.-S. (2016). Cross-protection induced by Toxoplasma gondii virus-like particle vaccine upon intraperitoneal route challenge. Acta Trop. *164*, 77–83.

Lehmann, T., Marcet, P.L., Graham, D.H., Dahl, E.R., and Dubey, J.P. (2006). Globalization and the population structure of Toxoplasma gondii. Proc. Natl. Acad. Sci. U.S.A. *103*, 11423–11428.

Lekutis, C., Ferguson, D.J., Grigg, M.E., Camps, M., and Boothroyd, J.C. (2001). Surface antigens of Toxoplasma gondii: variations on a theme. Int. J. Parasitol. *31*, 1285–1292.

Lemgrüber, L., Lupetti, P., Martins-Duarte, E.S., De Souza, W., and Vommaro, R.C. (2011). The organization of the wall filaments and characterization of the matrix structures of Toxoplasma gondii cyst form. Cell. Microbiol. *13*, 1920–1932.

Leriche, M.A., and Dubremetz, J.F. (1991). Characterization of the protein contents of rhoptries and dense granules of Toxoplasma gondii tachyzoites by subcellular fractionation and monoclonal antibodies. Mol. Biochem. Parasitol. *45*, 249–259.

Liu, C.-H., Fan, Y., Dias, A., Esper, L., Corn, R.A., Bafica, A., Machado, F.S., and Aliberti, J. (2006). Cutting edge: dendritic cells are essential for in vivo IL-12 production and development of resistance against Toxoplasma gondii infection in mice. J. Immunol. *177*, 31–35.

Lopez, J., Bittame, A., Massera, C., Vasseur, V., Effantin, G., Valat, A., Buaillon, C., Allart, S., Fox, B.A., Rommereim, L.M., et al. (2015). Intravacuolar membranes regulate CD8 T cell recognition of membrane-bound Toxoplasma gondii protective antigen. Cell Rep. *13*, 2273–2286.

Luft, B.J., and Remington, J.S. (1992). Toxoplasmic encephalitis in AIDS. Clin. Infect. Dis. *15*, 211–222.

Luu, L., and Coombes, J.L. (2015). Dynamic two-photon imaging of the immune response to Toxoplasma gondii infection. Parasite Immunol. *37*, 118–126.

Ma, J.S., Sasai, M., Ohshima, J., Lee, Y., Bando, H., Takeda, K., and Yamamoto, M. (2014). Selective and strain-specific NFAT4 activation by the Toxoplasma gondii polymorphic dense granule protein GRA6. J. Exp. Med. *211*, 2013–2032.

Machado, F.S., Johndrow, J.E., Esper, L., Dias, A., Bafica, A., Serhan, C.N., and Aliberti, J. (2006). Anti-inflammatory actions of lipoxin A4 and aspirin-triggered lipoxin are SOCS-2 dependent. Nat. Med. *12*, 330–334.

Mack, D.G., Johnson, J.J., Roberts, F., Roberts, C.W., Estes, R.G., David, C., Grumet, F.C., and McLeod, R. (1999). HLA-class II genes modify outcome of Toxoplasma gondii infection. Int. J. Parasitol. *29*, 1351–1358.

Magno, R.C., Lemgruber, L., Vommaro, R.C., De Souza, W., and Attias, M. (2005a). Intravacuolar network may act as a mechanical support for Toxoplasma gondii inside the parasitophorous vacuole. Microsc. Res. Tech. *67*, 45–52.

Magno, R.C., Straker, L.C., de Souza, W., and Attias, M. (2005b). Interrelations between the parasitophorous vacuole of Toxoplasma gondii and host cell organelles. Microsc. Microanal. *11*, 166–174.

Makioka, A., and Ohtomo, H. (1995). An increased DNA polymerase activity associated with virulence of Toxoplasma gondii. J. Parasitol. *81*, 1021–1022.

Marchant, J., Cowper, B., Liu, Y., Lai, L., Pinzan, C., Marq, J.B., Friedrich, N., Sawmynaden, K., Liew, L., Chai, W., et al. (2012). Galactose recognition by the apicomplexan parasite Toxoplasma gondii. J. Biol. Chem. *287*, 16720–16733.

Marti, M., Good, R.T., Rug, M., Knuepfer, E., and Cowman, A.F. (2004). Targeting malaria virulence and remodeling proteins to the host erythrocyte. Science. *306*, 1930–1933.

Masatani, T., Matsuo, T., Tanaka, T., Terkawi, M.A., Lee, E.-G., Goo, Y.-K., Aboge, G.O., Yamagishi, J., Hayashi, K., Kameyama, K., et al. (2013). TgGRA23, a novel Toxoplasma gondii dense granule protein associated with the parasitophorous vacuole membrane and intravacuolar network. Parasitol. Int. *62*, 372–379.

Mashayekhi, M., Sandau, M.M., Dunay, I.R., Frickel, E.M., Khan, A., Goldszmid, R.S., Sher, A., Ploegh, H.L., Murphy, T.L., Sibley, L.D., et al. (2011). CD8α(+) dendritic cells are the critical source of interleukin-12 that controls acute infection by Toxoplasma gondii tachyzoites. Immunity. *35*, 249–259.

Mehlhorn, H., and Frenkel, J.K. (1980). Ultrastructural comparison of cysts and zoites of Toxoplasma gondii, Sarcocystis muris, and Hammondia hammondi in skeletal muscle of mice. J. Parasitol. *66*, 59–67.

Meissner, M., Reiss, M., Viebig, N., Carruthers, V.B., Toursel, C., Tomavo, S., Ajioka, J.W., and Soldati, D. (2002). A family of transmembrane microneme proteins of Toxoplasma gondii contain EGF-like domains and function as escorters. J. Cell. Sci. *115*, 563–574.

de Melo, E.J., and de Souza, W. (1996). Pathway of C6-NBD-ceramide on the host cell infected with Toxoplasma gondii. Cell Struct. Funct. *21*, 47–52.

de Melo, E.J., and de Souza, W. (1997). A cytochemistry study of the inner membrane complex of the pellicle of tachyzoites of Toxoplasma gondii. Parasitol. Res. *83*, 252–256.

de Melo, E.J., de Carvalho, T.U., and de Souza, W. (1992). Penetration of Toxoplasma gondii into host cells induces changes in the distribution of the mitochondria and the endoplasmic reticulum. Cell Struct. Funct. 17, 311–317.

Mercier A, Devillard S, Ngoubangoye B, Bonnabau H, Bañuls AL, Durand P, Salle B, Ajzenberg D, Dardé ML. (2010). Additional haplogroups of Toxoplasma gondii out of Africa: population structure and mouse-virulence of strains from Gabon. PLoS Negl. Trop. Dis. 4, e876.

Mercier, C. and Delauw, M. F. (2012) Safe living within a parasitophorous vacuole: the recipe of success by Toxoplasma gondii. Pathogen Interaction. At the Frontiers of Cellular Microbiology (Ghigo, E. ed.) pp. 1-18, Transworld Research Network.

Mercier, C., and Cesbron-Delauw, M.-F. (2015). Toxoplasma secretory granules: one population or more? Trends Parasitol. *31*, 60–71.

Mercier, C., Cesbron-Delauw, M.F., and Sibley, L.D. (1998a). The amphipathic alpha helices of the toxoplasma protein GRA2 mediate post-secretory membrane association. J. Cell. Sci. *111* (Pt 15), 2171–2180.

Mercier, C., Travier, L., Bittame, A., Gendrin, C., and Cesbron-Delauw, M.F. (2010) The dense granule proteins of Toxoplasma gondii. In Parasitology Research Trends (De Bruyn, O. and Peeters, S., eds), pp. 1–31, Nova Publishers

Mercier C, Howe DK, Mordue D, Lingnau M, Sibley LD. (1998b). Targeted disruption of the GRA2 locus in Toxoplasma gondii decreases acute virulence in mice. Infect. Immun. *66*, 4176-4182.

Mercier, C., Dubremetz, J.-F., Rauscher, B., Lecordier, L., Sibley, L.D., and Cesbron-Delauw, M.-F. (2002). Biogenesis of nanotubular network in Toxoplasma parasitophorous vacuole induced by parasite proteins. Mol. Biol. Cell *13*, 2397–2409.

Mercier, C., Adjogble, K.D.Z., Däubener, W., and Delauw, M.-F.-C. (2005). Dense granules: are they key organelles to help understand the parasitophorous vacuole of all Apicomplexa parasites? Int. J. Parasitol. *35*, 829–849.

Miller, M., Conrad, P., James, E.R., Packham, A., Toy-Choutka, S., Murray, M.J., Jessup, D., and Grigg, M. (2008). Transplacental toxoplasmosis in a wild southern sea otter (Enhydra lutris nereis). Vet. Parasitol. *153*, 12–18.

Min, J., Qu, D., Li, C., Song, X., Zhao, Q., Li, X., Yang, Y., Liu, Q., He, S., and Zhou, H. (2012). Enhancement of protective immune responses induced by Toxoplasma gondii dense granule antigen 7 (GRA7) against toxoplasmosis in mice using a prime-boost vaccination strategy. Vaccine. *30*, 5631–5636.

Montoya, J.G., and Liesenfeld, O. (2004). Toxoplasmosis. Lancet. *363*, 1965–1976.

Moore, K.W., de Waal Malefyt, R., Coffman, R.L., and O'Garra, A. (2001). Interleukin-10 and the interleukin-10 receptor. Annu. Rev. Immunol. *19*, 683–765.

Morris, M.T., and Carruthers, V.B. (2003). Identification and partial characterization of a second Kazal inhibitor in Toxoplasma gondii. Mol. Biochem. Parasitol. *128*, 119–122.

Morris, M.T., Coppin, A., Tomavo, S., and Carruthers, V.B. (2002). Functional analysis of Toxoplasma gondii protease inhibitor 1. J. Biol. Chem. *277*, 45259–45266.

Morrissette, N.S., and Sibley, L.D. (2002). Cytoskeleton of apicomplexan parasites. Microbiol. Mol. Biol. Rev. *66*, 21–38.

Mortensen, P.B., Nørgaard-Pedersen, B., Waltoft, B.L., Sørensen, T.L., Hougaard, D., and Yolken, R.H. (2007). Early infections of Toxoplasma gondii and the later development of schizophrenia. Schizophr. Bull. *33*, 741–744.

Muñiz-Hernández, S., Carmen, M.G. del, Mondragón, M., Mercier, C., Cesbron, M.F., Mondragón-González, S.L., González, S., and Mondragón, R. (2011). Contribution of the residual body in the spatial organization of Toxoplasma gondii tachyzoites within the parasitophorous vacuole. J. Biomed. Biotechnol. *2011*, 473983.

Nadipuram, S.M., Kim, E.W., Vashisht, A.A., Lin, A.H., Bell, H.N., Coppens, I., Wohlschlegel, J.A., and Bradley, P.J. (2016). In vivo biotinylation of the Toxoplasma parasitophorous vacuole reveals novel dense granule proteins important for parasite growth and pathogenesis. MBio. *7*, pii: e00808-16.

Nagamune, K., Hicks, L.M., Fux, B., Brossier, F., Chini, E.N., and Sibley, L.D. (2008). Abscisic acid controls calcium-dependent egress and development in Toxoplasma gondii. Nature. *451*, 207–210.

Naguleswaran, A., Elias, E.V., McClintick, J., Edenberg, H.J., and Sullivan, W.J. (2010). Toxoplasma gondii lysine acetyltransferase GCN5-A functions in the cellular response to alkaline stress and expression of cyst genes. PLoS Pathog. *6*, e1001232.

Narasimhan, J., Joyce, B.R., Naguleswaran, A., Smith, A.T., Livingston, M.R., Dixon, S.E., Coppens, I., Wek, R.C., and Sullivan, W.J. (2008). Translation regulation by eukaryotic initiation factor-2 kinases in the development of latent cysts in Toxoplasma gondii. J. Biol. Chem. *283*, 16591–16601.

Ngô, H.M., Yang, M., and Joiner, K.A. (2004). Are rhoptries in Apicomplexan parasites secretory granules or secretory lysosomal granules? Mol. Microbiol. *52*, 1531–1541.

Nichols, B.A., Chiappino, M.L., and Pavesio, C.E. (1994). Endocytosis at the micropore of Toxoplasma gondii. Parasitol. Res. *80*, 91–98.

Nicolle, C, and Manceaux, L. (1908). Sur une infection a corps de Leishman (ou organismes voisons) du gondi. C R Acad Sci. *147*: 763-766.

Nolan, S.J., Romano, J.D., Luechtefeld, T., and Coppens, I. (2015). Neospora caninum recruits host cell structures to its parasitophorous vacuole and salvages lipids from organelles. Euk. Cell *14*, 454–473.

Okada T, Marmansari D, Li ZM, Adilbish A, Canko S, Ueno A, Shono H, Furuoka H, Igarashi M. (2013). A novel dense granule protein, GRA22, is involved in regulating parasite egress in Toxoplasma gondii. Mol Biochem Parasitol. *189*, 5-13.

Olias, P., Etheridge, R.D., Zhang, Y., Holtzman, M.J., and Sibley, L.D. (2016). Toxoplasma effector recruits the Mi-2/NuRD complex to repress STAT1 transcription and block IFN-γ-dependent gene expression. Cell Host Microbe. *20*, 72–82.

Opitz, C., and Soldati, D. (2002). "The glideosome": a dynamic complex powering gliding motion and host cell invasion by Toxoplasma gondii. Mol. Microbiol. *45*, 597–604.

Oz HS. (2015). Novel synergistic protective efficacy of atovaquone and diclazuril on fetal-maternal toxoplasmosis. Int J Clin Med. *5*, 921-932.

Paul, A.S., Saha, S., Engelberg, K., Jiang, R.H.Y., Coleman, B.I., Kosber, A.L., Chen, C.-T., Ganter, M., Espy, N., Gilberger, T.W., et al. (2015). Parasite calcineurin regulates host cell recognition and attachment by Apicomplexans. Cell Host Microbe. *18*, 49–60.

Peixoto, L., Chen, F., Harb, O.S., Davis, P.H., Beiting, D.P., Brownback, C.S., Ouloguem, D., and Roos, D.S. (2010). Integrative genomic approaches highlight a family of parasite-specific kinases that regulate host responses. Cell Host Microbe. *8*, 208–218.

Pena, H.F.J., Gennari, S.M., Dubey, J.P., and Su, C. (2008). Population structure and mouse-virulence of Toxoplasma gondii in Brazil. Int. J. Parasitol. *38*, 561–569.

Pernas, L., and Boothroyd, J.C. (2010). Association of host mitochondria with the parasitophorous vacuole during Toxoplasma infection is not dependent on rhoptry proteins ROP2/8. Int. J. Parasitol. *40*, 1367–1371.

Pernas, L., Adomako-Ankomah, Y., Shastri, A.J., Ewald, S.E., Treeck, M., Boyle, J.P., and Boothroyd, J.C. (2014). Toxoplasma effector MAF1 mediates recruitment of host mitochondria and impacts the host response. PLoS Biol. *12*, e1001845.

Persat, F., Mercier, C., Ficheux, D., Colomb, E., Trouillet, S., Bendridi, N., Musset, K., Loeuillet, C., Cesbron-Delauw, M.-F., and Vincent, C. (2012). A synthetic peptide derived from the parasite

Toxoplasma gondii triggers human dendritic cells' migration. J. Leukoc. Biol. *92*, 1241–1250.

Pizarro-Cerdá, J., Charbit, A., Enninga, J., Lafont, F., and Cossart, P. (2016). Manipulation of host membranes by the bacterial pathogens Listeria, Francisella, Shigella and Yersinia. Semin. Cell Dev. Biol. *60*, 155–167.

Plattner, F., Yarovinsky, F., Romero, S., Didry, D., Carlier, M.-F., Sher, A., and Soldati-Favre, D. (2008). Toxoplasma profilin is essential for host cell invasion and TLR11-dependent induction of an interleukin-12 response. Cell Host Microbe. *3*, 77–87.

Pszenny, V., Ehrenman, K., Romano, J.D., Kennard, A., Schultz, A., Roos, D.S., Grigg, M.E., Carruthers, V.B., and Coppens, I. (2016). A lipolytic lecithin:cholesterol acyltransferase secreted by Toxoplasma facilitates parasite replication and egress. J. Biol. Chem. *291*, 3725–3746.

Que X, Engel JC, Ferguson D, Wunderlich A, Tomavo S, Reed SL. (2007). Cathepsin Cs are key for the intracellular survival of the protozoan parasite, Toxoplasma gondii. J Biol Chem. *282*, 4994-5003.

Que, X., Ngo, H., Lawton, J., Gray, M., Liu, Q., Engel, J., Brinen, L., Ghosh, P., Joiner, K.A., and Reed, S.L. (2002). The cathepsin B of Toxoplasma gondii, toxopain-1, is critical for parasite invasion and rhoptry protein processing. J. Biol. Chem. *277*, 25791–25797.

Raetz, M., Kibardin, A., Sturge, C.R., Pifer, R., Li, H., Burstein, E., Ozato, K., Larin, S., and Yarovinsky, F. (2013). Cooperation of TLR12 and TLR11 in the IRF8-dependent IL-12 response to Toxoplasma gondii profilin. J. Immunol. *191*, 4818–4827.

Rahimi, M.T., Sarvi, S., Sharif, M., Abediankenari, S., Ahmadpour, E., Valadan, R., Ramandie, M.F.-, Hosseini, S.-A., and Daryani, A. (2017). Immunological evaluation of a DNA cocktail vaccine with co-delivery of calcium phosphate nanoparticles (CaPNs) against the Toxoplasma gondii RH strain in BALB/c mice. Parasitol. Res. *116*, 609–616.

Ravindran, S., and Boothroyd, J.C. (2008). Secretion of proteins into host cells by Apicomplexan parasites. Traffic. *9*, 647–656.

Reese, M.L., and Boothroyd, J.C. (2009). A helical membrane-binding domain targets the Toxoplasma ROP2 family to the parasitophorous vacuole. Traffic. *10*, 1458–1470.

Reichmann, G., Długońska, H., and Fischer, H.-G. (2002). Characterization of TgROP9 (p36), a novel rhoptry protein of Toxoplasma gondii tachyzoites identified by T cell clone. Mol. Biochem. Parasitol. *119*, 43–54.

Ribet, D., and Cossart, P. (2015). How bacterial pathogens colonize their hosts and invade deeper tissues. Microbes Infect. *17*, 173–183.

Robert-Gangneux, F., and Dardé, M.-L. (2012). Epidemiology of and diagnostic strategies for toxoplasmosis. Clin. Microbiol. Rev. *25*, 264–296.

Romano JD, de Beaumont C, Carrasco JA, Ehrenman K, Bavoil PM, Coppens I. (2013a). Fierce competition between Toxoplasma and Chlamydia for host cell structures in dually infected cells. Euk. Cell. *12*, 265-277.

Romano, J.D., Sonda, S., Bergbower, E., Smith, M.E., and Coppens, I. (2013b). Toxoplasma gondii salvages sphingolipids from the host Golgi through the rerouting of selected Rab vesicles to the parasitophorous vacuole. Mol. Biol. Cell *24*, 1974–1995.

Rome, M.E., Beck, J.R., Turetzky, J.M., Webster, P., and Bradley, P.J. (2008). Intervacuolar transport and unique topology of GRA14, a novel dense granule protein in Toxoplasma gondii. Infect. Immun. *76*, 4865–4875.

Rommereim, L.M., Bellini, V., Fox, B.A., Pètre, G., Rak, C., Touquet, B., Aldebert, D., Dubremetz, J.-F., Cesbron-Delauw, M.-F., Mercier, C., et al. (2016). Phenotypes associated with knockouts of eight dense granule gene loci (GRA2-9) in virulent Toxoplasma gondii. PLoS One. *11*, e0159306.

Rosowski, E.E., Lu, D., Julien, L., Rodda, L., Gaiser, R.A., Jensen, K.D.C., and Saeij, J.P.J. (2011). Strain-specific activation of the NF-kappaB pathway by GRA15, a novel Toxoplasma gondii dense granule protein. J. Exp. Med. *208*, 195–212.

Saeij JP, Boyle JP, Boothroyd JC. (2005). Differences among the three major strains of Toxoplasma gondii and their specific interactions with the infected host. Trends Parasitol. 21, 476-481.

Saeij JP, Coller S, Boyle JP, Jerome ME, White MW, Boothroyd JC. (2007). Toxoplasma co-opts host gene expression by injection of a polymorphic kinase homologue. Nature. *445*, 324-327.

Saksouk, N., Bhatti, M.M., Kieffer, S., Smith, A.T., Musset, K., Garin, J., Sullivan, W.J., Cesbron-Delauw, M.-F., and Hakimi, M.-A. (2005). Histone-modifying complexes regulate gene expression pertinent to the differentiation of the protozoan parasite Toxoplasma gondii. Mol. Cell. Biol. *25*, 10301–10314.

Sanchez Y, Rosado Jde D, Vega L, Elizondo G, Estrada-Muñiz E, Saavedra R, Juárez I, Rodríguez-Sosa M. (2010). The unexpected role for the aryl hydrocarbon receptor on susceptibility to experimental toxoplasmosis. J Biomed Biotechnol. *2010*, 505694

Sanders, K.L., Fox, B.A., and Bzik, D.J. (2015). Attenuated Toxoplasma gondii stimulates immunity to pancreatic cancer by manipulation of myeloid cell populations. Cancer Immunol. Res. *3*, 891–901.

Sautel, C.F., Ortet, P., Saksouk, N., Kieffer, S., Garin, J., Bastien, O., and Hakimi, M.-A. (2009). The histone methylase KMTox interacts with the redox-sensor peroxiredoxin-1 and targets genes involved in Toxoplasma gondii antioxidant defences. Mol. Microbiol. *71*, 212–226.

Scanga, C.A., Aliberti, J., Jankovic, D., Tilloy, F., Bennouna, S., Denkers, E.Y., Medzhitov, R., and Sher, A. (2002). Cutting edge: MyD88 is required for resistance to Toxoplasma gondii infection and regulates parasite-induced IL-12 production by dendritic cells. J. Immunol. *168*, 5997–6001.

Shastri AJ, Marino ND, Franco M, Lodoen MB, Boothroyd JC. (2014) GRA25 is a novel virulence factor of Toxoplasma gondii and influences the host immune response. Infect. Immun. *82*, 2595-2605

Schatten, H., and Ris, H. (2004). Three-dimensional imaging of Toxoplasma gondii-host cell interactions within the parasitophorous vacuole. Microsc. Microanal. *10*, 580–585.

Schwab, J.C., Beckers, C.J., and Joiner, K.A. (1994). The parasitophorous vacuole membrane surrounding intracellular Toxoplasma gondii functions as a molecular sieve. Proc. Natl. Acad. Sci. U.S.A. *91*, 509–513.

Sehgal, A., Bettiol, S., Pypaert, M., Wenk, M.R., Kaasch, A., Blader, I.J., Joiner, K.A., and Coppens, I. (2005). Peculiarities of host cholesterol transport to the unique intracellular vacuole containing Toxoplasma. Traffic. *6*, 1125–1141.

Shen, B., Buguliskis, J.S., Lee, T.D., and Sibley, L.D. (2014). Functional analysis of rhomboid proteases during Toxoplasma invasion. MBio. *5*, e01795-01714.

Shwab, E.K., Zhu, X.-Q., Majumdar, D., Pena, H.F.J., Gennari, S.M., Dubey, J.P., and Su, C. (2014). Geographical patterns of Toxoplasma gondii genetic diversity revealed by multilocus PCR-RFLP genotyping. Parasitology. *141*, 453–461.

Sibley, L.D. (1989) Active modification of host cell phagosomes by Toxoplasma gondii. In "Intracellular parasitism". Ed: J. Moulder. CRC Press. pp 245-257

Sibley, L.D. (2003). Toxoplasma gondii: perfecting an intracellular life style. Traffic. *4*, 581–586.

Sibley, L.D., and Boothroyd, J.C. (1992). Virulent strains of Toxoplasma gondii comprise a single clonal lineage. Nature. *359*, 82–85.

Sibley, L.D., Pfefferkorn, E.R., and Boothroyd, J.C. (1991). Proposal for a uniform genetic nomenclature in Toxoplasma gondii. Parasitol. Today. *7*, 327–328.

Sibley, L.D., Niesman, I.R., Asai, T., and Takeuchi, T. (1994). Toxoplasma gondii: secretion of a potent nucleoside triphosphate hydrolase into the parasitophorous vacuole. Exp. Parasitol. *79*, 301–311.

Sibley, L.D., Niesman, I.R., Parmley, S.F., and Cesbron-Delauw, M.F. (1995). Regulated secretion of multi-lamellar vesicles leads to formation of a tubulo-vesicular network in host-cell vacuoles occupied by Toxoplasma gondii. J. Cell. Sci. *108 (Pt 4)*, 1669–1677.

Silverman, J.A., Qi, H., Riehl, A., Beckers, C., Nakaar, V., and Joiner, K.A. (1998). Induced activation of the Toxoplasma gondii nucleoside triphosphate hydrolase leads to depletion of host cell ATP levels and rapid exit of intracellular parasites from infected cells. J. Biol. Chem. *273*, 12352–12359.

Sinai, A.P., and Joiner, K.A. (2001). The Toxoplasma gondii protein ROP2 mediates host organelle association with the parasitophorous vacuole membrane. J. Cell Biol. *154*, 95–108.

Sinai, A.P., Webster, P., and Joiner, K.A. (1997). Association of host cell endoplasmic reticulum and mitochondria with the Toxoplasma gondii parasitophorous vacuole membrane: a high affinity interaction. J. Cell. Sci. *110 (Pt 17)*, 2117–2128.

Singh, S., Alam, M.M., Pal-Bhowmick, I., Brzostowski, J.A., and Chitnis, C.E. (2010). Distinct external signals trigger sequential release of apical organelles during erythrocyte invasion by malaria parasites. PLoS Pathog. *6*, e1000746.

Soête, M., Camus, D., and Dubremetz, J.F. (1994). Experimental induction of bradyzoite-specific antigen expression and cyst formation by the RH strain of Toxoplasma gondii in vitro. Exp. Parasitol. *78*, 361–370.

De Souza, W. (2006). Secretory organelles of pathogenic protozoa. *An Acad. Braz. Cienc.* **78**, 271-291.

Spillman, N.J., Beck, J.R., and Goldberg, D.E. (2015). Protein export into malaria parasite-infected erythrocytes: mechanisms and functional consequences. Annu. Rev. Biochem. *84*, 813–841.

Splendore A. (1908). Un nuovo protozoa parassita deconigli incontrato nelle lesioni anatomiche d'une malattia che ricorda in molti punti il Kala-azar dell'uoma. Nota preliminare pel. Rev Soc Sci Sao Paulo. *3*, 109-112.

Straub, K.W., Peng, E.D., Hajagos, B.E., Tyler, J.S., and Bradley, P.J. (2011). The moving junction protein RON8 facilitates firm attachment and host cell invasion in Toxoplasma gondii. PLoS Pathog. *7*, e1002007.

Striepen, B. (2007). Switching parasite proteins on and off. Nat. Methods *4*, 999–1000.

Sturge, C.R., Benson, A., Raetz, M., Wilhelm, C.L., Mirpuri, J., Vitetta, E.S., and Yarovinsky, F. (2013). TLR-independent neutrophil-derived IFN-γ is important for host resistance to intracellular pathogens. Proc. Natl. Acad. Sci. U.S.A. *110*, 10711–10716.

Sturge CR, Yarovinsky F (2014). Complex immune cell interplay in the gamma interferon response during Toxoplasma gondii infection. Infect Immun. *82*: 3090-3097.

Su, C., Evans, D., Cole, R.H., Kissinger, J.C., Ajioka, J.W., and Sibley, L.D. (2003). Recent expansion of Toxoplasma through enhanced oral transmission. Science. *299*, 414–416.

Su, C., Shwab, E.K., Zhou, P., Zhu, X.Q., and Dubey, J.P. (2010). Moving towards an integrated approach to molecular detection and identification of Toxoplasma gondii. Parasitology. *137*, 1–11.

Su, C., Khan, A., Zhou, P., Majumdar, D., Ajzenberg, D., Dardé, M.-L., Zhu, X.-Q., Ajioka, J.W., Rosenthal, B.M., Dubey, J.P., et al. (2012). Globally diverse Toxoplasma gondii isolates comprise six major clades originating from a small number of distinct ancestral lineages. Proc. Natl. Acad. Sci. U.S.A. *109*, 5844–5849.

Suss-Toby, E., Zimmerberg, J., and Ward, G.E. (1996). Toxoplasma invasion: the parasitophorous vacuole is formed from host cell plasma membrane and pinches off via a fission pore. Proc. Natl. Acad. Sci. U.S.A. *93*, 8413–8418.

Suzuki, Y. (2002). Immunopathogenesis of cerebral toxoplasmosis. J. Infect. Dis. *186 Suppl 2*, S234-240.

Suzuki Y, Wang X, Jortner BS, Payne L, Ni Y, Michie SA, Xu B, Kudo T, Perkins S. (2010). Removal of Toxoplasma gondii cysts from the brain by perforin-mediated activity of CD8+ T cells. Am J Pathol. *176*, 1607-1613

Suzuki, Y., Yang, Q., Yang, S., Nguyen, N., Lim, S., Liesenfeld, O., Kojima, T., and Remington, J.S. (1996). IL-4 is protective against development of toxoplasmic encephalitis. J. Immunol. *157*, 2564–2569.

Swisher, C.N., Boyer, K., and McLeod, R. (1994). Congenital toxoplasmosis. The Toxoplasmosis Study Group. Semin. Pediatr. Neurol. *1*, 4–25.

Tahara M, Andrabi SB, Matsubara R, Aonuma H, Nagamune K. (2016). A host cell membrane microdomain is a critical factor for organelle discharge by Toxoplasma gondii. Parasitol Int. *65* (5 Pt A): 378-388.

Tan, T.G., Mui, E., Cong, H., Witola, W.H., Montpetit, A., Muench, S.P., Sidney, J., Alexander, J., Sette, A., Grigg, M.E., et al. (2010). Identification of T. gondii epitopes, adjuvants, and host genetic factors that influence protection of mice and humans. Vaccine. *28*, 3977–3989.

Taylor, S., Barragan, A., Su, C., Fux, B., Fentress, S.J., Tang, K., Beatty, W.L., Hajj, H.E., Jerome, M., Behnke, M.S., et al. (2006). A secreted serine-threonine kinase determines virulence in the eukaryotic pathogen Toxoplasma gondii. Science. *314*, 1776–1780.

Tomavo, S., and Boothroyd, J.C. (1995). Interconnection between organellar functions, development and drug resistance in the protozoan parasite Toxoplasma gondii. Int. J. Parasitol. *25*, 1293–1299.

Tomita T, Bzik DJ, Ma YF, Fox BA, Markillie LM, Taylor RC, Kim K, Weiss LM (2013). The Toxoplasma gondii cyst wall protein CST1 is critical for cyst wall integrity and promotes bradyzoite persistence. PLoS Pathog. *9*, e1003823.

Torpier, G., Charif, H., Darcy, F., Liu, J., Darde, M.L., and Capron, A. (1993). Toxoplasma gondii: differential location of antigens secreted from encysted bradyzoites. Exp. Parasitol. *77*, 13–22.

Torrey, E.F., Bartko, J.J., Lun, Z.-R., and Yolken, R.H. (2007). Antibodies to Toxoplasma gondii in patients with schizophrenia: a meta-analysis. Schizophr. Bull. *33*, 729–736.

Travier, L. (2007) Caracterisation des proteines de granules denses de toxoplasma gondii : Etude des interactions protéiques et lipidiques et du rôle des hélices alpha-amphipatiques de GRA2. Thèse Université Joesph Fourier, Grenoble.

Travier, L., Mondragon, R., Dubremetz, J.-F., Musset, K., Mondragon, M., Gonzalez, S., Cesbron-Delauw, M.-F., and Mercier, C. (2008). Functional domains of the Toxoplasma GRA2 protein in the formation of the membranous nanotubular network of the parasitophorous vacuole. Int. J. Parasitol. *38*, 757–773.

Van, T.T., Kim, S.-K., Camps, M., Boothroyd, J.C., and Knoll, L.J. (2007). The BSR4 protein is up-regulated in Toxoplasma gondii bradyzoites, however the dominant surface antigen recognised by the P36 monoclonal antibody is SRS9. Int. J. Parasitol. *37*, 877–885.

Villard, O., Cimon, B., L'Ollivier, C., Fricker-Hidalgo, H., Godineau, N., Houze, S., Paris, L., Pelloux, H., Villena, I., and Candolfi, E. (2016). Help in the choice of automated or semiautomated immunoassays for serological diagnosis of toxoplasmosis: evaluation of nine immunoassays by the French National Reference Center for Toxoplasmosis. J. Clin. Microbiol. *54*, 3034–3042.

Vivier, E., and Petitprez, A. (1969). [The outer membrane complex and its development at the time of the formation of daughter cells in Toxoplasma gondii]. J. Cell Biol. *43*, 329–342.

Walker, R., Gissot, M., Croken, M.M., Huot, L., Hot, D., Kim, K., and Tomavo, S. (2013). The Toxoplasma nuclear factor TgAP2XI-4 controls bradyzoite gene expression and cyst formation. Mol. Microbiol. *87*, 641–655.

Weidner, J.M., Kanatani, S., Uchtenhagen, H., Varas-Godoy, M., Schulte, T., Engelberg, K., Gubbels, M.-J., Sun, H.S., Harrison, R.E., Achour, A., et al. (2016). Migratory activation of parasitized dendritic cells by the protozoan Toxoplasma gondii 14-3-3 protein. Cell. Microbiol. *18*, 1537–1550.

Weissenhorn, W., Hinz, A., and Gaudin, Y. (2007). Virus membrane fusion. FEBS Lett. *581*, 2150–2155.

Werner-Meier, R., and Entzeroth, R. (1997). Diffusion of microinjected markers across the parasitophorous vacuole membrane in cells infected with Eimeria nieschulzi (Coccidia, Apicomplexa). Parasitol. Res. *83*, 611–613.

Whitelaw JA, Latorre-Barragan F, Gras S, Pall GS, Leung JM, Heaslip A, Egarter S, Andenmatten N, Nelson SR, Warshaw DM, Ward GE, Meissner M. (2017). Surface attachment, promoted by the actomyosin system of Toxoplasma gondii is important for efficient gliding motility and invasion. BMC Biol. *15*:1. doi: 10.1186/s12915-016-0343-5.

Wilson DC, Grotenbreg GM, Liu K, Zhao Y, Frickel EM, Gubbels MJ, Ploegh HL, Yap GS. (2010). Differential regulation of effector- and central-memory responses to Toxoplasma gondii Infection by IL-12 revealed by tracking of Tgd057-specific CD8+ T cells. PLoS Pathog. *6*, e1000815.

Wu, X.-N., Lin, J., Lin, X., Chen, J., Chen, Z.-L., and Lin, J.-Y. (2012). Multicomponent DNA vaccine-encoding Toxoplasma gondii GRA1 and SAG1 primes anti-Toxoplasma immune response in mice. Parasitol. Res. *111*, 2001–2009.

Yamamoto, M., Okuyama, M., Ma, J.S., Kimura, T., Kamiyama, N., Saiga, H., Ohshima, J., Sasai, M., Kayama, H., Okamoto, T., et al. (2012). A cluster of interferon-γ-inducible p65 GTPases plays a critical role in host defense against Toxoplasma gondii. Immunity. *37*, 302–313.

Yap, G.S., and Sher, A. (1999). Cell-mediated immunity to Toxoplasma gondii: initiation, regulation and effector function. Immunobiology. *201*, 240–247.

Yarovinsky, F. (2014). Innate immunity to Toxoplasma gondii infection. Nat. Rev. Immunol. *14*, 109–121.

Zhang, M., Joyce, B.R., Sullivan, W.J., and Nussenzweig, V. (2013). Translational control in Plasmodium and toxoplasma parasites. Euk. Cell *12*, 161–167.

Zhang, Y.W., Halonen, S.K., Ma, Y.F., Wittner, M., and Weiss, L.M. (2001). Initial characterization of CST1, a Toxoplasma gondii cyst wall glycoprotein. Infect. Immun. *69*, 501–507.

Zinecker, C.F., Striepen, B., Tomavo, S., Dubremetz, J.F., and Schwarz, R.T. (1998). The dense granule antigen, GRA2 of Toxoplasma gondii is a glycoprotein containing O-linked oligosaccharides. Mol. Biochem. Parasitol. *97*, 241–246.

SUMMARY

Toxoplasmosis, which is caused by the intracellular parasite *Toxoplasma gondii* is characterized by a life-long chronic infection. The parasites replicate inside a parasitophorous vacuole (PV), which evolves into a persistent cyst. The molecular mechanisms governing the differentiation process are poorly characterized. It is known that the dense granules proteins (GRA) are major components of both the PV and the cyst wall, enabling their interaction with the host cells. Using a *Prugniaud* cystogenic type II strain in which the *gra5* gene was invalidated and a combination of cellular and proteomic approaches, we discovered that GRA5 regulates *i)* the molecular content of the PV, *ii)* the PV interaction with the host endoplasmic reticulum and *iii)* host cell homeostasis necessary to ensure the formation of a stable cyst wall.

Key words: Toxoplasma *gondii,* dense granule proteins, chronic infection, cyst, host-pathogen interaction, knocked-out mutant

RESUME

Toxoplasma gondii est un parasite intracellulaire responsable de la toxoplasmose. Lors de l'infection aiguë, le parasite se divise dans une vacuole parasitophore (VP), compartiment d'interactions avec la cellule hôte. La VP se modifie pour former un kyste qui persiste au cours de la phase chronique. Le rôle des protéines de granules denses (GRA) dans ce processus est suggéré par leur abondance dans la VP et la paroi kystique. Par des approches de génétique inverse et de protéomique, le but de ce travail visait à préciser au plan moléculaire, le rôle de la protéine GRA5. En utilisant un modèle de différenciation parasitaire *in vitro*, l'étude des phénotypes d'un mutant invalidé du gène *gra5* a permis de découvrir son rôle clé dans la formation des kystes par le maintien 1/ de l'intégrité de la membrane délimitant la VP en cours de différenciation, 2/ de l'accumulation d'autres composants parasitaires dans la VP et 3/ de son interaction avec le reticulum endoplasmique de l'hôte.

Mots-clés : *Toxoplasma gondii*, protéines de granules denses, infection chronique, kyste, interaction hôte-pathogène, mutant knocked-out